DOE/PC/93053--T3

Cooperative Research Program in Coal Liquefaction

Technical Report on DOE Contract No. DE-FC22-93PC93053 Period: May 1, 1994 - October 31, 1994

Submitted to the

U.S. Department of Energy

On behalf of the

Consortium for Fossil Fuel Liquefaction Science

University of Kentucky
University of Utah
University of Pittsburgh
West Virginia University
Auburn University

CONSORTIUM FOR FOSSIL FUEL LIQUEFACTION SCIENCE

TABLE OF CONTENTS

DISCLAIMER

SUMMARY

Coliquefaction of Coal with Waste Materials

The liquefaction of a number of lignocellulosic wastes and the coprocessing of Wyodak coal with several lignocellulosic wastes was investigated using a CO/H_2(COSTEAM) atmosphere(500 psig cold) in the presence of an alkali catalyst(Na_2CO_3). Oil and asphaltene yields were higher and gas yields higher for lignocellulosic wastes with higher lignin content. Oil and asphaltene yields from the coal were increased by ~5-8% by coprocessing. Although the gas yields were high(~ 70% from the wastes alone and ~30% from the coal and coal-waste mixtures, the gas was rich in hydrogen(typically ~ 45%) which could be separated and used in the process.

The COSTEAM process has also been applied to the liquefaction of a number of plastic resins. Greater than 90% conversion was achieved for PPE, PS, and low density PE. When these resins were coliquefied with Wyodak coal under the same conditions, the oil yield from the coal decreased for coal-PE and coal-PS, but increased markedly(from 20% to 62%) for coal-PPE. Coliquefaction experiments using the COSTEAM method were also performed on 1:1 mixtures of PPE and a mixed plastic with newsprint. Oil yields increased somewhat(~5-10%) and, more importantly, the oxygen content of the oil product decreased significantly(from 9 to 4%).

A systematic study was carried out of the depolymerization-liquefaction reactions of high density polyethylene(PE) and isotatic polypropylene(PPE) as a function of temperature, time and H_2 pressure. Three types of superacid catalysts were investigated in the study of PPE. For PE, using 2 wt.% of a ZrO_2/SO_4 catalyst, 2 hrs. reaction time, and initial hydrogen pressure of 1500 psig, maximum liquid yield(87%) was obtained at 435 °C, while maximum gasoline range yield(63%) was

obtained at 450 °C. At 450 °C, 1500 psig initial hydrogen pressure, using 1 wt.% ZrO_2/SO_4, liquid yield and gasoline yield were maximized at reaction times of 0.5-1.0 hours. With a constant reaction time(1 hr.) and temperature(450 °C), using 1 wt.% ZrO_2/SO_4, liquid yield was approximately constant as a function of initial hydrogen pressure from 500 to 2000 psig, while gasoline yield increased from 53% at 500 psig to 58% at 1500 psig and remained constant at higher pressures. Similar studies of PPE conducted at 410 °C and 1500 psig initial hydrogen pressure using 1 wt.% ZrO_2/SO_4 showed that both liquid yield and gasoline yield were maximized at 1.0 hr. of reaction time at 90 and 65 %, respectively. At the same conditions, it was demonstrated that PPE could be liquefied fairly efficiently at ambient (15 psig) hydrogen pressure(86% liquid yield, 58% gasoline range yield). A comparison of several superacid catalysts (ZrO_2/SO_4, Fe_2O_3/SO_4, and Al_2O_3/SO_{42}) for PPE liquefaction showed Al_2O_3/SO_4 to be slightly superior to the other catalysts and only slightly better than thermal liquefaction.

The liquefaction of a commingled waste plastic obtained from the American Plastics Council(APC) has been studied as a function of temperature and time, and the coliquefaction of the APC plastic with Blind Canyon bituminous coal(DECS-6), both with no added solvent, have been investigated. It is found that the optimum temperature for solvent-free liquefaction of the plastic alone and for coliquefaction with Blind Canyon coal is approximately 430 °C. A fairly large suite of catalysts were tried in the solvent-free coliquefaction experiments, but none of them were found to be particularly effective.

Coliquefaction of Black Thunder subbituminous coal with PE and PPE established that under the same conditions, both oil yields and total liquid yields were much higher with PPE than with PE. It was also demonstrated that the catalytic(HZSM-5) liquefaction of PE alone was not very sensitive to hydrogen pressure, at least insofar as total yield and oil yield, defined by THF and pentane solubles, were concerned. Moreover, the yields under nitrogen were approximately the same as those under hydrogen. Experiments using a waste oil solvent, rather than tetralin look promising. The waste oil appears to give significantly higher total

and oil yields for the APC commingled plastic than tetralin or waste oil-tetralin mixtures.

A comparison of several commercial cracking catalysts for the liquefaction of a mixed plastic(50% PE, 30% PET, and 20% PS) has been carried out. The best results were obtained using HZSM-5. Mixtures of the mixed plastic with 20% of PE, PS, or PPE were liquefied; oil yield and total conversion was highest with the PPE additive.

Comparative coliquefaction experiments on Blind Canyon coal has been carried using several solvents: tetralin, waste oil, prehydrocracked waste oil, prehydrocracked polystyrene, and mixtures of prehydrocracked PS and waste oil. It appears that the prehydrocracking treatment significantly improves both oil and total liquid yields.

Tire liquefaction studies continue to demonstrate that the organic portion of tires, except for the carbon black which typically is about 30-35% of the tire is easily liquefied. It has further been demonstrated that nitrogen can serve as well as hydrogen as the liquefaction atmosphere for tire rubber, at least insofar as total conversion, oil yields and oil composition are concerned. Characterization studies of the oil products produced from tire rubber under nitrogen or hydrogen are underway to determine what differences in structure may exist. The coliquefaction of tire rubber with coal exhibits synergistic effects, exhibiting higher total conversion and asphaltene yields from the coal although the oil yield is not much affected. The result suggests that tire hydrogen plays a role in capping asphaltene radicals. The increase in total conversion from the coal in a 1:1 tire-coal mixture relative to that of the coal alone increases with increasing pressure from about 8% at 0 H_2 pressure to 22% at 1600 psig H_2(cold). Catalytic coliquefaction using an impregnated iron sulfide catalyst exhibited mixed results: with one tire, conversion from the coal was increased by increasing the tire to coal ratio, while with a second tire it was decreased.

Catalyst Research

Sulfated zirconia(ZrO_2/SO_4) and metal promoted ZrO_2/SO_4 have investigated as

acid cracking catalysts by studying model reactions with diphenylmethane(DPM). ZrO_2/SO_4 was active for cracking DPM at room temperature at atmospheric pressure of hydrogen. $ZrO_2/SO_4/Pt$ was quite active in cracking of DPM at 200 °C at elevated hydrogen pressure(500 psi). Anion-modified and metal(Mo or W) promoted Fe_2O_3 catalysts are being investigated for their activity at lower temperatures(<300 °C) and hydrogen pressures(500 psig cold) using various model compounds and Blind Canyon coal(DECS-17).

Noble metals(Pt, Ir, and Ru) are being investigated as promoters for Al_2O_3 supported upgrading catalysts(NiMo, CoMo, and NiW). Both Ru and Ir promotion(1 wt.% Ir or Ru) improved the HDN activity of NiMo and CoMo supported catalysts for pyridine reactions in a tubing bomb, but did not significantly improve the HDN of coal liquid. $AlPO_4$-Al_2O_3 is being investigated as a new support material; surface areas up to 250 m^2/g have been achieved.

Mixed metal Fe-Mo sulfide catalysts have been prepared by in situ impregnation and precipation techniques on the coal. the Mo/(Fe + Mo) ratio varied from O to 0.25. Maximum activity for liquefaction of Blind Canyon coal(DECS-6), using a phenanthrene solvent to enhance catalytic effects, occurred at a ratio of 0.1-0.15. Highly dispersed iron sulfide catalysts were generated using an aerosol reactor produced a 10% increase in total conversion of Blind Canyon coal at 350 °C.

Mo_2C, Mo_2N, and MoS_2 catalysts synthesized by laser pyrolysis have been characterized by XPS and other methods and tested for their activity for deoxygenation, desulfurization, and denitrogenation of model compounds. Although the XPS results indicate that the catalysts are coated by MoO_3 and polymeric carbon, they show high activity for deoxygenation of diphenyl ether and desulfurization of benzothiophene, and moderate activity for hydrogenation of naphthalene.

Nanoscale ferrihydrite(FHYD) catalysts have been treated under DCL conditions and investigated subsequently to determine the effect of adding secondary anionic groups to the surfaces of the particles. Binary FHYD catalysts (M/FHYD, where M= ~5% of Si, Mo, citric acid, etc.) have previously been shown to have better DCL activity than pure FHYD of similar particle size. The current experiments

demonstrate that the pyrrhotite phase formed from binary FHYD under DCL conditions has significantly smaller particle size, by a factor of ~10, than that formed from pure FHYD. Furthermore, the hexagonal to monoclinic phase transition of pyrrhotite appears to be retarded for the binary FHYD relative to pure FHYD, yield higher vacancy content for the pyrrhotite formed from binary FHYD.

Fundamental Studies

A variety of structural characterization studies were completed. These included: Mossbauer analyses of DCL residue samples from the iron catalyst testing program at Sandia National Laboratory; XAFS analysis of Zn in waste oils and in the residues from coprocessing waste oil with coal; XAFS analysis of Mo and W sulfide catalysts prepared by laser pyrolysis; XPS depth profile studies of a binary ferrihydrite (FHYD/$Si_{0.05}$) catalyst and related DCL residues; and Mossbauer analyses of a hydrothermal Fe-S catalyst and related residues from model compound reactions.

New two dimensional(2-D) ^{13}C NMR techniques are being developed and applied to the coal-waste liquefaction problem. It appears that application of these methods to the liquefaction residues will be valuable in tracking the degree of reaction of the plastics with the coal in the coliquefaction process.

Biohydrogentation of fumarate was investigated using *D. desulfuricans* with ambient and high pressure(500 psig) hydrogen in a multipurpose bioreactor. Complete reduction of fumarate was achieved in 24 hours. A preliminary bioprocessing study was carried out on a mixture of polyethylene and an Illinois coal. After 10 days of biotreatment, the biotreated coal exhibited an increase of 10% in total conversion over a control sample.

Using a new quantum mechanical calculation method, the reaction of PE with toulene in the presence of hydrogen has been modeled. H addition is found to weaken the C-C bond near a branch point in the PE. Calculations are continuing to elucidate the catalytic mechanisms of Mo-promoted Fe catalysts. It appears that hydrogenation is the principal function of the Mo.

In Situ Analytical Techniques

In situ ESR measurements of the free radical density for tire rubber-Blind Canyon coal mixtures as a function of temperature indicate a decrease in cracking temperature and increased capping of free radicals by hydrogen from the rubber. Similar effects are observed for mixtures of polyethylene and polystyrene with coal. The free radical density of the APC commingled plastic under vacuum shows a much more rapid increase with time at 460 °C than at 410 °C.

A unique high pressure TGA/GC-MS system, constructed earlier as part of the CFFLS program, is being applied to determine the catalytic activity of a variety of catalysts for plastic depolymerization. In this method, 1% of the catalyst is mixed with a small sample of the APC plastic and the TGA and GC-MS measurements are carried out in situ at a hydrogen pressure of 900 psig. At temperatures of 400- 430 °C, the most active depolymerization catalysts are found to HZSM-5 and a coprecipated silica-alumina.

Further in situ XAFS experiments using a high temperature, high pressure XAFS cell were conducted using a beamline that featured an energy dispersive XAFS setup. In principal, this would allow spectra to be collected in 5-10 seconds, making more realistic kinetic studies of catalyst reactions possible. Unfortunately, the beamline proved to have insufficient flux to obtain good spectra using the high pressure cell. Other options for rapid XAFS data collection are being investigated.

A recently constructed in situ FTIR cell is being tested to determine optimum methods for investigating the reactions of iron-based catalysts.

TASK I

COLIQUEFACTION OF COAL WITH WASTE MATERIALS

TASK 1

Project I.1

FUNDAMENTAL REACTION STUDIES IN CO-PROCESSING OF COAL AND WASTE POLYMERS

Joseph S. Shabtai, W. Zmierczak and X. Xiao
University of Utah

The main research activities during the May 1, 1994 - October 31, 1994 period of this project were in the following directions:

1. Systematic studies on the catalytic depolymerization-liquefaction reactions of high density polyethylene as a function of processing variables, i.e., reaction temperature, time and H_2 pressure.
2. Continuation of systematic studies on the catalytic depolymerization-liquefaction of isotatic polypropylene as a function of additional processing variables, i.e., reaction time, catalyst type and H_2 pressure.
3. Initiation of systematic coprocessing studies of coal and commercial polymers, based on results from 1 and 2.

Following is a description of research performed and results obtained:

I.1.1. Systematic Studies on the Catalytic Depolymerization-Liquefaction Reactions of High Density Polyethylene

In previous work we have obtained some basic information on the catalytic depolymerization-liquefaction behavior of high density polyethylene (see Annual Report for the period May 1993-April 1994).

During the reporting period, a detailed study on the depolymerization-liquefaction reactions of high density polyethylene (M.W., 125,000; d, 0.959 g/cm^3; Tm, 130 °C; Aldrich) as a function of reaction variables was performed. Runs with this polymeric feed were conducted in a 50 ml Microclave reactor (Autoclave Engineers). The effect of reaction temperature, time and hydrogen pressure were examined.

In a typical run, 10.0 g of the feed was mixed with 0.10 g of solid catalyst and the mixture (without any solvent) was introduced in the autoclave reactor. The latter was sequentially purged with nitrogen and hydrogen, and then charged with H_2 to a selected initial pressure in the range of ambient to 2000 psig (the reaction pressure was between 350 - 3600 psig). The reactor was heated with constant mixing (500 rpm) to the desired temperature (heat-up time, 15 min). Typical reaction times were in the range of 0.5 - 3.0 h. At the end of the run, the gas product was passed through a stainless steel trap kept at liquid nitrogen temperature. After weighing, the condensed gas was analyzed by GC (mostly C_1 - C_4 components, accompanied by some C_5 and C_6, and traces of C_7, C_8 components). The liquid and solid products were removed from the reactor and weighed. Liquid was separated by decantation and filtration. The solid was rinsed with a little n-hexane, dried, and weighed. The solid was then washed with hot (~ 80 °C) hexadecane and filtered, dried and weighed in order to determine the approximate weight of recovered catalyst. In this way, the product was separated and the weights of gas, liquid, solid and recovered catalyst were determined. Usually the mass balance of the runs was 90 - 95 wt% (relative to the weight of the feed). Gas and liquid products were identified mainly by GC, GC/MS and FTIR, and quantitatively analyzed by gas chromatography.

A. Effect of Reaction Temperature

Results on the change in product composition as a function of reaction temperature are given in Table I.1.1. At 420 - 450 °C and an initial H_2 pressure of 1500 psig, with 2 wt% of ZrO_2/SO_4^{2-} as catalyst, and a reaction time of 2.0 hours, the polyethylene was converted mostly (76-87 wt%) into a low-boiling liquid. The gasoline range increased from 35.1 wt% at 420 °C to a maximum of 62.9 wt% at 450 °C; then it decreased to 51.6 wt% at 465 °C. C_{13+} components decreased from 58.9 to 6.8 wt% in the same temperature range. By increasing the temperature from 420 to 450 °C, gas (C_1-C_4) increased from 6.0 wt% to 21.6 wt%. This demonstrates a stepwise break-down of the polymeric chains.

B. Effect of Reaction Time

The change in product composition as a function of reaction time (between 0.5-3.0 hr) is summarized in Table I.1.2 (the other processing conditions were kept

constant, i.e., temperature, 450 °C, 1.0 wt% of ZrO_2/SO_4^{2-} as catalyst and 1500 psig initial H_2 pressure). The conversion was essentially complete in all runs. For the reaction time range of 0.5-3.0 h, the gas product increased from 12.5 to 29.3 wt%, C_{13+} decreased from 35.8 to 15.3 wt%. This is in good agreement with the above indicated temperature effect and again demonstrates the stepwise break-down of the polymer.

C. Effect of Hydrogen Pressure

The effect of H_2 pressure on the product composition is given in Table I.1.3. At 450 °C and a reaction time of 1.0 h, with 1.0 wt% ZrO_2/SO_4^{2-} as catalyst, polyethylene was fully converted in the entire H_2 pressure range examined. As H_2 pressure was increased from 500 to 1500 psig initial (950 to 2600 psig final), the gasoline boiling range increased and C_{13+} decreased. However, for H_2 initial pressure higher than 1500 psig , the gasoline range fraction remained around 57 wt%, while the C13+ fraction was about 24-26 wt%

I.1.2 Systematic Studies on the Catalytic Depolymerization-Liquefaction Reactions of Isotatic Polypropylene

In this part of the project, previous systematic studies on the catalytic depolymerization-liquefaction reactions of polypropylene as a function of reaction variables (see Annual Report for the period May 1993 - April 1994) were continued as follows:

A. Effect of Reaction Time

The depolymerization-liquefaction of polypropylene (isotatic; M.W., 250,000; d, 0.900 g/cm^3; Tm, 189 °C; Aldrich) was investigated also as a function of reaction time in the range of 0.5-3.0 hr. The change in product composition found is summarized in Table I.1.4 (other processing variables were kept constant in all runs, i.e., temperature 410 °C, initial H_2 pressure 1500 psig, 1.0 wt% ZrO_2/SO_4^{2-} catalyst). As seen, conversion to liquid products increased from 87.1 wt% at 0.5 h reaction time to ~100 wt% at 2.0 h, while the yield of gasoline range components increased from 52.1 wt% at 0.5 h to a maximum of 67.9 wt% at 2.0 h. On the other hand gas production (C_1-C_4 gases) increased from 5.8 wt% at 0.5 h to 14.1 wt% at 3.0 h. These results are consistent with the previously reported effect of reaction temperature, viz., they

confirm the existence of a controllable stepwise depolymerization of polypropylene into light liquid hydrocarbons.

B. Effect of Catalyst Type

A comparative study of three different types of solid superacid, i.e., Fe_2O_3/SO_4^{2-}, Al_2O_3/SO_4^{2-} and ZrO_2/SO_4^{2-} was also performed, keeping other processing variables constant (reaction temperature, 410 °C, time 1.0 h, initial H_2 pressure 1500 psig, catalyst amount, 1.0 wt%). A run without catalyst was also carried out. Results obtained are summarized in Table I.1.5. As seen, the extent of depolymerization of the feed into gasoline range hydrocarbons was higher in the catalytic runs as compared with that in the thermal (non-catalytic) run. Among the catalysts examined, Al_2O_3/SO_4^{2-} was indicated as the most efficient. Comparative studies at lower temperature and conversion are presently underway.

C. Effect of Hydrogen Pressure

At 410 °C and a reaction time of 1.0 h, with 1.0 wt% ZrO_2/SO_4^{2-} as catalyst, four different initial H_2 pressures, i.e., 15 (ambient), 500, 1000 and 1500 psig were applied in comparative depolymerization-liquefaction runs with polypropylene. This represents actual reaction pressures of 350, 900, 1500 and 2600 psig, respectively. Results obtained are summarized in Table I.1.6. As seen, increase in H_2 pressure from 15 to 500-1500 psig suppressed gas formation, decreased the amount of C_{13+} products, and increased gasoline boiling range production. The data obtained during the reporting period are presently being used in selecting suitable conditions for coprocessing of coal with polyethylene, polypropylene and other waste polymeric feeds.

TABLE I.1.1

Product Composition from Depolymerization-Liquefaction of High Density Polyethylene as a Function of Reaction Temperature[a,b]

Temperature, °C	420	435	450	465
Conversion, wt%	82.53	98.91	100	100
Product Distribution, wt%[c]:				
Gas (C_1-C_4)	5.98	11.80	21.59	41.64
Liquid	76.55	87.11	78.41	58.36
Solid	17.47	1.09	0.00	0.00
Gas Product Distribution, wt%[d,e]:				
C_1	0.12	0.56	2.05	0.96
C_2	0.79	1.65	3.98	6.00
C_3	2.07	3.91	6.98	14.54
C_4	3.00	5.68	8.58	20.14
Higher Product Distribution, wt%[d,e]:				
C_5H_{12}	3.51	6.62	8.39	12.19
C_6H_{14}	4.07	6.86	8.61	8.26
C_7H_{16}	5.40	9.17	10.65	8.64
C_8H_{18}	5.81	10.19	11.68	7.82
C_9H_{20}	4.50	7.35	7.53	4.96
$C_{10}H_{22}$	4.51	6.95	6.95	4.74
$C_{11}H_{24}$	3.85	5.46	5.18	2.91
$C_{12}H_{26}$	3.49	4.69	3.95	2.04
C_{13+}	58.88	30.91	15.47	6.81
Gasoline Range, wt%:				
C_5-C_{12}	35.14	57.29	62.94	51.55

[a] In each run was used 10.0 g of polymer and 0.20 g of ZrO_2/SO_4^{2-} catalyst; reaction time, 2.0 hr; H_2 initial pressure, 1500 psig.
[b] Data are given by weight percentage based on the total product.
[c] Liquid and solids were separated by decantation and filtration in which the solid was rinsed with little hexane.
[d] All products of a given C number consist of mixtures of normal and branched paraffins.
[e] All paraffin fractions contain trace amount (< 1 wt%) of corresponding olefins.

TABLE I.1.2

Product Composition from Depolymerization-Liquefaction of High Density Polyethylene as a Function of Reaction Time[a,b]

Reaction Time, hr	0.5	1.0	2.0	3.0
Conversion, wt%	99.35	99.87	100	100
Product Distribution, wt%[c]:				
Gas (C_1-C_4)	12.45	17.86	26.12	29.33
Liquid	86.90	82.01	73.88	70.67
Solid	0.65	0.13	0.00	0.00
Gas Product Distribution, wt%[d,e]:				
C_1	0.31	0.90	1.30	1.10
C_2	1.81	2.85	4.73	5.25
C_3	4.36	6.21	9.61	12.30
C_4	5.98	7.90	10.48	10.69
Higher Product Distribution, wt%[d,e]:				
C_5H_{12}	4.34	7.53	3.48	3.35
C_6H_{14}	5.46	7.39	13.42	4.62
C_7H_{16}	10.42	8.93	8.33	13.78
C_8H_{18}	6.42	8.59	5.71	7.93
C_9H_{20}	7.00	8.64	5.92	8.06
$C_{10}H_{22}$	6.36	6.66	3.52	7.24
$C_{11}H_{24}$	5.91	5.53	5.90	5.61
$C_{12}H_{26}$	5.80	4.57	3.27	4.79
C_{13+}	35.84	24.30	24.33	15.29
Gasoline Range, wt%:				
C_5-C_{12}	51.71	57.83	49.55	55.37

[a] In each run was used 10.0 g of polymer and 0.10 g ZrO_2/SO_4^{2-} catalyst; reaction temperature, 450 °C; H_2 initial pressure, 1500 psig.

[b] Data are given by weight percentage based on the total product.

[c] Liquid and solids were separated by decantation and filtration in which the solid was rinsed with little hexane.

[d] All products of a given C number consist of mixtures of normal and branched paraffins.

[e] All paraffin fractions contain trace amount (< 1 wt%) of corresponding olefins.

TABLE I.1.3

Product Composition from Depolymerization-Liquefaction of High Density Polyethylene as a Function of Hydrogen pressure[a,b]

H_2 pressure, psig	500	1500	1850	2000
Conversion, wt%	~100	~100	~100	~100
Product Distribution, wt%[c]:				
Gas (C_1-C_4)	16.73	17.86	19.42	17.30
Liquid	83.27	82.14	80.58	82.70
Solid	0.00	0.00	0.00	0.00
Gas Product Distribution, wt%[d,e]:				
C_1	1.03	0.90	0.85	0.52
C_2	2.95	2.85	3.37	2.76
C_3	5.69	6.21	7.01	6.11
C_4	7.06	7.90	8.19	7.92
Higher Product Distribution, wt%[d,e]:				
C_5H_{12}	3.88	7.53	4.30	4.41
C_6H_{14}	9.93	7.39	11.84	11.56
C_7H_{16}	7.86	8.93	8.93	9.29
C_8H_{18}	6.84	8.59	7.00	7.28
C_9H_{20}	6.84	8.64	7.25	7.02
$C_{10}H_{22}$	4.92	6.66	4.79	4.81
$C_{11}H_{24}$	7.44	5.53	7.69	7.26
$C_{12}H_{26}$	4.79	4.57	4.55	4.55
C_{13+}	30.77	24.30	24.22	26.52
Gasoline Range, wt%:				
C_5-C_{12}	52.50	57.83	56.35	56.18

[a] In each run was used 10.0 g of polymer and 0.10 g ZrO_2/SO_4^{2-} catalyst; reaction temperature, 450 °C; reaction time, 1.0 hr.
[b] Data are given by weight percentage based on the total product.
[c] Liquid and solids were separated by decantation and filtration in which the solid was rinsed with little hexane.
[d] All products of a given C number consist of mixtures of normal and branched paraffins.
[e] All paraffin fractions contain trace amount (< 1 wt%) of corresponding olefins.

TABLE I.1.4

Product Composition from Depolymerization-Liquefaction of Isotatic Polypropylene as a Function of Reaction Time[a,b]

Reaction Time, hr	0.5	1.0	2.0	3.0
Conversion, wt%	87.08	97.75	99.96	100
Product Distribution, wt%[c]:				
Gas (C_1-C_4)	5.84	7.67	11.12	14.09
Liquid	81.24	90.08	88.84	85.91
Solid	12.92	2.25	0.04	0.00
Gas Product Distribution, wt%[d,e]:				
C_1	0.14	0.24	0.48	0.73
C_2	0.71	1.10	2.09	3.65
C_3	1.99	2.69	4.19	4.78
C_4	3.00	3.64	4.36	4.93
Higher Product Distribution, wt%[d,e]:				
C_5H_{12}	4.74	5.50	5.85	5.90
C_6H_{14}	8.35	11.43	11.98	11.77
C_7H_{16}	6.81	8.60	8.73	8.43
C_8H_{18}	6.01	7.64	8.75	8.71
C_9H_{20}	10.60	13.11	13.26	12.62
$C_{10}H_{22}$	5.50	6.86	7.22	7.36
$C_{11}H_{24}$	5.73	6.72	6.75	6.50
$C_{12}H_{26}$	4.33	4.81	5.38	4.95
C_{13+}	42.09	27.66	20.92	19.67
Gasoline Range, wt%:				
C_5-C_{12}	52.07	64.67	67.92	66.24

[a] In each run was used 10.0 g of polymer and 0.10 g ZrO_2/SO_4^{2-} superacid catalyst; reaction temperature, 410 °C; H_2 initial pressure, 1500 psig.

[b] Data are given by weight percentage based on the total product.

[c] Liquid and solids were separated by decantation and filtration in which the solid was rinsed with little hexane.

[d] All products of a given C number consist of mixtures of branched paraffins.

[e] All paraffin fractions contain trace amount (< 1 wt%) of corresponding olefins.

TABLE I.1.5

Product Composition from Depolymerization-Liquefaction of Isotatic Polypropylene as a Function of Catalyst Type[a,b]

Catalyst Type	None	Fe_2O_3/SO_4^{2-}	ZrO_2/SO_4^{2-}	Al_2O_3/SO_4^{2-}
Conversion, wt%	97.77	99.81	97.75	99.98
Product Distribution, wt%[c]:				
Gas (C_1-C_4)	6.41	10.25	7.67	10.81
Liquid	91.36	89.56	90.08	89.17
Solid	2.23	0.19	2.25	0.02
Gas Product Distribution, wt%[e]:				
C_1	0.05	0.18	0.24	0.23
C_2	0.77	1.39	1.10	1.63
C_3	2.70	4.12	2.69	4.83
C_4	2.89	4.56	3.64	4.13
Higher Product Distribution, wt%[d,e]:				
C_5H_{12}	6.39	5.93	5.50	6.44
C_6H_{14}	10.37	14.48	11.43	13.24
C_7H_{16}	7.34	8.16	8.60	8.37
C_8H_{18}	6.16	7.15	7.64	7.37
C_9H_{20}	17.32	15.03	13.10	14.71
$C_{10}H_{22}$	5.50	5.80	6.86	6.92
$C_{11}H_{24}$	6.64	5.93	6.72	6.69
$C_{12}H_{26}$	4.37	3.92	4.81	4.48
C_{13+}	29.49	23.16	27.66	20.95
Gasoline Range, wt%:				
C_5-C_{12}	64.10	66.40	64.67	68.21

[a] In each run was used 10.0 g of polymer and 0.10 g of catalyst; reaction temperature, 410 °C; reaction time, 1.0 hr; H_2 initial pressure, 1500 psig.

[b] Data are given by weight percentage based on the total product.

[c] Liquid and solids were separated by decantation and filtration in which the solid was rinsed with little hexane.

[d] All products of a given C number consist of mixtures of branched paraffins.

[e] All paraffin fractions contain trace amount (< 1 wt%) of corresponding olefins.

TABLE I.1.6

Product Composition from Depolymerization-Liquefaction of Isotatic Polypropylene as a Function of Hydrogen pressure[a,b]

H_2 pressure, psig	15	500	1000	1500
Conversion, wt%	95.21	95.97	95.05	97.75
Product Distribution, wt%[c]:				
Gas (C_1-C_4)	9.65	7.63	7.74	7.67
Liquid	85.56	88.34	88.31	90.08
Solid	4.79	4.03	3.95	2.25
Gas Product Distribution, wt%[d,e]:				
C_1	0.32	0.29	0.21	0.24
C_2	1.60	1.05	1.00	1.10
C_3	3.88	2.80	2.55	2.69
C_4	3.85	3.49	3.98	3.64
Higher Product Distribution, wt%[d,e]:				
C_5H_{12}	4.90	5.34	5.22	5.50
C_6H_{14}	8.60	9.28	12.86	11.43
C_7H_{16}	7.88	8.02	9.70	8.60
C_8H_{18}	6.86	6.84	8.42	7.64
C_9H_{20}	11.70	12.09	13.26	13.10
$C_{10}H_{22}$	6.44	6.45	6.20	6.86
$C_{11}H_{24}$	6.30	6.44	4.80	6.72
$C_{12}H_{26}$	4.85	4.83	3.37	4.81
C_{13+}	32.82	33.08	28.43	27.66
Gasoline Range, wt%:				
C_5-C_{12}	57.53	59.29	62.83	64.67

[a] In each run was used 10.0 g of polymer and 0.10 g ZrO_2/SO_4^{2-} catalyst; reaction temperature, 410 °C; reaction time, 1.0 hr.
[b] Data are given by weight percentage based on the total product.
[c] Liquid and solids were separated by decantation and filtration in which the solid was rinsed with little hexane.
[d] All products of a given C number consist of mixtures of branched paraffins.
[e] All paraffin fractions contain trace amount (< 1 wt%) of corresponding olefins.

TASK I

Project I.2

COLIQUEFACTION OF COAL AND WASTE POLYMERS

Edward M. Eyring and Edward C. Orr
University of Utah

Introduction

In our recent work we have continued to investigate the optimum conditions for coprocessing waste rubber tires with coal and added catalyst. Samples were coprocessed at two different temperatures, and amounts were varied of waste tire rubber and Blind Canyon DECS-6 coal mixed with a molybdenum catalyst. In earlier experiments we had coprocessed powdered Blind Canyon DECS-17 coal and ground up rubber from a Michelin tire. At the end of the quarter (Oct. 31, 1994) we were concluding experiments with samples composed of Blind Canyon DECS-6 coal and ground waste rubber tire (sample # 5) obtained from the University of Utah Waste Material Bank. We had also started a study of the effect of a hydrogen atmosphere on the breakdown of tire rubber at elevated temperatures with no coal present.

Experimental

Blind Canyon (Utah) coal (DECS-6, -60 mesh) was obtained from the Penn State Coal Sample Bank and ground under nitrogen to -100 mesh. The ground waste rubber tire (-20 mesh) was obtained from the University of Utah Center for Microanalysis. The ground waste rubber tire was stored under air at ambient conditions. Samples were composed of 40% waste rubber tire and 60% Blind Canyon DECS-6 coal by weight. The catalyst precursor, ammonium tetrathiomolybdate (Aldrich), was used to make an aqueous solution of molybdenum. The Blind Canyon DECS-6 coal and waste rubber tire mixture was impregnated with Mo catalyst solution using the incipient wetness technique. The resulting mixture was 1% by weight ammonium tetrathiomolybdate. The resulting mixture was vacuum dried for 2 hours at 100° C. The dried mixture was placed in glass tubes that were stoppered

with glass wool. The glass tubes were placed in 27 cm^3 tubing bombs, purged with nitrogen, and pressurized to 1000 psig H_2 (cold). Tubing bombs were placed in a fluidized sandbath held at 350 ° C. The tubing bombs were shaken vertically at 160 rpm for various lengths of time and removed. The tubing bombs were allowed to cool overnight while under pressure. Samples were then removed and extracted with tetrahydrofuran (THF). The insoluble portion is referred to as ash/char. Products soluble in THF were isolated using a rotary evaporator and then dried two hours under vacuum at 100 ° C. The THF solubles were subsequently extracted with cyclohexane. The cyclohexane was removed with a rotary evaporator and the residue was dried under vacuum for two hours.

Results

The breakdown of the tire is interesting because of its possible importance as a coal dissolution solvent and hydrogen donor solvent. It is possible that the high content of aromatic molecules in tire oil and the breakdown of the styrene-butadiene will provide a useful coal solvent. To understand the products that arise from the breakdown of tire rubber under coprocessing conditions, tire samples were heated under hydrogen and nitrogen atmospheres with a molybdenum catalyst precursor to determine the effect of the hydrogen gas that is normally used in liquefaction. The first two columns of Table I.2.1 show the conversion for the waste rubber tire and catalyst mixtures heated under a hydrogen atmosphere, and under a nitrogen atmosphere, respectively. The oil yields (cyclohexane solubles) indicate that the THF soluble material is entirely cyclohexane soluble. There are no measured asphaltenes or preasphaltenes from the breakdown of the waste rubber tires under either atmosphere. The conversion for reactions under hydrogen and nitrogen are comparable suggesting that the hydrogen in the presence of the molybdenum catalyst has little or no effect on the reaction pathways of the tire conversion to cyclohexane soluble oil at 350° C. The elemental analyses of the cyclohexane soluble oils also indicate small difference in H, C, N, or S content for either a hydrogen or a nitrogen atmosphere (Table I.2.2). Table I.2.2 indicates that the hydrogen content of the derived cyclohexane oils is approximately 10%. This is similar to what Farcasiu and

Smith[1] obtained for the quality of oil products from tire and coal mixtures (Farcasiu and Smith defined oils as hexane solubles). These results indicate that the composition of the atmosphere is not an important factor in the breakdown of the tire rubber into products that are suitable as a coprocessing solvent for producing transportation liquids from coal. The yields of oils are similar and the composition of the oils appears to be the same. Recently, Badger and coworkers[2] reported that pre-hydrogenated tire oils (hydrogenation took place under a hydrogen atmosphere and in the presence of CoMo catalyst) are effective for dissolution of coal. There may be some subtle differences between the hydrogen derived tire oils and the nitrogen derived tire oils. Thus we are beginning to analyze oils produced under a nitrogen and a hydrogen atmosphere with NMR to determine the ratio of aromatic to aliphatic species present in each type of oil.

It is noteworthy that the oil products from tires processed under both a hydrogen and a nitrogen atmosphere are of the same quality as are oils derived from coal/tire/molybdenum mixtures coprocessed under hydrogen as shown in Table I.2.2. We are in the process of coprocessing a coal/tire/molybdenum sample under nitrogen to make a comparison.

Figure I.2.1 shows the breakdown of products and the total conversion for various mixtures of tire rubber and Blind Canyon DECS-6 coal that have been coprocessed under hydrogen for 1 hour. Total conversions reported here are reproducible within $\pm$ 2%. The graph indicates that as the rubber tire content of the mixture increases, so also does the oil yield increase with gas yields increasing only slightly. Accordingly, as the tire rubber percentage decreases and the coal becomes the dominant reactant, the percentage of asphaltenes increases, oil yields decrease, and gas yields decrease. Since tire rubber breaks down into THF soluble components quite readily, the increase of gas and oil products and the decrease in preasphaltenes and asphaltenes with increasing tire rubber content is not surprising. The straight diagonal line is drawn to indicate the typical conversion expected for a tire and coal sample calculated from samples consisting only of tire rubber and of only coal. The total conversion points above the solid line show that there is some synergism for sample composition between 10% tire rubber and 30% tire rubber by weight. It

appears from the preasphaltene-asphaltene curve in Fig. I.2.1 that his may be related to an increase in production of asphaltenes and preasphaltenes.

Figure I.2.2 presents the results of further work with various mixes of tire rubber and coal with the same molybdenum catalyst but at a much higher temperature of 430°C. The most significant enhancement in conversion occurs between 50% and 70% tire rubber by weight in the sample. Again the line indicates a theoretical value for the total conversion based on samples consisting of only coal liquefied at 430°C and only tire at 430 °C assuming no interaction of the two components takes place that would inhibit or enhance total conversion. It is interesting to note that the synergism that takes place at 350 °C does not seem to occur at the same tire/coal composition at which synergism is observed for samples processed at 430 °C. The synergistic effect appears with samples of higher tire rubber content at 430 °C.

Currently, oils from the 350 °C and 430 °C runs are being analyzed for overall zinc content. It is important to know how the zinc content varies with overall conversion in order to determine if one mix of tire rubber and coal is optimum for minimizing the amount of zinc found in the oil. As we have shown in our previous work, some zinc may be scavenged by the coal particles.[3]

While processing samples at different temperatures we have noted a difference in the amount of carbon black found in the product oils. The carbon black is to be unsuited to hydrotreatment, but during the extraction procedure utilizing THF, some carbon black passes through the cellulose filters into the extraction mixture. The carbon black tends to stick to the solvent extraction apparatus. We have further noted that samples coprocessed at 430 °C tend to dirty the glassware less. In order to calculate conversion to products accurately the carbon black is filtered out. We then observed for some of these samples coprocessed at higher temperatures and made up of more than 50% tire rubber that less carbon black was being filtered out. Figure 3 compares the amount of carbon black that was filtered out for samples coprocessed at 350°C and 430 °C. The percentage of carbon black filtered out of the THF solubles is plotted versus the composition of the tire/coal mixture. At the lower temperatures and at a higher tire rubber percentage a large amount of the carbon

black passes through the cellulose filter. This result may only be related to conditions of coprocessing with a tubing bomb and the manner in which we extract our samples, but the result may be of some use in decreasing the amount of carbon black that becomes mixed into the oil products in a commercial operation.

Summary

The most interesting observation arising from our recent work is that a tire rubber/coal synergism producing increased yields of oil and gas occurs at a higher rubber content when coprocessing is carried out at 430 °C than when the reaction is run at 350 °C.

References

1. Farcasiu, M.; Smith, C.,**1992**, Prepr. Pap. Am. Chem. Soc., Div. Fuel Chem., 37 (1), 472.

2. Badger, M. W.; Harrison, G., Ross, A. B., **1994**, Prepr. Pap. Am. Chem. Soc., Div. of Petroleum Chem., 39 (3), 438.

3. Orr, E. C.; Tuntawiroon, W.; Anderson, L. L.; Eyring, E. M., **1994**, Prepr. Pap. Am. Soc., Div. Fuel Chem., 39 (4), 1065.

Table I.2.1

Conversion Results for Organic Tire Components at 350 °C

	Tire/Mo/N_2	Tire/Mo/H_2
Pre Asphaltenes and Asph.	0.0	0.0
Oil	88.0	90.1
Gas	10.0	8.0
Total Conversion	98.0	98.1

Table I.2.2

Elemental Analyses of Oils (Cyclohexane) Derived from Various Mixtures

	Tire/Mo/H_2	Tire/Mo/N_2	Tire/Coal/Mo/H_2
Carbon	82.8	82.7	81.6
Hydrogen	10.9	10.8	10.5
Nitrogen	0.4	0.4	0.4
Sulfur	0.9	.09	.08

Figure 1

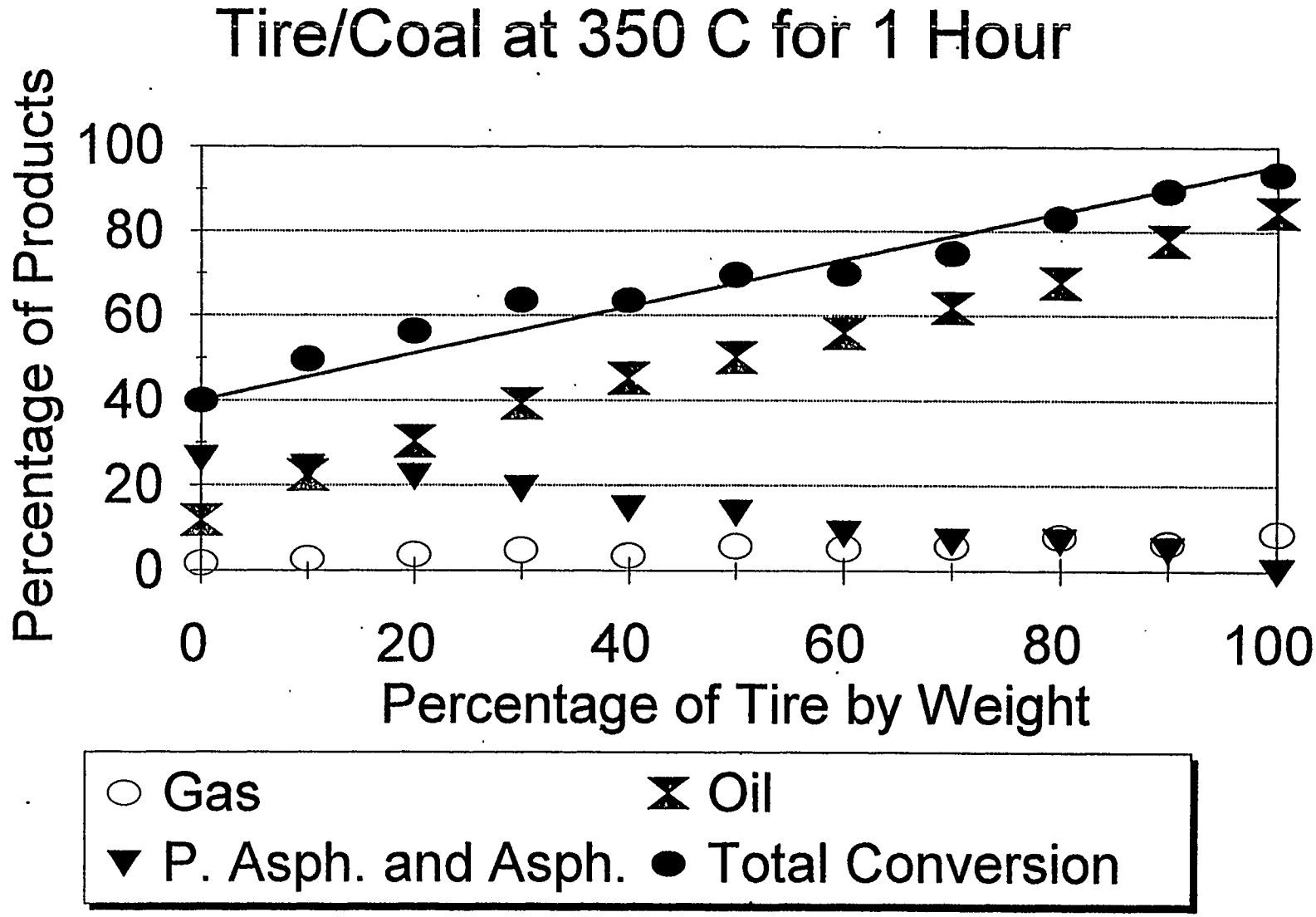

Figure I.2.1.

Figure 2

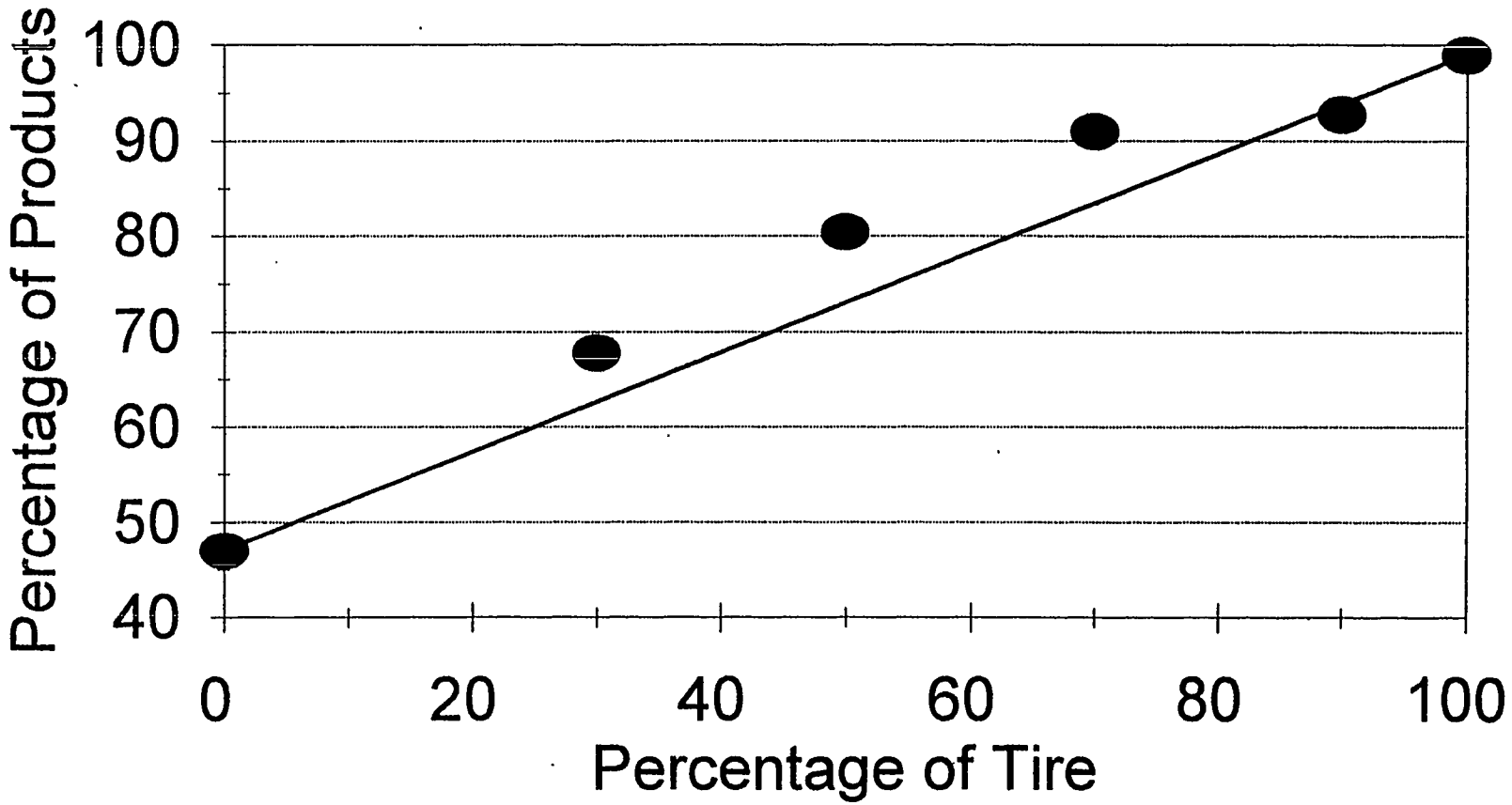

Figure I.2.2.

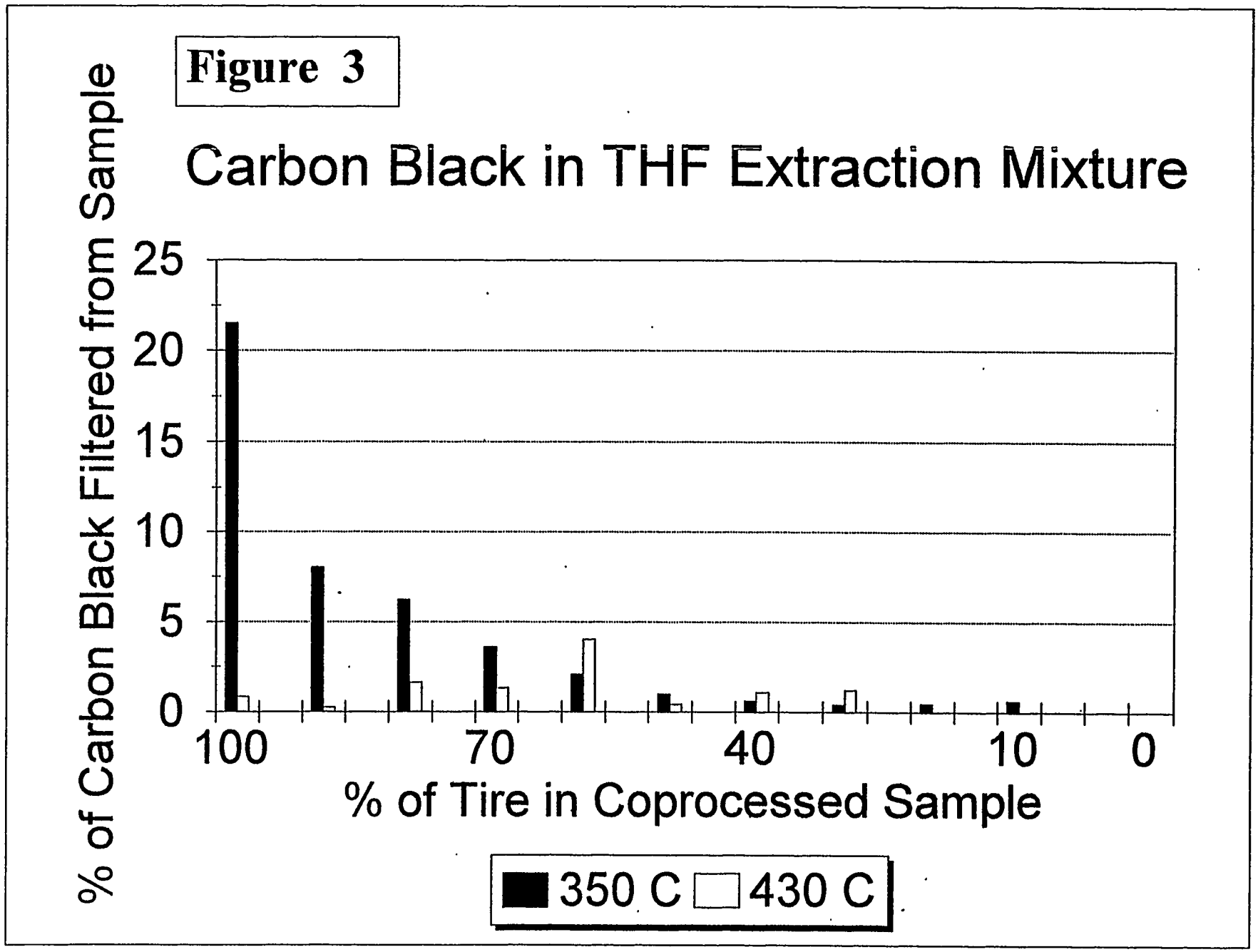
Figure 3
Carbon Black in THF Extraction Mixture
% of Carbon Black Filtered from Sample
25
20
15
10
5
0
100
70
40
10
0
% of Tire in Coprocessed Sample
350 C
430 C

Figure I.2.3.

TASK I

Project I.3

USE OF MIXED PYRRHOTITE/PYRITE CATALYSTS FOR CO-LIQUEFACTION OF COAL AND WASTE RUBBER TIRES

Dady B. Dadyburjor, John W. Zondlo and Ramesh K. Sharma
Department of Chemical Engineering
West Virginia University

Work this quarter continued on a systematic investigation of the liquefaction of coal and tire rubber. The coal used is DECS-6 (-60 mesh), which is a high-volatile A bituminous coal from the Blind Canyon seam in Utah, and was received from the Pennsylvania State University Coal Bank (PSCB). Three different tire materials have been tested. The first sample was prepared from a Goodyear Invicta tire, recycled in-house at WVU (Tire-1). Another sample, obtained from the University of Utah, was a recycled tire ground to -30 mesh (Tire-2). The third sample consists of tire buffings (Tire-3), also obtained from the University of Utah. Table I shows the proximate and ultimate analyses of the tire materials (performed by Galbraith Laboratories) and DECS-6 coal (from PSCB). As seen in the table, the contents of volatile matter and ash in Tire-2 are each about 4 percentage points higher than those in Tire-1. The oxygen content of Tire-2, as indicated by the elemental analysis (by difference), is also about 4 percentage points higher than in Tire-1. The results suggest differences in the composition of the two tire samples. On the other hand, the differences between the compositions of Tire-3 and Tire-1 appear to be small.

Most of our work with Tire-1 sample has been completed and presented earlier [1]. Work this quarter was mainly focused on the Tire-2 sample, which is expected to be a common sample for all consortium members. The effect of time, temperature and hydrogen pressure on the product slate from the uncatalyzed liquefaction of coal and Tire-2 is being studied systematically using a statistical experimental design. Work has also begun on the use of catalysts in the co-liquefaction runs. The catalysts

are pyrrhotite/pyrite mixtures, obtained from the disproportionation of ferric sulfide.

Finally, along with other laboratories in the consortium, we carried out preliminary experiments on coal+plastic and coal+rubber co-liquefaction prior to HRI's PDU run.

For all the data reported below, total conversion was based on the measurement of tetrahydrofuran (THF)-insoluble matter. The asphaltene yield was found from the measurement of hexane-insoluble matter. The oil+gas fraction was found by difference. For some runs, the gas fraction was measured separately, using gas chromatography as described in earlier reports.

I. Uncatalyzed Liquefaction

Previously, we have reported that the organic matter in the tire (69 wt% in Tire-2) is completely liquefied at 400°C in 30 min [2]. The conversion is strongly dependent on temperature and decreases from 69 wt% at 400°C to 54 wt% at 350°C. The oil+gas fraction is the major product and the yield of asphaltenes from tire is negligible.

The co-liquefaction of tire and coal showed a strong synergistic effect of tire on the coal conversion. The conversion of coal increased steadily with increase in the tire/coal ratio at 350°C and 375°C. However, at 400°C, there appeared to be a maximum in coal conversion at a tire/coal ratio of around 3. The oil yields were greatest at a ratio of around 2, and at higher ratios, the gas yield increased. Further details of the results are presented in Ref. [2].

Statistical analysis of the data obtained from the liquefaction of coal and tire is still in progress. Figure 1 shows the effect of hydrogen pressure on conversion and product slate from separate liquefaction of coal and Tire-2 at 400°C for a run time of 30 min. The conversion and oil+gas yield from the tire appear to be independent of hydrogen pressure. However, the conversion of coal increases from 28 wt% in the absence of hydrogen to 37 wt% at a hydrogen pressure of 1500 psi (cold). The yields of both asphaltenes and oil+gas fraction from coal also increase slightly with an increase in the hydrogen pressure. The results indicate that the fraction of hydrogen which is consumed in the stabilization of asphaltenic free radicals is higher than that used for the stabilization of free radicals in the oil range.

Figure 2 shows the effect of hydrogen pressure on coal conversion when it is liquefied with Tire-2 at 400°C. The tire/coal ratio in these co-liquefaction runs was unity. It should be noted that the results in the figure are computed on coal-alone basis by subtracting the weighted contribution of the tire from the overall results. As indicated by the figure, the coal conversion increases with hydrogen pressure. However, the increase is higher in this case compared to that observed with coal in Figure 1 (in the absence of tire). This indicates that the synergistic effect of tire increases with hydrogen pressures. The yields of both the asphaltenes and oil+gas fraction also increase with hydrogen pressure (Figure 2). Again, the increase is higher compared to those in the coal alone runs. Interestingly, the yields of asphaltenes in the co-liquefaction runs are nearly double of those in the coal-alone runs suggesting that the major role of tire is to stabilize the asphaltenes radicals. Similar observations were made earlier when the coal was liquefied with Tire-1 [1]

II. Catalytic Liquefaction

The catalytic runs were carried out with catalysts based on iron sulfide, Fe_2S_3. Work with Tire-1 and Coal has indicated that highly active catalysts are obtained when the ferric sulfide is impregnated *in-situ* on the coal. According to this method, the coal is first mixed with a dilute aqueous solution of Na_2S and agitated vigorously before adding $FeCl_3$ solution. The suspension containing coal and the catalyst is filtered, washed and dried in N_2 under vacuum. A catalyst loading of 1.67 wt% based on dry, ash-free coal was used.

Figure 3 shows the results from the catalytic runs at 400°C. The catalyst was dried at 85-92°C for 24h in vacuum under N_2. The tire/coal ratio in these runs varies from 0 (coal only) to 4. For comparison, the results from the uncatalyzed runs are also shown in the figure. In the absence of catalyst, both the coal conversion and the asphaltene yield increase with tire/coal ratio as mentioned earlier. With the use of catalyst, the conversion of coal increases from 35 wt% (uncatalyzed) to around 70 wt% in the absence of tire. The yield of asphaltenes increases similarly but the increase in the oil+gas fraction is small. However, when the catalytic liquefaction is performed in the presence of tire (Tire-2), the coal conversion decreases sharply as the tire/coal

ratio is increased. The yields of asphaltenes and oil+gas fraction decrease similarly. Earlier, in the case of Tire-1, it was observed that the conversion of coal in the catalytic runs increased when tire was added to the coal at a tire/coal ratio of 1. The addition of Tire-2 to the coal in the catalytic runs did not show the similar increase. Thus it seems that Tire-1 and Tire-2 behave differently in the presence of the catalyst. The presence of Tire-2 may be poisoning or somehow blocking the catalyst in these runs. This major difference may be due to the small differences in the composition of the two tire samples.

Finally, in this quarter, along with other laboratories in the consortium, we carried out preliminary experiments on coal+plastic co-liquefaction prior to HRI's PDU run under consistent conditions using Wyodak Black Thunder coal and different plastic materials. Experiments were also done on coal+tire co-liquefaction prior to HRI's PDU run with those co-feeds. Again conditions were consistent with those of HRI: 430°C, 1h, 800 psi(cold) H_2, solvent/solid (coal+rubber)/catalyst = 4.7/2/2. Conversions (from cyclohexane solubility, DAF coal+rubber basis) were 75% for R_{TC}= 1 and 73% for R_{TC} = 0.5. The gas yield was 12% in both cases. The H_2S content of the gas (on a hydrogen-free basis) was 11 and 12%, respectively.

III. FUTURE DIRECTIONS

In the next quarter, the liquefaction of other coals, namely, Wyodak Black Thunder and Illinois No. 6 will be studied. Also, runs will be made in which these coals will be co-liquefied with Tire-2 sample both with and without catalyst.

IV. REFERENCES

1. Liu, Z., Zondlo, J.W., and Dadyburjor, D.B., Energy & Fuels 8, 607 (1994).

2. Dadyburjor, D., Liu, Z., Sharma, R.K., and Zondlo, J.W., Abstracts, 8th Ann. Tech. Meeting, Consortium for Fossil Fuel Liquefaction Science, Snowbird, UT (1994).

Table I

Proximate and Ultimate Analyses of Coal and Tires Used
Tire-1: Ground Goodyear Invicta tire from WVU sample
Tire-2: 30 mesh recycled tire from Utah sample bank
Tire-3: 80 mesh tire buffings from Utah sample bank

Sample	H_2O %	ASH % dry	VOLATILE MATTER, %daf	FIXED CARBON, %daf	C %	H %	N %	S %
Tire-1	0.3	4.7	67.1	32.9	82.29	7.39	<0.5	1.6
Tire-2	0.4	8.1	71.0	29.0	79.65	7.45	<0.5	1.7
Tire-3	0.5	7.3	67.1	32.9	81.82	7.32	<0.5	1.4
DECS-6	1.8	6.3	49	51	81.9	6.3	1.5	0.9

daf = dry, ash-free basis

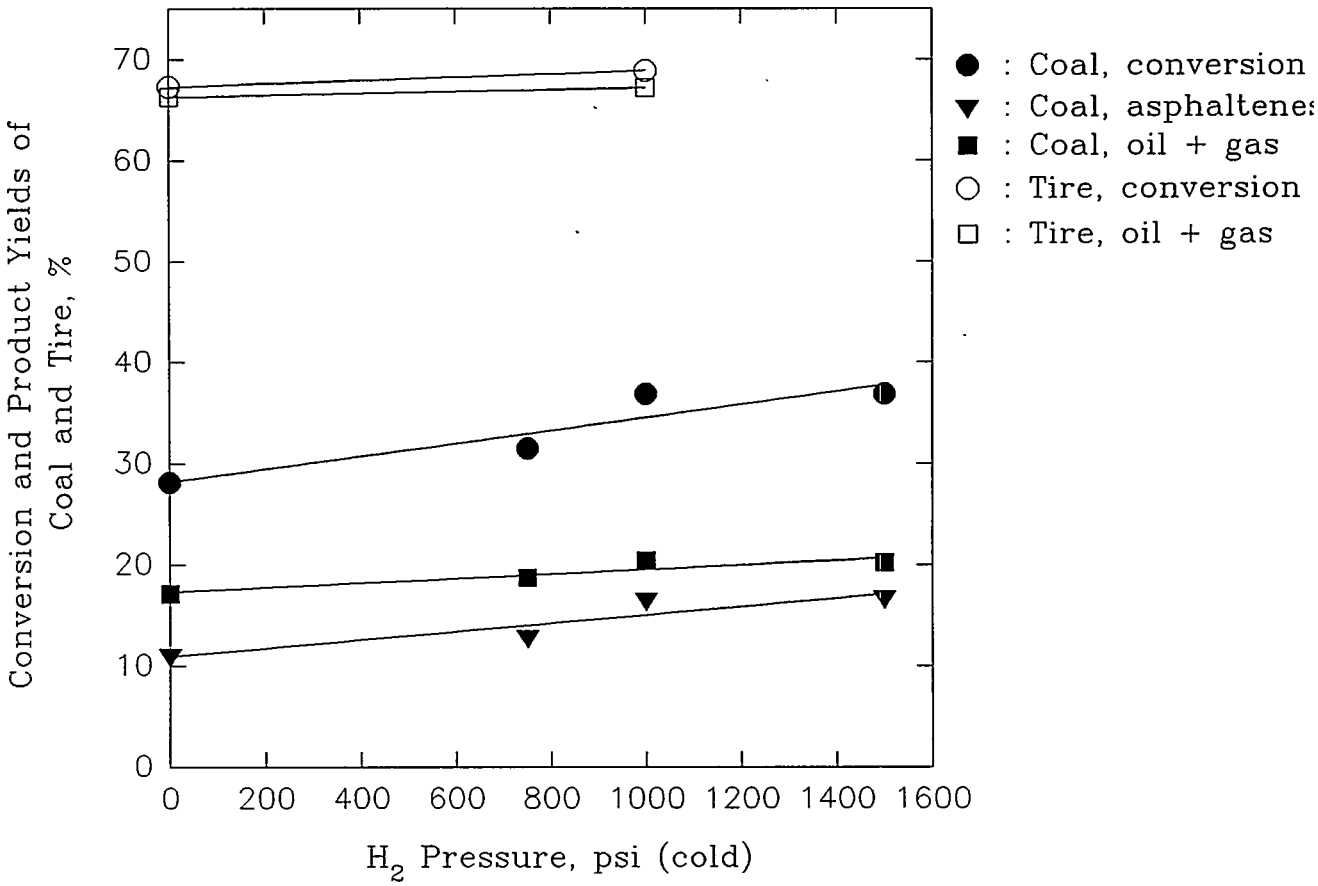

Figure 1. Effect of H_2 pressure on conversion and yields of coal–alone and tire–alone. Conditions: 400°C, 30 min. Tire–2 and DECS–6 coal were used.

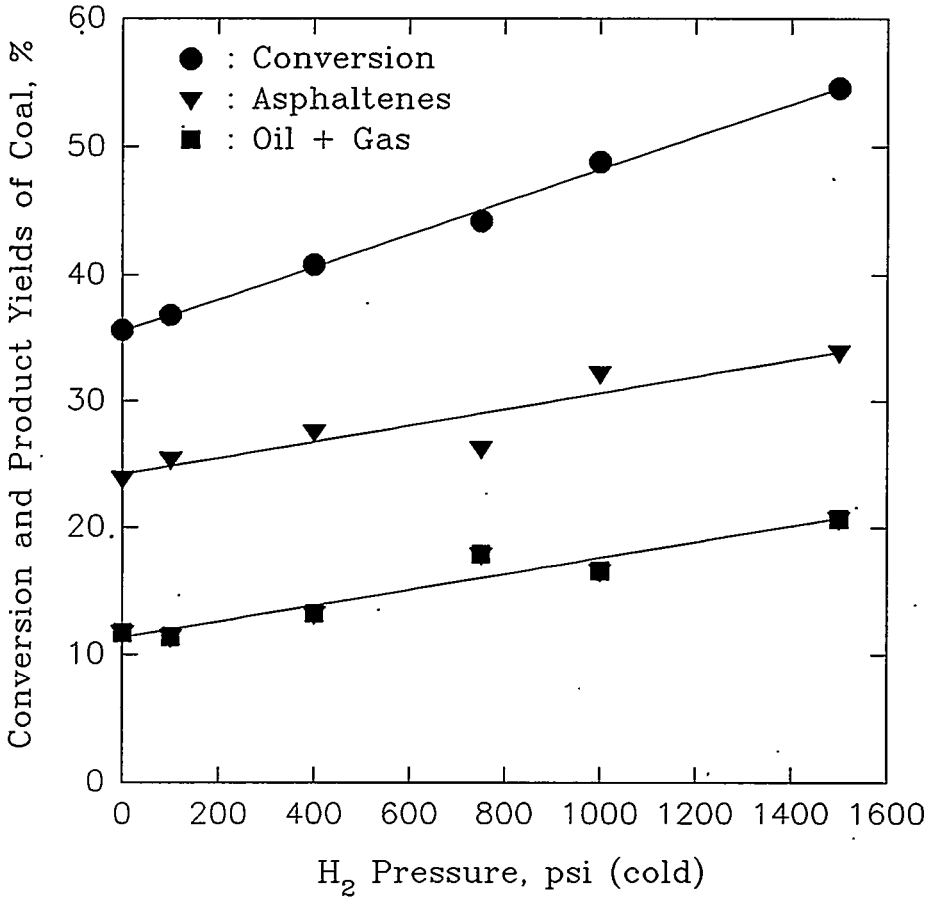

Figure 2. Effect of H_2 pressure on conversion and yields of coal in a coal/tire mixture. Conditions: 400°C, 30 min, tire/coal =1. Tire-2 and DECS-6 were used.

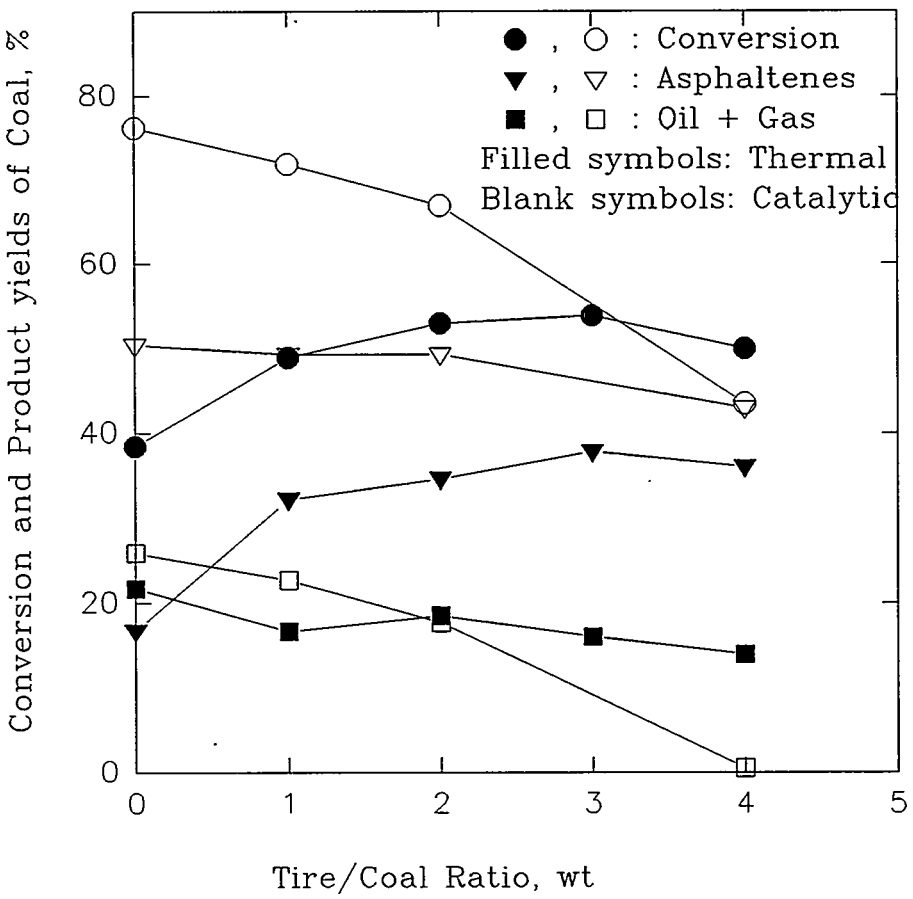

Figure 3. Conversion and yields of coal in a coal/tire mixture, as functions of tire/coal ratio. Conditions: 400°C, 1000 psi H_2 (cold), 30 min. Tire-2 and DECS-6 were used. The catalyst loadiung was 1.67 wt%.

TASK I

Project I.4

COPROCESSING COAL WITH WASTE OILS, PLASTICS, AND OTHER MATERIALS

A.R. Tarrer
Auburn University

Introduction

Research continued this quarter into the effects of coprocessing coal with waste plastic. For this phase of the work, we obtained a quantity of pyrolyzed plastic oil. Initial investigation showed that the response to coal conversion/product selectivity was high and comparable to that of prehydrocracked plastic and waste oil studied earlier. The best results, however, were obtained when using a mixture of polystyrene and waste oil with prehydrocracking.

Kinetic studies of coprocessing coal with waste grease and waste oil were also done this quarter. These results validated the improvements in coal conversion and selectivity when coprocessing with the grease. However, no one reaction pathway was observed by which the grease appears to enhance reaction rates; instead, all reaction pathways appeared to be enhanced.

To date, due to experimental limitations, we have not been able to evaluate the relative effect of premelting the plastics and then mixing with coal prior to reaction. The effects we are observing due to prehydrocracking may prove to be a mixing phenomena; regardless, prehydrocracking does render the waste oils, greases and plastics easier to handle and to transport.

Coprocessing With Waste Plastic

Studies have previously been conducted using coal, polystyrene and waste oil in differing ratios and under various prehydrocracking conditions. Our study this quarter involved a liquid obtained from a commercial plastic pyrolyzing unit (CPPU).

A DECS 6 coal was coprocessed with the pyrolyzed plastic oil (PPO) obtained from the CPPU and also in combination with a waste oil from the Auburn waste oil sample bank. Even though coprocessing the coal with the PPO resulted in better

conversion and selectivity than coprocessing with waste oil, the best results were obtained when using prehydrocracked virgin polystyrene oil. The results are summarized in Table 1.

Table 1
RESPONSE OF COAL CONVERSION/PRODUCT SELECTIVITY TO ADDITION OF PYROLYZED PLASTIC OIL, POLYSTYRENE & WASTE OIL

Solvent	Hexane Conversion (%)	Total Conversion (%)	Selectivity (%)
Waste Oil	43	73	59
Prehydrocracked Waste Oil	60	86	70
Prehydrocracked Polystyrene	63	97	65
Pyrolyzed Plastic Oil	64	91	70
PPO[1]/Waste Oil 1:1	56	81	69
Prehydrocracked PS[2]/Waste Oil 1:1	73	100	73

Reaction conditions: 2.5g DECS 6 coal, 10g solvent, 0.25g Fe_2O_3, 425 °C, 1250 psig H_2, 1 hour.
[1]Pyrolyzed Plastic Oil
[2]Polystyrene

The pyrolyzed plastic oil was obtained from Conrad Industries in Chehalis, Washington. The oil was filtered before using as it contained about 10% tar. It was assumed that the oil resulted from the pyrolysis of several types of plastic and is therefore representative of the pyrolysate from a typical waste plastic stream.

The oil will be analyzed by proton NMR for aromatic content and compared with that of waste oil.

Kinetic Model Development

Kinetic studies of coprocessing provides a better understanding of the process as a disposal alternative. In this study, waste grease and waste oil were taken as the waste organic materials.

Coprocessing reactions were carried out with DECS 6 coal in a tubing bomb microreactor at temperatures of 375-425 °C and a hydrogen pressure of 1250 psig cold

for 15-90 minutes. Waste grease was obtained from Texaco Lubricants Company and waste oil from the Auburn waste oil sample bank. Reactions were carried out with various mixtures of coal, waste oil and waste grease. Total conversion, conversion to asphaltenes, preasphaltenes and oils were monitored.

Mechanism Assumed:

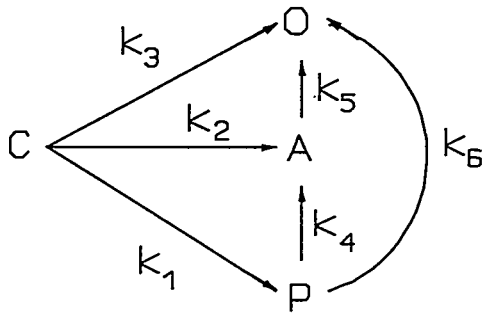

where, C = unreacted coal O = oil
A = asphaltenes p = preasphaltenes

Assumptions:

The following assumptions were made in the kinetic model development:

1. All the reactions are irreversible.
2. All the reactions are pseudo first order with respect to the mass of the reacting species.
3. There are no mass transfer limitations.

Experiments were conducted at three different temperatures (375 °C, 400 °C and 425 °C) in order to evaluate the kinetic rate parameters. Experiments were also conducted with and without waste grease. Figures 1 and 2 show the model predictions along with the experimental data used for parameter estimation. All the reactions were carried out with 10% coal loading and 1250 psig cold hydrogen pressure. In order to verify the validity of the model, experiments were done in temperature ranges other than that used for parameter estimation.

From Figures 3 and 4, we find that the model predictions are good even in the

other temperature ranges. The model predictions are within ± 3%. The kinetic rate constants for both cases (with and without grease) were evaluated for all the reactions involved in coal liquefaction. They are listed in Table 2. All of the rate constants for the case with grease are higher than in the case without grease. This explains the occurrence of higher conversion of coal when grease is present in the system. The higher conversion obtained with waste grease may be due to its higher aromatic and metals contents (particularly Fe and Mo). These metals may act as catalysts for coal liquefaction. The rate constant k_3, which indicates the rate of conversion of coal directly to oil, increases at a much faster rate compared to the rate constants for the other reactions, thus indicating higher conversion of coal and higher selectivity. The kinetic rate parameters, namely activation energy and frequency factor, were obtained at three different temperatures for the various reactions involved in coal liquefaction. The values of these parameters are listed in Table 3. From the table we see that the activation energies for the coal/waste oil/waste grease system are lower than in the coal/waste oil system. This kinetically justifies the higher conversion we obtain with waste grease in the system.

Table 2
KINETIC RATE PARAMETERS FOR THE DISSOLUTION OF COAL, FORMATION OF OILS, PREASPHALTENES AND ASPHALTENES

	Coal+Waste Oil		**Coal+Waste Oil+Waste Grease**	
	A 1/min	E cal/mole	A 1/min	E cal/mole
k_1	0.287	4885	5.97	8644
k_2	878	16387	876	15957
k_3	960683	24990	491	14718
k_4	0.021	2222	0.021	2184
k_5	0.23	2897	0.246	2923
k_6	511	16566	512	16184

Table 3 RATE CONSTANTS FOR THE FORMATION OF OILS, PREASPHALTENES AND ASPHALTENES			
Coal+Waste Oil			
Rate Constants (min^{-1})	375 °C	400 °C	425 °C
k_1	0.00625	0.00722	0.00822
k_2	0.00240	0.00356	0.00603
k_3	0.00433	0.00673	0.01010
k_4	0.00366	0.00380	0.00415
k_5	0.02387	0.02550	0.02810
k_6	0.00129	0.00159	0.00330
Coal+Waste Oil+Waste Grease			
Rate Constants (min^{-1})	375 °C	400 °C	425 °C
k_1	0.00695	0.00852	0.01130
k_2	0.00331	0.00505	0.00810
k_3	0.00490	0.00719	0.01120
k_4	0.00379	0.00382	0.00429
k_5	0.02542	0.02590	0.03000
k_6	0.00165	0.00240	0.00410

Reaction Kinetics/Mechanisms of Coal Intermediates

Small amounts of asphaltene fractions of coal were collected from various microreactor runs (avg. conversion = 70%, avg. selectivity = 50%). These were further subjected to liquefaction conditions at relatively lower temperatures in order to obtain information on the rate of conversion of asphaltenes to oils and to coke. Some preliminary results are shown in Table 4.

Table 4						
Run No.	Temp. (°C)	Time (min)	Total Conversion (%)	Conversion		Selectivity (%)
				To Oils (%)	To Coke Residue (%)	
1	303	15	28	19	9	67
2	362	20	49	46	4	95

Reaction conditions: 1g asphaltenes, 6g waste oil, 0.15g Fe_2O_3, 1250 psig H_2.

Additional runs will be done where asphaltenes from a single batch run will be subjected to liquefaction conditions at different temperatures and times to obtain the general reaction mechanisms for upgrading asphaltenes to oils.

Figure 1: Comparison of kinetic model with experimental data

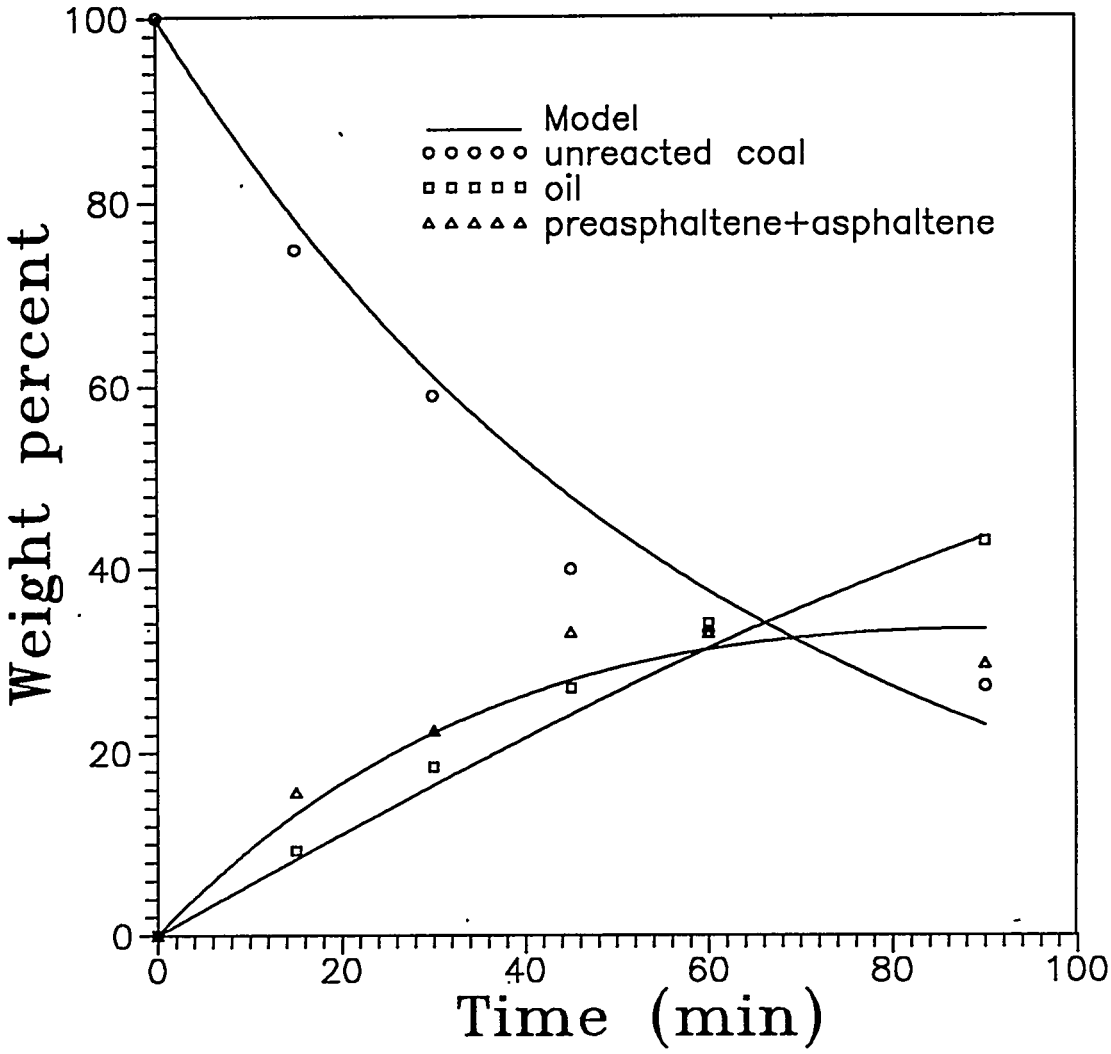

Reaction conditions: DECS 6 coal = 10 wt % Waste Oil = 90 wt %
Temperature = 400 C H2 Pressure = 1250 psig
Time = 60 min

Figure 2: Comparison of kinetic model with experimental data

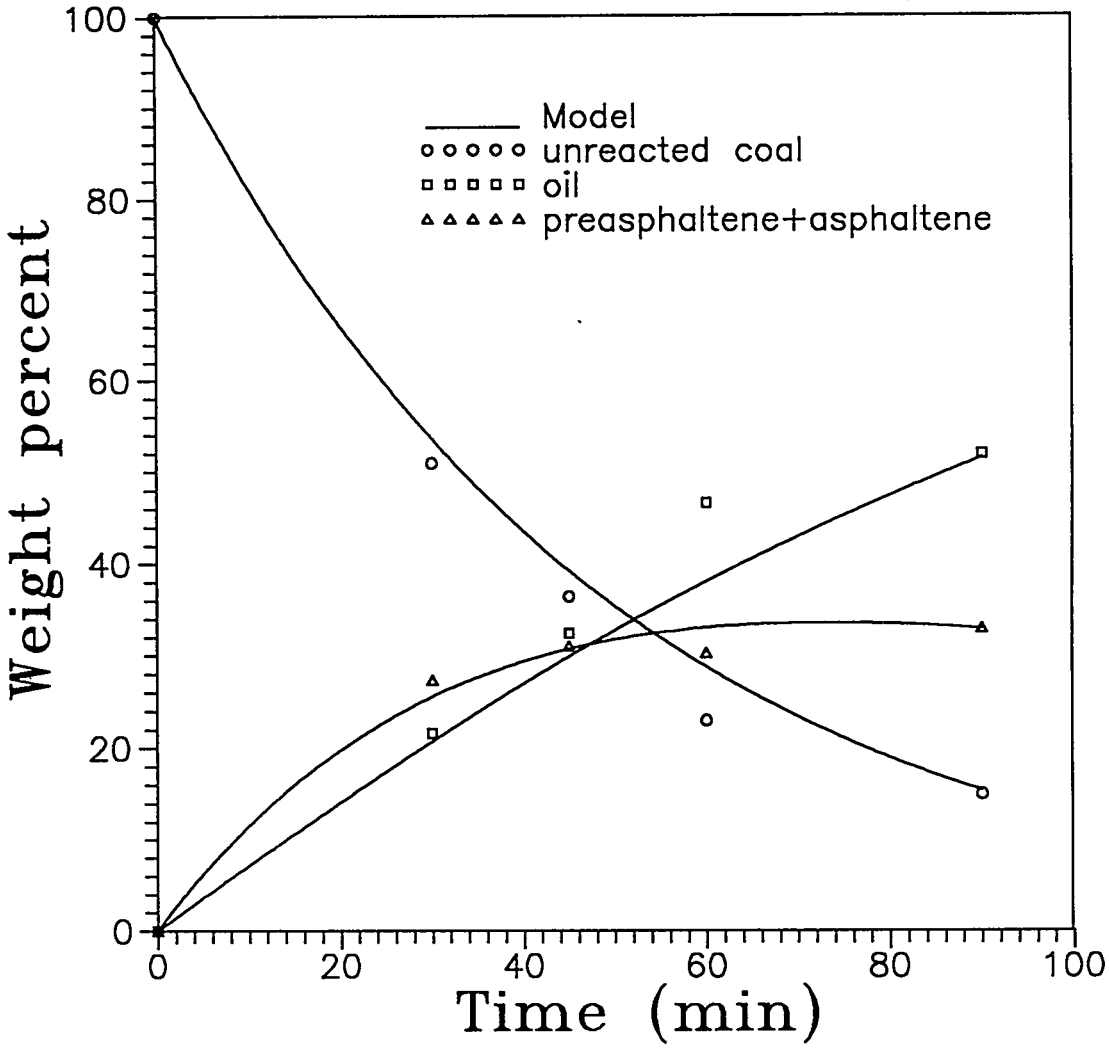

Reaction conditions: DECS 6 coal = 10 wt %
Temperature = 400 C
H2 Pressure = 1250 psig
Waste Oil = 45 wt %
Waste Grease = 45 wt %
Time = 60 min

MODEL VALIDATION

Figure 3: Comparison of kinetic model with experimental data

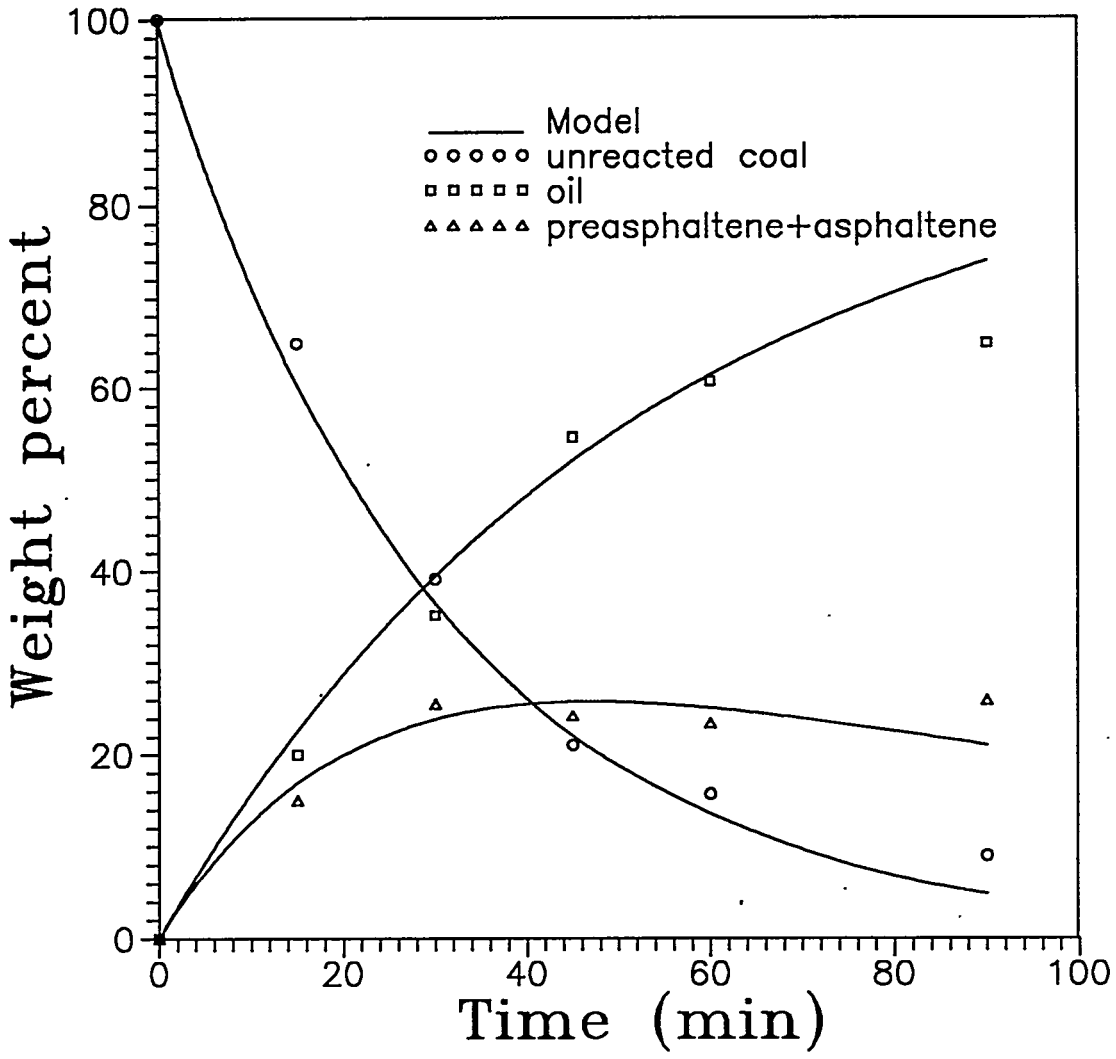

Reaction conditions: DECS 6 coal = 10 wt %
Temperature = 435 C
H2 Pressure = 1250 psig
Waste Oil = 45 wt %
Waste Grease = 45 wt %
Time = 60 min

MODEL VALIDATION

Figure 4: Comparison of kinetic model with experimental data

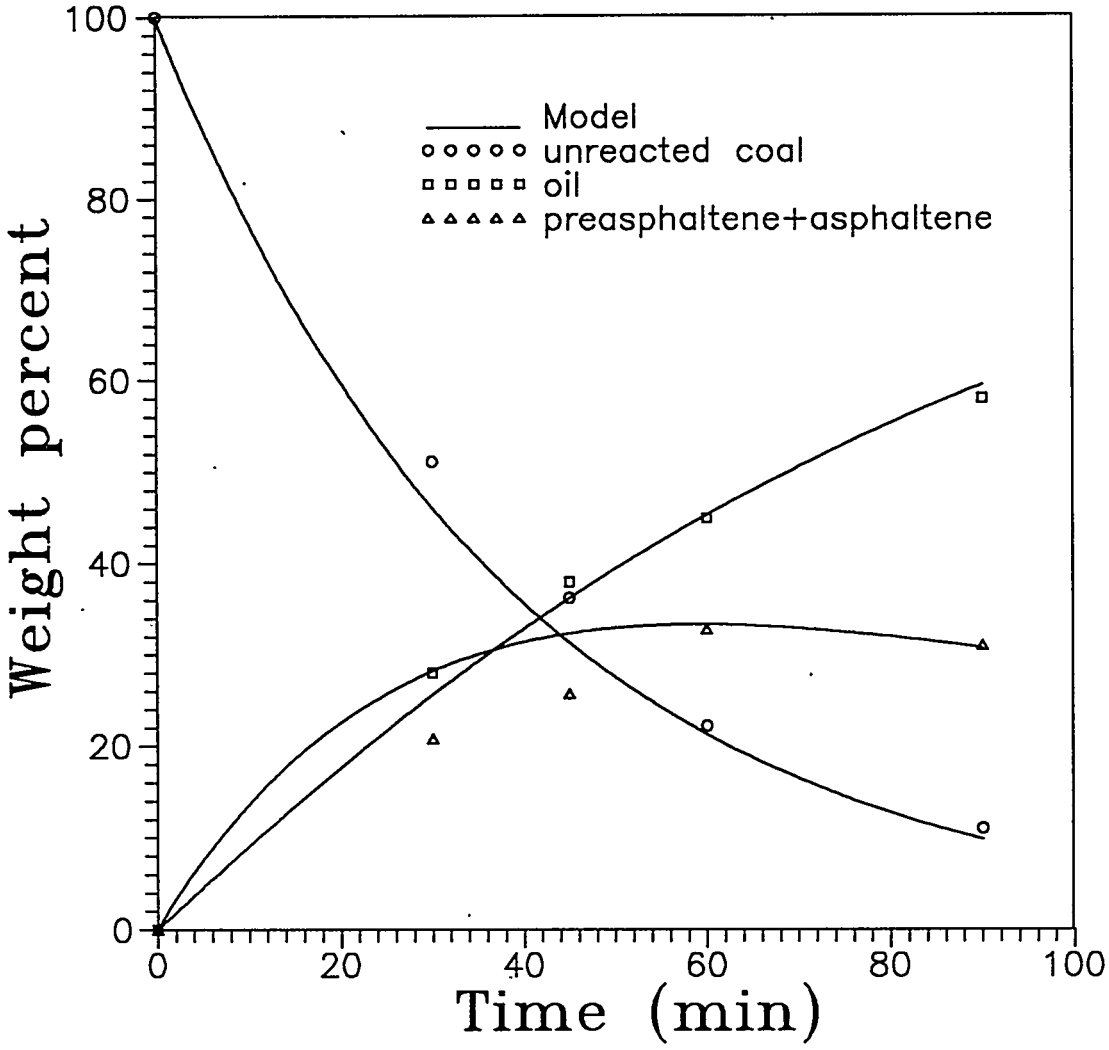

Reaction conditions: DECS 6 coal = 10 wt % Waste Oil = 90 wt %
Temperature = 410 C H2 Pressure = 1250 psig
Time = 60 min.

TASK I

Project I.5

COLIQUEFACTION OF COAL WITH LIGNOCELLULOSIC AND POLYMERIC WASTES: LIQUID FUELS FROM COAL WHILE CLEANING THE ENVIRONMENT

Irving Wender, John W. Tierney and Gerald D. Holder
Chemical and Petroleum Engineering Department
University of Pittsburgh

Introduction

Coal is usually liquefied in the presence of hydrogen, donor solvent and a hydrogenation catalyst (Route A). An alternate process uses carbon monoxide, water and an alkali catalyst (Route B: Costeam process)[1,2]. The Costeam process can be operated using synthesis gas obtained from natural gas, coal or biomass. In the presence of an alkali, hydrogen is generated by the water gas shift reaction. Some of the hydrogen produced may be incorporated in the products and the remainder could be used in upgrading the liquid fuels. Lignocellulosic wastes and plastic wastes constitute a major fraction of the municipal solid waste stream. It has been shown that lignocellulosic wastes can be converted to oils in the same way as coal, but at less severe conditions[3]. We have evidence for an enhancing effect when lignocellulosic wastes are coprocessed with coal[4]. Exploratory work on the feasibility of conversion of plastic wastes to oil using Routes A and B indicates that plastics can be converted essentially in the same way as coal or lignocellulosic wastes. Plastics used in packaging are sometimes associated with cellulosic or lignocellulosic material.

Accomplished Experimental Work

All the CO/H_2O (Route B) liquefaction experiments were carried in a 300 ml stirred autoclave. Eight grams of reactant were charged with 24 g of water and 1.02 g of Na_2CO_3. The reactor was pressurized with CO at 575 psi and then heated to 400°C in one hour and maintained at this temperature for an hour (reaction pressure

in the range of 4000 psi). The reaction products are extracted with tetrahydrofuran (THF) for 2 hours. After removing the THF in a rotary evaporator, an extraction with pentane is carried out. Oils are the pentane-soluble product and asphaltenes are the THF soluble but pentane insoluble products. As shown in Table 1, with almost 100% conversion, more than 40% of polypropylene and polystyrene were converted to oil at 400°C using Route B. At 430°C, 90% of low density polyethylene was converted to oils and gases. When polypropylene was coprocessed with coal, the conversion with respect to coal increased and the oil yield increased from 17.5% to 61.7%. The observed increase in oil yield may be due to the fact that the gas formation from the polymer (>50% when liquefied alone) is reduced in the presence of coal. However, when polystyrene and coal (and low density polyethylene and coal) were coprocessed, a decrease in oil yield was observed. It is possible that the free radicals that are formed during the reaction undergo polymerization reactions that yield high molecular weight products. This is substantiated by the data in Figure 1 which shows the simulated distillation curve of the oil product from coprocessing of LDPE and coal at 430°C using Route B.

Liquefaction of polypropylene in supercritical water and helium (thermal) and in Route B with CO and Na_2CO_3 as catalyst showed identical results in terms of conversion and oil yield. However, the oil product from the thermal reaction contained more naphthenic compounds when liquefied in Route B. In contrast, polypropylene liquefied via Route A with $Mo(CO)_6$ at 400°C, gave only a 15% conversion. These results show that more hydrogenation takes place in Route B than in route A with tetralin as a solvent.

Since formate is the proposed reaction intermediate in Route B, use of potassium formate (HCOOK) instead of K_2CO_3 was investigated with DECS-17 (high volatile bituminous coal) at 400°C (Table 2)[5]. There was no appreciable difference in coal conversion, asphaltene and oil yields and the quality of the oil as determined by simulated distillation was identical. This result corroborates that formate is a possible intermediate. Evidence for this has also been given by NMR[6].

Liquefaction of newsprint using Route A at 325°C (Table 3) has shown that various catalysts such as SiO_2/Al_2O_3 and superacids such as $Pt/ZrO_2/SO_4$ and

$Mo/Fe_2O_3/SO_4$ gave results that were identical to the thermal conversion of newsprint. However with a $NiMo/Al_2O_3$ catalyst, the asphaltene fraction was reduced. Using $Mo(CO)_6$ with added sulfur resulted in the highest conversion with the lowest asphaltene yield.

Liquid fuels derived from biomass have high oxygen contents which largely reduce the heating value of the fuels. Numerous efforts have been made to reduce the oxygen content of the liquids obtained from the hydroliquefaction of biomass[7]. When newsprint is liquefied, the product contains large amounts of phenolic compounds. Table 4 shows the results from the coliquefaction of polypropylene and newsprint; the oils from newsprint increased from 14.7% to 28.4%. At 420°C, 50% of low density polyethylene was converted to oils in the presence of newsprint compared to less than 15% when liquefied alone. When a mixed plastic containing 85% polypropylene and 15% polyethylene was coprocessed with newsprint, an overall conversion of 70% was achieved.

Reported values of the oxygen content of the oil from the hydrogenation of newsprint or of cellulose using tetralin as a solvent via Route A are greater than 20% by weight[7]. The elemental analysis of the oil products obtained via Route B is shown in Table 5. The oil product from the coprocessing of polypropylene and newsprint has a lower oxygen content and hence the product is of higher quality than when newsprint is liquefied alone. The H/C ratio of the oil product from the coprocessing experiment is more than that of the oil product from newsprint.

Future Work

The use of acid catalysts such as zeolites (H-ZSM-5, HY) in the liquefaction of coal, plastics and lignocellulosic wastes will be explored. The regeneration ability of these catalysts will be examined. Since it is quite likely that catalysts such as nickel and molybdenum are poisoned by the alkali catalysts used in Route B, solid bases such as Ni/MgO, Ni/Na_2O will be tried so that the hydrogen from the water gas shift reaction is utilized in the hydrogenation of the oil product.

Our experiments on the liquefaction of polystyrene and polyethylene with coal showed decreased conversion of coal and decreased oil yield. This will be investigated further. Further reactions with plastic wastes (polyethylene, PET) with biomass are

planned to determine the optimum conditions for maximum oil yield.

References

1. Appell, H.R., R.D. Miller, and I. Wender, Division of Fuel Chemistry, 163rd National Meeting of the American Chemical Society, April 1972.

2. Appell, H.R., Y.C. Fu, S. Friedman, P.M. Yavorsky, and I. Wender, *U. S. Bureau of Mines, Pittsburgh, Report of Investigations 7560*, 1971.

3. Coughlin, R.W. and P. Altieri, *Fuel*, **65**, 95, 1975.

4. Jung, H., J.W. Tierney, and I. Wender, *ACS Fuel Chemistry Division*, **38**(3), 880, 1993.

5. Appell, H.R., I. Wender, and R.D. Miller, *Prepr. Pap. Am. Chem. Soc. Div. Fuel. Chem.*, **13**, 39,1969.

6. Howrath, I.T., and M. Siskin, *Energy & Fuels*, **5**,933, 1991.

7. Vasilakos, P.N., and D.M. Austgen, *Ind. Eng. Chem. Process. Des. Dev.*, **24**, 304, 1985.

Table 1. Results of the coliquefaction of Wyodak coal and polypropylene at 400°C and 575 psi (cold) CO in the presence of Na_2CO_3 as catalyst (Costeam reaction).

Expt. No.	Material	Conversion %	Asphaltene %	Oil %	Gases + water %
ska-13	Wyodak (8g)	71.3	19.2	19.6	32.5
d0503a	Polyprop. (PP) (8g)	97.6	4.2	41.6	51.8
ska-1	Polyethy-lene terephtha-late, PET (8g)	87.0	16.0	8.3	62.7
d0503b	Polystyr. (PS) 8g	99.6	2.6	58.6	38.4
d0504b	Wy/PP* (4g/4g)	81.4	11.9	61.7	7.8
d0504a	Wy/PS* (4g/4g)	61.6	12.2	-1.3	50.70
d0602a	PVC (8g)	68.0	31.3	12.6	24.10
ska-31	LDPE(6g)&	90.6	9.2	58.5	22.90
ska-33	Wyodak (6g)&	94.0	20.0	30.0	44.00
ska-32	Wy/LDPE (3g/3g)&	68.3	37.5	25.2	5.60

* Conversion, asphaltene and oil yields are calculated for coal with the assumption that the behavior of polypropylene is the same as when it is liquefied alone.

& Reaction at 430°C

Table 2. Comparison of HCOOK and K_2CO_3 as catalysts in Route B in the liquefaction of DECS-17. 8 g DECS-17 coal, 24 g water, 575 psi CO and catalyst at 400°C for 1 hour in a 300 mL autoclave (rpm=1800).

Run No.	Catalyst	Conversion	Asp.	Oils
SKA-19	HCOOK (1.62g)	96.8%	40.5%	30.7%
SKA-20	K2CO3 (1.33g)	92.5%	40.2%	31.4%

Table 3. Liquefaction of newsprint using Route A. 3 g of newsprint in 12 g tetralin and 900 psig (cold) H_2 at 325°C for 1 hour.

Run	Catalyst	Conversion %	Asp. %
SK-1	SiO_2/Al_2O_3 (1%)	87.0	35.7
SK-2	ZrO_2/SO_4(1%)	89.8	37.2
SK-4	Fe_2O_3/SO_4 (1%)	88.5	34.5
SK-5	Fe_2O_3/SO_4(1%) +S(1%)	88.7	33.7
SK-7	No Catalyst	86.4	38.2
SK-12	NiMo/Alumina (Shell)	0.874	0.23
SK-13	$Mo(CO)_6$/S	0.948	0.21
SK-14	$NiMo/Al_2O_3$/S	0.875	0.214

Table 4. Coliquefaction of newsprint and plastics by Route at 400°C and 575 psi (cold) CO with Na_2CO_3 as catalyst (Costeam reaction).

Expt. No.	Material	Conversion %	Asphaltenes %	Oils %	Gases + Water %
ska-16	Newsprint Np (8g)	94.4	8.2	17.7	68.5
d0503a	Polyprop. PP (8g)	97.6	4.2	41.6	51.8
ska-17	Np/PP (4g/4g)	97.7	3.4	25.7	68.6
ska-5	LDPE/Np** (2g/6g)	82.2	6.0	27.0	49.20
ska-18	Mixed Plastic/Np** (4g/4g)	70.0	6.5	20.3	43.20

* Conversion, asphaltene and oil yields are calculated for newsprint with the assumption that the behavior of polypropylene is the same as that when it is liquefied alone.

** Conversion, asphaltene and oil yields are based on the total moisture and ash free reaction mixture.

Table 5. Elemental analysis of the newsprint and the oil products from the Costeam experiments. Values given below are wt% of the dry sample.

Oil Sample	Description	C	H	N	S	O (by diff.)
---	newsprint	51.07	5.40	0.20	0.04	43.29
ska-15	oil product from polypropylene	85.38	13.62	0.28	0.02	0.70
ska-16	oil product from newsprint	82.12	9.15	0.10	0.07	8.56
ska-17	oil product from polypropylene/ newsprint	83.12	13.07	0.11	0.01	3.69

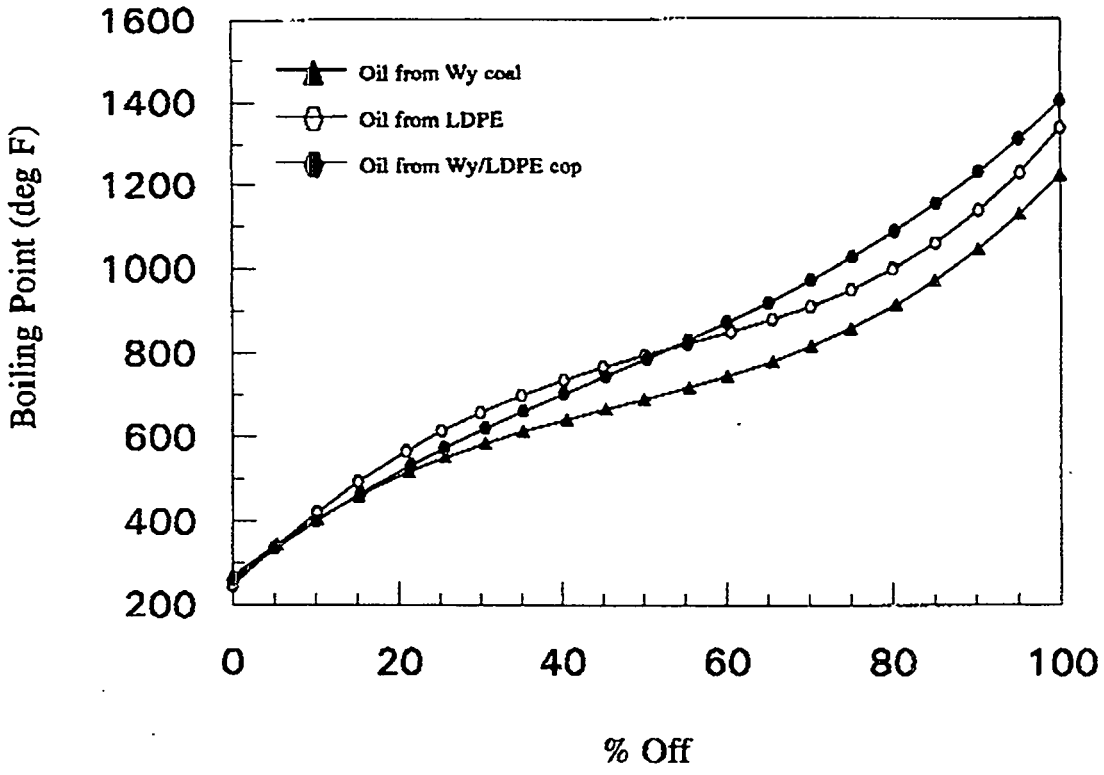

Figure 1. Simulated distillation curve of the oil products from Wyodak coal, LDPE and Wyodak/LDPE coprocessing at 430°C in Route B.

TASK I

Project I.6

COPROCESSING OF COAL WITH WASTE POLYMERS USING FINELY DISPERSED IRON CATALYSTS

Christine W. Curtis
Auburn University

Research performed this quarter involved two primary areas: waste tire coprocessing and waste plastics coprocessing. In both of these areas, the research has continued in the vein that was predicated by the results obtained and reported previously. The waste tire research has focused on two areas: evaluation of waste tire residue as catalytic agents using model compounds as test cases and evaluation of the waste liquefaction behavior in the absence of coal. This individual behavior is important because the chemistry and reactivity of the waste tires at coprocessing conditions will affect the liquefaction behavior and conversion of coal when coliquefied with waste tires. Research in waste plastics coprocessing focused this quarter on the cosolvating effect that different polymers have on each other during coprocessing at elevated temperatures and pressures. The effect of coprocessing solvent and reaction time was examined as well.

Waste Tire Coprocessing

The objective of this research is to evaluate the chemistry and reactivity of waste tires in coprocessing reactions with coal. A discovery that the residue from liquefied waste tires that has been extracted and heat-treated at 560 °C had catalytic activity was further evaluated using two model systems. The compound 4-(1-napththylmethyl)bibenzyl (NMBB) was used to evaluate the hydrocracking activity of these residues and other additives from waste tires. Dibenzothiophene (DBT) was used to evaluate the desulfurization activity of these materials. In addition, the liquefaction behavior of waste tires was examined to determine the reactivity of these materials. Two different waste tire materials were used. One was obtained from Rouse Rubber and the other from Uniroyal-Michelin. These waste tires were reacted thermally and catalytically using as catalysts residues from liquefied waste tires, additives such as carbon black, and combinations of waste tire residues with slurry phase catalysts, Mo naphthenate and Fe naphthenate.

Experimental. The model compounds used were NMBB (99% purity) obtained from TCI America and DBT (99%) obtained from Aldrich; both were used as received. The catalysts used in this work were Mo naphthenate (MoNaph) (6% Mo) from Shepherd Chemical and Fe naphthenate (FeNaph) (6.0%) from Strem. Elemental sulfur used in conjunction with the two slurry phase catalysts was obtained from Aldrich. The two waste tires were supplied by Rouse Rubber Industries, Vicksburg, MS. and Uniroyal-Michelin, Opelika, AL. Carbon black as Black Pearls 2000 was supplied by Cabot Industries and had a surface area of 1440 m^2/g.

Reaction Procedures. The waste tires were reacted in stainless steel tubular microreactors of ~20 cm^3 at 400 °C for 30 min with a H_2 pressure of 6.8 MPa introduced at ambient temperature. The liquefied waste tire products were extracted with THF to obtain the solid residue. The residue was then heated in a tubular furnace at 560±30 °C for 1 or 4 hr in a stream of N_2 flowing at 3L/min. The carbon black used in the reactions was also heat-treated by the same method as the waste tire residue.

Model compound reactions were performed in horizontally agitated stainless steel tubular microreactors of ~20 cm^3 at 400 °C for 30 min with a H_2 pressure of 8.7 MPa introduced at ambient temperature. The reaction system consisted of 0.25 g of NMBB; when additives were used, each material was added at 0.25 g. Model desulfurization reactions contained 0.2 g of DBT; the additive amount in those reactions was 0.04 g. When a catalyst precursor was used in the reaction, Mo or Fe was added at a level of 900 to 1000 ppm of active metal on a total reactor charge basis. When sulfur was added, elemental sulfur was added in a stoichiometric ratio of sulfur to metal assuming that MoS_2 or FeS_2 was formed in situ.

The reaction products produced from the model reactions of NMBB or DBT with the different additives were analyzed by gas chromatography using a Varian Model 3700 gas chromatograph equipped with J&W DB-5 30 m capillary column and flame ionization detector. The products obtained from NMBB were primarily hydrocracked products, although trace amounts of hydrogenated products were also formed. Percent hydrocracking (HYC) of NMBB was used to describe the HYC activity of the different additives and is defined as the moles of hydrocracked liquid products as a percentage of the total moles of liquid products produced. The products produced from DBT were primarily hydrogenolysis products although a small amount of hydrogenation also occurred. Percent hydrodesulfurization (HDS) is defined as the moles of desulfurized liquid products a percentage of the total moles of liquid products.

Two different waste tires from Rouse and Uniroyal were reacted in the stainless steel microreactors at 400 °C for 30 min with 6.9 MPa H_2 pressure introduced at ambient temperature. For each reaction, 4 g of waste tire were added. When additives were used in the reaction, 0.4 g were used. In the catalytic reactions the slurry phase catalysts, MoNaph and FeNaph, were added at a level of 1000 ppm of active metal; sulfur was added to these reactions on the same basis as in the catalytic model reactions. The liquefied products from the waste tires were first extracted with hexane to obtain the hexane soluble material and then with THF to obtain the THF soluble but hexane insoluble material. The organic material that was not soluble in THF was defined as insoluble organic matter or IOM which is calculated on an ash-free basis. The unreacted waste tires were also extracted to determine the amount soluble at room temperature.

Results of 4-(1-Naphthylmethyl)bibenzyl Reactions. The model compound NMBB was used as a model to test the activity of waste tires and components in waste tires for HYC. Neither the waste tires themselves, SBR rubber, slurry phase Fe and Mo catalysts nor combinations of these material showed much HYC activity. Carbon black, however, showed substantial HYC activity as reported previously[1]. Since the residue from the liquefied waste tires should contain a fairly high percentage of carbon black as well as any mineral matter present in the waste tire, this material offered the potential for being an active catalyst. Therefore, the residue from liquefied waste tire was extracted with THF, then heat treated at 560 °C for 1 or 4 hr, and tested as a catalyst for NMBB HYC after each step in the process. After reaction, the products from NMBB were analyzed by gas chromatography and % HYC was determined. Under these reaction conditions, NMBB only hydrocracked at three bond cleavage sites; the selectivity for the different bond ruptures are given in the Table 1: SA represents bond cleavage at a, SB represents bond cleavage at b, and SD represents bond cleavage at d[1].

When reacted thermally, only 4.9% HYC of NMBB occurred with 60% selectivity for SA and 40% for SD. The direct addition of both waste tire material increased the NMBB HYC to 11.3% for Rouse and 7.4% for Uniroyal; the selectivity for SD decreased to 23 and 32%, respectively. Introduction of carbon black to the NMBB yielded 79.1% HYC with a selectivity of 6% SB and 16% SD. Adding extracted Rouse and Uniroyal waste tire residue resulted in 32.5 and 22.0% HYC, respectively, with a selectivity for SA of 93 and 87%. Rouse residue was carbon black-rich compared to the Uniroyal residue and was a more effective catalytic agent after extraction. Heat treatment, however, changed the relative activities of the two residues.

When the Rouse residue was heat-treated at 560 °C for 1 to 4 hr prior to reaction with NMBB, the HYC activity increased to 51.5% and 52.9%, respectively. Similarly, heat-treated Uniroyal residues yielded increased HYC of NMBB, giving 99.6% and 99.7%, respectively. Heating these residues at elevated temperatures effectively removed any remaining organic or rubber coating from the waste tires. The waste tire residues were quite different in composition as presented in Table 2. The Rouse waste tire residue was primarily carbon although some Zn was present. By contrast, Uniroyal waste tire residue was composed primarily of inorganic constituents of Al, Si, Ti, and Zn; some carbon black was also present. The differences in the compositions of these residues were not only reflected in different HYC activity but also in different selectivities. Rouse residue gave selectivities for HYC activity that was very similar to the extracted but not heat-treated residue. By contrast, heat-treating Uniroyal residue decreased the SA selectivity to 61% from 87% and SD selectivity to 1 or 2 from 4 or 6%. The greatest difference observed with Uniroyal residue was the high selectivity for SB at 36 or 38%; this was the highest selectivity for SB obtained in any of the reactions.

Results from Dibenzothiophene Reactions. Hydrodesulfurization (HDS) of DBT was performed previously at 425 °C without solvent but using slurry phase catalyst: MoNaph, FeNaph, and Fe acetylacetonate, and Fe 2-ethylhexanoate[2]. The only catalyst that was active for either HDS or hydrogenation (HYD) was MoNaph reacted with or without sulfur. In this study, DBT was reacted at 400 °C in the absence of a solvent for 30 min with a H_2 pressure of 8.7 MPa which was introduced at ambient. The reason for selection of these conditions was that these DBT reactions will serve as a baseline for reactions to be performed next quarter.

The additives that were used in the DBT reactions were heat-treated residues from liquefied waste tires and heat-treated carbon black as shown in Table 3. These additives were reacted individually with DBT and also with MoNaph and excess sulfur. None of the additives alone showed much activity for either HDS or HYD with the values ranging from 2.5% HDS for heat-treated Rouse residue to 5.2% for carbon black. Their HYD activity was even less. When the additives were used in conjunction with MoNaph and excess sulfur, both HDS and HYD activities increased; HDS increased in the range of 10.2 to 14.3% with carbon black being the greatest; a similar increase in activity for HYD was observed. Neither carbon black nor the residues were nearly as active in the DBT system as in the NMBB system.

Waste Tire Reactions. Both waste tire materials used in this study were produced from

tire buffing processes; however, their compositions were quite different as shown in Table 4. Although the amount of volatile carbon was quite similar in both materials, the ash content and fixed carbon content were substantially different. Rouse waste tire was high in fixed carbon content at 29.8% but was low in ash at 3.6%. By contrast, Uniroyal waste tire had a low fixed carbon content of 5.5% and a high ash content of 31%. These considerable differences in the waste tire composition led to different liquefaction behaviors.

Both waste tires were thermally and catalytically liquefied; the amount of waste tire conversion was determined and the reaction products were fractionated into hexane solubles and THF solubles. The conversion of the waste tires is presented on two bases in Table 5: moisture and ash free (maf) and moisture, ash and carbon black free (macf). Rouse waste tire yielded 68.2% thermal conversion on a maf basis but a 97.7% conversion on a macf basis. The difference in those conversions is the carbon black present in the waste tire. By contrast, Uniroyal waste tire thermal reaction resulted in 81.6% conversion of a maf basis and 89.7% conversion on a macf basis, which left approximately 10% of the total material unconverted. The solubility of the unreacted waste tire was tested using the same solvent fractionation procedure as was used after liquefaction. Both waste tires showed similar solubility with about 13% of the waste tire being soluble in hexane plus THF. The differences observed in the thermal liquefaction behavior of the two waste tires were directly attributable to their differences in composition.

The addition of additives and catalysts to the waste tire liquefaction reaction affected the liquefaction behavior as well as the amount of waste tire conversion achieved. When Rouse waste tire was reacted with either MoNaph or FeNaph, the conversion remained very high at 98.3 and 99.8% conversion on a macf basis, respectively. By contrast, the addition of carbon black or heat-treated waste tire residues inhibited the conversion of a portion of the convertible waste tire. Carbon black lowered macf conversion of Rouse waste tires to 86.9% while the residues lowered the conversions to 91 and 94%. The Uniroyal waste tire reacted differently than the Rouse. Addition of both slurry phase catalysts and both heat-treated residues resulted in more conversion of Uniroyal waste tire than in the Uniroyal thermal reaction. The highest conversion was achieved with MoNaph yielding 98.1% conversion on macf basis. By contrast, carbon black inhibited the macf conversion of Uniroyal waste tire and yielded a lower conversion than the thermal reaction.

Summary. Waste tires liquefy readily at coprocessing conditions. The residues from the liquefied waste tires serve as active catalysts particularly in conjunction with slurry phase catalysts. Future work will include further evaluation of the waste tire residue's catalytic activity. Coprocessing reactions of preliquefied waste tires and coal will also be performed.

Waste Plastics Coprocessing

The coprocessing of coal with plastics to produce a fuel is a reasonable alternative for the recycling of used plastics that contain colorizing metals or are contaminated with various materials. Previous research performed by this group has shown that certain waste plastics are readily dissolved at liquefaction temperatures while others are quite difficult to convert. Polymers like polystyrene, polyisoprene, polypropylene, and even polyethylene terephthalate are readily liquefiable but low, medium and high density polyethylenes are not. Coprocessing reactions of coal with polymers and commingled plastics have varying levels of success depending upon the type of waste plastic and type of catalyst used. The research performed this quarter involved liquefying waste polymers individually and combinatorially to evaluate the effect of cosolvation and reaction conditions on the conversion and reactivity of the different polymers and polymer combinations.

Experimental. The polymers representing waste plastics used this quarter were high density polyethylene (HDPE), low density polyethylene (LDPE), polyethylene terephthalate (PET), polypropylene (PP), and polystyrene (PS). These polymers were obtained from Aldrich Chemical Co. and were used as received. Three different catalysts were used: HZSM-5 obtained from United Catalyst Inc., low alumina and super nova-d fluid cracking catalysts from Davison Chemical Division of W.R. Grace and Co. For some of the reactions, the solvents, tetralin and hexadecane, were used; tetralin was obtained from Aldrich while hexadecane was obtained from Fisher.

Coprocessing reactions using polymers were performed in ~20 cm^3 stainless steel tubular microreactors which were agitated horizontally. The reaction conditions in the coprocessing reactions were a reaction temperature of 440 °C, H_2 pressure of 5.5 MPa introduced at ambient and a 30 min reaction time. The products from the reactions were solvent fractionated using hexane followed by THF. The unconverted plastic composed the IOM which is defined as insoluble organic matter and is ash free.

The conversion of waste plastics is defined as:

$$\% \text{ conversion} = \left(1 - \frac{\text{unreacted polymer}}{\text{polymer charged}}\right) \times 100\%.$$

Reactions of Individual Polymers. Each individual polymer was reacted with low alumina at 440 °C without a catalyst as given in Table 6. All of the polymers tested showed conversions of more than 90% except for PET which gave a conversion of 69%. The highest gas make was also produced by PET. The polymers, HDPE, LDPE, and PP, produced hexane solubles between 70 and 80%, while PS and PET yielded 61.2 and 33.3%, respectively.

Polymer Combinations. The second set of experiments that was performed involved a base combination of three polymers: 50% HDPE, 30% PET, and 20% PS. The base polymer combination was reacted with three different catalysts: HZSM-5, low alumina, and super nova-d as presented in Table 7. The base polymer was then introduced at 80% and 20% of another polymer was added. The additions included HDPE, LDPE, PP, PS, and PET. Each of these reactions was performed in the presence of a solvent composed of 30% tetralin and 70% hexadecane. The catalysts used in these reactions was the same as in the base combination reaction.

The conversion and product distribution of the base polymer combination served as a baseline for the other reactions. The most active catalyst for the base combination was HZSM-5 for both polymer conversion and hexane solubles. When LDPE, PP, and PS were added to the base combination, the conversion and hexane solubles increased for each catalyst. For all the reactions, HZSM-5 was the most active catalyst while low alumina and super nova-d showed similar activity. Addition of HDPE was detrimental to the conversion obtained with low alumina and super nova-d while PET showed similar conversion with HZSM-5 and low alumina but increased conversion with super nova-d; their hexane solubles yields were similar to the base case.

Another set of reactions begun this quarter tested the synergism for cosolvation among the different polymers. The reactions performed to date used low alumina as the catalyst in individual reactions of each polymer (Table 8). Both conversion and product distribution were obtained for each polymer. Then the hypothetical mean, defined as the weighted average from the individual base component reactions, of the conversion and product distribution was

calculated and compared to the conversion and product distribution obtained from the base combination reaction. In reactions with low alumina, the conversion difference between the hypothetical mean and base combination was 25.6%. Therefore, the individual reactions with low alumina converted substantially more polymer individually than did the combined reaction.

Effect of Reaction Parameters. The effect of the solvent type (Table 9) and reaction time (Table 10) on conversion and product distribution of the base polymer combination was evaluated. The solvents that were evaluated were tetralin, a hydroaromatic, and hexadecane, a straight chain alkane. Reactions with HZSM-5 and super nova-d used tetralin alone and 30% tetralin in hexadecane. The reactions using the combined alkane and hydroaromatic solvent yielded higher conversions as well as higher hexane soluble materials. In reactions with low alumina, hexadecane was also used individually. The highest conversion for any of the reactions was obtained with hexadecane alone as solvent.

In addition, the effect of reaction time was also evaluated. The system used was the base polymer combination, low alumina as the catalyst, and reaction times of 30 and 60 minutes. Two different solvents were used: 30% tetralin and 70% hexadecane. For both solvents increased reaction resulted in increased polymer conversion and hexane soluble yields.

Summary. Therefore, in the liquefaction of polymers, reaction parameters, catalyst type, and solvent composition, all affect the conversion and product slate of the polymers. At this point, combining the polymers appears to be detrimental to polymer conversion and hexane soluble yields. Further work is being done to evaluate the synergism or lack thereof among polymers during liquefaction.

References

1. Tang, Y.; Curtis, C.W., *ACS Fuel Chem. Div. Prepr.*, 39, 3, 1994, 865-869.
2. Curtis, C.W.; Chen, J.H.; Tang, Y., *Energy and Fuels*, in press, 1994.

Table 1. Activity and Selctivity of the Additives for Hydrocracking 4-(1-Naphthylmethyl)bibenzyl

Reaction Systems	Residue Treatment Conditions	%HYC[a]	Cleavage of a+b+d[b]	Selectivity * 100 %		
				SA	SB	SD
NMBB		4.9±1.3	2.5	61	0	39
NMBB + Rouse Waste Tire		11.3±2.2	5.7	77	0	23
NMBB + Uniroyal Waste Tire		7.4±2.3	3.7	68	0	32
NMBB + Carbon Black	Heated: 1 hr	79.1±2.7	39.6	78	6	16
NMBB + Rouse Residue	Extracted	32.5±3.1	16.3	93	2	4
NMBB + Rouse Residue	Heated: 1 hr	51.1±3.4	25.6	93	4	3
NMBB + Rouse Residue	Heated: 1 hr	52.9±1.7	26.5	92	4	4
NMBB + Uniroyal Residue	Extracted	22.0±3.2	11.1	87	7	6
NMBB + Uniroyal Residue	Heated: 1 hr	99.6±2.4	49.8	61	38	1
NMBB + Uniroyal Residue	Heated: 4 hr	99.7±2.1	49.8	62	36	2

[a] %HYC = the moles of hydrocracked liquid products as a precentage of the total moles of liquid products produced.
[b] Cleavage of bonds a, b, and d is defined as bond cleavage of bond a, b, and d in NMBB.
[c] Selectivity is defined as bond cleavage at a or b or d divided by the combined bond cleavage of a, b, and d.

Table 2. Analysis of Waste Tire Residue and Carbon Black

Weight %	Carbon Black	Rouse Residue	Uniroyal Residue
C	NM	85.0±0.2	14.5±0.1
H	NM	<0.5	<0.5
S	0.61±0.03	3.02±0.02	1.90±0.08
Si	NM	NM	19.06±0.1
Al	NM	NM	16.52±0.1
Ti	NM	NM	17.28±0.1
Zn	NM	4.64±0.02	6.03±0.03
Ash	0.5±0.1	10.9±0.2	84.2±0.3
Surface Area (m^2/g)	1432±26	98±1	27±1

[a] The residue were obtained by liquefying waste tire, extracting the reaction products with solvents, and then heating the solid residue in N_2 at 560 °C.
[b] Carbon, hydrogen, and metal contents were determined by Galbraith Laboratories, Inc., Knoxville, TN.
[c] The ash amounts were determined by ASTM D3174-82
[d] The sulfur content was determined using a Leco Sulfur Analyzer Model SC32.
[e] The surface area were determined using a Quantasorb BET analyzer.

Table 3. Effect of Additives and/or Catalysts on Dibenzothiophene Reactions[a]

Additive	Catalyst	Product Distribution (mol%)					HDS (%)	HYD (%)	Recovery (%)
		DBT[b]	TDBT	BPN	CHB	BCH			
None	None	100.0±0.0	0.0±0.0	0.0±0.0	0.0±0.0	0.0±0.0	0.0±0.0	0.0±0.0	92.5±1.4
None	MoNaph + S	94.3±1.2	trace	5.7±1.2	0.0±0.0	0.0±0.0	5.7±1.2	1.4±0.4	93.3±1.2
Carbon Black	None	94.8±0.8	0.0±0.0	5.2±0.8	0.0±0.0	0.0±0.0	5.2±0.8	1.3±0.4	92.8±2.3
Uniroyal Residue	None	95.3±0.7	0.0±0.0	4.7±0.7	0.0±0.0	0.0±0.0	4.7±0.7	1.2±0.5	91.9±1.1
Rouse Residue	None	97.5±0.9	0.0±0.0	2.5±0.9	0.0±0.0	0.0±0.0	2.5±0.9	0.6±0.2	92.0±1.6
Carbon Black	MoNaph + S	84.0±1.6	1.6±0.4	11.4±0.8	2.9±0.8	0.0±0.0	14.3±1.6	5.1±0.8	90.1±1.8
Uniroyal Residue	MoNaph + S	86.0±1.2	1.4±0.4	9.9±0.8	2.7±0.4	0.0±0.0	12.6±1.2	4.5±0.4	92.0±1.0
Rouse Residue	MoNaph + S	89.0±1.0	0.8±0.3	8.6±0.6	1.7±0.4	0.0±0.0	10.2±1.0	3.4±0.4	90.8±1.9

[a] Reaction Conditions: 400 °C; 30 min, 1250 psig H_2 at ambient temperature; catalyst loading of 1000 ppm Mo; 3:1 S to Mo; 0.2 gram dibenzothiophene without solvent; stainless steel tubular reactor agitated at 550 cpm.

[b] DBT = dibenzothiophene; TDBT = tetrahydrodibenzothiophene; BPN = biphenyl; CHB = cyclohexylbenzene; BCH = bicyclohexyl.

Table 4. Analysis of Waste Tires and Coals[a]

	Uniroyal Waste Tires[b]	Rouse Waste Tire[b]
Ultimate Analysis (%)[c]		
C	56	85
H	8.0	7.4
N	NM[d]	NM
S	1.0	1.6
O	NM	NM
Proximate Analysis (%)		
Moisture	0.15	0.83
Ash	31.04	3.60
Volatile Matter	63.29	65.81
Fixed Carbon	5.52	29.76
Product Distribution of Liquefied Waste Tire (%), maf Basis[f]		
	Uniroyal Waste Tire	**Rouse Waste Tire**
Hexane Solubles	78.0±1.0	63.4±1.5
THF Solubles	3.6±1.2	4.8±1.1
IOM[e]	18.4±1.0	31.8±1.5
Conversion	81.6±1.0	68.2±1.5
Product Distribution of Liquefied Waste Tire (%), macf Basis[f]		
	Uniroyal Waste Tire	**Rouse Waste Tire**
Gas + Hexane Solubles	85.7±1.1	90.8±2.2
THF Solubles	4.0±1.3	6.9±1.6
IOM	10.3±1.1	2.3±2.2
Conversion	89.7±1.1	97.7±2.2
Distribution of Untreated Waste Tire (%), maf Basis		
	Uniroyal Waste Tire	**Rouse Waste Tire**
Hexane Solubles	10.3±1.6	10..1±1.7
THF Solubles	2.3±0.7	2.7±0.5
IOM	87.4±1.6	87.2±1.7

[a] Reaction Conditions: 400 °Cm 30 min, 1000 psig H_2,
[b] Uniroyal = waste tire from Uniroyal-Michelin Tire Company, Opelika, AL; Rouse = waste tire from Rouse Rubber, Vicksburg, MS.
[c] Coal data were quoted from Argonne Premium coal Sample Program User Handbook. Ultimate and proximate analysis of waste tires were performed by Galbraith Laboratories, Inc. Other waste tire analysis was performed by the authors;
[d] NM = not measured; [e] IOM = insoluble organic matter; [f] maf Basis = moisture and ash free basis, macf Basis = moisture, ash, and carbon black free basis.

Table 5. Reaction of Waste Tire with Catalysts or Aditives[a]

Waste Tire	Catalysts and Additives	Product Distribution (wt%)		Waste Tire Conversion (%) (maf)[b]	Waste Tire Conversion (%) (macf)[b]
		Gas + Hexane Solubles	THF Solubles		
Rouse[c]	None	63.4±1.5	4.8±1.1	68.2±1.5	97.7±2.2
	FeNaph + S[e]	65.3±1.9	3.3±0.9	68.6±1.9	98.3±2.7
	MoNaph + S	66.9±2.0	2.7±0.8	69.6±2.0	99.8±2.9
	Carbon Black[f]	56.1±1.5	4.5±0.8	60.6±1.5	86.9±2.2
	Uniroyal Residue	62.5±1.2	3.1±0.7	65.6±2.1	94.0±3.0
	Rouse Residue	59.2±2.0	4.3±0.9	63.5±2.0	91.0±2.9
Uniroyal[d]	None	78.0±1.0	3.6±1.2	81.6±1.0	89.7±1.1
	FeNaph + S[e]	85.1±1.5	2.5±0.5	87.6±1.5	96.6±1.7
	MoNaph + S	86.1±1.8	2.9±0.7	89.0±1.8	98.1±2.0
	Carbon Black[f]	74.6±1.9	2.9±0.7	77.5±1.9	85.4±2.1
	Uniroyal Residue	80.2±2.0	5.2±1.6	85.4±2.0	94.2±2.2
	Rouse Residue	76.5±2.3	8.0±1.9	84.5±2.3	93.2±2.5

[a] Reaction Conditions: 400 °C, 30 min, 1000 psig H_2 introduced at ambient temperture.
[b] maf = moisture and ash free basis; macf = moisture, ash, and carbon black free basis.
[c] waste tire from Rouse Comapny.
[d] waste tire from Uniroyal Company.
[e] 1000 ppm Fe or Mo. S: Fe or S: Mo = 3:1 in the catalytic reaction systems.
[f] Weight ratio of waste tire to additives was 10:1.

Table 6. Product Distribution from the Liquefaction of Polymers

Polymer	Product Distribution (%)				Conversion (%)
	Gas	Hexane Solubles	THF Solubles	IOM	
High Density Polyethylene	17.5±1.6	71.9±1.9	2.6±0.2	8.0±0.4	92.0±0.2
Low Density Polyethylene	14.2±0.0	79.6±1.1	3.3±1.0	3.0±0.1	97.0±0.2
Polypropylene	15.5±0.1	70.5±0.5	12.3±1.2	1.7±0.6	98.3±0.1
Polystyrene	6.1±0.0	61.2±0.8	25.3±0.7	7.5±0.0	92.5±0.0
Polyethylene Terephthalate	27.9±0.1	33.3±1.3	7.9±0.9	30.8±0.6	69.2±0.3

IOM = unreacted polymer.
Reaction Conditions: 440 °C, 30 min, 800 psig H_2 at ambient, 2 g polymer 0.44 g of low alumnia.

Table 7. Reaction Results of Different Polymer Combination

Polymer	Catalyst	Product Distribution (%)				Conversion (%)
		Gas	Hexane Solubles	THF Solubles	IOM	
Base Polymer Combination	HZSM-5	11.4±0.8	56.0±0.2	9.0±0.5	23.6±1.1	66.4±1.6
	Low Alumina	10.4±0.0	41.6±0.0	6.6±0.4	41.3±0.4	58.7±0.4
	Super Nova-D	10.1±0.2	36.8±0.0	10.7±1.4	42.3±1.6	57.7±1.7
80% Base + 20% HDPE	HZSM-5	17.8±1.3	52.4±0.5	6.8±0.4	22.9±2.3	77.1±3.3
	Low Alumina	8.6±0.4	36.0±2.0	4.0±0.4	51.4±2.1	48.6±2.2
	Super Nova-D	9.1±0.2	34.6±0.7	7.4±1.1	48.9±0.2	51.1±0.2
80% Base + 20% LDPE	HZSM-5	15.4±0.4	66.8±0.7	4.6±0.2	13.1±0.9	86.9±1.4
	Low Alumina	8.6±0.1	50.4±0.3	3.2±0.5	37.8±0.3	62.2±0.4
	Super Nova-D	8.7±0.1	38.7±0.7	8.0±1.4	44.6±2.0	55.4±2.1
80% Base + 20% Polypropylene	HZSM-5	21.1±0.8	61.6±2.0	7.4±1.5	9.8±0.4	90.2±0.8
	Low Alumina	10.7±0.1	53.1±0.5	5.0±0.6	31.1±0.0	68.9±0.0
	Super Nova-D	11.6±0.1	47.4±0.9	6.0±1.2	35.1±0.1	64.9±0.1
80% Base + 20% Polystyrene	HZSM-5	17.8±0.6	66.8±0.2	6.0±0.5	9.3±0.2	80.7±0.3
	Low Alumina	8.8±0.2	51.2±1.1	5.7±0.3	34.2±1.0	65.8±1.1
	Super Nova-D	8.9±0.0	53.8±4.0	5.6±1.0	31.6±3.0	68.4±3.2
80% Base + 20% PET	HZSM-5	12.5±0.2	53.8±2.4	9.0±1.2	24.8±3.4	65.2±5.0
	Low Alumina	11.4±0.4	37.4±1.3	9.0±1.0	42.2±0.8	57.8±0.8
	Super Nova-D	12.6±0.0	40.0±2.7	11.3±0.4	36.1±3.2	63.9±3.4

Base Combination: 50% HDPE, 30% PET, and 20% Polystyrene
Reaction Conditions: 440 °C, 30 min, 800 psig H_2 at ambient, 2 g polymer, 2 g of solvent (30% tetralin and 70% hexadecane), 0.44 g of catalyst.
Product distribution given on a solvent-free basis.

Table 8. Evaluation of Synergism for Liquefaction of Base Polymer Combination

Polymer	Catalysts	Product Distribution (%)				Conversion (%)
		Gas	Hexane Solubles	THF Solubles	IOM	
HDPE	Low Alumina	5.6±0.0	76.0±1.0	15.0±1.5	3.4±0.5	96.6±0.5
PET	Low Alumina	21.7±0.0	35.5±1.0	18.8±0.6	23.9±1.7	76.1±1.7
PS	Low Alumina	9.2±0.2	68.2±0.5	3.5±1.1	19.0±0.8	81.0±0.9
Hypothetical Mean		11.2	62.3	13.8	12.7	87.3
Base Charge	Low Alumina	10.4±0.0	41.6±0.0	6.6±0.4	41.3±0.4	58.7±0.4
Difference		0.8	20.7	7.2	-28.6	25.6

1. Hypothetical mean is the weighted average of the base charge component, HDPE, PET and PS;
2. Difference is the hypothetical mean less the base charge reaction value;
3. The individual polymer reaction was run under the same conditions as the base charge.

Table 9. Solvent Effects on Base Charge Liquefaction

Catalyst	Solvent	Product Distribution (%)				Conversion (%)
		Gas	Hexane Solubles	THF Solubles	IOM	
HZSM-5	Tetralin	10.2±0.5	55.5±0.3	4.9±2.0	29.4±2.3	70.6±3.3
	Tetralin + Hexadecane	11.4±0.8	66.0±0.2	9.0±0.5	23.6±1.1	76.4±1.1
Super Nova-D	Tetralin	9.2±0.3	34.9±1.7	7.4±0.1	48.5±1.9	51.5±2.1
	Tetralin + Hexadecane	10.1±0.2	36.9±0.0	10.7±1.4	42.3±1.6	57.7±1.7
Low Alumina	Tetralin	8.5±0.0	40.7±0.3	5.2±0.3	45.6±0.1	54.4±0.1
	Tetralin + Hexadecane	10.4±0.0	41.6±0.0	6.6±0.4	41.3±0.4	58.7±0.4
	Hexadecane	12.5±0.1	53.7±0.7	5.4±0.5	28.4±1.3	71.6±1.3

Reaction Conditions: Reaction Conditions: 440 °C, 30 min, 800 psig H_2 at ambient, 2 g polymer, 2 g of solvent.

Table 10. Reaction time Effect on Base Charge Liquefaction

Reaction Time (min)	Solvent	Product Distribution (%)				Conversion (%)
		Gas	Hexane Solubles	THF Solubles	IOM	
30	Tetralin + Hexadecane	10.4±0.0	41.6±0.0	6.6±0.4	41.3±0.4	58.7±0.4
60	Tetralin + Hexadecane	12.4±0.0	55.4±2.4	3.4±0.8	28.9±1.6	71.1±1.7
Difference,%		2.0	13.8	-3.2	-12.4	13.3
30	Hexadecane	12.5±0.1	53.7±0.7	5.4±0.5	28.4±1.3	71.6±1.3
60	Hexadecane	16.6±0.0	61.8±1.0	6.8±0.0	14.9±1.0	85.1±1.1
Difference,%		4.1	8.1	1.4	-13.5	14.4

TASK I

Project I.7

COLIQUEFACTION OF WASTE PLASTICS WITH COAL

G.P. Huffman, Zhen Feng, and Vikram Mahajan
University of Kentucky

Introduction

In previous work,[1] we have investigated the direct liquefaction of medium and high density polyethylene(PE), polypropylene(PPE), poly(ethylene terephthalate) (PET), and a mixed plastic waste, and the coliquefaction of these plastics with coals of three different ranks. The results established that a solid acid catalyst(HZSM-5 zeolite) was highly active for the liquefaction of the plastics alone, typically giving oil yields of 80-95% and total conversions of 90-100% at temperatures of 430-450 °C. In the coliquefaction experiments, 50:50 mixtures of plastic and coal were used with a tetralin solvent(tetralin:solid = 3:2). Using ~1% of the HZSM-5 catalyst and a nanoscale iron catalyst, oil yields of 50-70% and total conversions of 80-90% were typical.

In more recent work, we have conducted further investigations of the liquefaction reactions of PE and the coliquefaction reactions of PE, PPE and Black Thunder subbituminous coal. Liquefaction of a commingled waste plastic obtained from the American Plastics Council has also been investigated.

Experimental Procedure

The feedstock materials used in the work reported in this paper included medium density polyethylene (PE), polypropylene (PPE), a commingled waste plastic obtained from the American Plastics Council(APC), and a subbituminous coal (Black Thunder). Proximate and ultimate analyses for the coal and APC waste plastic are shown in Table 1. The experiments used 3 types of catalysts: a commercial HZSM-5 zeolite catalyst[2], an ultrafine ferrihydrite treated with citric acid(FHYD/CA), and a ternary Al/Si/ferrihydrite with Al:Si:Fe=1:1:18 ($FHYD_{0.90}/Al_{0.05}Si_{0.05}$). The ultrafine ferrihydrite catalysts are synthesized in our laboratory. For all runs, 1 wt.% of catalyst was added. Dimethyl disulfide (DMDS) was sometimes added to convert the ultrafine ferrihydrite to pyrrhotite during the reaction. The preparation, structure, and liquefaction activity of the ferrihydrite catalysts has been discussed in detail elsewhere[3,4].

The liquefaction experiments were conducted in tubing bomb reactors with a volume of 50ml which were shaken at 400 rpm in a fluidized sand bath at the desired

temperature. The reaction times were 20-60 min. and the atmosphere in the bomb was either hydrogen or nitrogen (cold pressure 100-800 psi). Usually 5 g of plastic or plastic + coal with 7.5 g of solvent(tetralin and/or waste oil) were charged in the tubing bombs. The reactor was cooled in a second sand bath, and gas products were collected and analyzed by gas chromatography[5]. The other products were removed from the reactor with tetrahydrofuran (THF) and extracted in a Soxhlet apparatus. The THF solubles were subsequently separated into pentane soluble (oils) and pentane insoluble (PA + AS) fractions. Total THF conversion was determined from the amount of insoluble material that remained (residue). Any added catalyst was subtracted from the residue sample weight.

Table 1. Proximate and ultimate analyses of Black Thunder coal and APC commingled waste plastic used in this research.

Proximate[a]	Black Thunder Coal	APC Waste Plastic
% Ash	6.33	0.45
% Volatile	45.40	98.8
% Fixed Carbon	48.27	0.74
Ultimate[b]		
% Carbon	71.59	84.65
% Hydrogen	4.83	13.71
% Nitrogen	1.51	0.65
% Sulfur	0.49	0.01
% Oxygen	15.24	0.98

a = Dry basis, b = Dry ash free basis.

Results and Discussion

Previously, we have shown that a solid acid catalyst(HZSM-5 zeolite) is highly active for the liquefaction of PE, PPE, and mixed waste plastic. Some interesting new results for PE are shown in Figure 1, where it is shown that oil yields are not strongly dependent on hydrogen pressure. Moreover, the oil yield as determined by pentane solubility is as high under moderate pressures of nitrogen as it is under hydrogen. The total conversion(THF soluble) was nearly 100% in all cases. Figure 1 also shows the time dependence of the reaction for PE in the presence of HZSM-5.

Figure 1. Liquefaction results for PE as a function of time and pressure. T=430 C, t=60 min., tetralin:PE=3:2, 1 wt.% HZSM-5

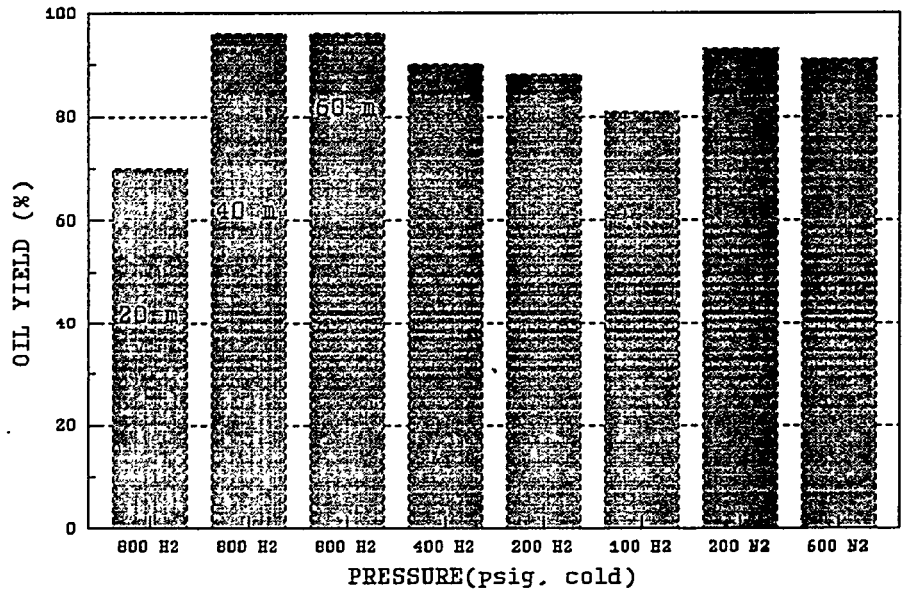

Our previous paper[1] examined the coliquefaction of a mixed waste plastic with both a bituminous and a subbituminous coal. Oil yields of 60-70% and total conversions of over 90% were observed in the presence of both the HZSM-5 catalyst and an iron catalyst(430 °C, 800 psi H_2-cold, 60 min., tetralin solvent). We are currently studying the response of individual plastic resins to various catalysts and conditions in more detail. Some typical results are shown in Table 2. PE and PPE both respond strongly to the HZSM-5 catalyst. PPE also responds very well to the citric acid-treated ferrihyrite although PE does not. It is also seen that the mixtures of PE and coal do not liquefy as well as PPE-coal mixtures or as well as we observed previously for a mixed plastic[1]. Neither the HZSM-5 or the FHYD/CA catalyst has a strong effect on the liquefaction of PE-coal mixtures.

Table 2. Liquefaction results(yields in wt.%) for medium density polyethylene(PE), polypropylene(PPE), and 50:50 mixtures of PE and PPE with Black Thunder coal.

FEED	CATALYST	T (°C)	OIL	GAS	PA+A	TOT.
PE	NONE	430	26	1	39	65
PE	FHYD/CA	430	33	1	34	68
PE	HZSM-5	430	96	1	2	99
PE/COAL	NONE	430	41	3	26	69
PE/COAL	FHYD/CA	430	42	4	22	68
PE/COAL	HZSM-5	430	41	4	28	72
PPE	NONE	420	83	<1	4	88
PPE	FHYD/CA	425	98	2	0	100
PPE	HZSM-5	425	100	<1	0	100
PPE/COAL	HZSM-5	430	71	4	18	93

Some interesting results for a commingled waste plastic provided by the American Plastics Council are shown in Table 3. Here, we have examined the effect of varying both the catalyst and the solvent. It is seen that at 445 °C the nature of the solvent has a larger effect on the oil yield and total conversion than the catalyst. Both catalysts are moderately effective at this temperature; however, the solvent has a much larger effect, with the oil yields increasing from 30-40% to ~90% as tetralin is replaced with a waste motor oil.

Table 3. Liquefaction results(yields in wt.%) for APC waste plastic with different solvents and catalysts. Experiments conducted at 445 °C, 800 psig H_2(cold) in a tubing bomb, with 7.5 g of solvent and 5 g of plastic.

FEED	CAT.	SOLV.	OIL+GAS	OIL	GAS	PA+AS	TOTAL
W.PL	HZSM-5	OIL-7.5	89.3			5.1	94.4
W.PL	HZSM-5	TET.-2.5 OIL-5.0	88.4			5.7	94.1
W.PL	HZSM-5	TET.-5.0 OIL-2.5	66.8	63.7	3.1	17.8	84.6
W.PL	HZSM-5	TET.-7.5	42.9			12.3	55.2
W.PL	NONE	OIL-7.5	87.1			7.9	95.0
W.PL	NONE	TET.-2.5 OIL-5.0	48.6			27.1	75.7
W.PL	NONE	TET.-5.0 OIL-2.5	51.0	48.3	2.7	15.2	66.2
W.PL	NONE	TET.-7.5	35.8			23.2	58.9
W.PL	FHYD AlSi	OIL-7.5	90.9			4.8	95.7
W.PL	FHYD AlSi	TET.-2.5 OIL-5.0	61.8	58.4	3.4	21.2	83.0
W.PL	PHYD AlSi	TET.-5.0 OIL-2.5	51.2	48.6	2.6	22.2	73.4
W.PL	FHYD AlSI	TET.-7.5	30.2			16.5	46.7

Summary

New results for plastics liquefaction and coal-plastic coliquefaction suggest that the nature of the plastic, the solvent, and the reaction atmosphere can all have a significant on product yields. A thorough experimental matrix is needed to explore this parameter space. Further catalyst development aimed at producing cheaper, more robust catalysts for coal-waste plastic coliquefaction is required.

TASK I

Project I.8

TECHNICAL AND ECONOMIC ASSESSMENT OF CO-LIQUEFYING COAL AND PLASTIC WASTES

Mahmoud El-Halwagi
Auburn University

SUMMARY

Efforts have been undertaken to assess the technical and economic feasibility of a new process for co-liquefying coal and waste plastics. This assessment is based on incorporating recent experimental data on plastic/coal liquefaction within a conceptual process framework. A preliminary design was developed to co-liquefy 30,000 kg/hr of plastic waste with and equivalent amount of coal on a weight basis. The plant products include hydrocarbon gases, naphtha, jet fuel and diesel fuel. Material and energy balances along with plant-wide simulation were conducted for the process. Furthermore, the fixed capital investment and production cost for the facility have been evaluated.

INTRODUCTION

Recent research efforts (Taghiei et al., 1993: Anderson and Tuntawiroon, 1993) have shown that the conversion of coal and plastic waste into liquid fuel is possible on a lab scale. This conversion is achieved by processing coal and waste plastics at a relatively high temperature (400 - 450 °C) and moderate to high hydrogen pressure (800 - 2000 psi). Experiments are reported to yield hydrocarbon mixtures. Conversion as high as 100% is achievable for reactions involving plastic waste alone with yields to the oils fraction ranging between 86 - 92% (Taghiei et al., 1993). However, coal/plastic mixtures are able to attain somewhat lower conversions and yields ranging from 53 - 93% and 26 - 83%, respectively.

The objective of this research is to provide a technical and economic assessment of co-liquefying coal and plastic waste. A process flowsheet was first conceptualized.

Subsequently, the material and energy balances for the process along with a plant-wide simulation using the software ASPEN PLUS were undertaken. Finally, preliminary economic aspects of the process were analyzed.

PROCESS CONCEPTUALIZATION AND TECHNICAL ASSESSMENT

The first step in assessing the process involved developing a conceptual flowsheet to co-liquefy coal with waste plastics (Figure 1). The waste plastics are sent to a shredder which chips the plastics into pieces with manageable size. Coal is first crushed then distributed to the slurry mixer and to hydrogen generation. The waste plastics and crushed coal are mixed with a recycled solvent to form a slurry. This slurry mixture is fed to a preheater. The preheated slurry is then forwarded to an adiabatically operated reactor which yields vapor, liquid and solid products. The vapor, leaving the reactor at 800 °F and 2200 psi, is first relinquished of hydrogen which is recycled back to the reactor after being mixed with the fresh hydrogen feed. The remainder of the stream is then separated into vapor and liquid products by using a flash column. The gas leaving this flash column is sent to an acid gas removal system. The remaining gas consists of light petroleum fuel gases. The hydrogen sulfide removed is processed in a Claus unit to yield elemental sulfur. The slurry leaving the reactor is first flashed is the gas oil column. The column yields a vapor product which contains most of the valuable hydrocarbon fractions. The bottom product leaving the column includes heavy hydrocarbons along with the unreacted coal, ash and tire inorganics. The vapor stream leaving the gas-oil flash column is hydrotreated and distilled to yield light, middle and heavy distillates. A hydroclone is employed to process the bottoms from the gas oil flash column. The product leaving the top of the hydroclone contains the heavy boiling point fraction (>650 °F). This fraction is recycled to the slurry mixer as a hydrogen solvent donor. Additional liquid from the fraction is removed using the Wilsonville evolved Residuum Oil Supercritical Extraction-Solid Rejection [ROSE-SR] unit. This liquid is combined with the recycled solvent and the mixture is returned to the slurry mixer. The solid effluent from the ROSE-SR unit along with some fresh coal are then used to generate

hydrogen needed for processing. A useful fuel gas is also produced in the hydrogen generation process.

Having developed a conceptual flow sheet for the process, It was then possible to simulate the plant and conduct the necessary calculations for material and energy balances. In addition, a plant-wide simulation has also been undertaken using the software ASPEN Plus. Optimization of some units/systems has been carried out to minimize capital and operating costs. In order to yield an environmentally benign plant, the removal and recovery of the sulfur by-product has been achieved via a desulfurization system. Heat integration has also been done by using the pinch techniques to synthesize a heat exchange network. Figure 2 summarizes the overall material balance for the plant.

ECONOMIC ANALYSIS

Fixed Cost Estimation

Estimation of fixed cost is done by identifying the total purchased equipment cost by relating equipment capacity to cost utilizing available data in literature. In particular, the cost of several pieces of equipment was determined by scaling-down based on a recent Bechtel/Amoco study (US DOE-PETC, 1993). This DOE-Funded study provides an extensive economic evaluation of direct coal-liquefaction in which Illinois #6 coal is liquefied to yield naphtha, light, middle, and heavy distillates. Design aspects throughout the plant were taken from several pre-existing liquefaction projects (Breckinridge, Wilsonville, HRI, etc.). Based on the capacities of the pieces of equipment needed in this co-liquefaction study, the cost may be calculated using the suggested Bechtel/Amoco scaling exponent of 0.71. The plant economics depends on the extent of conversion and yield to oil. For instance, for a 70% conversion and 90% yield, the purchased equipment cost of the major pieces of equipment was calculated to be $78 million. The liquefaction system (reactor, Ebullating pumps, etc.), accounted for 55% of the total purchased equipment cost. This is due to the very specialized design of the ebullated-bed liquefaction system needed for this type of conversion. From this purchased equipment cost, the fixed and total capital investments are estimated to be $373 million and $439 million, respectively. An

itemized account of the contributing elements to these investment costs appears in Fig. 3.

Operating Cost Estimation

In order to estimate the operating cost of the facility, four elements were considered; raw materials, shredding of plastics, labor and depreciation of fixed capital. The annual operating cost is a function of conversion and yield to oil. For example, when the conversion and the yield were taken as 70 and 90%, respectively, it was found that the annual production cost is $59 million. Figure 4, shows the main contributors to this cost. As can be seen, the two principal cost elements are depreciation ($36 million/year) followed by raw materials ($17 million/year).

RESEARCH UNDERWAY

At present, a complete profitability analysis is being developed. This analysis accounts for several additional aspects such as annual sales, tipping fees, break-even conditions and return on investment.

REFERENCES

Anderson, L. L. and W. Tuntawiroon, "Co-liquefaction of Coal and Polymers to Liquid Fuels", Preprints of ACS Meeting, Chicago, pp. 816 - 822, August 1993.

Taghiei, M. M., F. E. Huggins and G. P. Huffman, "Co-liquefaction of Waste Plastics with Coal", Preprints of ACS Meeting, Chicago, pp. 810 - 815, August 1993.

US DOE, PETC, "Direct Coal Liquefaction; Baseline design and system analysis", March 1993, Pittsburgh.

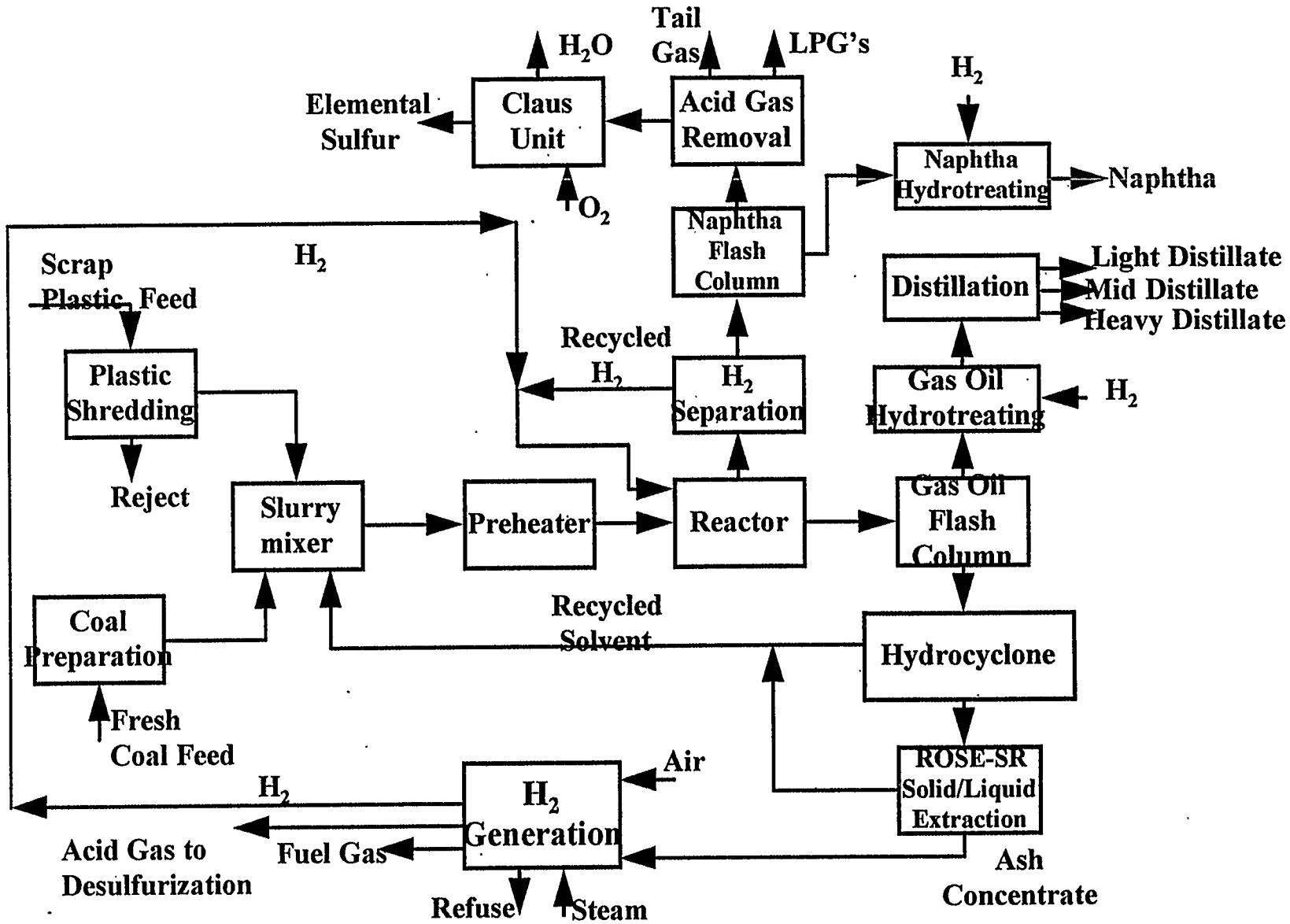

Fig. 1 Conceptual Process Flow Diagram for the Co-Liquefaction Plant

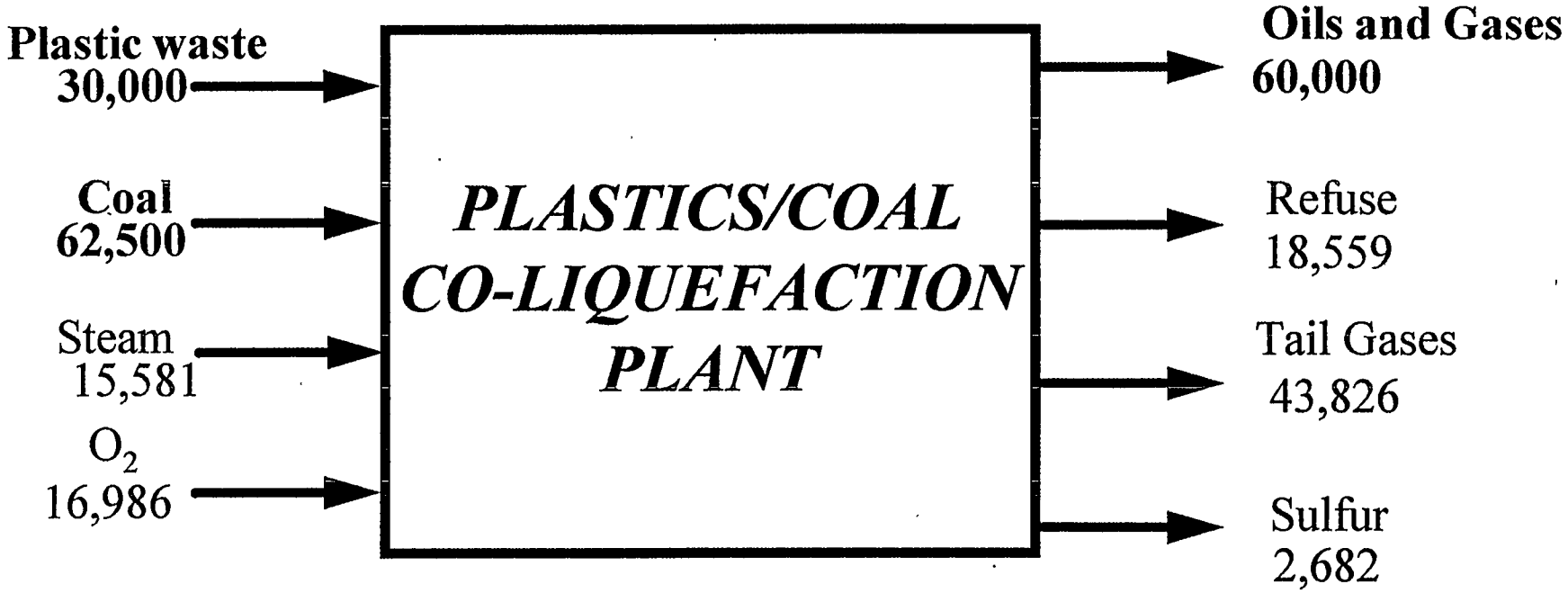

Fig. 2 Example of Overall Material Balance

(70% conversion of feed to reactor, 90% yield, all numbers are kg/hr)

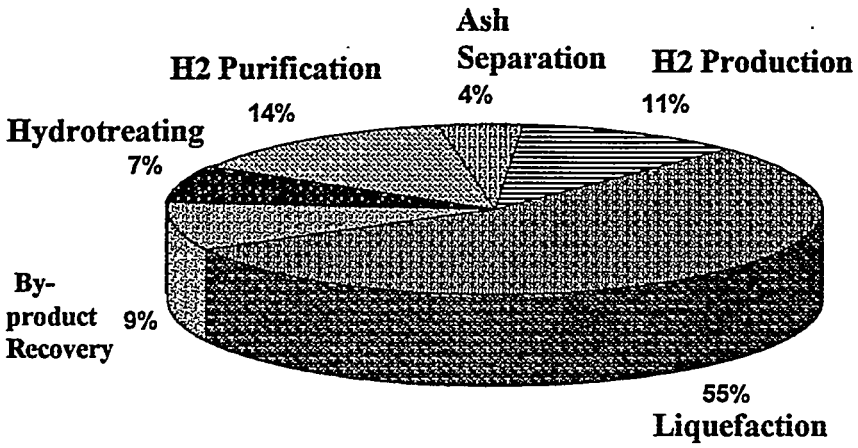

TOTAL = $373 MILLION

FIG. 3 EXAMPLE OF FIXED CAPITAL INVESTMENT (70% conversion, 90% yield)

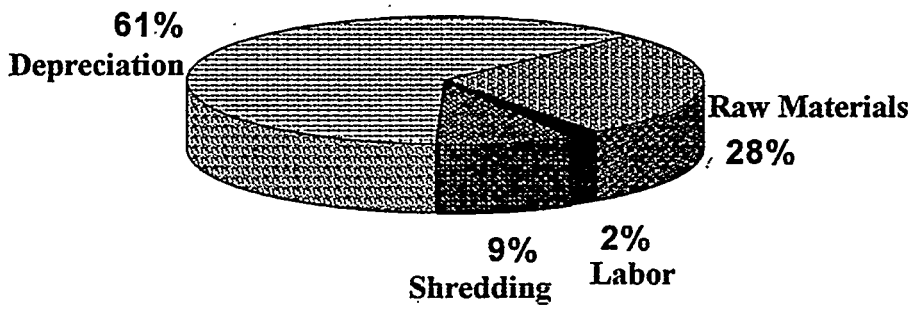

ANNUAL PRODUCTION COST = $59 MILLION /YR

FIG. 4 EXAMPLE OF TOTAL PRODUCTION COST (70% Conversion, 90% yield)

TASK I

Project I.9

COLIQUEFACTION

Larry L. Anderson and Wisanu Tuntawiroon
University of Utah

Disposal of municipal solid waste presents a serious environmental problem. Coprocessing of coal with waste polymers or waste rubber tires would have the beneficial effect of utilizing hydrogen from waste which is needed to make high quality liquid products. The relationship of product yield to the reaction variables of temperature, time, catalyst, and plastic to coal ratio were investigated by a series of laboratory coprocessing experiments.

Commingled plastic was obtained from Oregon through American Plastic Council. Samples of -100 mesh DECS 6 Blind Canyon Coals were obtained from the Penn State Coal Bank and stored at 0°C until use in experiments. The mixture of coal and polymer waste was shaken in an ultrasonic bath for about 1 hour before being put into a tubing reactor. Reactants were then pressurized by Hydrogen gas to 1000 psig. Samples were then reacted in a shaken tubing reactor at 160 rpm in a fluidized sand bath for various length of times. Different ratios of plastic and coal with different ranges of temperature were studied. All samples were extracted with cyclohexane (oil yield) and THF (total liquid yield) respectively then were characterized by simulated distillation.

Experiments were run in order to determine the effect of temperature and catalyst on coprocessing mixtures of coal and plastic. As seen in Figure I.9.1, the conversion yield from conversion of commingled plastic increases with temperature up to 430 °C, after which there is no significant change in conversion. Results show an increase in conversion due to cracking of high density polyethylene only at or above a temperature of 430 °C. Gas production amounted to as much as 85 percent at reaction temperature up to 480°C. Figure I.9.2. shows conversion of DECS 6 coal at temperatures from 400 to 480°C. Oil yields were constant with increasing

reaction temperature while gas product yields were increasing to a maximum at 450°C. From Figure I.9.3, one can observe that the conversion of coal and plastic waste depends on the reaction temperature. Oil yield and conversion reach their maximum values at 430°C.

Several sets of experiments done involved the use of iron based or zeolite catalysts. These experiments were run in order to determine catalytic effect on the coprocessing coal and plastic mixtures. From Figures I.9.5 and I.9.6, one can see that most of the catalysts tested show retrogressive reactions since the total liquid yield and/or the total conversion values were actually less than the thermal runs. Maximum oil product yields from hydroliquefaction of commingled plastic with DECS-6 coal were obtained with Fe_2O_3/SO_4 and H-ZSM5 Zeolite. Conversion and liquefaction yields for use of both catalysts are comparable to the thermal run. Further analyses and characterization of oil and gases by methods such as GC/MS, TGA/MS, and SFC/ MS need to be done to investigate the effect of plastic type, mixture composition, and other feed related variables. Some results on these studies, which are being done will be given in the next report.

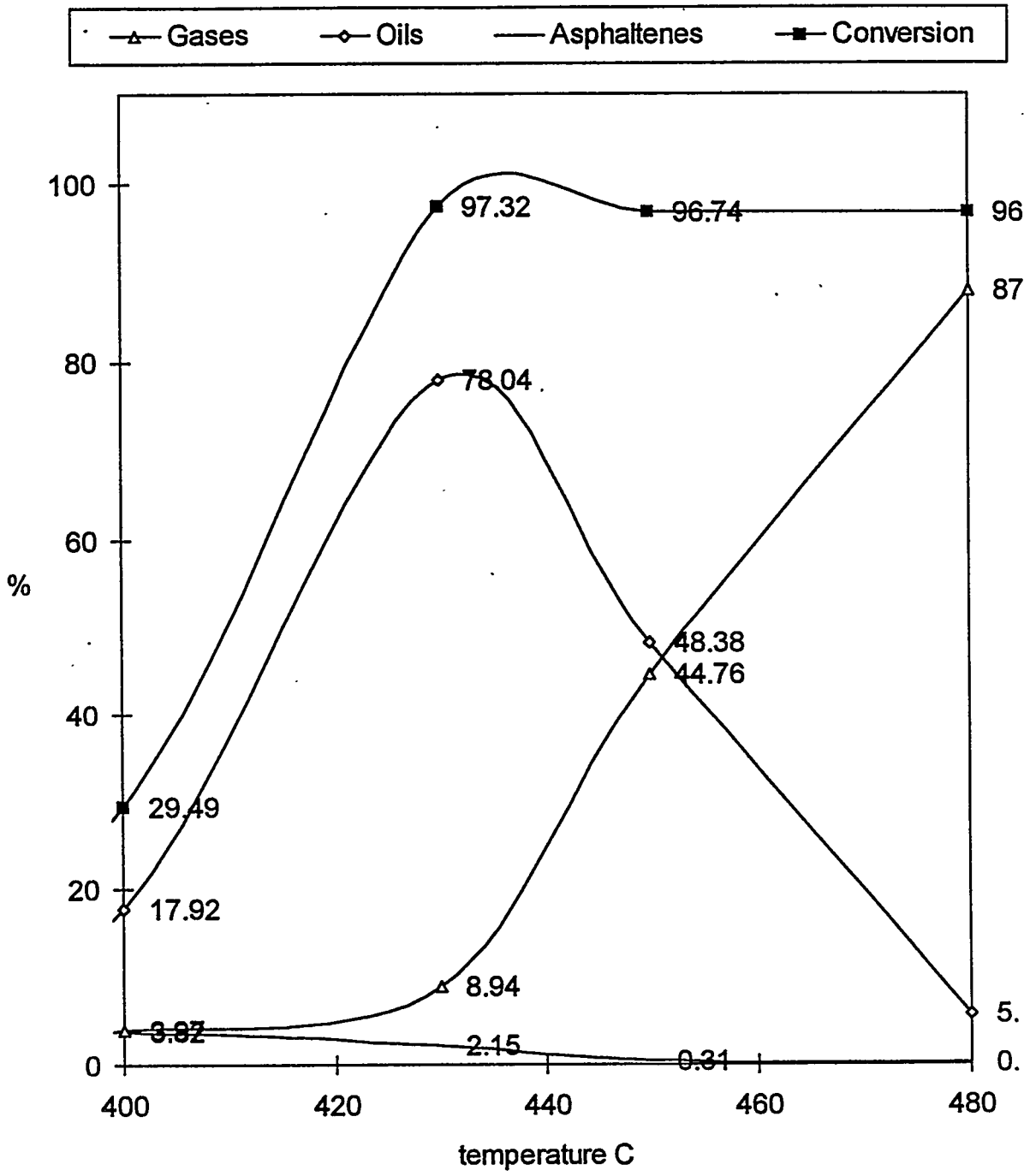

Fig I.9.1. Liquefaction of Commingled plastic for 1 hour, 100 psig H_2; values are weight percent of total feed material.

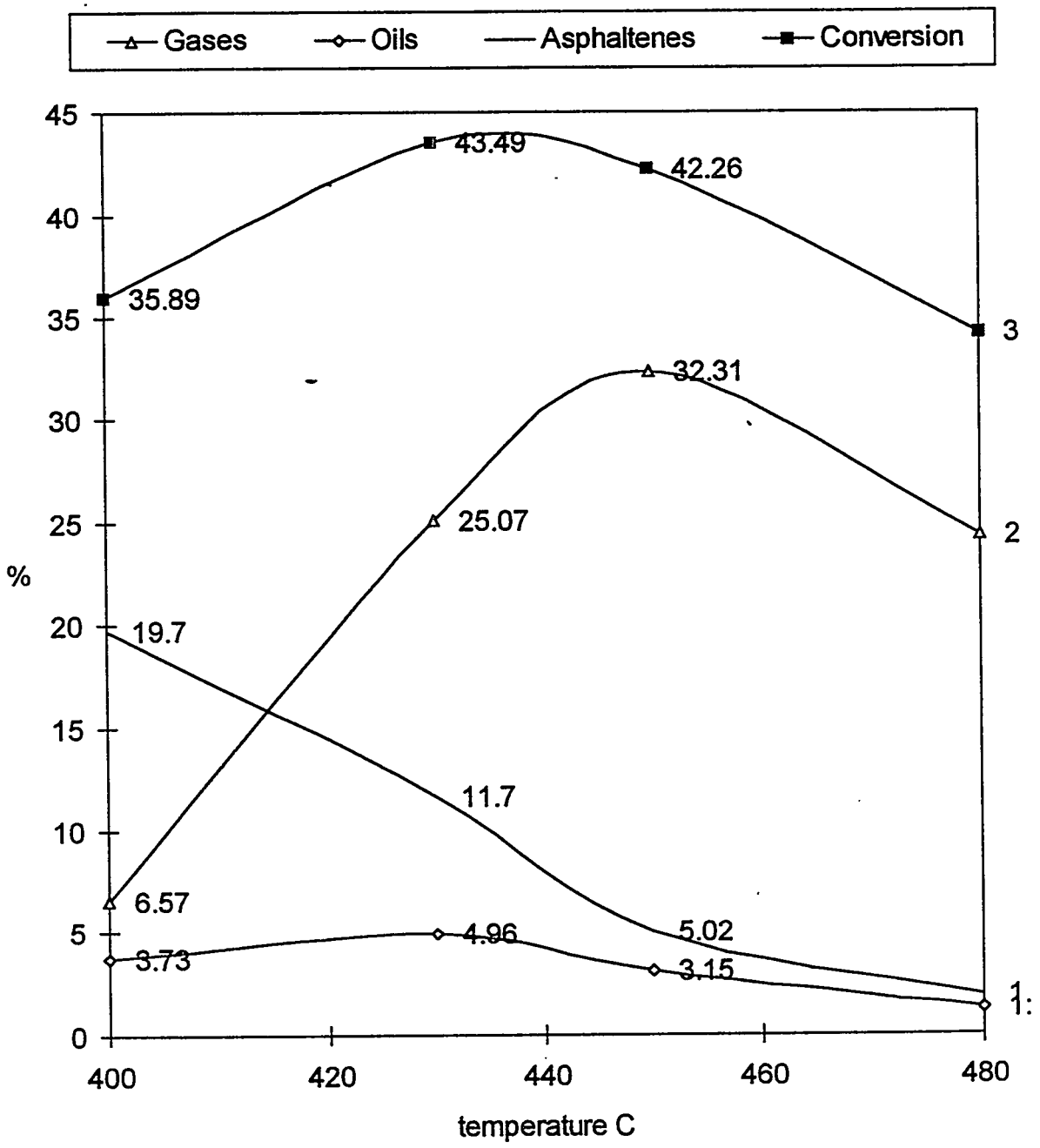

Fig I.9.2. Liquefaction of DECS 6, for 1 hour, 1000 psig H_2; values are weight percent of total feed material.

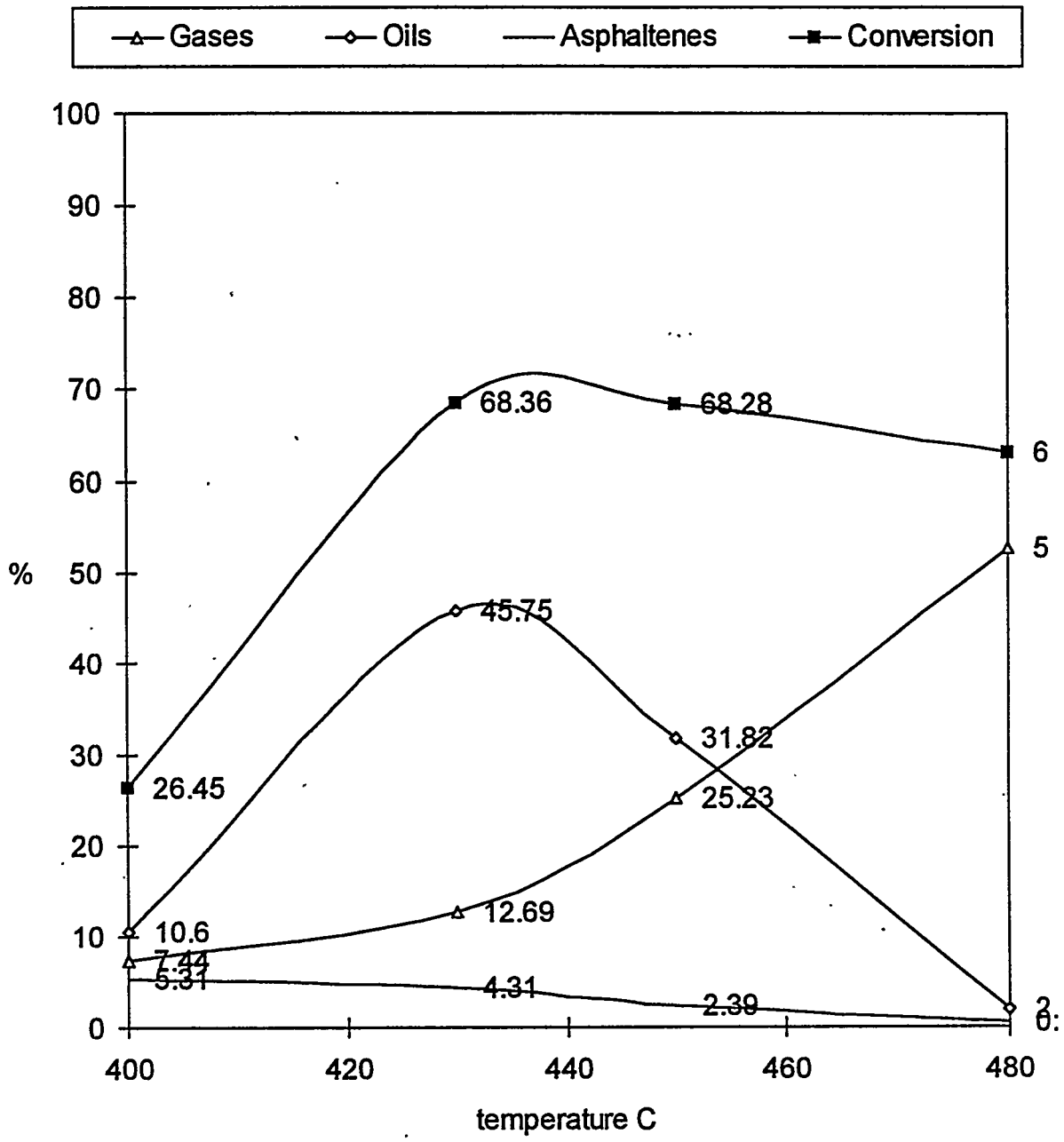

Fig I.9.3. Coprocessing of DECS 6 and commingled plastic for 1 hour, 1000 psig H_2, values are weight percent of total feed material.

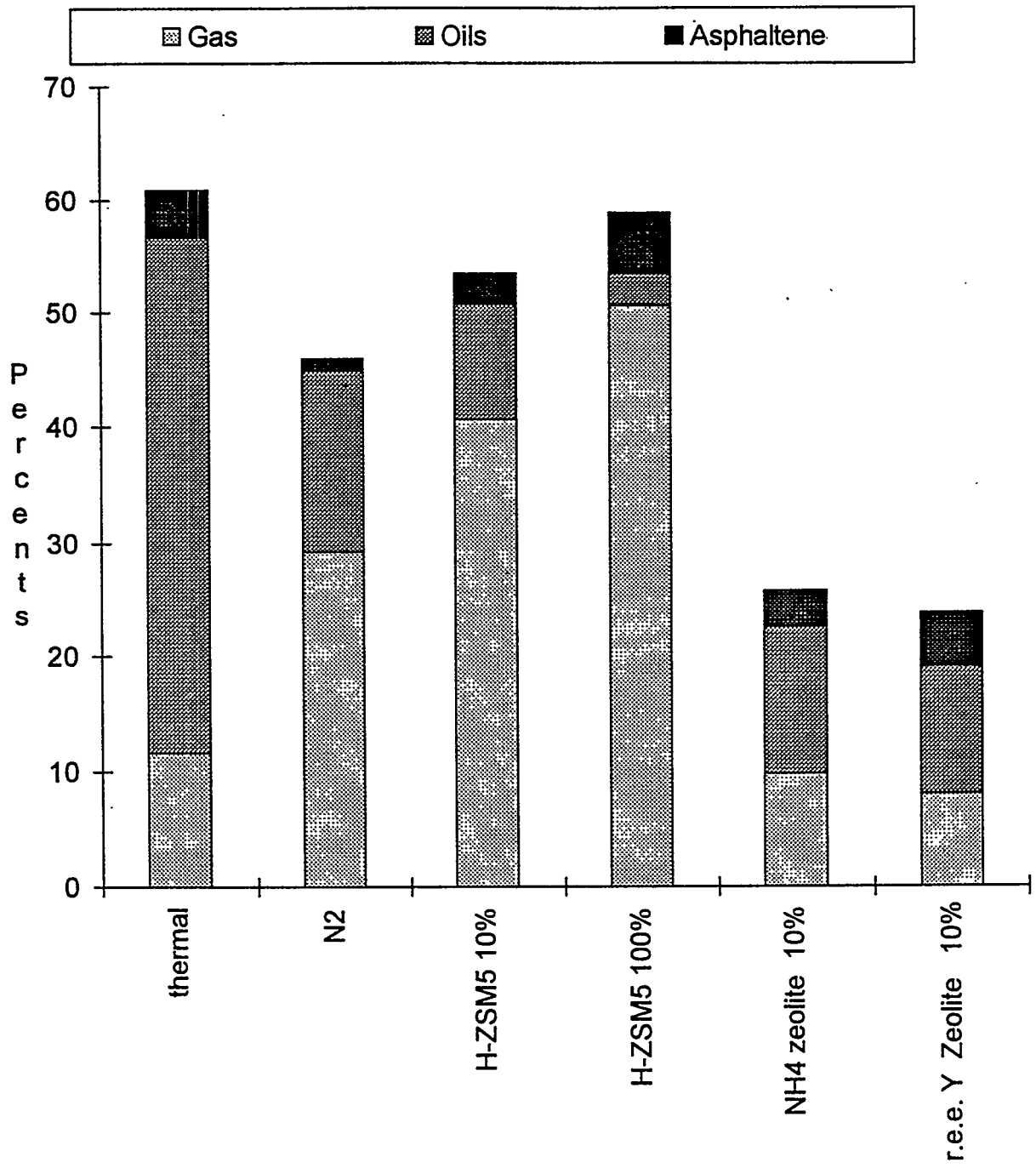

Fig I.9.4. Catalytic coprocessing of coal and commingled plastic with zeolite catalyst for 1 hour, 1000 psig H_2, 430°C. (values are weight percent of total feed material)

Fig I.9.5. Catalytic coprocessing of coal and commingled plastic with iron base catalysts for 1 hour, 1000 psig H_2, 430°C. (values are weight percent of total feed material)

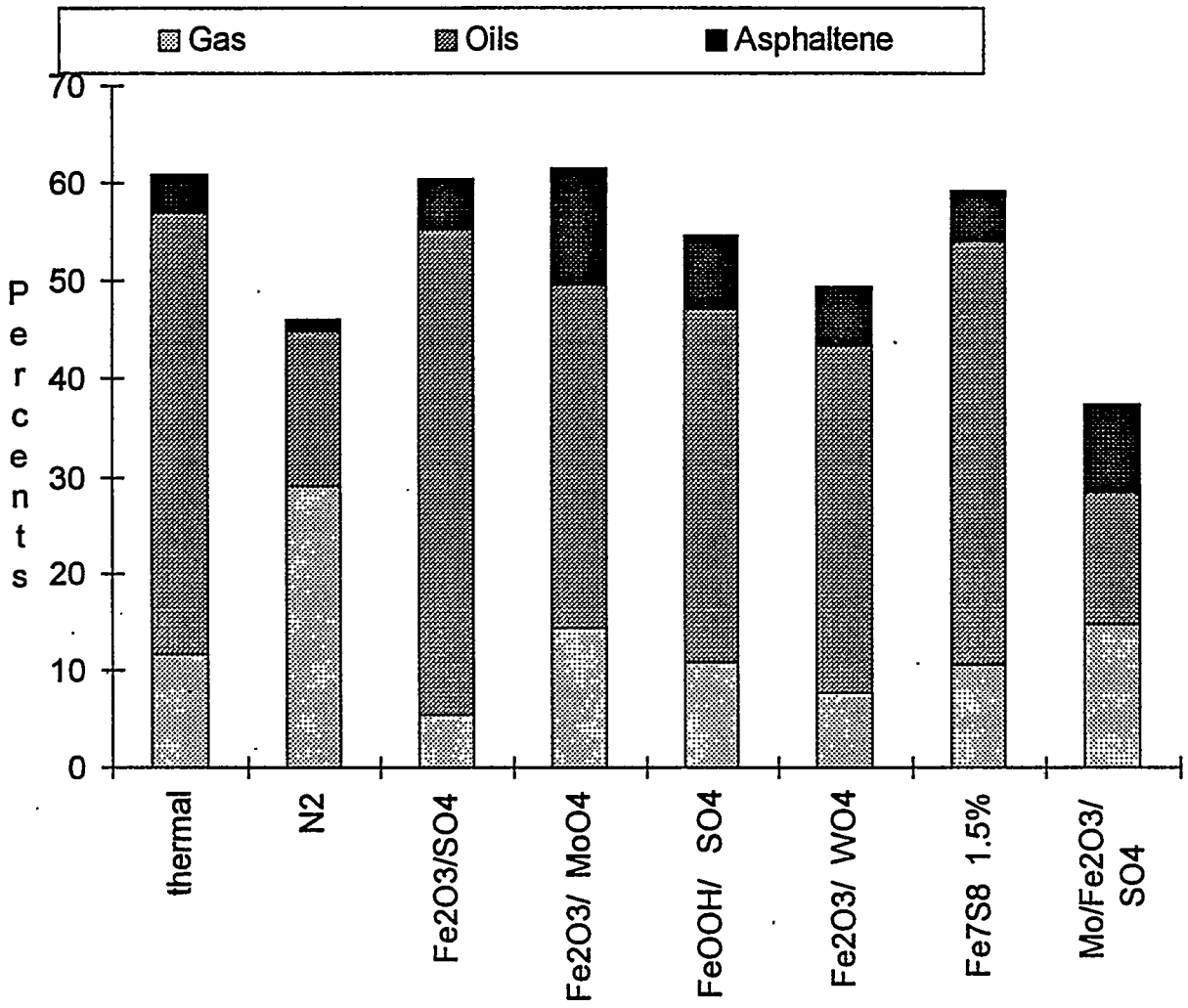

TASK II

CATALYSTS FOR COAL LIQUEFACTION TO CLEAN TRANSPORTATION FUELS

TASK II

Project II.1

BIFUNCTIONAL METAL-PROMOTED SOLID SUPERACIDS FOR COPROCESSING OF WASTES WITH COAL AND HEAVY OILS

Irving Wender, John W. Tierney and Gerald D. Holder
University of Pittsburgh

Introduction and Background

We have developed iron and tin-based catalysts (e.g. $Mo/Fe_2O_3/SO_4$ and SnO_2/SO_4) in recent years and found that they show significant activity in coal liquefaction and coal-heavy oil coprocessing reactions at 400°C and 1000 psig (cold) H_2[1-3]. These catalysts are comprised of three components, a metal oxide (Fe_2O_3 or SnO_2), an anion (SO_4^{2-}, MoO_4^{2-} or WO_4^{2-}) and a promoter metal (such as Mo) which provides a hydrogenation function to the catalyst. Promotion of 3-5 wt% of anions (especially SO_4^{2-}) on the metal oxides helps in the generation of strong acid sites on the catalyst surface[4]; however, the activity of the anion-modified iron oxides (with added sulfur) in coal liquefaction and coal-heavy oil coprocessing reactions is believed to be due to the *in-situ* formation of non-stoichiometric pyrrhotites[3]. In the past year, our work was focussed on determining the role of acidity of these catalysts during the heatup period (< 300°C) in coal liquefaction, since at higher temperatures and pressures, the acidity of the catalyst is lost due to reduction of the anionic component in the catalyst.

Accomplished Experimental Work

Experiments during the first half year were conducted with model compounds such as benzyl phenyl ether, bibenzyl, and alkylaromatics at mild conditions to understand the nature of the reactions that occurred over these solid acid catalysts. A few experiments were also carried out with DECS-17 (Blind Canyon) coal at mild

conditions to determine the effect of acidity on the quality of products obtained. The reactions were conducted in a 27 cc microautoclave and the products (from model compounds) were analyzed using GC and GC-MS. Coal liquefaction products were determined based on their solubility in THF and n-pentane. Simulated distillation was used to determine the quality of the oils obtained from coal.

Results and Discussion

Based on cracking and alkylation of long-chain alkylaromatics such as 1-phenyldecane and p-dodecylphenol that occur over the sulfated iron oxide catalysts at mild conditions (200°C and 500 psig (cold) H_2), we conducted reaction studies with polyaromatic compounds such as benzyl phenyl ether and bibenzyl, which contain strong linkages postulated to exist in coal. The results of reaction of benzyl phenyl ether over a $Mo/Fe_2O_3/SO_4$ catalyst at 200°C and 500 psig (cold) H_2 are shown in Table 1; about 63 wt% conversion of benzyl phenyl ether was achieved. Benzyl cations from the cleavage of C-O bond are readily formed over this solid acid catalyst at these conditions; there were also significant amounts of unidentified high molecular weight products (compounds with three or more aromatic rings) formed, possible precursors to coke formation. However, the reaction of bibenzyl over this catalyst at the same conditions resulted in almost no conversion indicating that this catalyst lacks the acidity to cleave the C-C bond at these mild conditions. Experiments with other model compounds such as diphenylmethane and 4-(1-naphthylmethyl) bibenzyl were also conducted over the sulfated iron oxide catalysts to determine the role of catalyst acidity in the cleavage of strong bonds. The strong alkyl-aryl carbon bonds in these compounds could not be cleaved over the sulfated iron oxide catalysts at 200°C and 500 psig (cold) H_2.

Experiments were also conducted with a low-sulfur (0.44 wt%) DECS-17 (Blind Canyon) coal with n-dodecane at mild conditions (250°C and 800 psig (cold) H_2) over sulfated iron oxide to determine whether the aromatic structures in coal could be alkylated with a paraffin. As shown in Table 2, use of the Fe_2O_3/SO_4 catalyst gave similar conversions but significantly higher selectivities to oils (n-pentane solubles) compared to the thermal reaction. The $(H_\gamma/H_\beta)_{alkyl}$ ratio of oils from ^{1}H-NMR

indicated that the oils of the catalytic run had slightly more isomerized or short chain paraffins compared to the thermal run. Analysis of asphaltenes (from $(H/C)_{atomic}$ ratios) between the thermal and catalytic runs of DECS-17 coal showed negligible improvement in hydrogen uptake due to the presence of a catalyst at these conditions. The simulated distillation results of the oils obtained from DECS-17 coal over a Fe_2O_3/SO_4 catalyst at mild conditions is shown in Figure 1. The boiling point curve seems to support the 'mobile phase concept' in vogue in the coal liquefaction literature in the 1970-80s. Many of the large polynuclear aromatic, aliphatic and heteroatom linkages present in coal are believed to exist as macro-cages and smaller molecules (lighter boiling compounds)--known as 'the mobile phase'--are postulated to be trapped inside the macromolecular framework. Liquefaction under relatively milder conditions can lead to opening of the macro-cages by cleavage of weak bonds in their structure leading to release of the trapped mobile phase. This could be a reason for the dramatic increase in boiling points after ~450°F in Figure 1. The oils from the thermal run also gave a very similar boiling point distribution as Figure 1, indicating that the catalyst is not effective in improving the quality of oils at these conditions.

Nevertheless, the catalyst seems to be useful in increasing the oil yield and decreasing the asphaltene yield; this is expected of an active catalyst because the conversion of asphaltenes to oils in coal liquefaction is almost entirely a catalytic step[5]. By promotion with a variety of active metals in small amounts along with a suitable anionic modification of iron or other oxides, we hope to enhance the quality of oils produced from coal in conjunction with depolymerization of waste plastics.

Future Work

By incorporating various promoter metals and anions onto metal oxides (such as ZrO_2 and Fe_2O_3), we hope to obtain novel catalysts which are effective in achieving high yields of improved quality products (based on boiling points) from plastics depolymerization and coal plus plastic coprocessing reactions. Metals such as ruthenium (10-100 ppm) which are known to be extremely active in coal liquefaction[6] would be suitable candidates for promotion onto anion-modified iron oxides and can

also be employed as such in small amounts (e.g. as RuS_2) and the effect of such modifications on oil yields from coal+plastics will be ascertained. Since ruthenium forms oxides of a variety of oxidation states, novel catalyst formulations such as Ru_2O_3/SO_4 will be developed and used in our reaction studies. Other metal oxides such as TiO_2, Al_2O_3 and SnO_2 will be promoted with SO_4^{2-} or other suitable anions and active hydrogenation metals and their activities in plastics depolymerization reactions as well as in coprocessing reactions will be ascertained.

Some experiments with model compounds will be performed in order to understand the nature of catalysis occurring over these dispersed catalysts. An aim would be to conduct these experiments in the presence of small amounts of sulfur or nitrogen compounds; the results will help determine the tolerance of the solid acid catalysts towards organic sulfur/nitrogen and also may help in developing novel solid acid catalysts in the future which are resistant to these deactivating agents. We will also investigate the use of multifunctional solid acid catalysts, especially in the presence of paraffins/olefins that can furnish carbenium ions (R^+) which can alkylate aromatic structures in coal. Addition of C_5-C_{16} paraffins derived from plastic wastes to model compounds and to coal will be carried out in the presence of these multifunctional solid acid catalysts.

Based on the results, we would characterize active catalysts, before and after reaction, by XRD, TEM/SEM, and EXAFS to determine physicochemical properties and by FT-IR and TPD of ammonia/pyridine to determine acidity-related properties.

References

1. Pradhan, V.R., J. W. Tierney and I. Wender, *Energy & Fuels*, **5**, pp. 712-720 (1991).

2. Pradhan, V.R., J. Hu, J. W. Tierney and I. Wender, *Energy & Fuels*, **7**, pp. 446-454 (1993).

3. Pradhan, V.R., Ph.D. dissertation, University of Pittsburgh, Pittsburgh, PA (1993).

4. Tanabe, K., H. Hattori, T. Yamaguchi, *Critical Reviews in Surface Chemistry*, **1**(1), p.1 (1990).

5. Pradhan, V.R., G. D. Holder, I. Wender and J. W. Tierney, *Ind. Eng. Chem. Res.*, **31**, pp. 2051-2056 (1992).

6. De Los Reyes, J. A., Vrinat, M., Geantet, C. and Breysse, M., *Catalysis Today*, **10**, pp. 645-654 (1991).

Table 1. Products obtained from the reaction of benzyl phenyl ether over a $Mo/Fe_2O_3/SO_4$ catalyst at 200°C and 500 psig (cold) H_2 for 60 minutes. Total conversion was 63.2 wt%. The unidentified products (~ 60 wt% selectivity) consisted of higher molecular weight compounds.

PRODUCT	SELECTIVITY (wt%) OF IDENTIFIED PRODUCTS
toluene	0.10
phenol	19.0
2-methylphenylphenol	8.9
4-methylphenylphenol	11.7

Table 2. Results obtained from reactions of Blind Canyon (DECS-17) coal + n-dodecane (1:2) at 250°C and 800 psig (cold) H_2.

Catalyst Used	Total Conversion (wt%)	% Oils + Gases (% selectivity)	$(H/C)_{atomic}$ of asphaltenes	$(H_\gamma/H_\beta)_{alkyl}$ of oils (from ^{1}H-NMR)
None	15.6	8.5 (54.7)	0.986	0.457
Fe_2O_3/SO_4	19.2	12.8 (66.7)	0.987	0.561

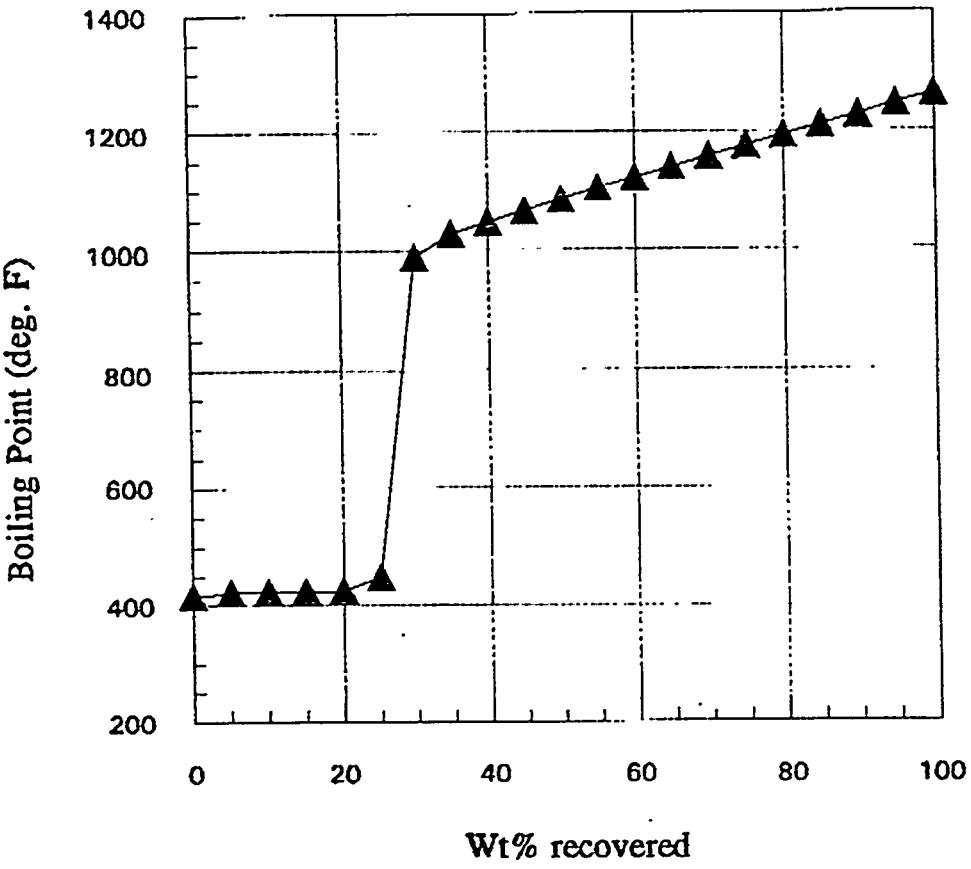

Figure 1. Simulated distillation of oils from DECS-17 coal over Fe_2O_3/SO_4 catalyst at mild conditions (250°C, 800 psig (cold) H_2).

TASK II

Project II.2

USE OF AEROSOL-GENERATED FINE PARTICLE MIXED-METAL CATALYSTS FOR DIRECT COAL LIQUEFACTION TO TRANSPORTATION FUELS

Dady B. Dadyburjor, Alfred H. Stiller,
Charter D. Stinespring and Ramesh K. Sharma
West Virginia University

Our work on coal liquefaction is focused on the use of ferric-sulfide-based catalysts generated by using both an aerosol reactor [1] and the non-aerosol techniques [2]. The objective of the aerosol reactor work is to optimize the synthesis conditions in the aerosol reactor to obtain the catalyst particles which are in the nanometer size range. We are also studying the effect of adding a second metal such as cobalt, nickel, magnesium and molybdenum on the activity of iron-sulfide catalysts. For experimental convenience these mixed-metal catalysts are generated by the non-aerosol techniques. These catalysts are characterized by various spectroscopic techniques such as Auger electron spectroscopy (AES) and x-ray diffraction (XRD) in order to correlate the structural properties with their catalytic activity.

In this report, we present the results of coal liquefaction experiments using the above two families of catalysts, i.e. a series of (non-aerosol) mixed-metal catalysts containing molybdenum, in combination with iron sulfide, and the aerosol-generated iron-alone catalysts. In the case of mixed-metal catalysts particular attention is paid to the effect of exposure of the catalyst to air on its activity and product slate. Attempts are also being made to investigate the role of catalyst during liquefaction using model compounds such as cumene and phenanthrene.

The details of the design and construction of aerosol reactor and the method of preparation of aerosol catalysts have been described elsewhere [1]. The mixed-metal catalysts containing molybdenum were impregnated *in-situ* on the coal. These catalysts are designated as Bx1 and Bx2. Catalysts of type Bx1 were prepared by first

mixing the coal in aqueous sodium sulfide solution and then reacting the slurry with the aqueous ferric acetate (made by reacting ferric hydroxide and acetic acid) and ammonium heptamolybdate solutions. The resulting suspension was filtered and vacuum dried at 85°C to obtain the mixed-metal catalysts. The catalysts designated Bx2 were prepared similarly except that the ammonium heptamolybdate solution was added after filtering and drying the iron-sulfide/coal slurry. For both Bx1 and Bx2 catalysts, x is 2 or 3, depending upon the loading. The catalyst loading in most runs in this report was 1.67 wt% based on dry, ash-free coal. The Mo/(Mo+Fe) ratios were 0.05, 0.08, 0.1, 0.15 and 0.25.

The liquefaction was performed at 350-440°C for 30 min using a hydrogen pressure of 1000 psi (cold). To ensure the presulfiding of the catalyst, 0.1 ml of CS_2 was also added to the reaction mixture. The coal used is a high-volatile A bituminous coal from the Blind Canyon seam in Utah (DECS-6). It was received from the coal bank at the Pennsylvania State University and ground to -60 mesh under nitrogen. It contains 49% volatile matter and 51% fixed carbon. Its ash content is 6.3%.

I. Mixed-Metal Catalysts

Previously, it was observed that the conversion of coal in the absence of catalyst was nearly 16 percentage points lower when phenanthrene was used as solvent compared to that with tetralin as solvent. This indicates that the use of phenanthrene can more easily differentiate between the activities of various catalysts than the use of tetralin. Hence all the runs in this report were made with phenanthrene as solvent.

Figure 1 shows the effect of f_{Mo}, i.e., Mo/(Mo+Fe) on coal conversion. Most points in the figure represent an average of two or more runs. The conversion increases slightly with f_{Mo} and the maximum value is obtained at f_{Mo} of around 0.08-0.15. The oil+gas yield is maximum when f_{Mo} is 0.1. It is not clear if the activity and selectivity of the catalyst are affected by its exposure to air. To study this aspect, runs were made such that the catalyst was not exposed to air at any time during or after the impregnation. The results are presented in Figure 2. It is seen that the conversion with iron-alone catalyst (f_{Mo}= 0) increased to 87% when the catalyst was prepared and

stored in N_2 atmosphere. The conversion to oil plus gas fraction also increased by 4 percentage points to 26%. With the addition of molybdenum, the catalytic activity increased further. The highest conversion is obtained at f_{Mo} of 0.1 when the catalyst is not exposed to air. The oil+gas yield is also highest at the same f_{Mo} ratio. This indicates that the activity and selectivity of the mixed-metal catalysts are significantly altered by their exposure to air. This may be due to the oxidation of active phase. Also, it seems that the catalytic activity was not dependent on the stage at which Mo was added to the catalyst i.e. before filtration or after filtration. This suggests that no molybdenum was lost to the filtrate during the preparation of the catalyst.

The effect of temperature on conversion and yield is shown in Figure 3. Again, the catalysts in these runs were not exposed to air. It is seen that both the conversion and oil+gas yield increase with temperature. In the absence of catalyst (thermal), the conversion was highest at 70% at 400-440°C. The oil+gas yield was highest (40%) at 440°C. With iron-alone catalyst (f_{Mo}=0), the conversion increased further and was about 90% at 440°C. However, the highest oil+gas yield, which was obtained at 440°C, remained unchanged by the addition of the catalyst. Using the Fe-Mo-S catalyst (f_{Mo}=0.1), the conversion and oil+gas yield increased further and were highest at 92% and 42%, respectively, at 440°C. These results indicate that the addition of molybdenum is beneficial to the activity and selectivity of the catalyst especially above 400°C.

II. Aerosol-Generated Catalysts

The iron-alone aerosol catalysts were prepared under various conditions shown in Table I. The catalyst particles were found to be spherical in shape, about 0.5 micron in diameter and the surface of the spheres appeared to be an assemblage of very small crystals with an edge length in the nanometer range. The particle size determinations were made by laser light scattering and by transmission electron microscopy (TEM) measurements. The pyrrhotite /pyrite ratios, PH/PY, as determined by the acid dissolution technique, are around 1, which is in agreement with hydrothermal disproportionation experimental results for ferric sulfide. The

characterization of the catalyst by pycnometry, AES and XRD indicated interesting crystal structures. The S/Fe ratios at the surface were found to be higher compared to those in the bulk. Some of the aerosol catalysts were subjected to Mossbauer spectroscopy and transmission electron microscopy (TEM) in the laboratory of Professor Huffman at the University of Kentucky. The Mossbauer spectra show mainly oxides, consistent with the catalysts being exposed to the air. The TEM results indicate that very small, sub-micron particles can indeed be seen in the aerosol catalyst samples.

These catalysts were used for coal liquefaction at 350°C with tetralin as solvent. CS_2 was used to ensure the presulfiding of the catalyst. The run time was 60 min. A catalyst loading of 5 wt% based on iron was used. The results are presented in Table II. Again, the data represent averages over multiple runs. With these catalysts, both the conversion and asphaltenes yield increase by about 10 percentage points over the thermal values. The increase is consistent with the corresponding values for the iron-alone catalysts made by the non-aerosol techniques. However, the oil and gas yield does not increase by the addition of aerosol catalyst. These catalysts were generated without regard to exposure to air. As observed earlier with the non-aerosol catalysts, both the conversion and yield are affected by the exposure of the catalyst to air.

III. Model Compounds

We have initiated an investigation of the role of the catalyst and solvent during cracking and hydrogenation reactions. Phenanthrene and cumene are being used as model compounds to measure the hydrogenation and cracking activities, respectively. Three catalysts, namely, an aerosol catalyst, a hydrothermally disproportionated catalyst, and a catalyst disproportionated at high temperatures in hydrogen are being studied. Runs are made in the tubing bomb reactor at conditions similar to those for coal liquefaction, i.e., 400°C, 1000 psi H_2 (cold), 30 min run time. The catalyst is characterized before and after the reaction by the auger electron spectroscopy (AES) and the atomic absorption (AA). Preliminary results indicate that the hydrogenation activity of the catalyst is dependent in PH/PY ratio and decreases at high PH/PY ratios. This is consistent with the observations made with coal. The AA analysis

showed that the PH/PY ratios in the spent catalysts are higher than those in the fresh catalysts and the increase is dependent on the availability of hydrogen during liquefaction. Further work is necessary to completely analyze the data and correlate it with the surface properties of the catalyst.

IV. Spectroscopic Techniques

Three separate studies were started to characterize the catalysts using spectroscopic techniques. In the first study, the catalyst is characterized from start to finish during coal liquefaction; the second establishes procedures for removing elemental S from the as-prepared catalyst, to improve the reliability of the surface S/Fe ratio; and the third confirms the acid dissolution technique for distinguishing FeS_2 from pyrrhotites.

V. REFERENCES

1. Stiller, A.H., Agarwal, S., Zondlo, J.W., and Dadyburjor, D.B., Proc. 10th Ann. Intern. Pittsburgh Coal Conference, Chiang, S.-H., Editor, Pittsburgh Coal Conference, 258 (1993).

2. Dadyburjor, D.B., Stiller, A.H., Stinespring, C.D., Zondlo, J.W., Wann, J.-P., Sharma, R.K., Tian, D., Agarwal, S., and Chadha, A., Prepr. Amer. Chem. Soc., Div. Fuel Chem., Washington DC (1994).

Table I

Characterization of Aerosol-Generated Fe-S Catalysts

#	Precursor Conc. M	Prep Pres. psi	Prep Temp °C	PH/PY	Density g/cc	Bulk S/Fe EDX	Surface S/Fe AES
A7	0.01	200	200	0.96	-	2.5	3.6
A8	0.01	100	200	0.66	4.6	2.5	3.3
A9	0.1	100	200	0.92	4.27	0.9	2.0
A12	0.01	100	250	-	4.66	1:9	-

Table II

Coal Liquefaction with Aerosol-Generated Iron Sulfide Catalysts

DECS-6 coal, tetralin, 0.1 ml CS_2, 5% catalyst loading,
350°C, 1000 psi (cold) H_2, 60 min, 500 cpm

Run	Conversion	Asphaltene Yield	Oil + Gas Yield
----------wt % of coal----------			
Thermal	54.9	41.2	13.6
A8	64.9	55.6	9.3
A9	63.0	52.1	10.8
A12	64.4	54.8	10.9

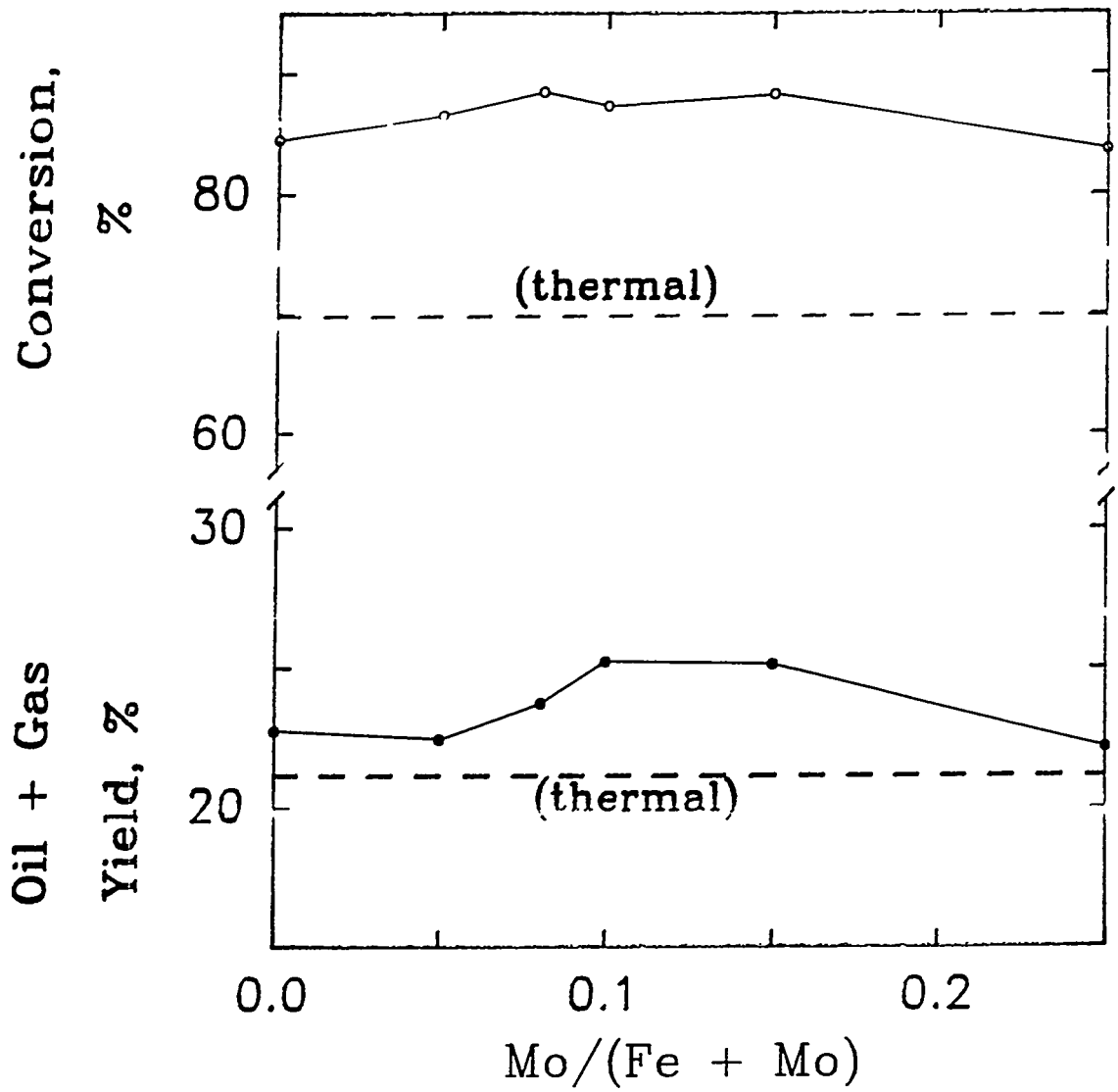

Figure 1. Effect of f_{Mo} on conversion and yield of coal. Conditions: 400°C, 30 min, 1000 psi H_2, phenanthrene solvent, 0.1 ml CS_2, 1.67% catalyst loading.

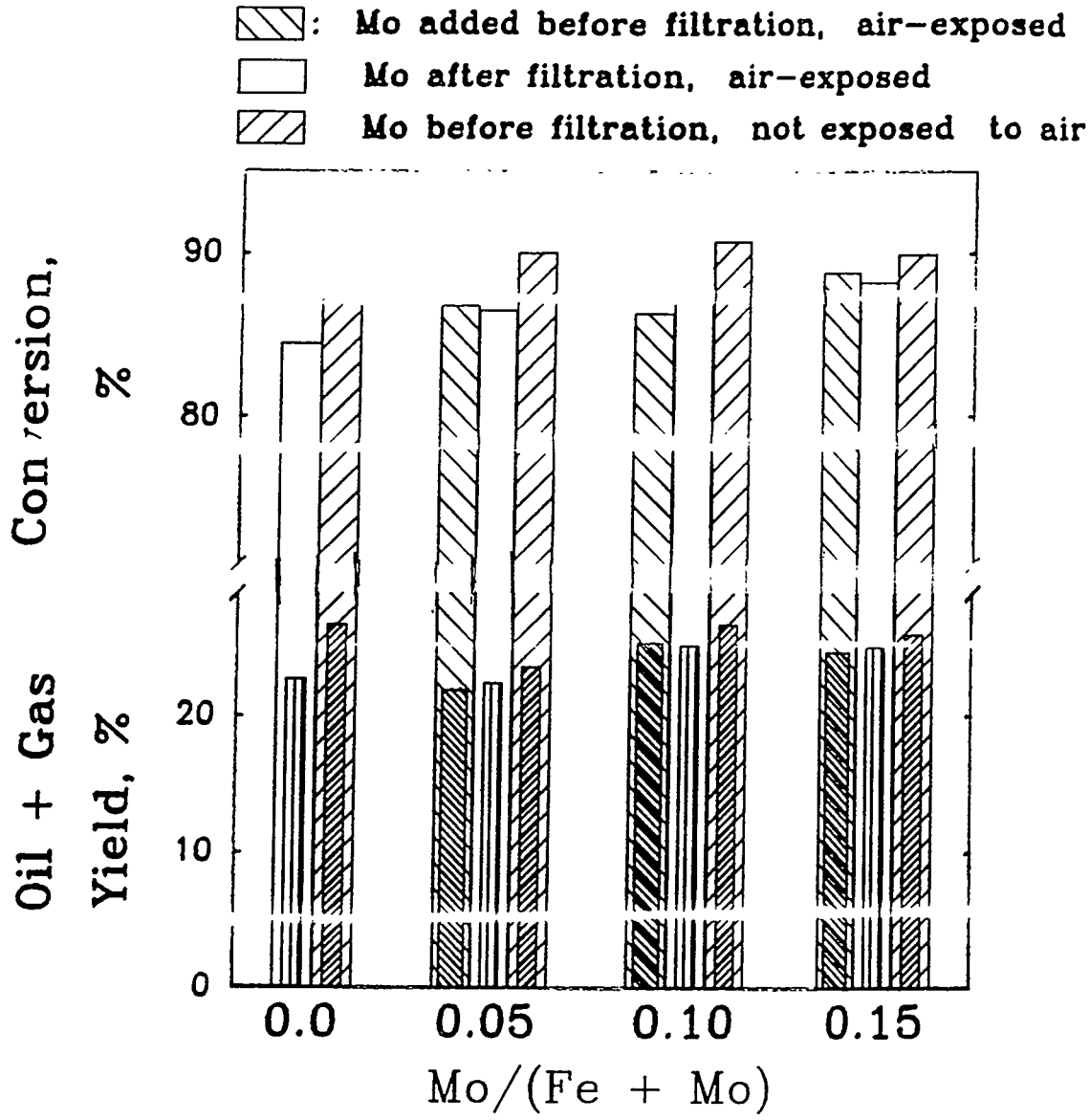

Figure 2. Effect of preparation conditions on conversion and yield. Conditions same as in Figure 1.

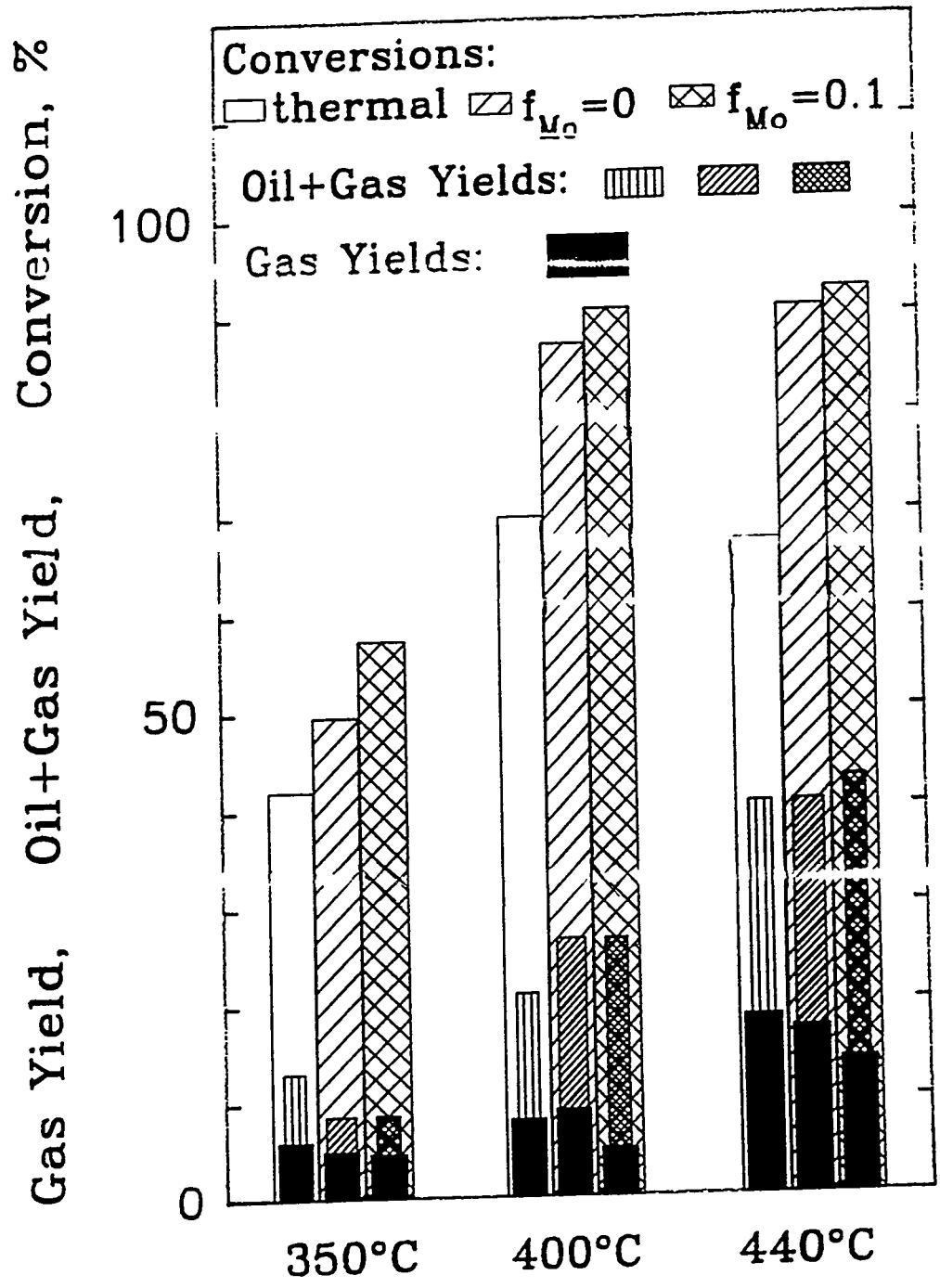

Figure 3. Effect of temperature on conversion and yield of coal. Other conditions same as in Figure 1.

TASK II

Project II.3

STUDIES IN CATALYTIC HYDROPROCESSING FOR UPGRADING PRIMARY COAL DERIVED LIQUIDS TO CLEAN TRANSPORTATION FUELS

J.A. Guin, X. Zhan, H.S. Joo, and R. Menon
Auburn University

Some of our work on the development of hydrotreating catalyst promoted with noble metals has been summarized in a recent article which will be presented at the AICHE meeting in Houston, April 1995. This quarter we continued our work in this area to study the promotion effect of noble metals other than Pt , e.g., Ir and Ru. Both model compounds and coal derived liquid were used to examine the catalyst activities. We also have successfully modified our continuous reactor to upgrade coal derived liquid. Several runs have been performed with satisfaction and the work is now in progress. More results in this regard will be reported later as some of the product analysis information is still not available so far. Future work includes the upgrading of HRI coprocessing liquid from coal/waste polymers.

TUBING BOMB REACTIONS

Catalyst Preparation. Three types of commercial Al_2O_3 supported catalysts (Criterion 424 NiMo, Cyanamid 1442B CoMo and Crosfield 550S NiW) were used to investigate the noble metal promotion effect. Catalysts were crushed and sieved to between 100 and 200 mesh. The noble metal promoted catalysts were prepared by an incipient wetness technique and then dried in air overnight and calcined at 450°C for 3 h. An aqueous solution of 37% HCl was used to dissolve Ru salts ($RuCl_3$ and $Ru_3(CO)_{12}$). The Ir precursor was H_2IrCl_6 in aqueous solution. Sulfided catalysts were used in all experiments. Sulfidation was performed with dimethyldisulfide (DMDS) in a tubing bomb at 300°C for 2 h.

Experimental. All reactions took place in 20 cc 316 ss tubing bomb

microreactors (TBMR) which were agitated in a fluidized sand bath. A reactant solution (6g) containing 2 wt% pyridine in hexadecane was used for model compound studies and coal liquid (3g) for upgrading. Experiments with tubing bombs were charged with 1000 psig cold hydrogen pressure and performed at 350°C using 0.1 g catalyst for model compound reactions and at 375°C for 1 hr using 0.4 g catalyst for upgrading coal liquid. DMDS as a sulfur compound was added to maintain the catalysts in a sulfided state.

Results. The effect of Ru and Ir loadings on pyridine HDN activity was examined in the range of 0-2 wt% loadings and the results are in Figs. 1 and 2. In Fig. 1, RuNiMo (1.0 wt%) and RuCoMo (0.5 wt%) exhibited increased HDN activity compared to original catalysts where the catalysts were made using the precursor, $RuCl_3$. For other catalysts, Ru promotion effects were generally negligible or negative. In Ir promoted NiMo and CoMo experiments, the HDN activity increased with increasing Ir wt% in the range of 0-2 wt% as shown in Fig. 2. Ir did not affect the activity of NiW.

In succeeding experiments, 1.0 wt% Ru and Ir loaded catalysts were chosen. Pyridine HDN activities with original and promoted catalysts under the same condition are compared in Fig. 3 where Ru (A) and Ru(B) catalysts were made using $RuCl_3$ and $Ru_3(CO)_{12}$, respectively. In NiMo and CoMo experiments, Ru(A)NiMo, IrNiMo, and IrCoMo catalysts showed higher activity than the original ones and the activity of IrNiMo was highest among them. As before, promotion effects on NiW were negligible. The effect of different Ru precursors was examined. In NiMo, the activity of Ru(A) was 10 % higher than that of Ru(B) as shown in Fig. 3. For CoMo and NiW, little effect was observed. The product distributions with original, Ru(A), and Ir promoted NiMo are shown in Fig. 4. For IrNiMo, slightly higher pyridine hydrogenation (lower pyridine concentration) and relatively higher C-N bond scission (lower pentylamine and higher n-pentane) was observed compared to the unpromoted catalyst. The product distribution with RuNiMo was between original and IrNiMo. The increased pyridine HDN activity with IrNiMo was thought to mainly result from enhanced C-N bond scission by Ir.

Coal liquid was reacted with the above catalysts in TBMR's and the HDN

activity of each run is shown in Fig. 5. In contrast to the result of model compound reactions, the promotion effect was negligible in NiMo and negative in CoMo and NiW. In order to examine the effect of H_2S, experiments with IrNiMo with and without added DMDS were performed. Some researchers[1-3] had reported that H_2S enhanced HDN, but H_2S had little effect on the reaction in this experiment.

CONTINUOUS UPGRADING STUDIES

Experiment. The upgrading studies also were conducted in a continuous upflow reactor with a coal middle distillate. Three commercial catalysts, NiMo, CoMo, and NiW supported on alumina, and their Pt promoted forms were used to examine the catalytic activity maintenance and product distribution. The impregnation of Pt on the catalysts was the same as described previously in the TBMR work. The catalysts were crushed to 16-25 mesh and packed in the center of the 18-inch reactor tube. Typically, 5 g of catalyst was diluted with about 20 g of 1.0 mm glass beads to extend the length of catalytic bed to 6 inches. The catalysts were preceded and followed by 6 inches of the same glass beads.

Prior to the start of a run the catalyst was presulfided using 5 wt% CS_2 in cyclohexane at a flow rate of 0.05 ccm and hydrogen at 100 sccm. The pressure was 1400 psig and temperature was programmed as follows: 210°C for 6 hours and then raised to 310°C at 15°C/h, 310°C for 2 hours and then raised to 400°C at 25°C/h, and 400°C for 2 hours. At the end of presulfidation, the reaction feeds were started immediately at 1400 psig and 400°C with flow rates of 0.2 ccm for coal liquid and 100 sccm for hydrogen. These flow rates give a WHSV of 2.34 and hydrogen rate of 2800 scf/bbl.

The reaction product was collected periodically and subjected to analysis for specific gravity and elemental analyses for C, H, and N contents. Product distribution of paraffins, naphthenes, monoaromatics, and polyaromatics was estimated using existing empirical correlations for coal liquids from the literature[4].

Results. Figure 6 shows the effect of catalyst on the specific gravity (correlated to H/C ratio) of product oil with time on stream. It can be seen that under our experimental conditions, the effect of thermal reaction on the reduction of

specific gravity of oil is not as great as that of the catalytic reactions. Of the three alumina supported commercial catalysts, it appears that NiMo and CoMo have approximately the same activity for aromatic hydrogenation, which is related to the specific gravity. NiW is the least active of the three catalysts, in contrast to reports in the literature[5] that NiW is superior to Mo catalysts for aromatics saturation in synthetic crudes. An interesting observation is that for these unpromoted catalysts, the specific gravity of first sample (produced in the first 24 hours) is much lower than those collected afterwards indicating a significant deactivation of the catalysts in the initial reaction stage. After 36 hours, the reaction reaches steady state and the product specific gravity is essentially stable. For Pt promoted NiMo, the catalyst deactivation behavior is different from that of NiMo as the specific gravity increases gradually after 36 hours to approach that of NiMo at steady state. The high specific gravity of the first sample with PtNiMo may indicate that the catalyst deactivates more rapidly in the initial stage than unpromoted NiMo. It is probable that catalyst deactivation occurs in the first few hours of reactions when oils of low specific gravity are produced. The specific gravity of the first sample depends on the sampling time and the deactivation behavior of the catalyst.

Figure 7 shows the calculated product distribution with the assumption that the olefin content is negligible in the oils. The results show that under steady state conditions, the reduction of the polyaromatics (PA) content is due to thermal reactions instead of catalytic reaction. However, in the initial stage, as shown in Figure 8, catalytic effects on the reduction of polyaromatics were observed. In both of these stages, catalysts improved the formation of paraffins (P) and naphthenes (N) and the conversion of monoaromatics (MA), while thermal reactions result in the formation of MA only. Figure 9 shows that the Pt promoted NiMo catalyst had no significant advantage over NiMo in product distribution, although the products with this catalyst generally had lower specific gravities and better H/C ratio. The nitrogen contents in the products are shown in Figure 10 with NiMo and PtNiMo catalysts. It is clear that catalysts significantly promoted the removal of nitrogen with PtNiMo slightly superior to NiMo.

The four catalysts tested here showed essentially the same activity in product

distribution with different behaviors in product specific gravity and nitrogen removal. It is suspected that the catalytic function for the conversion of polyaromatics was lost partially during the initial stage because of the deposit of carbonaceous materials or poisoning.

CATALYST SUPPORT STUDIES

The objective of this study is to explore the performance of metal phosphates of aluminum, titanium and zirconium as potential new supports for stage 2 upgrading catalysts. There is considerable evidence of metal phosphate utility as possible catalyst support material in light of their high stable surface area, pore geometry and surface acidity properties. Experimental studies were begun using $AlPO_4$ - metal oxide systems such as Alumina-Aluminum Phosphate(AAP). Several methods were investigated for the preparation of AAP support.

Method A. Supports were prepared by a coprecipitation method (Chen et al 1990; Marcelin et al 1983). Aluminum nitrate $Al(NO_3)_3 .9H_2O$ (98%) was completely dissolved into distilled water to form a 0.5M solution; phosphoric acid H_3PO_4(85%) was then added to this slowly. After the addition, the acidic solution was well stirred for at least 10 minutes. A pH controlling solution was prepared by mixing NH_4OH (28-30%) and distilled water with a volume ratio 1:1. Both the acidic and the basic solutions were slowly added to a well stirred vessel of distilled water. The pH value was maintained at 8.0 throughout the precipitation process. The titration was continued until the acidic solution was consumed.

The resulting precipitates were centrifuged, washed with distilled water three times and dried at 393 K overnight followed by 12h calcination at 773 K in the muffle furnace. Controlling the Al/P atomic ratio allowed a desired AAP composite to be obtained. The surface areas of the samples were determined by nitrogen adsorption(BET) using a Quantasorb adsorption unit manufactured by Quantachrome Corp (Figure 11). The samples were degassed at 350°C.

The next aim was to prepare a finished catalyst by adding nickel nitrate and ammonium molybdate to the catalyst support. The support AAP2 (10.02gms) was pressed under 20,000psi and was made into a tablet. Another tablet was made using

AAP6 (8.07gms) again by pressing under 20,000psi. This was crushed and screened through 16/25 mesh sieves. Since the screened particles were not strong enough to be used in the continuous reactor for further studies, another method of preparing the finished catalyst was chosen.

After calcination, dry AAP and 3wt% methyl cellulose (lubricant) were well ground, and an appropriate amount of distilled water was added. The mixture was then extruded. The wet extrusion was dried in air at room temperature, dried at 383 K for 4h, and calcined at 773 K for 4h. Still the strength of the catalyst support was not satisfactory. Since the extrudates made of alumina using acetic acid as a peptizing agent gave much stronger catalyst supports, combinations of AAP1 and boehmite with AAP1/boehmite ratio varying from 1 to 0.2 were tried. 5%(vol) acetic acid was used as peptizing agent. The mixture was forced through the die hole (1/8"diameter) using an extruder. Extrudates were dried overnight and calcined at 773 K. The resulting AAP pellets could be impregnated with Ni and Mo compounds by incipient wetness method and used for further studies if desired.

Method B. Another preparation method (Kearby, 1960) was sought in order to obtain a higher surface area for the AAPs. 0.5M solutions of $Al(NO_3)_3.9H_2O$ and H_3PO_4 (85%) were stirred and cooled to 0^0C while slowly adding portions of a 13% ammonia solution. Two sets of experiments were done; one with varying Al/P ratio keeping the pH at 5.0 and the second by changing pH at a constant Al/P ratio of 1.0. After standing overnight the gel was thoroughly extracted with 99% isopropanol and dried for 12h at 106-110^0C in the vacuum oven. The samples were then calcined at 500^0C for 12h.

Six samples were prepared with different Al/P ratios. The surface area of AAP1 was found to be $140m^2/g$ by this method. The areas remained between 140-100 m^2/g for a pH range of 5-9 (Fig.11).

Method C. 0.5M solutions of $Al(NO_3)_3.9H_2O$ and H_3PO_4 were stirred together to form an acidic solution to which ammonium hydroxide solution was added. Precipitation was done rapidly. This preparation was a little different from the previous methods: during precipitation pH was not held constant. As ammonia was added to the aluminum and phosphate containing solution, the pH rose from less

than one to neutrality, and precipitation occurred during the interval. After neutralization with ammonium hydroxide to pH 7-8 the gel was dried overnight in air. The gel was centrifuged and extracted with 99% isopropanol three times. This was followed by drying in the vacuum oven at 108^{0}C for 12h and calcination in the muffle furnace in air at 649^{0}C for 3h. Surface area of the samples were measured by nitrogen adsorption (Figure 11) after degassing at 350^{0}C for 5h.

REFERENCES

1. Satterfield, C. N. and S. Gultekin, *Ind. Eng. Chem. Process Des. Dev..*, **20**, 62 (1981).

2. Yang, S. H. and C. N. Satterfield, *J. Catal.*, **81**, 168 (1983).

3. Hanlon, R. T., *Energy & Fuels,* **1**, 424 (1987).

4. Riazi, M. and T. E. Daubert, *Ind. Eng. Chem. Process Des.. Dev.*, **25**, 1009 (1986).

5. Wilson, M.F. and J. F. Kirz, *Fuel*, **63**, 190 (1984).

6. Chen et al, *Ind. Eng. Chem. Res.,* 29, 1830 (1990).

7. Marcelin et al, *Journal of Catalysis,* 83, 42 (1983).

8. Kearby, K., *Proceedings of the Second International Congress on Catalysis* 1960, p2567, Technip, Paris 1961.

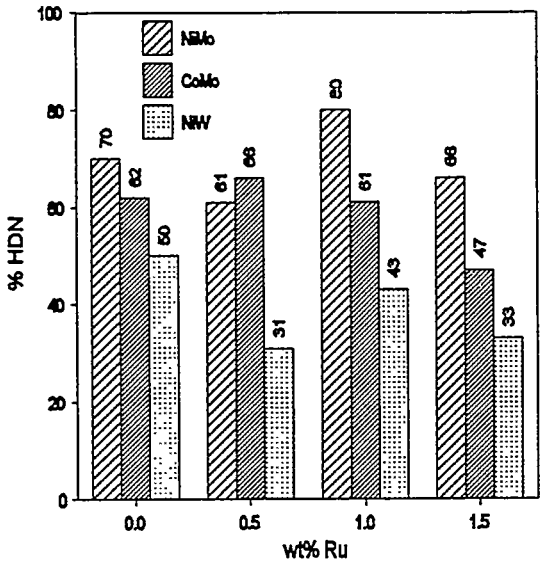

Figure 1 Effect of Ru Loading on Pyridine HDN (350°C, 20 min.).

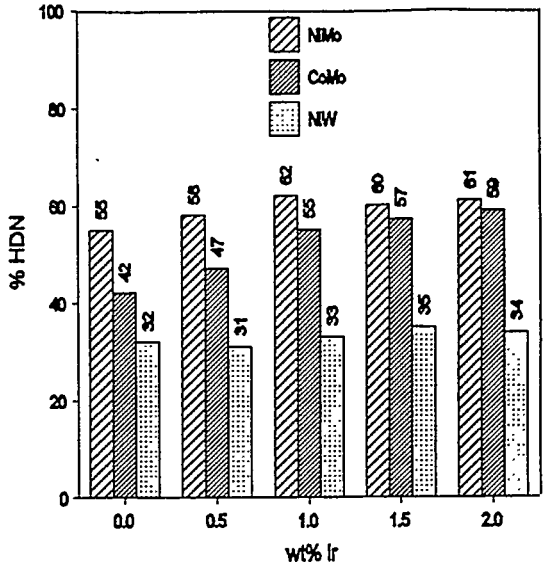

Figure 2 Effect of Ir Loading on Pyridine HDN (350°C, 10 min.)

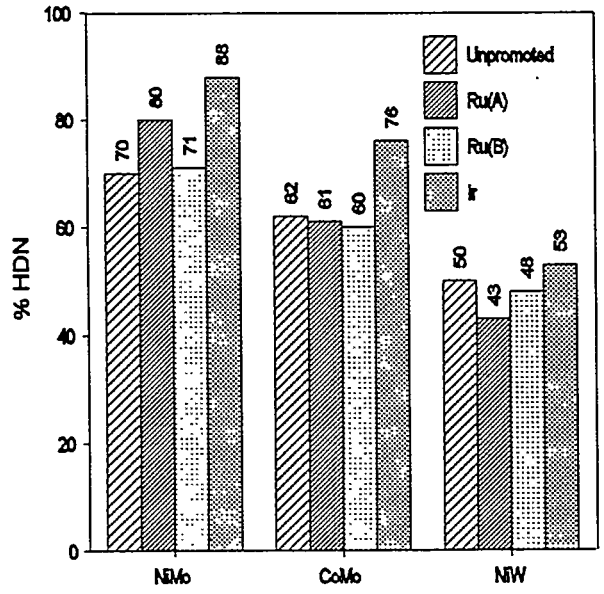

Figure 3 HDN of Pyridine with Various Catalysts (350°C, 20 min.).

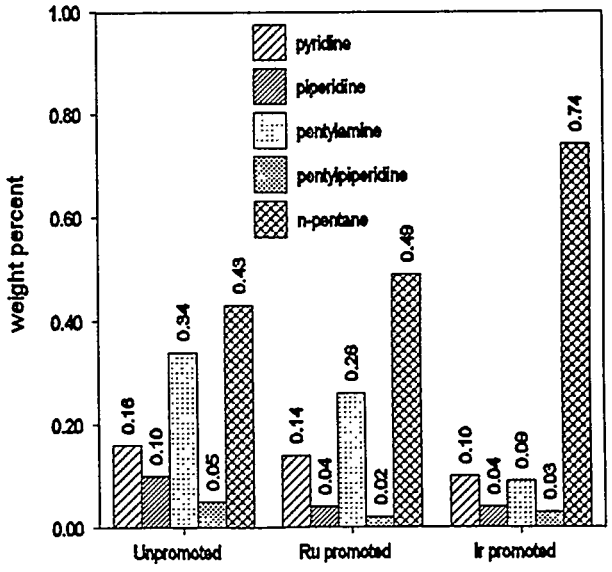

Figure 4 Product Distribution of Pyridine HDN (350°C, 20 min.)

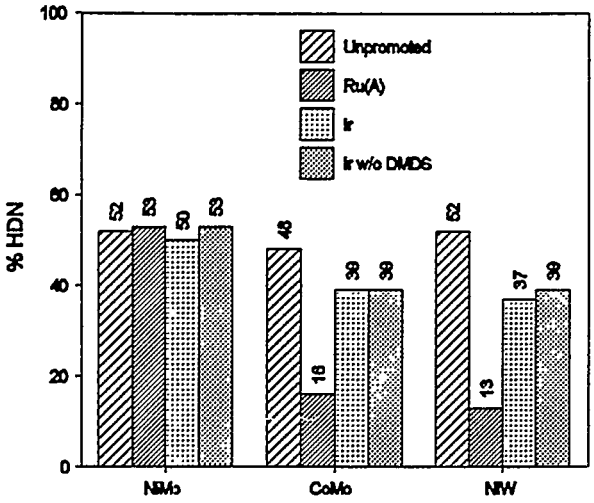

Figure 5 HDN Activity with Coal Liquid (375 °C, 1 hr)

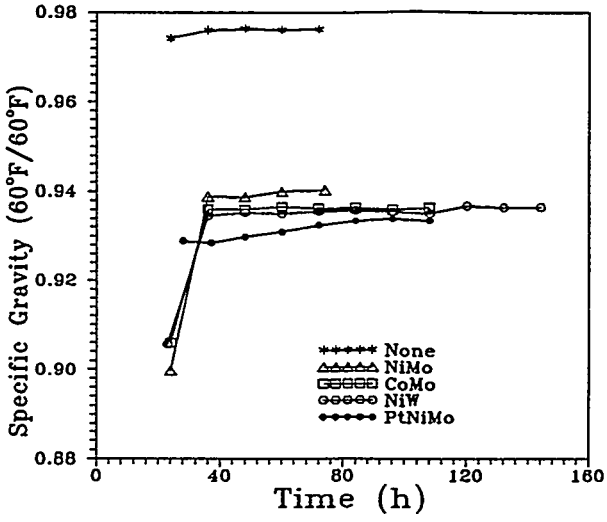

Figure 6 Dependence of Specific Gravity of Product on Reaction Time

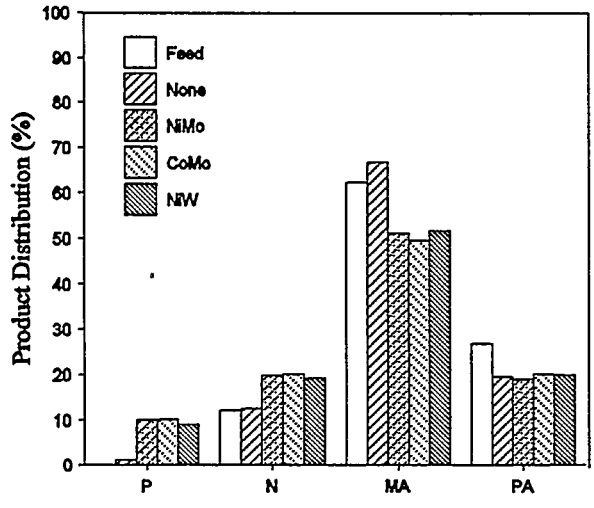

Figure 7 Product Distribution at Steady State

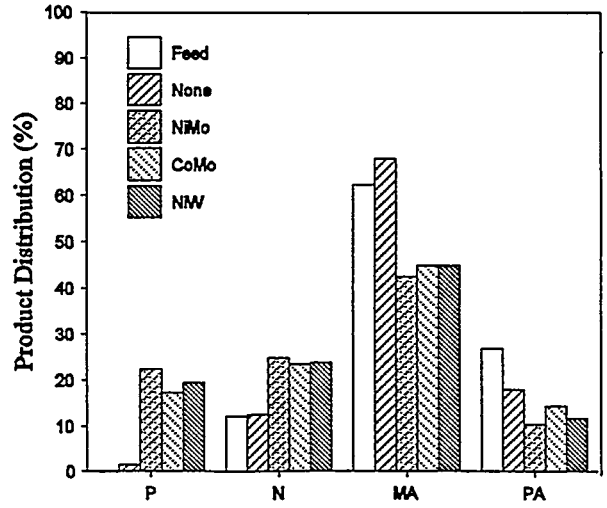

Figure 8 Product Distribution in the Initial Stage (24-hr sample)

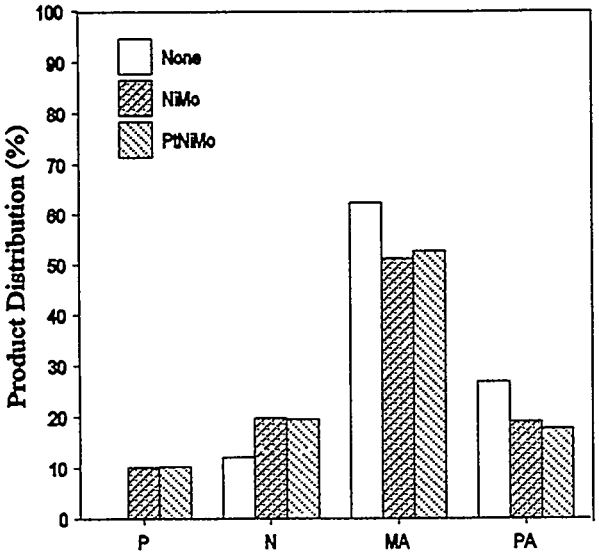

Figure 9 Effect of Pt Promotion on Product Distribution with NiMo Catalyst

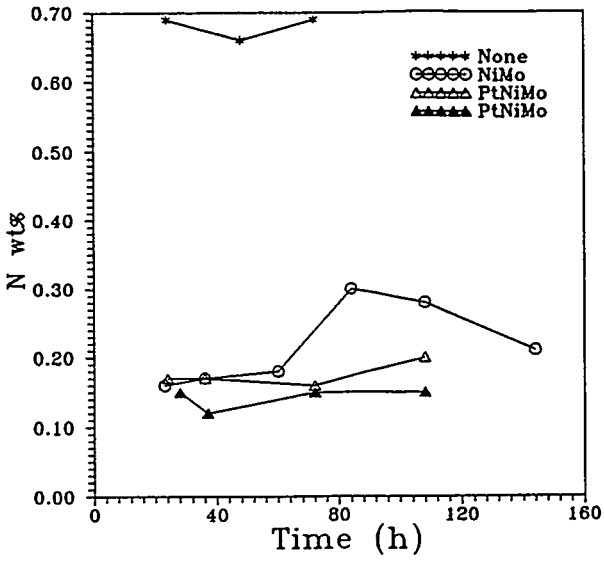

Figure 10 Nitrogen content in the product with time on stream

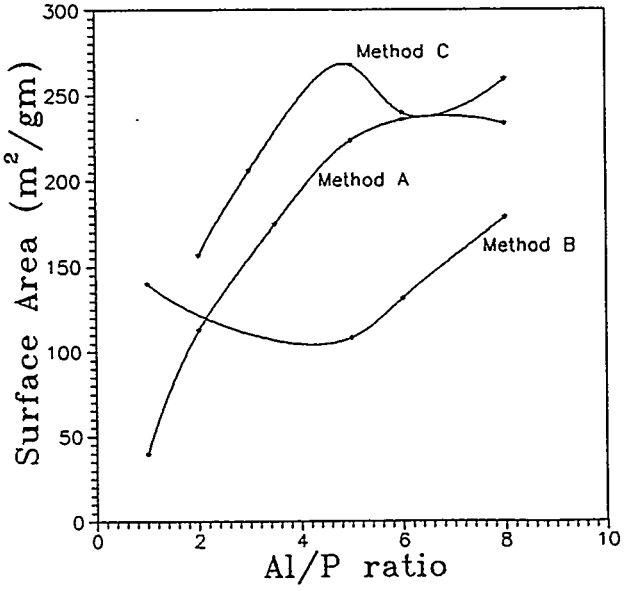

Figure 11 Effect of Al/P Ratio on Surface Area of Catalyst Support AAP.

TASK II

Project II.4

NANOSCALE CATALYSTS FOR COAL AND PLASTIC WASTE LIQUEFACTION

P.C. Eklund
Center for Applied Energy Research
and Department of Physics and Astronomy
University of Kentucky

Summary

In the last six months, we have continued the evaluation of Mo_2C, Mo_2N and MoS_2 ultrafine particle catalysts and have also applied X-ray photoelectron spectroscopy and CO irreversible chemisorption to characterize their surface. These catalysts have been synthesized by laser pyrolysis from the decomposition of $Mo(CO)_6$ in the presence of ammonia, ethylene or hydrogen sulfide [1]. XPS provided us with information regarding the composition of the surface of the particle while CO chemisorption allowed us to quantify the actual number of active sites present on its surface. This information is invaluable, allowing us a correlation between structural and surface chemical properties of these materials with their catalytic activity and selectivity. We found that the particles are coated with approximately a monolayer of MoO_3 and that polymeric carbon is deposited on the particle surface as a result of the decomposition of the carbonyl precursor [1]. In spite of the presence of these surface species, the catalysts exhibited high activity toward the deoxygenation and desulfurization of diphenyl ether and benzothiophene and moderate activity for hydrogenation of naphthalene [2]. The measured density of active sites on nanoscale Mo_2N and Mo_2C synthesized by laser pyrolysis, was found to be lower than the values reported for Mo_2N and Mo_2C synthesized by Temperature Programmed Reduction [3]. The Mo_2N catalysts possesed higher number of active sites than the Mo_2C. This has been attributed to the excessive decomposition of the hydrocarbon reactant during the synthesis of Mo_2C.

Currently, we are trying to synthesize Mo_2C, Mo_2N and MoS_2 nanoparticles free of oxygen and polymeric carbon by utilizing metal precursors that do not contain either

carbon or oxygen, such as $MoCl_5$. Using the chloride, we have already produced ultrafine particles of Mo_2C, as indicated by X-ray diffraction spectra.The catalytic properties of this newly synthesized Mo_2C catalyst are being compared to our previous results.

During this period we also completed the characterization of the catalytic activity of the Mo-based ultrafine particles by studying the hydrodenitrogenation of quinoline as a model compound reaction of coal representing nitrogen containing molecules. Quinoline was found to undergo a rapid hydrogenation to form 1234 -tetrahydroquinoline, which in turn reacted more slowly to produce cis- and trans- decahydroquinoline and 2-propyl aniline as the main products [1]. In the absence of additional sulfur, Mo_2C and Mo_2N showed no HDN activity at the reaction conditions tested. MoS_2 showed a higher HDN activity than the nitride and the carbide. Molybdenum promoted sulfated hematite catalysts, used for comparison, did not show any HDN activity, even when sulfur was present. When sulfur was added to the reaction mixture containing the Mo_2N, Mo_2C or MoS_2, higher HDN activity was observed, producing propylcyclohexane as the main denitrogenated product. In the next period we intend to compare the observed catalytic activity of these catalyst during model compound reactions of coal to their performance using real coal-derived liquids.

In the last part of this period, we started to synthesize high surface area silica-alumina catalysts to study the role that catalyst acidity (nature and strength) plays in the conversion and quality of products derived from the liquefaction of plastic waste and plastic/coal mixtures. Using sol-gel chemistry techniques we have prepared Al_2O_3, $75\%SiO_2/25\%Al_2O_3$ and pure SiO_2 catalysts. In the next quarter we will prepare two more SiO_2/Al_2O_3 catalysts with different silica to alumina ratio (25% /75% and $50\%SiO_2/50\%Al_2O_3$). Increasing the silica content in these catalsyts is known to increase the ratio of Brönsted to Lewis acid sites, while maintaining constant the total acidity content [4]. Furthermore, we will evaluate these catalysts using commercially available pure plastics like polyethylene and polystyrene, and later we will employ commingled plastics and mixtures of coal and plastics for our tests. The experiments will be done in microautoclave reactors at conditions similar to those reported in the literature. The products will be analyzed by solubility class and simulated distillation in collaboration with Professor Edwin L. Kugler from the Chemical Engineering Department of West Virginia University.

Surface Characterization of UFP particles (Ultrafine)

XPS of Mo_2C and Mo_2N UFP.

The XPS measurements were performed on a Leybold-Hereaus EA-11 spectrometer using Mg K- α (1253.6 eV) radiation at 15 kV and 20 mA, and analyzed from 50 energy scans. The oxygen/helium-passivated samples were pressed into 13 mm diameter pellets and placed in the holder of the XPS preparation chamber, where they were evacuated for 2 hours.

Figure (1) shows the XPS spectra from samples of molybdenum carbide and molybdenum nitride that were passivated in oxygen prior to their removal from the laser pyrolysis chamber. Figure (1a) shows to the photoelectron lines of molybdenum 3d5/2 and 3d3/2 from molybdenum nitride, and figure (1b) presents the carbon 1s line from the same sample. Figures (1c) and (1d) correspond to the molybdenum and carbon peaks, respectively, from molybdenum carbide.

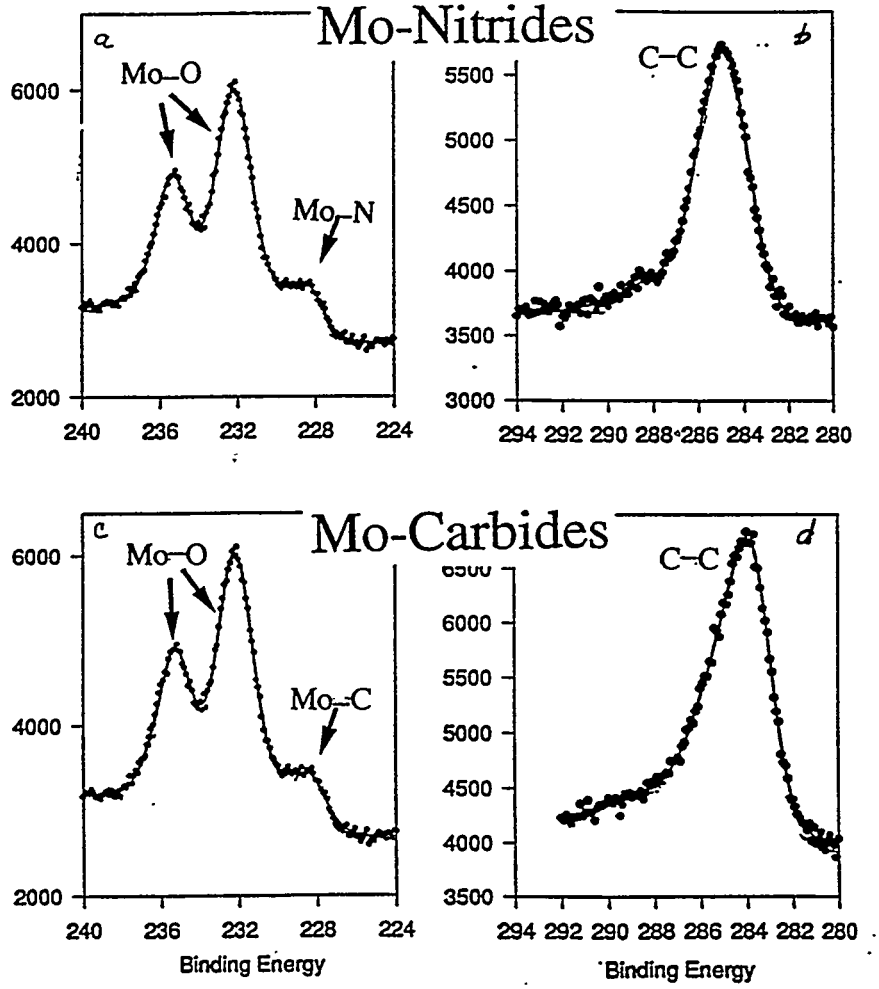

The peaks at 228.58 eV in figures (1a) and (1c) have been assigned [5] to the C-Mo and N-Mo bonding energies, whereas the ones at 232.2 eV to the +VI oxidation state of molybdenum , consistent with the presence of MoO_3 [6]. Deconvolution of the data gives 90% of surface molybdenum in the form of oxides (mainly MoO_3) for both Mo_2N and Mo_2C.

The carbon 1s peak in figure (1b), located at 284.5 eV, corresponds to carbon deposited on the particle surface during synthesis. No evidence was found of a carbidic phase in the molybdenum nitride sample. The presence of this carbon can only be explained in terms of the decomposition of the carbonyl precursor. Deconvolution of the carbon photoelectron line from the molybdenum carbide sample gives one peak at 283.7 eV which corresponds to carbidic carbon [5] together with the presence of amorphous carbon.

The average bulk composition of Mo_2N and Mo_2C was obtained by elemental analysis. The content of carbon and/or nitrogen and hydrogen was determined by combustion of a portion of the sample. The amount of molybdenum was determined by dissolving a second portion of the sample in a mixture of nitric and sulfuric acid and analyzing the solution by atomic absorption. The oxygen content was obtained by difference. The average composition obtained was $Mo_2N_{0.77}O_{1.88}C_{0.5}$ for the molybdenum nitride and $Mo_2C_5O_{0.9}$ for the molybdenum carbide. To rationalize the presence of such a high concentration of oxygen in the particle composition, a simple model consisting of a spherical particle coated with a single monolayer of oxide as MoO_3 was assumed [7]. Using the value for the Mo-Mo interlayer distance in this oxide and the bulk densities of MoO_3 and Mo_2N the calculated stoichiometry for the nitride nanoparticle was $Mo_2N_{0.7}O_{2.5}$. Despite the fact that this model allows only a monolayer of MoO_3, the resulting composition corresponds to an oxide fraction of about 40% of the total weight of the particle. This result stems from the small particle size ~ 5 nm diameter. The lower oxygen content observed in actuality may be due to a mixture of lower valence molybdenum oxides with MoO_3.

The density of active sites measured by irreversible CO chemisorption was $0.92x10^{14}$ site/cm^2 for the Mo_2N and $0.24X10^{14}$sites/cm^2 for the Mo_2C [1]. These numbers correspond to approximately half of that reported by Oyama et al for TPD derived Mo_2N and Mo_2C catalysts [3]. This low density of sites may be due, in part, to their obstruction

by the carbon deposited during the synthesis, together with the incomplete removal of the MoO_3 coating by the H_2 pretreatment prior to the CO absorption experiments. Notice also that the sites density of Mo_2N is almost four times larger than that of Mo_2C, and since the values of the overall conversion of the model compounds were similar for Mo_2N and Mo_2C [2], it follows that Mo_2C is a more active catalyts than the Mo_2N [1].

Denitrogenation of Quinoline

The experimental procedure for the synthesis and evaluation of the catalytic activity of the nanoscale particles has already been described [2].

Table 1 lists the values of final conversions of quinoline, product distribution and %HDN expressed as a mol percentage of denitrogenated products over total products of the reaction. The conversion and product distribution over Mo_2C (not listed) was very similar to that obtained from Mo_2N. Note in Table 1 that Mo_2N alone was not capable of removing the nitrogen from the quinoline molecule. Longer reaction time periods (2 hours) and higher temperatures (400°C) gave HDN values of about 2.4% This low activity was unexpected since there are reports of higher conversion and selectivity toward the production of propoylybenzene [3]. In the presence of sulfur, the HDN increased from 0 to 3% in the case of Mo_2N and Mo_2C and from 1 to 13 % in the case of MoS_2. The molybdenum-promoted sulfated hematite did not exhibit any HDN activity at all.

TABLE I

CONVERSION OF QUINOLINE *

CATALYST	CONV	HDN	THQ	O-PA	CHPYD	DHQ	PB	PCH+ PCHE
Mo_2N	93	0	82	2	4	5	0	0
Mo_2N+S	93	3	71	7	7	5	0	3
MoS_2	94	1	80	3	4	6	1	0
MoS_2+S	95	13	56	13	6	6	1	13
$Mo/Fe_2O_3/SO_4^{2-}$	94	0	83	5	2	3	0	1

THQ=tetrahydroquinolineo-PA=o-propylanilineDHQ=decahydroquinoline(c,t)
CHP=cyclohexenopyridinePB=propylbenzenePCHE+PCHE=propylcyclohexane+ propylcyclohexene
* Reaction time = 60 minutes at 800 psig hydrogen and 380°C.

Synthesis of Acidic Catalysts for Plastic Liquefaction

The experimental procedure for the synthesis of the Alumina catalysts is as follows: 75 g of $Al(NO_3)_3.9H_2O$ were dissolved in 250 ml of distilled water with a resulting pH of 1.6. This solution was placed on a heating table equipped with a magnetic stirrer. A solution of 40 g of NaOH in 150 ml of water was then added to the $Al(NO_3)_3.9H_2O$ solution. Then 11g of HNO_3 in 100 ml of water was added to the above $NaAl_2O_2$ solution under mechanical stirring and at a constant temperature of 70°C. The addition of nitric acid was continued until the pH reached 7. This suspension was filtered and washed with NH_4NO_3 to ion-exchange the sodium present in the precipitate. SiO_2 was prepared by weighing 47.3g of $Na_2SiO_3.9H_20$ and dissolving it in water (pH=11). HNO_3 was then added until a pH of 6 was reached. The precipitate was aged for 2 h at 35°C and for 6 h at 45°C. 35.5 g of sodium silicate dissolved in water were added to 18.38g of aluminum nitrate to prepare the 75:25 SiO_2/Al_2O_3 catalyst. The mixture was stirred for 10 minutes and 1:1 NH_4OH was then added dropwise until a pH of 6 was obtained. The precipitates obtained by these three methods were filtered and washed with hot ammonium nitrate, dried at 120°C and finally calcined at 550°C for 12 hours. Typical acidic properties of

these catalysts are listed in Table II [4].

TABLE II

	Surface Area(m^2/g)	Total Acidity(mmol/g)	Brönsted/Lewis
SiO_2	311	0.001	0
25%SiO_2:Al_2O_3	297	0.5	0.1
50%SiO_2:Al_2O_3	306	0.4	0.3
75%SiO_2:Al_2O_3	294	0.3	0.6
Al_2O_3	150	0.3	0

In the following period we will complete the synthesis of the remaining silica alumina catalysts and we will characterize their acidic properties by Infrared Spectroscopy and Temperature Programmed Desorption of chemisorbed ammonia.

Conclusions

Nanoscale Mo_2N, Mo_2C and MoS_2 produced by laser pyrolysis exhibited higher activity for heteroatom removal than $Mo/Fe_2O_3/SO_4$. MoS_2 appears to be the most active catalyst overall. Mo_2N gave similar conversion and product distribution as Mo_2C. On the basis of the number of active sites measured by CO chemisorption, Mo_2C was found to be more active than Mo_2N. A low number of active sites on the particles compared to values reported in the literature is attributed to coverage of carbon and oxide on the particle surface. More experiments are underway to study the benefits from removing or avoiding altogether this coating and reducing oxygen in the particles.

References

[1] R. Ochoa, G.T. Hager, W. Lee, S. Bandow, E. Givens and P.C. Eklund, Proc. Mat. Res. Soc. Symp. Proc. T. Boston, 1994 (paper T. 1. 4)

[2] P.C. Eklund, R. Ochoa, G.T. Hager, W.T. Lee, S. Bandow, CFFLS 1st quaterly report, 1994 pp. 82.

[3] S.T. Oyama, J. C. Schlatter, J. Metcalfe, J. Lambert, Ind. Eng. Chem. Res. 27, 1639 (1988).

[4] S. Rajagopal, H. Marini, J. Marzari and R, Miranda, J. of Catalysis, Submitted for Publication, 1994.

[5] M. J. Ledoux, C.P. Huu, J. Guille, H. Dunlop, J. of Catalysis 134, 383 (1992).

[6] C.D. Wagner, W.M. Riggs, L.E. Davis, J.F. Moulder, and G.E. Muilenberg in "Handbook of X-ray Photoelectron Spectroscopy". Perkin-Elmer, Eden Prairie, MN, 1979.

[7] X.X. Bi, K. Das Chowdhury, R. Ochoa, W.T. Lee, S. Bandow, P. Zhou, M.S. Dresselhaus and P.C. Eklund, Proc. Mat. Res. Soc. Symp. Proc. T. Boston, 1994 (paper T3.6)

TASK II

Project II.5

DEVELOPMENT OF CATALYSTS FOR DCL AND COLIQUEFACTION

J. Zhao, Z. Feng, F.E. Huggins, and G.P. Huffman
University of Kentucky

INTRODUCTION

In the past several years, considerable effort has been made to develop highly dispersed and low cost iron-based catalysts for direct coal liquefaction (DCL). Most iron-based catalysts are in fact the catalyst precursors as the catalysts convert to $Fe_{1-x}S$ (pyrrhotite) under DCL reaction conditions. There has been less work reported on the pyrrhotite phase, in terms of its morphology and structure, and how they influence DCL activity.

As for coliquefaction of coal with waste plastics, coal liquefaction principally involves hydrogenation and hydrogenolysis, while the liquefaction of plastics involves cracking and depolymerization. It would be difficult to find one catalyst to serve both functions. An alternative could be using two catalysts: a DCL active pyrrhotite and a cracking catalyst such as zeolite or alumina-silica. The advantage of using pyrrhotite instead of iron oxide precursors is that we can avoid adding sulfur, a poisoning gent for the cracking catalyst and contamination for fuel products.

We have extensively investigated the structure and DCL activity of ferrihydrite (FHYD) [1-3]. We found that the chemisorption of small amount of impurity anions at the ferrihydrite surface can effectively inhibit particle agglomeration, allowing the catalyst to maintain its dispersion. A number of binary ferrihydrite catalysts (M/FHYD, M/Fe $\approx$ 5%) with M = Si, Mo, P, and citric acid (CA) have been synthesized in our lab. DCL tests using Si/FHYD and Ca/FHYD show significant increase of coal liquefaction yields over those obtained from thermal reaction [4,5].

In this report, we present the characterization of pyrrhotite catalysts synthesized with simulated DCL conditions using binary ferrihydrites as the catalyst precursors. TEM, XRD, and Mössbauer spectroscopy were used for the investigation.

RESULTS AND DISCUSSION

Sulfidation of the catalyst was performed using a tubing bomb under simulated DCL condition. The tubing bomb reactor was charged with 0.25 g of catalyst mixed with tetralin along with dimethyl disulfide (DMDS) as a sulfur donor for the catalyst (S/catal = 2/1, by weight). The reactor was than pressurized with H_2 to 1000 psi at room temperature and agitated vertically at 400 cycles/min in a fluidized sand bath at 415 °C for one hour. After reaction, the samples were subjected to XRD, TEM and Mössbauer investigation.

Transmission electron microscopy For the pure ferrihydrite (30-Å catalyst by Mach I), after sulfidation, TEM shows the formation of well crystallized, hexagonal shaped $Fe_{1-x}S$ phase with average particle size > 1000 Å (Fig. 1). Markedly improved dispersions of the $Fe_{1-x}S$ phases are obtained with the binary ferrihydrites as indicated in Fig 1, showing significantly smaller particles of irregular shapes.

X-ray diffraction $Fe_{1-x}S$ has a NiAs structure in which each Fe is surrounded by six sulfur atoms, and each Fe has 1, 2, or 4 vacancies among its 12 nearest Fe neighbors. The monoclinic ($Fe_{0.881}S$) and hexagonal ($Fe_{0.909}S$) phases are the most common ones. The phase transition of monoclinic to hexagonal occurs at ~300°C. The XRD patterns for the three ferrihydrite catalysts after sulfidation are consistent with those for the hexagonal phase. However, the pyrrhotite phase formed with Si/FHYD shows diffraction features at the high 2θ sides of the major diffraction peaks, which are also seen in the monoclinic phase (Figure 1a, indicated by arrows). Because of decreased Fe:S ratio, the d spacing for the monoclinic phase is shorter than that for the hexagonal phase, thus the (102) peak for the monoclinic phase is shifted to higher 2θ. Such shifting is also found for the sulfided Si/FHYD and the 350°C sulfided 30-Å catalyst, indicating incomplete monoclinic-hexagonal transition, due the presence of the surface adsorbed Si and lower sulfiding temperature, respectively. For reasons unclear at the present , the (102) peak for the sulfided CA/FHYD is shifted to the low 2θ side.

Mössbauer spectra Quantitative analysis for the Fe vacancies in pyrrhotite are obtained using Mössbauer spectroscopy. The Mössbauer spectrum for the hexagonal phase contains three sextets with magnetic hyperfine fields of H_f = 302, 274, and 256 kOe, respectively. These three components are assigned to three Fe positions, which respectively have 0 (position A), 1(B), and 2(C) vacancies among their Fe neighbors. For the monoclinic pyrrhotite, the spectrum also consists of three sixtets of H_f = 300, 256, and 225 kOe, corresponding to the Fe atoms with 0

(A), 2(C), and 4(D) vacancies in their Fe neighbors. Figure 3 shows the Mössbauer spectra of the three pyrrhotite catalysts. The spectrum for the sulfided 30-A catalyst is very similar to that for the hexagonal phase, which is dominated by the A, B, and C positions. However, a fourth component (D) is discernable, hence the spectrum is fitted with four sextets. The spectrum for the sulfided Si/FHYD is similar to that for the monoclinic phase, showing splitting of the magnetic hyperfine fields, due to decreased population of the B position and increased population of the C and D positions. The spectrum is fitted with three sextets representing the A, C, and D positions, and a doublet at the center for the unsulfided ferrihydrite. The results are in agreement with the XRD results. The spectrum for the sulfided CA/FHYD also shows increased splitting of the magnetic components, indicating increased fractions of C and D components. The spectrum is fitted with four sextets and the Mössbauer parameters are listed in Table 1.

According to distribution of the four magnetic components (Table 1), the average vacancy in the nearest Fe shell for a pyrrhotite phase can be estimated by

$$N_{vac} = \frac{(m*1 + l*2 + k*4)}{(n + m + l + k)} \qquad (1)$$

where n, m, l, k represent the fractions of four positions with 0, 1, 2, 4 vacancies, respectively. N_{vac} for the three pyrrhotites are listed in Table 1. Significant increases of Fe vacancies are indicated in the sulfided Si/FHYD and CA/FHYD.

In conclusion, we found that in addition to improving the dispersion of the pyrrhotite phases, the presence of impurity anions at the ferrihydrite surface retards the monoclinic-hexagonal phase transition, resulting in more Fe vacancies retained in the pyrrhotite phase. The results will be presented at the ACS 1995 Anaheim Meeting, Division of Fuel Chemistry [6]. The effects of Fe vacancies on catalytic coal liquefaction will be further investigated.

SYNTHESIS OF BINARY OXIDES FOR COLIQUEFACTION

The development of binary ferrihydrite catalysts provides a novel way of improving the catalytic performance by modifying the surface with chemisorption of secondary components. Because of the difference of coordination numbers and valence states between the Fe ion and the secondary component, surface acidity of the binary ferrihydrite will vary as a result of

chemisorption. Liquefaction experiments using $Si_{0.05}/Al_{0.05}$/FHYD catalyst for waste plastic with waste oil as the solvent show improvement of liquid yield over thermal reaction.

The binary ferrihydrite catalysts which consists of a secondary component(s) chemisorbed at the surface are structurally different from binary metal oxides, which are regarded as the solid solution of two oxides. In most cases, mixing two metal oxides creates new acid sites at the surface. We are currently in the process of preparing several binary oxides including, SiO_2-Fe_2O_3 (Fe_2O_3 as the substituting oxide, at Si:Fe ~ 3:1), SiO_2-Al_2O_3, and TiO_2-Fe_2O_3. Co-liquefaction tests of the catalysts will be conducted in due course.

References

1. G. P. Huffman, B. Ganguly, J. Zhao, K. R. P. M. Rao, N. Shah, Z. Feng, F. E. Huggins, M. M. Taghiei, F. Lu, I. Wender, V. R. Pradhan, J. W. Tierney, M. S. Seehra, M. M. Ibrahim, J. Shabtai, and E. M. Eyring, *Structure and Dispersion of Fe-Based Catalysts for Direct Coal Liquefaction,* **Energy & Fuels 7**, 285 (1993).

2. J. Zhao, F. E. Huggins, Z. Feng, F. Lu, N. Shah, and G. P. Huffman, *Structure of a Nanophase Ultrafine Iron Oxide Catalyst,* **J. Catal. 143**, 499 (1993).

3. Z. Feng, J. Zhao, F. E. Huggins, and G. P. Huffman, *Agglomeration and Phase Transition of a Nanophase Iron Oxide Catalyst,* **J. Catal. 143,** 510 (1993).

4. J. Zhao, Z. Feng, F. E. Huggins, G. P. Huffman, *Binary Iron Oxide Catalysts for Direct Coal Liquefaction,* **Energy & Fuels 8**, 38 (1994).

5. J. Zhao, Z. Feng, F. E. Huggins, and G. P. Huffman, *Organic Acid Treatment of Ferrihydrite Catalyst for Improved Coal Liquefaction*, **Energy & Fuels 8,** 1152 (1994).

6. J. Zhao, Z. Feng, F. E. Huggins, K. P. R. M. Rao, and G. P. Huffman, *Characterization of Fe1-xS Catalysts Synthesized from Ferrihydrite under DCL Conditions,* preprint paper, ACS Divi. Fuel Chemistry, (1995) in press.

Table 1. Mossbauer parameters for the iron phases for the ferrihydrite catalysts after sulfidation without coal. H is for the magnetic hyperfine field; IS the isomer shift; QS the quadruple splitting. A, B, C, and D represent the Fe positions with 0, 1, 2, and 4 Fe vacancies among its Fe neighbors. The average vacancy is determined by Eqn. (1). All spectra were recorded at room temperature.

Sample	H (kOe)	IS (mm/s)	QS (mm/s)	Phase	% Fe	N_{Ave}
30-A	297	0.69	0.06	A	30.9	1.22
	274	0.72	0.04	B	31.2	
	257	0.69	0.07	C	30.5	
	232	0.60	0.11	D	7.4	
CA/FHYD	296	0.69	0.05	A	32.3	1.35
	273	0.71	0.04	B	23.9	
	255	0.68	0.05	C	32.1	
	227	0.63	0.09	D	11.8	
Si/FHYD,	294	0.68	0.05	A	30.0	1.59
	255	0.67	0.05	C	26.6	
	223	0.65	0.09	D	15.3	
		0.45	0.52	FHYD	28.0	

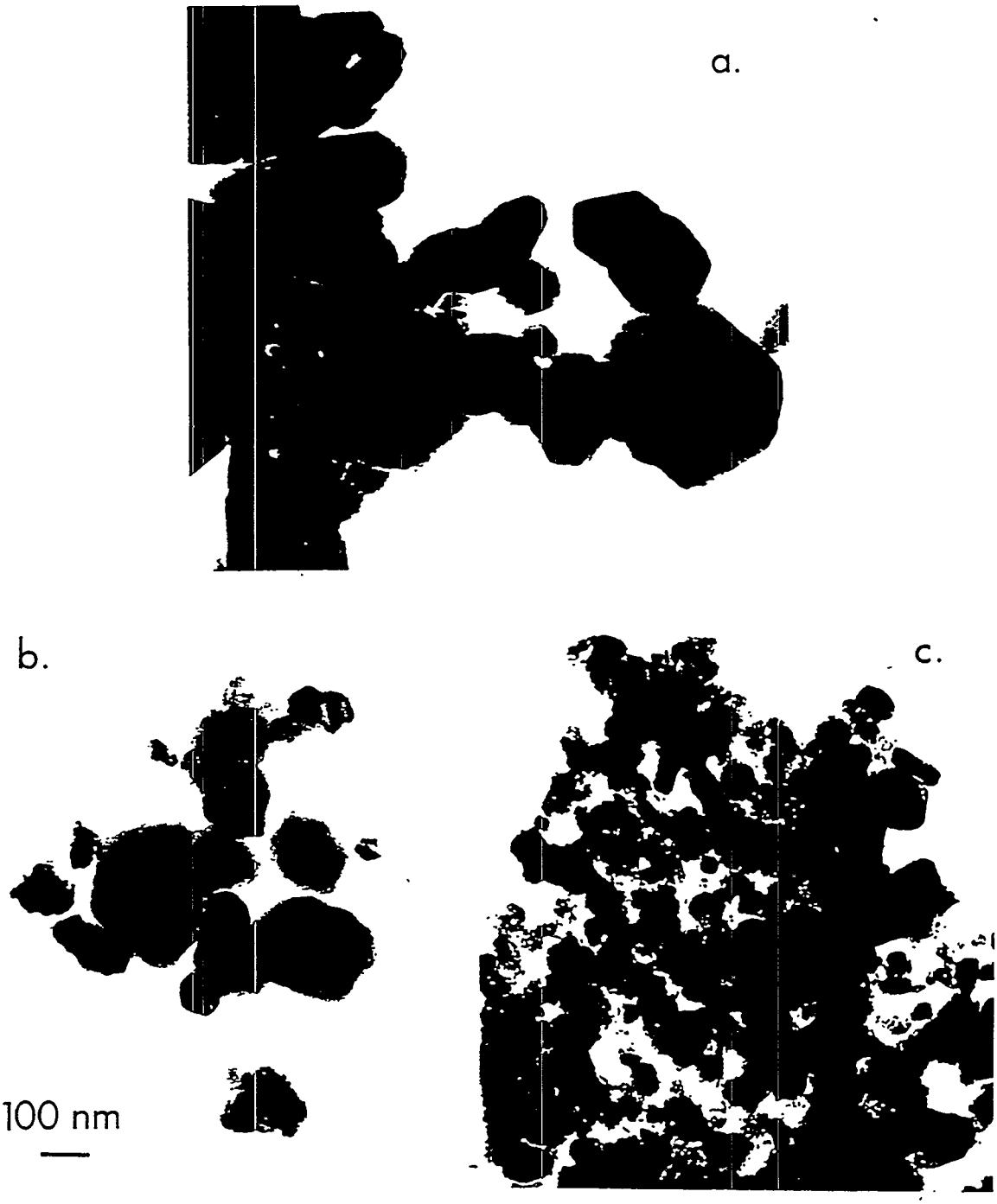

Figure 1. Transmission electron micrographs of three sulfided ferrihydrites: a) the 30-A catalyst; b) CA/FHYD; c) Si/FHYD.

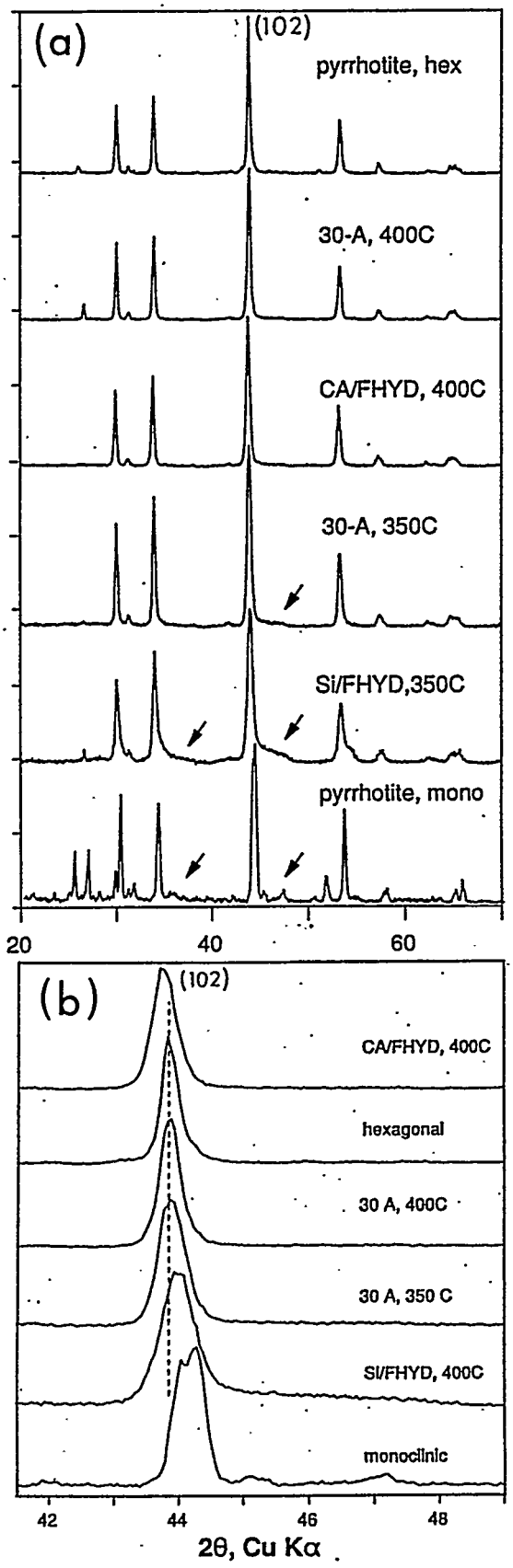

Figure 2. a) XRD patterns for the pyrrhotites and the sulfided ferrihydrite catalysts; b) the (102) peaks for the pyrrhotites and the sulfided ferrihydrite catalysts.

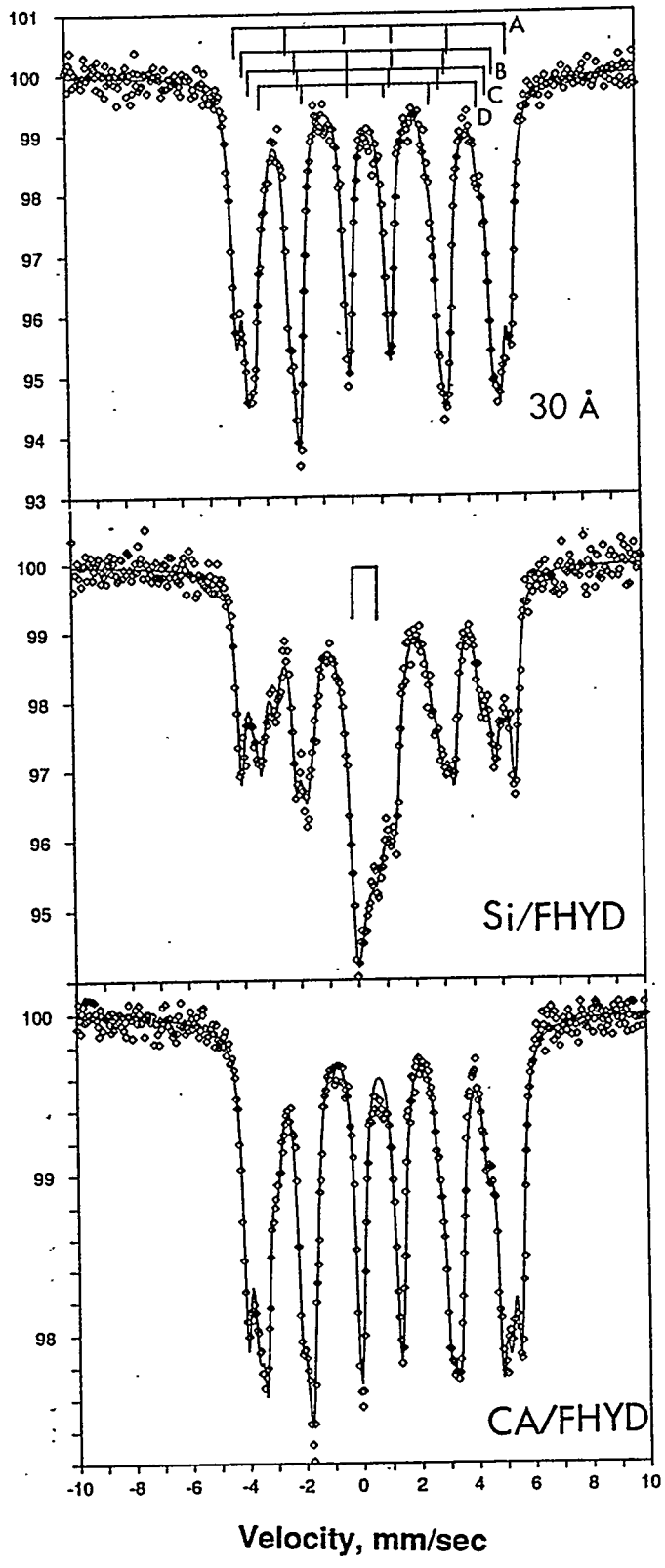

Figure 3. Mossbauer spectra of three sulfided ferrihydrites.

TASK II

Project II.6

CHARACTERIZATION OF INITIAL STEPS IN HYDROGENATION OF COAL MODEL COMPOUNDS BY COAL LIQUEFACTION CATALYSTS

S.D. Worley and W.C. Neely
Auburn University

The Interaction of Dihydrogen with Iron Catalysts

Using a recently-constructed high-pressure infrared cell reactor, and techniques utilized previously in these laboratories for investigating the FTIR of surface hydride species on transition metals,[1,2] studies of the interaction of dihydrogen with Fe_2O_3 and Fe_3O_4 films were begun. The purpose of these experiments was to use the integrated areas of the iron hydride infrared bands to measure the thermodynamic parameters ΔH and ΔS for Fe-H or Fe-H_2 adsorption, so that information concerning the binding strength of these species to the coal catalysts could be obtained. Previous studies here on the Fe-H_2 system with a first generation high-pressure infrared cell reactor were not successful presumably because the cell reactor could only be heated to about 250°C in the presence of static doses of dihydrogen which was apparently not sufficient to cause reduction of the Fe species. Thus the initial experiments failed to reveal infrared data for the species of interest.

During the past report period the newly-constructed infrared-cell reactor (see Figure 1 of the last report) was employed. In these experiments both static and flowing doses of dihydrogen at temperatures up to 250°C were employed for reduction. Figures 1 and 2 show the infrared spectra corresponding to an Fe_2O_3/Al_2O_3 sample containing 3% Fe by weight which was prereduced in flowing dihydrogen (3000 Torr) for 2 hours and then exposed to: (a) 1800 Torr H_2 for 15 min at 25°C, (b) 3500 Torr H_2 for 15 min at 25°C, (c) 3500 Torr H_2 for 10 min at 165°C and then cooled to 25°C, (d) 8400 Torr H_2 for 15 min at 25°C, and (e) a vacuum of 10^{-6} Torr at 25°C for 10 min. In the spectra an intense, broad band near 3200 cm^{-1} corresponding to water on the support was obtained, but unfortunately no band near 2000 cm^{-1} which could be attributed to an Fe-H or Fe-H_2

surface species was observed. The samples in this study were prepared by either pressing the Fe_2O_3/Al_2O_3 mixture into a stainless steel mesh grid or by spraying a slurry of the material onto the mesh grid. The latter method gave somewhat better film homogeneity and light transmission. However, we found that neither method provides sufficient sample in the infrared beam plus some blockage of the beam by the grid. Furthermore, it is difficult to control the temperature of the grid when dihydrogen is present in the cell. For these reasons we plan to return to our method of spraying slurries of the samples onto a CaF_2 infrared window, but we shall modify the original cell so as to allow continuous flow of the dihydrogen during the reduction procedure. Hopefully this will provide a higher concentration of Fe-H or Fe-H_2 oscillators in the beam so that we can observe these species spectroscopically.

Comparison of Reaction Products From Catalytic Hydrogenation of Model Compounds With Those Formed by Direct Reaction with Atomic Hydrogen

As discussed in the previous status report, it has been found necessary to fabricate an atomic hydrogen generator based on a microwave discharge plasma system operating at reduced pressure rather than a silent discharge plasma system operating at atmospheric pressure. Because of the reduced absolute concentration of gas and consequent reduction in the rate of generation of hydrogenation products, a system capable of accepting a large (50 mm diameter) sample holder has been constructed (see Figure 3). For this we are using an 80 L/sec vacuum diffusion pumping system and a 6 kW microwave generator. To avoid the production of artifacts caused by direct uv radiation from the microwave discharge plasma, we have designed an offset sample insertion port so that direct uv radiation can not impact the sample. By concentrating the reacted samples from the 20 cm^2 surface of the sample holder, we anticipate that sufficient quantities of hydrogenation products can be obtained for GC/MS and FTIR analyses.

References

1. Wey, J.P., Neely, W.C., and Worley, S.D., J. Phys. Chem., 95, 8881 (1991).
2. Fang, T.H., Wey, J.P, Neely, W.C., and Worley, S.D., J. Phys. Chem., 97, 5128 (1993).

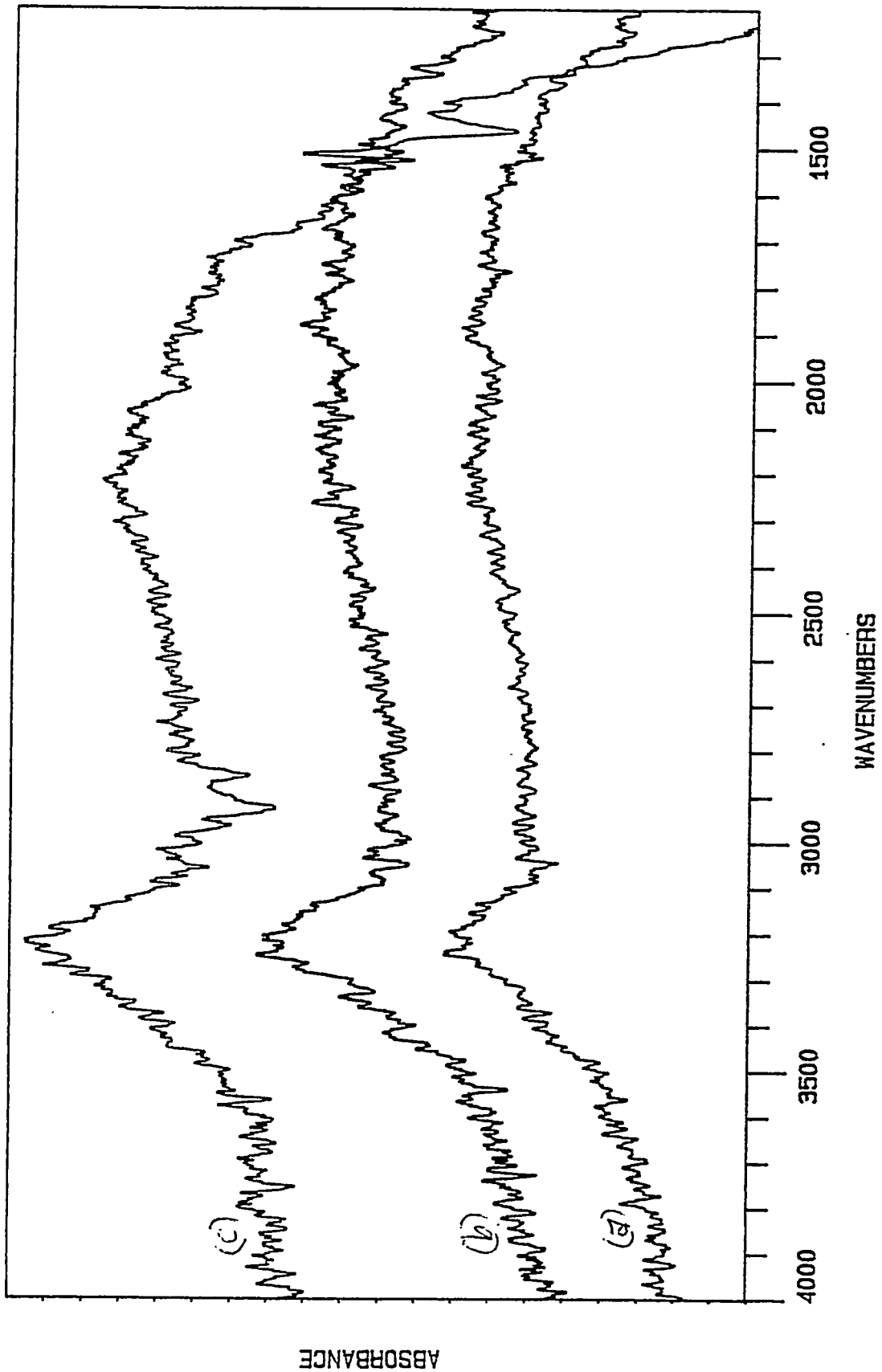

Figure 1

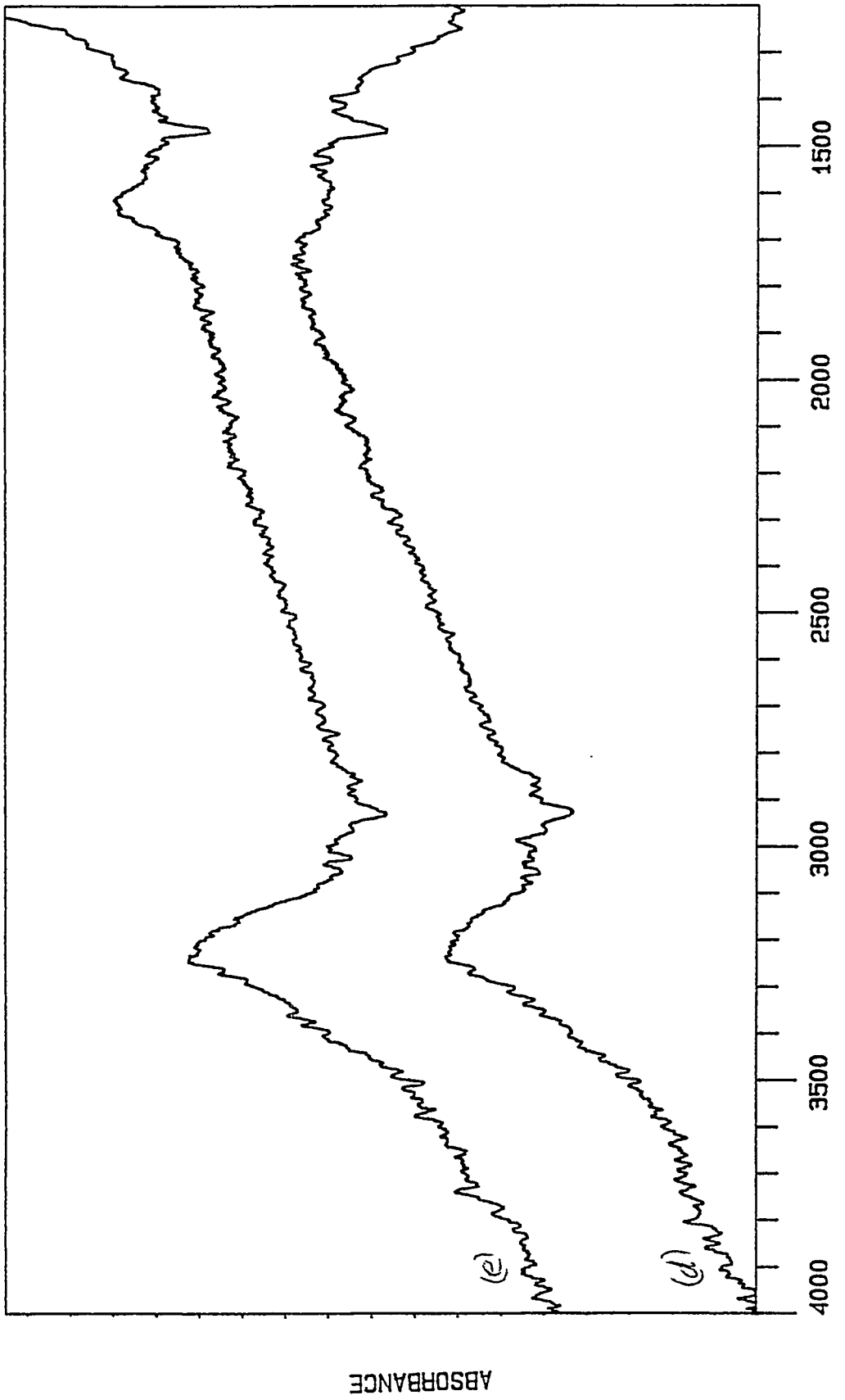

Figure 2

Figure 3

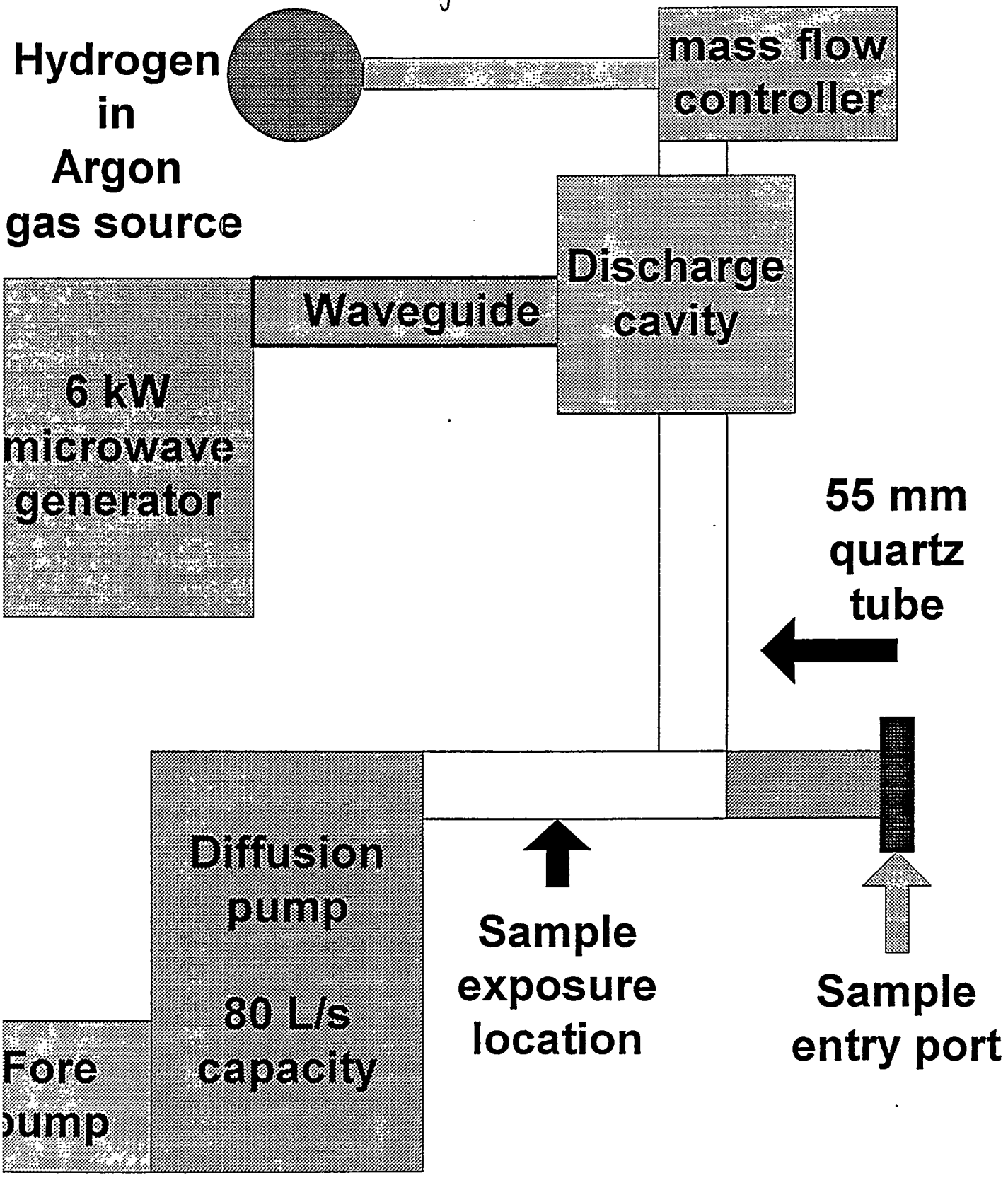

High Capacity Atomic Hydrogen Generation System

TASK III

FUNDAMENTAL RESEARCH IN COAL LIQUEFACTION

TASK III

Project III.1

GENERIC STRUCTURAL CHARACTERIZATION STUDIES

F.E. Huggins, P. Reucroft, J. Zhao, J.Y. Kim, K.R.P.M. Rao, and G.P. Huffman

The Consortium for Fossil Fuel Liquefaction Science and the Department of Chemical and Materials Engineering University of Kentucky, Lexington, KY 40506

The primary activity of the group in this project is to supply a characterization service for the Consortium as a whole with element-specific spectroscopic techniques, viz. Mössbauer spectroscopy and XAFS spectroscopy for bulk investigation and X-ray photoelectron spectroscopy (XPS) and other techniques for surface investigation, that are available only at the University of Kentucky. Such a service provides useful interaction among different Consortium groups, especially in view of the wide-ranging materials that are currently under investigation by the Consortium as the focus shifts more to coliquefaction of coals with various waste carbonaceous materials: catalysts, coals, plastics, waste oils, and their liquefaction residues. In addition, in a follow-up study to one done in the last fiscal year, Mössbauer analyses were requested of the CFFLS program for a closely allied project from outside the CFFLS program, viz. the DCL catalyst testing program at Sandia National Laboratory, New Mexico, (Dr. Frances Stohl).

1. Characterization of residue samples from DCL catalyst testing program at Sandia National Laboratory, (Dr. Frances Stohl, P.I.).

To complement characterization studies of catalysts undertaken by Sandia National Laboratory as part of their DCL catalyst testing program, some samples of the coal, catalyst and DCL residue samples from these tests are being analyzed by Mössbauer spectroscopy at the University of Kentucky. Mössbauer characterization work has now been completed for the following additional seven (7) samples:

6-line ferrihydrite catalyst (as received); source: PNL

THF-insoluble residue from thermal liquefaction run at 350°C, 20 min.

THF-insoluble residue from thermal liquefaction run at 400°C, 60 min.

THF-insoluble residue from catalytic liquefaction run at 350°C, 20 min.

THF-insoluble residue from catalytic liquefaction run at 375°C, 40 min.

THF-insoluble residue from catalytic liquefaction run at 400°C, 60 min.

THF-insoluble residue from catalytic liquefaction run at 400°C, 60 min, 2 wt% sulfur.

1 wt% of the catalyst was added to the liquefaction runs at 350°C and 400°C, and 0.5 wt% of the catalyst was added to the liquefaction run at 375°C. 1 wt% of sulfur was added to all tests, except for the one with 2 wt% sulfur. The coal used for the liquefaction tests is Blind Canyon (DECS-6); Mössbauer data for this coal was reported with the analysis of the first set of residue samples.

The Mössbauer data are summarized in Table 1; the results for the residue samples virtually duplicate those obtained previously for the liquefaction tests done with a sulfated hematite catalyst and reported in the previous Annual Report [1]. The catalyst spectrum was, of course, quite different; it consisted of a broad doublet with parameters consistent with those anticipated for 6-line ferrihydrite. With the possible exception of the Mössbauer spectrum of the catalytic residue obtained at 350°C, 20 mins, there was no evidence for this phase persisting in the catalytic residue samples and it appeared that all of the ferrihydrite had been converted to pyrrhotite.

These Mössbauer data add to the baseline data necessary for interpreting the behavior and transformations of the many different iron-based DCL catalysts to be tested at Sandia National Laboratory. These results have been forwarded to Dr. Stohl in an informal memorandum.

2. XAFS Investigation of Trace Elements in Waste Lubricating Oil and Residues of Co-processing Waste Oil with Coal, (Auburn University program, Prof. A. Tarrer, P.I.).

In the last year, an XAFS investigation was initiated on the behavior of zinc

TABLE 1: Mössbauer Data for Sandia Residue Samples
Using 6-line Ferrihydrite as catalyst

Sample	%Fe in			
	γ-Fe	Ankerite	Pyrrhotite	Ferrihyd.
6-line ferrihydrite, as received				100
THF Insol., 350°C, thermal	13	87		
THF Insol., 400°C, thermal	18	36	46	
THF Insol., 350°C, catalytic	6	28	42	24
THF Insol., 375°C, catalytic	6	25	57	10
THF Insol., 400°C, catalytic	1	13	68	18
THF Insol., 400°C, catalytic, with 2% S	10	18	67	5

and other minor and trace elements in co-liquefaction of waste lubricating oil (15W40) with a bituminous coal (Blind Canyon coal, UT). However, ICP analysis of the waste oil compared to reported [2] INAA data for Blind Canyon coal (Table 2) indicates that only Zn and P derive predominantly from the waste oil rather than the coal in the co-liquefaction experiments. From the zinc XAFS data, it was shown that zinc was present in the waste oil as a zinc dialkyldithiophosphate (ZDDP) compound, which is a commercial additive to motor oils designed to reduce oxidation and wear. From the ICP analysis of the waste oil, it was estimated that about 0.5 wt% of ZDDP had been added to the oil. Furthermore, XAFS data was able to confirm that the ZDDP compound was not present in the monomeric form in oil and in its liquid form, but in a dimeric or polymeric form (Figure 1), in agreement with conclusions made from ^{31}P NMR studies [3].

XAFS spectra of the liquefaction residues indicated that ZDDP in the waste oil was converted into a zinc sulfide (ZnS). In the current quarter, elemental analyses of the residue samples were obtained using PIXE/PIGE techniques (courtesy of Prof. J. David Robertson, Department of Chemistry, University of Kentucky). These data are presented in Table 3; by comparing data in this Table with those in Table 2, it is apparent that the residues are greatly enriched in most inorganic elements compared to both the waste oil and the coal. In Table 4, concentration data for elements in one of the residues (M7) are compared with the estimated elemental concentrations for the starting mixture of Waste Oil:Coal:Catalyst in the ratio 40:4:1. The concentration enhancement for elements in residue M7 compared to those in the starting mix varies from a low of 6.5 for sulfur to a high of 19 for Al; however, most enhancement values are in the vicinity of 10. Similar results were found for the other two samples: for residues M5 and M6 the mean enhancement values were about 11 and 18, respectively.

By means of calculations based on the data in Tables 2-4 and the weight of the THF residue fractions obtained in analysis of the tubing bomb experiments (courtesy M. Mulgaonkar, Auburn U.), it was shown that, except for sulfur, most of the major inorganic elements, including zinc, report to the residue in the 50 - 90% range (Table 5). Approximately 40% of the sulfur present in the starting

Postulated Structures for ZDDP

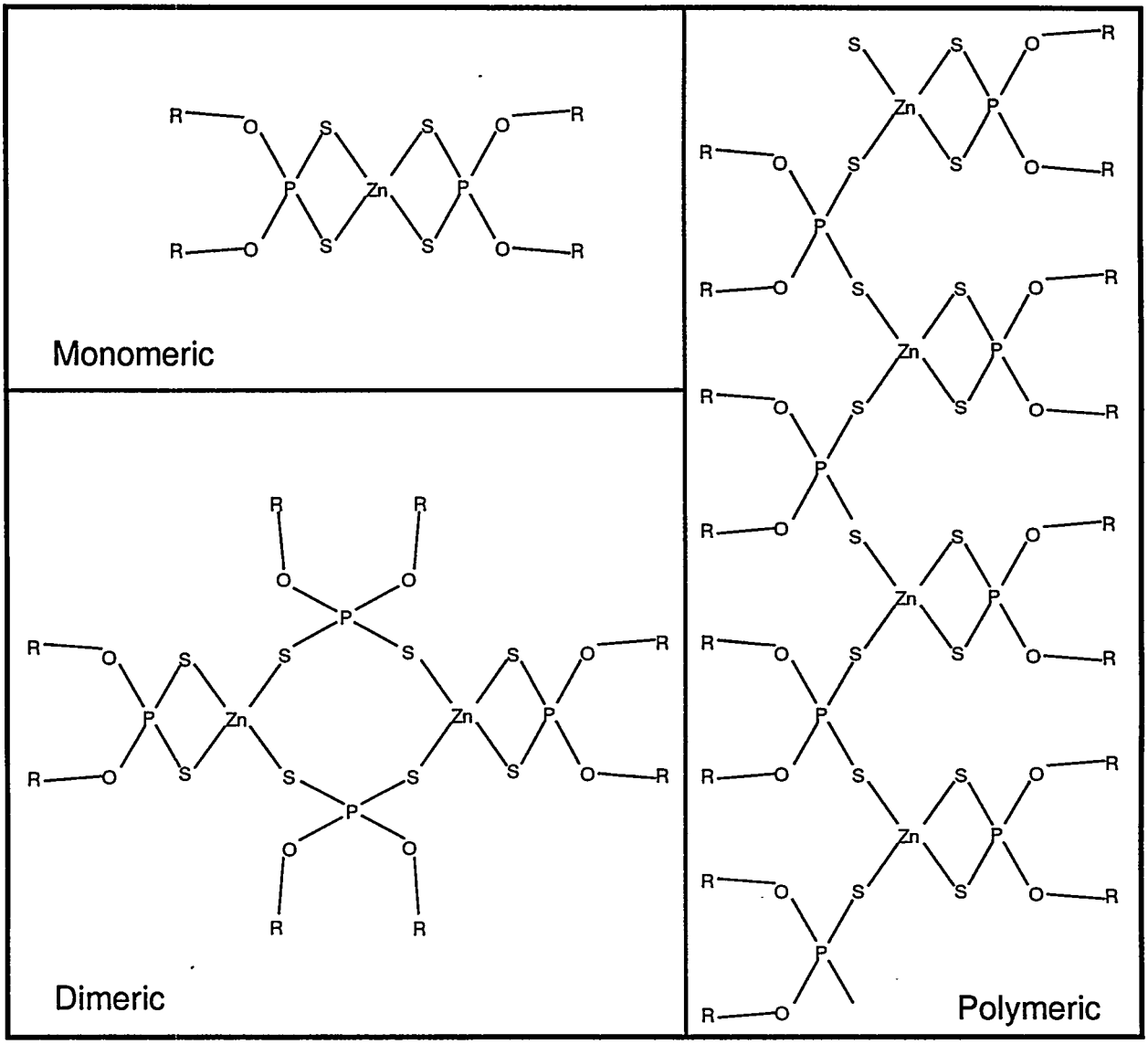

Zinc EXAFS Data is consistent with dimeric and polymeric structures only, not with monomeric structure.

Figure 1

TABLE 2: Analytical Data for Waste Oil Sample Compared to Typical Data for Blind Canyon Bituminous Coal*

Waste Oil		Blind Canyon Coal
Specific Gravity	0.89	1.4
Sulfur Content, wt%	1.01	0.6
Ash Content, wt%	0.45	4.7
Metals Analysis (ICP)		
Metal	**ppm**	**ppm**
Al	2.55	3500.
As	1.24	<1.
Ba	2.14	33.
Ca	1024.	4000.
Co	0.10	5.
Cr	0.15	1.
Cu	10.30	5.
K	0.81	200.
Mg	385.	400.
Mn	2.13	5.
Mo	0.50	2.
P	843.	10.
Pb	1.74	2.
Si	4.78	8600.
Zn	803.	6.

*Comparative data for trace element abundances in Blind Canyon coal obtained from database for the Argonne Premium Coal Sample [2].

TABLE 3: PIXE/PIGE Data for Elements in Coal Liquefaction Residues*

Element	Wt% of Residue		
	Residue M5	Residue M6	Residue M7
C	70.0	56.0	71.0
Na	0.64	0.72	0.42
Mg	0.34	0.57	0.25
Al	0.79	0.78	0.61
Si	0.91	1.05	0.83
P	0.68	1.39	0.63
S	5.38	10.97	6.16
Ca	1.40	2.35	1.12
Cr	0.03	<dl	0.03
Fe	18.2	23.8	17.7
Ni	0.02	0.03	0.05
Cu	0.36	0.33	0.46
Zn	0.90	1.73	0.88
Zr	0.01	<dl	<dl
Ba	0.10	<dl	0.10

*Data courtesy of J. D. Robertson, University of Kentucky.
<dl - below detection limit.

TABLE 4: Comparative Data for Elements in Coal Liquefaction Mixture and a Residue

Element	Est. Mix Conc.* (ppm)	Residue M7 (wt%)	Enhancement
Al	320	0.61	19
Si	770	0.83	11
P	750	0.63	8
S	9500	6.16	6.5
Ca	1250	1.12	9
Fe	17000	17.7	10
Zn	720	0.88	12

*Estimated starting mixture concentrations estimated from component elemental compositions and the ratio of Waste Oil:Coal:Catalyst = 40:4:1

TABLE 5: Percentage of Element That Ends Up in Residue

Element	Liquefaction Test Residue		
	M5	M6	M7
Al	155	92	105
Si	74	51	60
P	57	70	46
S	36	43	36
Ca	71	71	50
Fe	67	53	58
Zn	79	90	68

materials reports to the residue; the remaining 60% most likely reports to the liquid fraction or possibly the gas fraction.

A manuscript has been submitted to the J. Environment. Sci. Health [4], summarizing the above findings, in conjunction with a paper presented [5] at Waste Management VI (Special Symposium of the American Chemical Society, IE&C Division) held in September in Atlanta, GA.

3. XAFS Examination of Materials Prepared by Laser Pyrolysis, (University of Kentucky program, P. Eklund, P.I.)

XAFS spectra of Mo and W sulfide and carbide catalyst materials prepared by Dr Eklund and his group using their laser pyrolysis process have been obtained at SSRL since the last report. Although a detailed analysis of the data has not yet been fully completed, the laser pyrolysis products all gave significantly weaker spectra than those for closely related bulk standards. We are attempting to determine the significance of this observation; it may reflect small particle effects or a compositional complication (e.g. oxycarbide formation rather than pure carbide formation.)

4. Depth Profile Studies of a Ferrihydrite Catalyst ($Si_{0.05}$/FHYD) and Related Catalyst Co-Liquefaction Residues:

Previous XPS studies on a series of fresh binary ferrihydrite catalysts (M/FHYD), where secondary metallic- or non-metallic components were added to the particle surface to inhibit particle agglomeration at high temperature, showed that a surface enrichment of both oxygen and secondary components occurred at the surface of the FHYD particles [6]. In these studies, selected area X-ray photoelectron spectroscopy (SAXPS) depth profile techniques were employed to define the nature of the FHYD surface and any differences between the surface and bulk concentrations of the various elements.

The SAXPS experimental set-up employed in this work has been described previously [7,8]. *In situ* Ar^+ ion sputtering of the powdered sample was carried out using a differentially pumped and computer controlled 3M mini-beam ion gun.

The incident ion gun was operated at 3.5 kV and the sample current was maintained at 3 μA across a sample area of about 5 × 5 mm^2. The pressure in the main chamber was stabilized at 4 × 10^{-6} Torr during ion sputtering. Charge shifted binding energies were corrected by shifting the C 1*s* peak to 285 eV.

In this report, depth profile studies are described on one binary ferrihydrite catalyst prior to liquefaction and on three ferrihydrite catalyst residues (samples listed in Table 6) which were collected after processing in tetralin solvent without coal or waste materials at 400°C in a tubing bomb. Dimethyl disulfide was added in amounts stoichiometrically equivalent to FHYD in order to promote sulfidation of the catalyst, i.e., a standard procedure in catalyzed liquefaction processes. The objective was to simulate the conditions that the catalyst experiences in a typical reactor without the complicating presence of coal and/or waste materials.

XPS depth-profiling results for the $Si_{0.05}$/FHYD catalyst prior to liquefaction are shown in Figure 2. The data clearly indicate a surface enrichment in both oxygen and silicon, and a corresponding depletion in iron. Such trends are quite consistent with the structural models of binary ferrihydrites proposed by Zhao et al. [9], in which elements, such as Si, that are commonly tetrahedrally coordinated by oxygen favor the surface.

The initial chemical state of Fe $2p_{3/2}$ in all the catalyst residue samples showed a binding energy value of 711.4 eV with 13.6 ± 0.05 eV splitting between $2p_{1/2}$ and $2p_{3/2}$ peaks. The surface chemical state of Fe in the catalysts is thus similar to that of either Fe_2O_3 or FeOOH. No distinct changes in chemical state were observed after 10 minutes of Ar^+ ion sputtering.

Two peak components were initially observed in the case of the surface sulfur XPS signal of the $Si_{0.05}$/FHYD residue, as shown in Figure 3. Similar results were observed in all three catalyst residues. The peak at 169 eV was ascribed to oxidized sulfur, while the peak at 162.5 eV is characteristic of inorganic sulfide [10,11]. The sulfate peak disappeared as Ar^+ ion sputtering proceeded, while the sulfide peak increased in intensity. This observation is in agreement with the decrease in oxygen concentration which was also observed as the sputtering proceeded (Figure 4). Yoshimura et al. have also reported similar results from XPS

TABLE 6: Summary of catalyst and catalyst residues investigated by SAXPS Depth Profiling

Samples	Conditions
Si/FHYD	Si/Fe = 0.05 (atomic ratio), as-prepared catalyst before any processing.
30Å FHYD	Residue after tubing bomb processing without coal or waste material at 400°C for 1 hour with tetralin as solvent. Dimethyl disulfide was added.
CA/FHYD	Citric acid treated FHYD, Residues after tubing bomb processing without coal or waste materials at 400°C for 1 hour with tetralin as solvent. Dimethyl disulfide was added.
$Si_{0.05}$/FHYD	Si/Fe = 0.05 (atomic ratio). Residue after tubing bomb processing without coal or waste materials at 400°C for 1 hour with tetralin as solvent. Dimethyl disulfide was added.

TABLE 7: S/Fe atomic ratio in catalyst residues as a function of Ar^+ ion sputtering time.

Residue from Catalyst	Sputtering Time in minutes				
	0	5	10	15	20
30Å FHYD	0.63	0.80	0.85	0.92	0.95
$Si_{0.05}$/FHYD	0.5	0.65	0.72	0.81	0.87
CA/FHYD	0.40	0.62	0.80	0.85	0.89

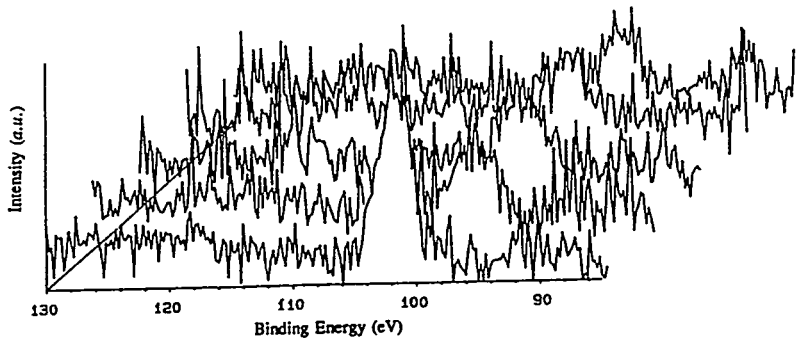

XPS depth profile spectra of Si 2*p* region for a binary ferrihydrite catalyst (Si/FHYD) as a function of Ar^+ ion etching time

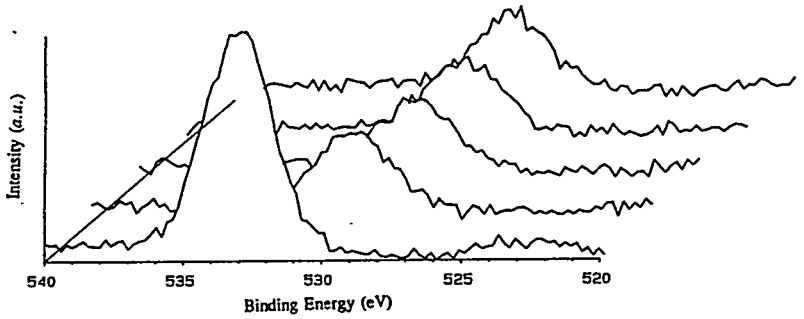

XPS depth profile spectra of O 1*s* region for a binary ferrihydrite catalyst (Si/FHYD) as a function of Ar^+ ion etching time

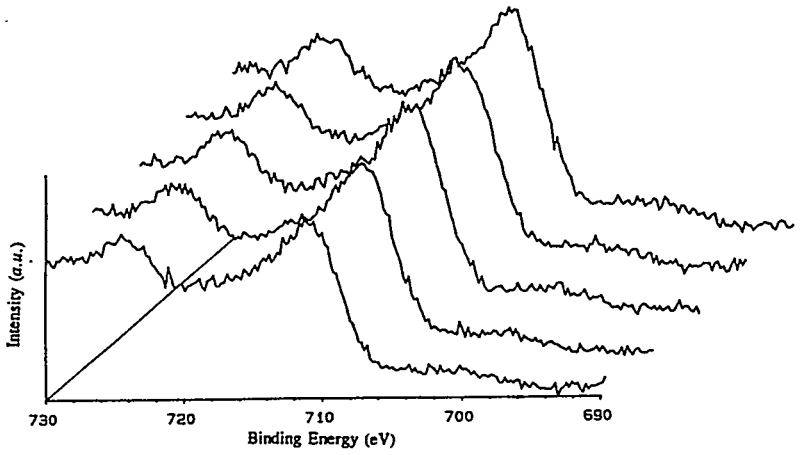

XPS depth profile spectra of Fe 2*p* region for a binary ferrihydrite catalyst (Si/FHYD) as a function of Ar^+ ion etching time

Figure 2

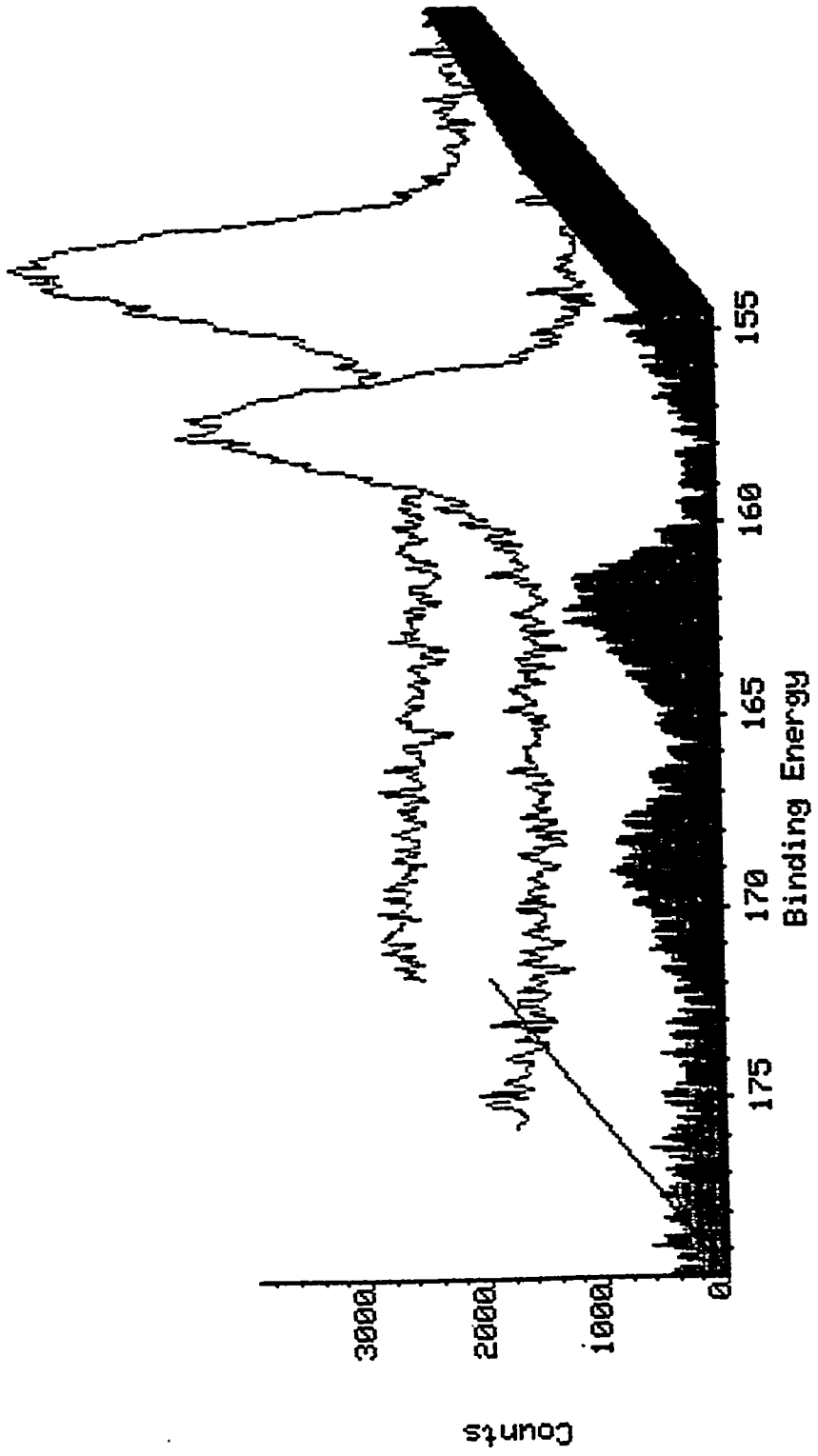

Figure 1. Typical SAXPS depth profile spectra of S 2p region for $Si_{0.05}$/FHYD residue

Figure 3

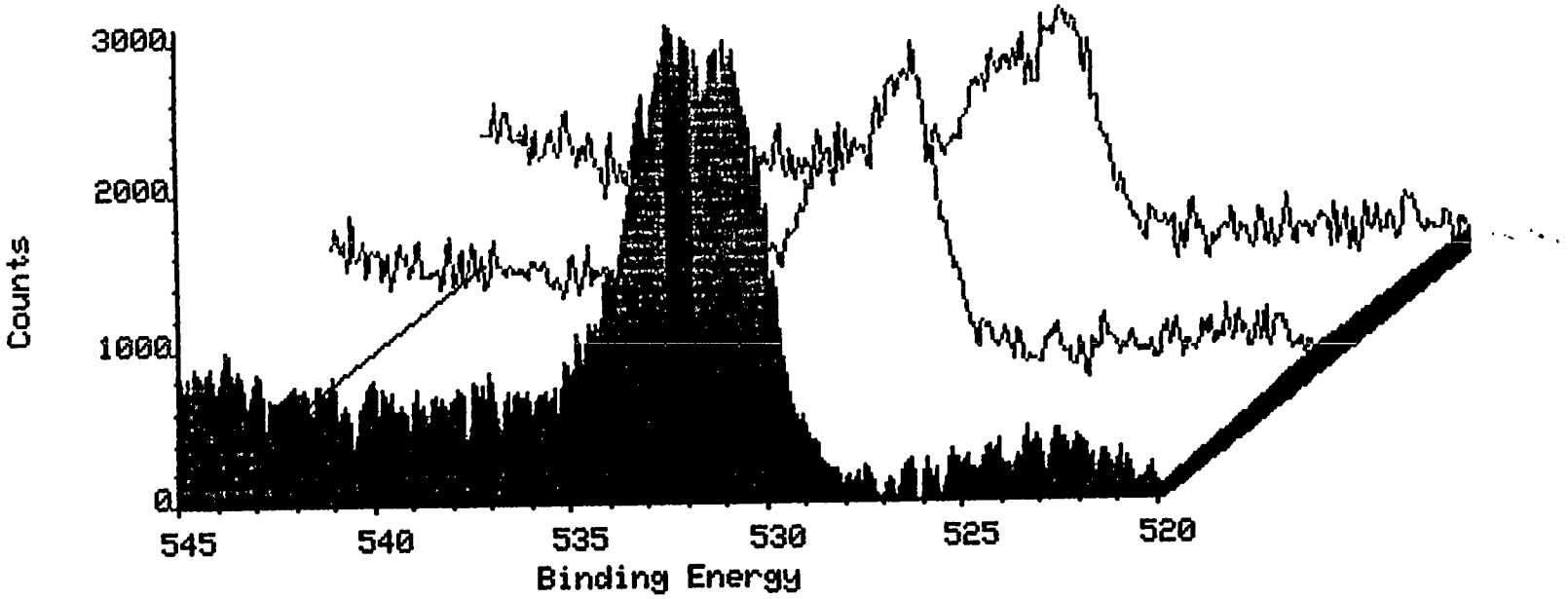

Figure 2. Typical SAXPS depth profile spectra of O 1s region for $Si_{0.05}$/FHYD residue

Figure 4

studies of catalysts where surface sulfide was covered with oxide/sulfate layers [12]. The surface enrichment of both oxygen and carbon was ascribed to atmospheric contamination on the surface resulting from exposing samples to air.

The surface chemical state of Si in the $Si_{0.05}$/FHYD sample was consistent with the most stable oxidation state (SiO_2) of Si with the expected binding energy of 103.3 eV. This chemical state was maintained throughout the bulk of the sample.

Figures 5, 6, and 7 show depth elemental concentrations, as a function of Ar^+ ion sputtering time, for the 30Å FHYD, $Si_{0.05}$/FHYD, and CA/FHYD catalyst residues, respectively. As Ar^+ ion sputtering proceeded and bulk composition is approached, increases in both the Fe and S concentrations were observed with corresponding decreases in both C and O concentrations. A slight decrease in the secondary element Si concentration was also observed with increased Ar^+ ion sputtering (Fig. 6).

The $S_{162.5\ eV}$/Fe ratio (from the peak area) which was initially (at the surface) much less than 1, generally increased with Ar^+ ion sputtering time. After Ar^+ ion sputtering for 20 minutes, the ratio approached closer to 1.1, the bulk pyrrhotite stoichiometry. The results are shown in Table 7. Previous EXAFS and Mössbauer studies have confirmed that these iron catalysts are converted to bulk iron sulfide (pyrrhotite) under liquefaction conditions [13]. The XPS studies are consistent with these findings but also show that significant deviation from the pyrrhotite stoichiometry can occur in the surface regions of the catalyst particles where presumably the active sites that promote the catalytic liquefaction process are to be found.

5. Mössbauer analysis of an hydrothermal Fe-S Catalyst and related residues from model hydrogenation and cracking tests (West Virginia University program, C. D. Stinespring, P.I.):

Mössbauer analysis of one sample of an iron sulfide catalyst prepared hydrothermally at 200°C and three samples of the catalyst residues from two model hydrogenation tests and a model cracking run has been completed. All four

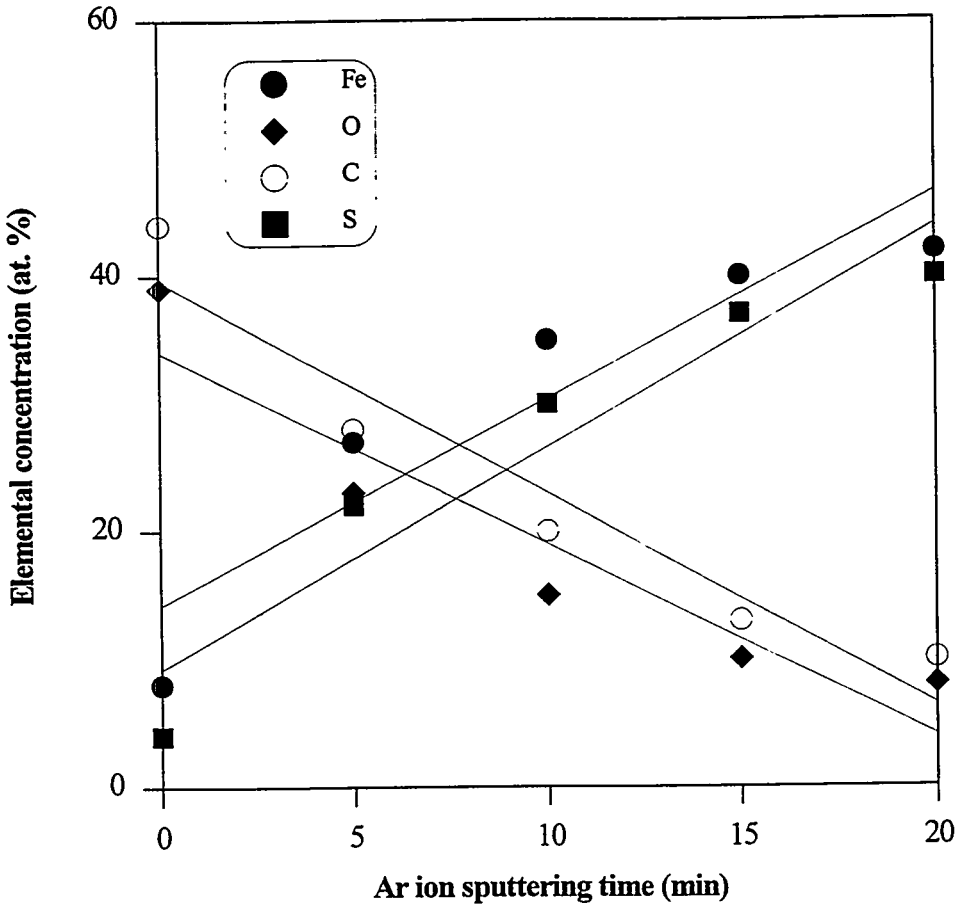

Figure 3. SAXPS depth profile of element concentrations (FHYD residue)

Figure 5

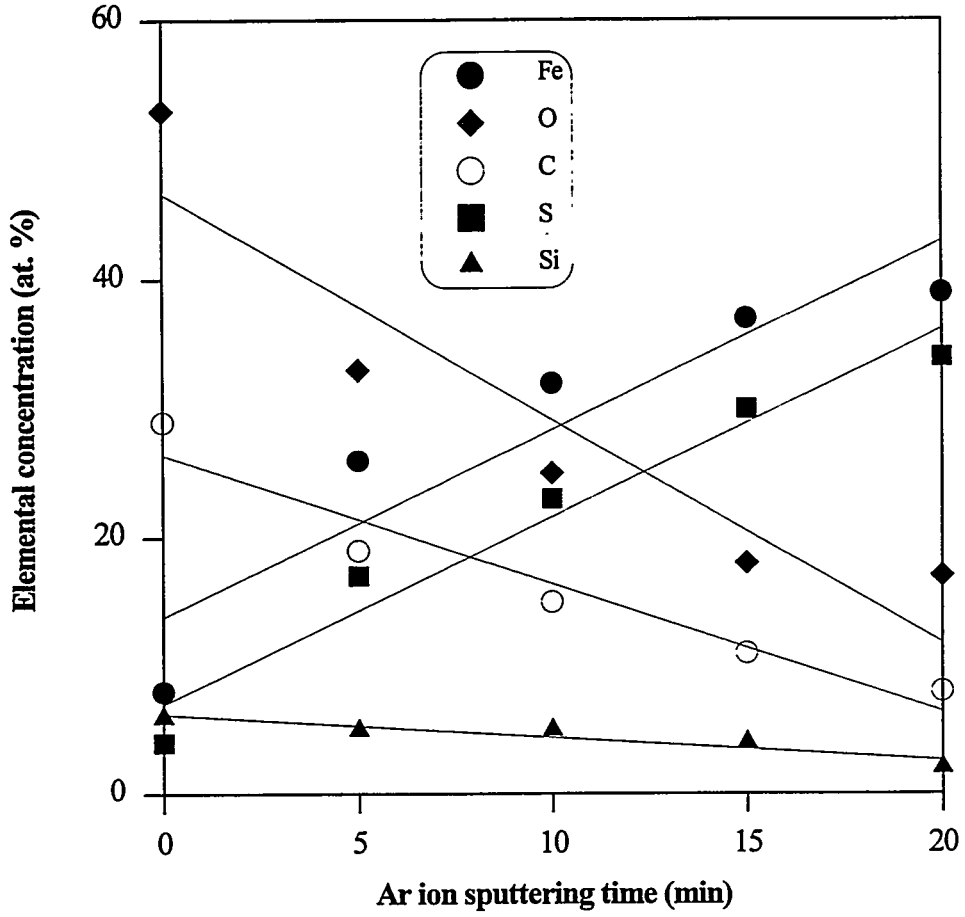

Figure 4. SAXPS depth profile of element concentrations ($Si_{0.05}$/FHYD residue)

Figure 6

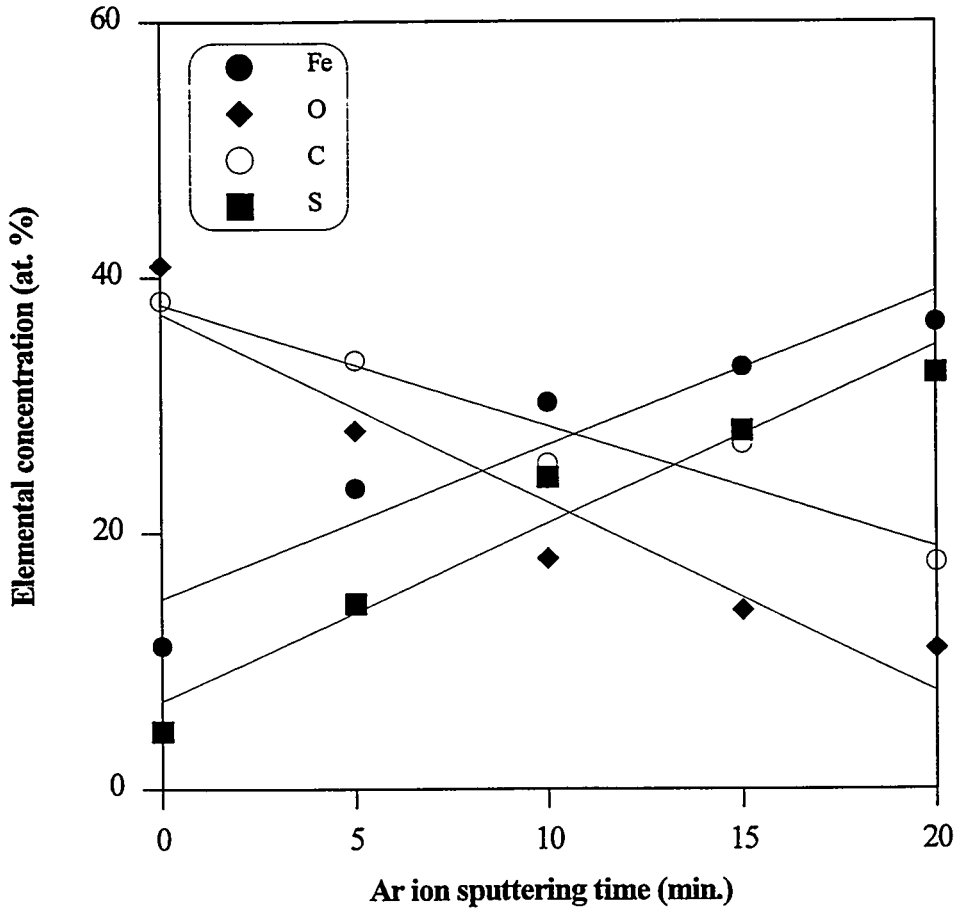

Figure 5. SAXPS depth profile of element concentrations (CA/FHYD residue)

Figure 7

samples were run at both room temperature and 13K. The data obtained at 13K were more informative as there was significant overlap between pyrite and oxyhydroxide absorption features in the RT spectra that made the analysis ambiguous. The data are summarized in Table 8.

The catalyst prepared at 200°C under hydrothermal conditions consists of at least four different absorption features: pyrite (FeS_2) accounts for almost half of the iron, with an iron oxyhydroxide phase constituting 35% of the iron, and the remainder of the iron (about 20%) in the form of two sulfates, jarosite (most likely, the hydronium jarosite: $H_3O^+Fe_3(SO_4)_2(OH)_6$) and melanterite ($FeSO_4.7H_2O$). Under hydrogenation and cracking conditions at 400°C, 1000 psi, for 30 min, there is some rearrangement of the iron: the amount of iron as pyrite decreases as it is converted into pyrrhotite, and the jarosite phase disappears completely. Both the oxyhydroxide phase and the ferrous sulfate increase relative to the corresponding fractions of these fractions present in the original catalyst prepared at 200°C. The amount of iron as ferrous sulfate after the model runs under He is approximately equivalent to the amounts of Fe present in the hydrothermal catalyst as jarosite and melanterite, suggesting conversion of the jarosite into ferrous sulfate. The conversion of pyrite to pyrrhotite is only partially completed in two of the model runs, whereas in the third model run the conversion is complete, but the amount of iron present as sulfide is significantly less than that in the original catalyst.

References:

1. F.E. Huggins, et al., Generic Structural Characterization Studies, 1993-94 CFFLS Annual Report to DoE, 1994.
2. C.A. Palmer, *Energy & Fuels*, **4(5)**, 436-439, 1990.
3. P.G. Harrison and T. Kikabhai, *J. Chem Soc. (Dalton Trans.)*, 807-814, 1987.
4. F.E. Huggins, J. Zhao, G.P. Huffman, M. Mulgaonkar, and A.R. Tarrer, *J. Environment. Sci. Health*, submitted, 09/94.
5. F.E. Huggins, et al., *Proceedings, Emerging Technologies in Hazardous Waste Management, VI*, ACS Special Symposium, Atlanta, GA, 993-996,

TABLE 8: Mössbauer Analysis of Hydrothermal Fe-S Catalyst and Residue Samples

(Prof. C.D. Stinespring, West Virginia University)

Sample	Phase	I.S.	ΔE_q	H_0	%Fe
Hydrothermally prepared 200C	Pyrite	0.38	0.61	-	44
	Jarosite	0.49	-0.13	388	14
	Oxyhydroxide	0.51	0.03	474	15
	Oxyhydroxide	0.49	-0.11	434	20
	$FeSO_4.7H_2O$	1.39	3.39	-	7
Model Run I Expt #6 Hydrothermally prepared cat. used to hydrogenate Phenanthrene 400C,1000psig H_2 pressure, 30min	Pyrite	0.40	0.61	-	21
	Pyrrhotite	0.88	-0.05	326	26
	Oxyhydroxide	0.50	-0.13	471	24
	Oxyhydroxide	0.49	-0.14	434	16
	$FeSO_4.7H_2O$	1.43	3.22	-	13
Model Run II, Expt #12 Hydrothermally prepared cat. used to hydrogenate Phenanthrene in tetralin at 400C,1000psig He pressure, 30min	Pyrrhotite	0.94	-0.07	327	18
	Oxyhydroxide	0.52	-0.10	493	36
	Oxyhydroxide	0.5	-0.17	453	25
	$FeSO_4.7H_2O$	1.4	3.38	-	21
Model Cracking Run,Expt #20 Hydrothermally prepared cat. used to crack cumene at 400C 1000psig He pressure,30min	Pyrite	0.39	0.61	-	26
	Pyrrhotite	0.88	0.02	331	8
	Oxyhydroxide	0.51	-0.09	493	15
	Oxyhydroxide	0.53	-0.09	462	18
	Oxyhydroxide	0.50	-0.11	428	16
	$FeSO_4.7H_2O$	1.41	3.29	-	17

1994.

6. J.Y. Kim and P.J. Reucroft, Surface characterization of binary ferrihydrite liquefaction catalysts, 1993-94 CFFLS Annual Report to DoE, 1994.
7. J.Y. Kim, P.J. Reucroft, M. Taghiei, V.R. Pradhan and I. Wender, *Energy and Fuels*, **8**, 886, 1994.
8. J.Y. Kim, P.J. Reucroft, V.R. Pradhan and I. Wender, *Fuel Processing Technology*, **34**, 207, 1993.
9. J. Zhao, et al., *Clays, Clay Minerals,* accepted for publication, 12/94.
10. D.L. Perry and A. Grint, *Fuel*, **62**, 1024, 1983.
11. D.C. Frost, W.R. Leeder and R.L. Tapping, *Fuel*, **53**, 206, 1974.
12. Y. Yoshimura, N. Matsubayashi, H. Yokokawa, T. Sata, H. Shimada and A. Nishijima, *Ind. Eng. Chem. Res.*, **30**, 1092, 1991.
13. P.A. Montano and B. Granoff, *Fuel*, **59**, 214, 1980.

TASK III

Project III.2

COAL STRUCTURE/LIQUEFACTION YIELD CORRELATIONS BY MEANS OF ADVANCED NMR TECHNIQUES

Ronald J. Pugmire
University of Utah

Introduction

The focus of our efforts in the Consortium for Fossil Fuel Liquefaction Science has been to use ^{13}C solid state NMR techniques to improve our understanding of the structure of coal and the relationship between structure and coal conversion processes, including the nature of the apparent synergistic interactions of coal and waste materials in these processes. While we have been pursuing collaborative efforts with consortium members to provide useful analytical information we continue to vigorously explore new spectroscopic techniques in order to increase the amount of information available from NMR experiments.

We have continued our engagement in a major program to develop new two-dimensional (2D) experiments that can provide more structural detail than is available from 1-D experiments. As there are only a few instances in the literature of shielding tensor components being measured from aromatic compounds with more than one benzene ring, we have begun a major effort to study the chemical shift tensor components of aromatic carbons in a variety of polycyclic aromatic hydrocarbons. The compounds chosen for study contain structural features that are believed to be important in the structure of clusters in coal. The development and application of the PHase cORrected Magic Angle Turning (PHORMAT) experiment has provided a major break-through in the types of data available from NMR experiments.

Another 2-D experimental technique (the 2-D flipper experiment) which has been developed in our laboratory has proven to be useful for the study of polymers. This experiment has proven to be especially useful for assessing the

amorphous/crystalline contents of polymers and the degree of orientation of such materials. Furthermore, this experiment can be used to study the orientational order of polymeric materials, including mesophase pitches.

Objectives

Our objectives continue to be the development of NMR techniques that provide new information about structural details in solids. Particular emphasis has been placed on those procedures that relate to coal, coal derived materials, and polymers. Our immediate objective is the measurement of the components of the chemical shielding tensors in model compounds and the application of these new techniques to coal structure studies and the study of simple polymeric materials.

Progress to Date

1. Spectroscopic Techniques Development

The PHORMAT experiment continues to be the focus of our development work. A new 400 MHz spectrometer was recently acquired with a specially designed rotor system that has enabled us to move from the VXR-200 spectrometer to the higher field strength. The new system operates as hoped and, with the addition of rotor-synchronization, the PHORMAT experiment at 400 MHz achieves resolution comparable to that obtained by the standard CP/MAS experiments. In Figure 1, the contour plots of each of the ten carbons in para-ethoxyphenyl acetic acid are clearly resolved. The projection of the data on to the isotropic shift axis displays the familiar isotropic shift spectrum. The isotropic chemical shift separation of carbons C-3 and C-5 are 1.8 ppm in a standard CP/MAS experiment and the excellent resolution obtained for these two carbons is apparent. The line width of the aromatic carbons is approximately 1 ppm.

The experimental data suffers somewhat from the lack of sufficient decoupling power. In Figure III.2.1, the proton decoupler was centered at the aromatic proton frequency which broadens the aliphatic carbons, particularly the CH_2 groups. Setting the decoupler frequency on the aliphatic proton frequency creates narrow aliphatic carbon lines but broadens the aromatic lines.

A correlation plot of the principal values of the ^{13}C chemical shift tensors is given in Figure III.2.2. The frequency (in ppm) of each line in Figure III.2.2

represents the three principal values for each carbon. From high to low chemical shift frequency (i.e., left to right) the principal values are designated δ_{11}, δ_{22}, and δ_{33}. The isotropic chemical shift is 1/3 ($\delta_{11} + \delta_{22} + \delta_{33}$).

The variation in principal values for each carbon provide much greater detail regarding the local environment than one can obtain from the isotropic chemical shift value. For instance, the isotropic chemical shift values of C-2 and C-6 are separated by 7 ppm. However, a major upfield shift (17 ppm) is noted in the δ_{33} component of C-6 compared to C-2. Our previous work on an aryl ether[1] allows us to ascribe this shift change to the steric interaction of the OCH_2 group lying in the plane of the molecule as shown in Figure III.2.2.

We have recently started to do a two-dimensional ^{13}C-NMR exchange experiment which employs rapid sample reorientation during the mixing time permitting the measurement of solid state ^{13}C resonance frequencies at two different sample orientations. This technique provides a method for probing the principal values of multiple ^{13}C chemical shift tensors from overlapping powder patterns of powders as well as the characterization of order in partially oriented materials. This experiment provides information not only on the ^{13}C chemical shift principal values but also provides data on the orientational distribution function of an ordered system. We have begun the study of polyethylene, polypropylene, as well as two mesophase pitches derived from naphthalene and methyl naphthalene. The two pitches have similar chemical shift tensors on the aromatic rings which indicates they have related aromatic ring structures. However, the significant differences in the molecular structure of these two pitches are also noted. The aromatic rings in both oriented pitches exhibit axial ordering with the preferential probability along the dominant axis. The probability distribution of the aromatic ring along the draw direction in the oriented mesophase pitch of methyl naphthalene is approximately three times greater than that in the oriented mesophase pitch of the naphthalene sample.

Publications

In 1994 one paper has appeared and three papers are in press. In addition, a summary of the work carried out under this project was presented at the recent

(November 6-11, 1994) Gordon Research Conference on The Chemistry of Hydrocarbon Resources.

1. Measurement of ^{13}C Chemical Shift Tensor Principal Values with a Magic Angle Turning Experiment, J.Z. Hu, A.M. Orendt, D.W. Alderman, R.J. Pugmire, C. Ye, and D.M. Grant, Solid State Nuclear Magnetic Resonance, 1994, 3, 181.

2. Solid State ^{13}C NMR, X-ray and Quantum Mechanical Studies of the Carbon Chemical Shift Tensors of p-Tolylether, J.C. Facelli, J.Z. Hu, A.M. Orendt, A.M. Arif, R.J. Pugmire, and D.M. Grant, J. Phys. Chem., 1994 (in press).

3. Magic Angle Turning Experiments for Measuring Chemical-Shift-Tensor Values In Powdered Solids, J.Z. Hu, W. Wang, F. Liu, M.S. Solum, D.W. Alderman, R.J. Pugmire, and D.M. Grant, J. Magn. Reson., 1994 (in press).

4. Coal Structure from Solid State NMR, R. J. Pugmire, Encyclopedia of NMR, John Wiley & Sons, Ltd., 1995 (in press).

References

1. J.C. Facelli, J.Z. Hu, A.M. Orendt, A.M. Arif, R.J. Pugmire, and D.M. Grant, J. Phys. Chem., 1944, in press

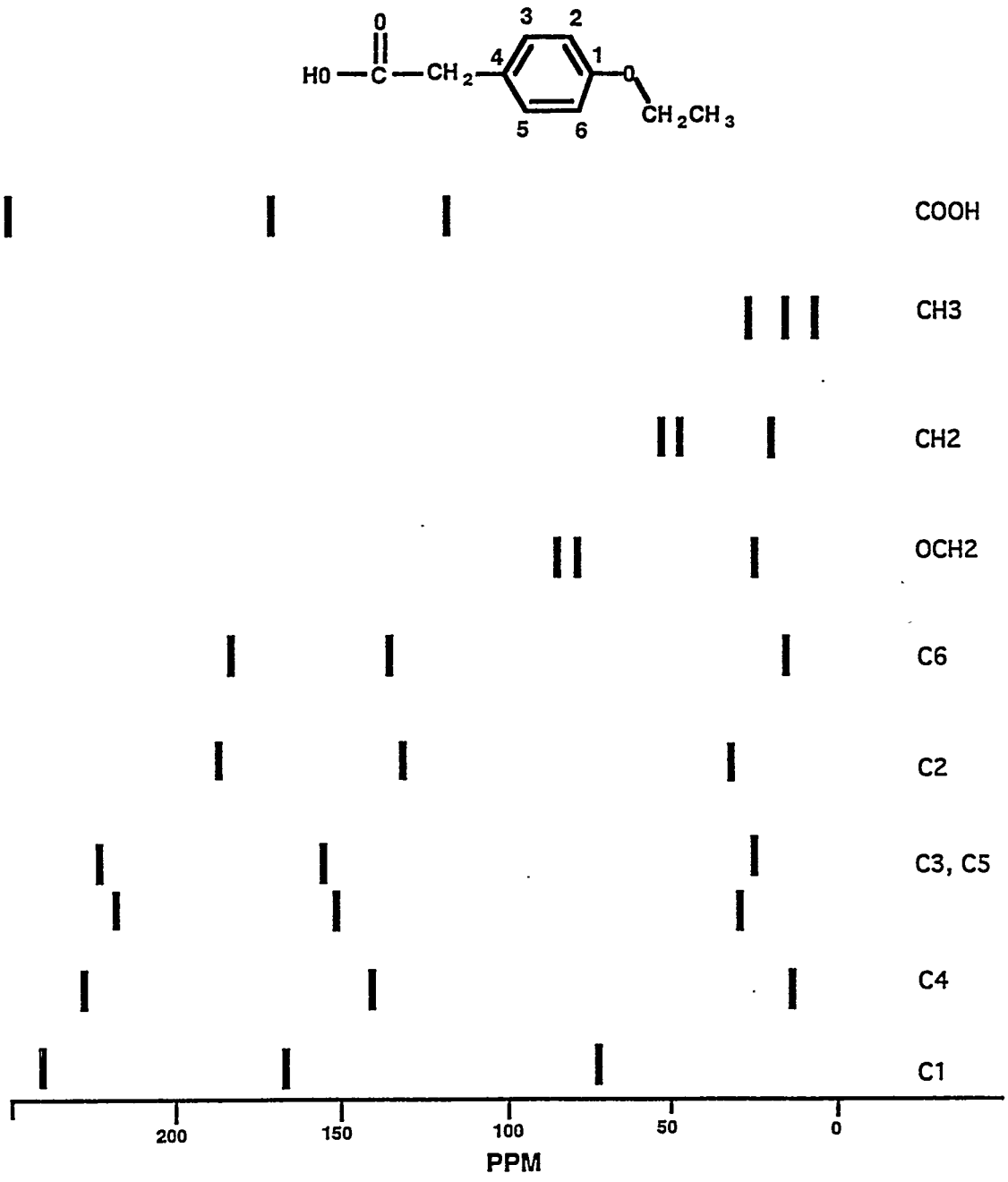

Figure III.2.1. PHORMAT spectra of para-ethyoxy phenyl acetic acid. The lower portion of the figure shows the contour plots for each peak. The upper portion is the projection of the data on the isotropic dimension showing the quality of the isotropic shift data obtained.

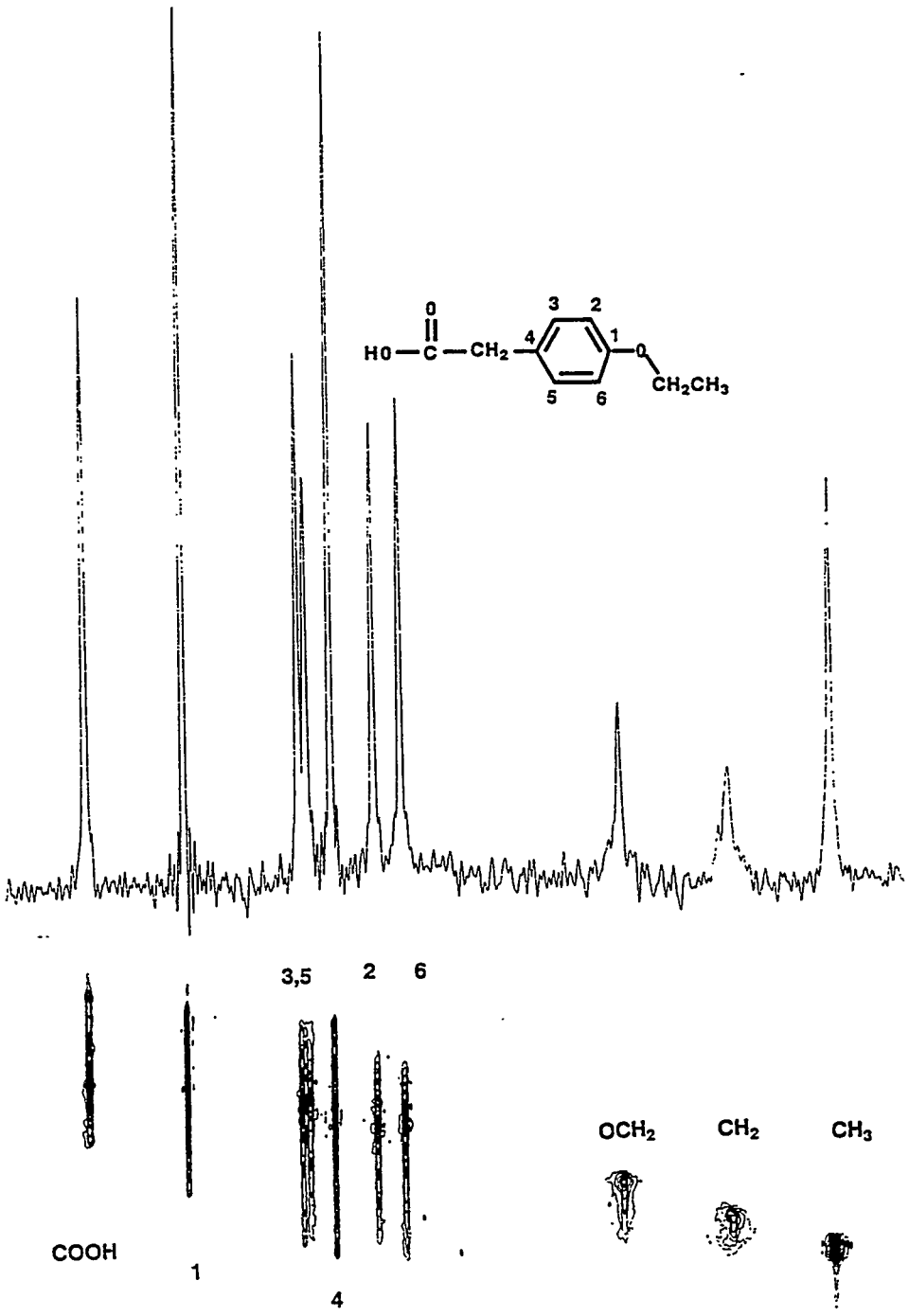

Figure III.2.2. Correlation plot of the ^{13}C chemical shift principal values for the 10 carbons in para-ethoxy phenyl acetic acid.

TASK III

Project III.3

CHARACTERIZATION OF COAL LIQUIDS BY HIGH PERFORMANCE LIQUID CHROMATOGRAPHY

Ramesh B. Subramanian, David M. Padlo and Edwin L. Kugler
West Virginia University

The goal of this research program is to develop rapid methods of characterizing coal liquids. The initial work had been focused on high performance liquid chromatography. We have reported previously that by using three HPLC columns, three solvents and at least one column switching valve, heavy hydrocarbon liquids can be separated into aliphatic, aromatic and polar fractions. Our current work has focused on quantitation of HPLC results, separation of THF soluble fractions using size exclusion chromatography, and simulated distillation by both gas chromatography and thermal-gravimetric analysis.

HPLC Aliphatics-Aromatics-Polars Analysis

The key detector for our HPLC aliphatics-aromatics-polars analysis is an evaporative light scattering detector. This detector functions by vaporizing the HPLC solvent stream into a heated tube where the solvent and light products evaporate. Higher boiling materials remain as small, discrete particles and are detected by light scattering. The initial problem solved with this detector was linearizing its highly non-linear response. A student wrote software to treat each individual time slice as a separate peak, and find the best exponential constant to linearize the detector output as a function of sample concentration.

After solving the non-linear response problem, we discovered that for a given weight of sample, the ELSD peaks were twice as large when methylene chloride was the solvent carrier as when pentane was used. We suspected this was related to viscosity, but did not know how to deal with it since we ran solvent gradients varying

from 100% pentane to 100% methylene chloride. We found that by increasing the flow of nebulizer gas, the response factors for the ELSD decreased, but converged toward a common value. Hence, we optimized the ELSD performance for dealing with solvent gradients.

The low molecular weight detection limit for the ELSD was determined by running a series of paraffins varying in size from 12 to 40 carbons. The results of this study are shown in Figure 1 where peak area of a specified weight of sample was studied as a function of sample boiling point and detector temperature. At 40°C sample detection begins at C_{16}, increases and levels off at C_{20}. The normal boiling point of C_{20} is approximately 340°C. As the detector temperature is increased, the threshold for uniform response increases. However, even though the detector temperature is varied, the maximum response goes to the same value for non-vaporizing solutes.

These detector studies resulted in our learning how to optimize ELSD response to a variety of solvent concentrations and gradients. The output can be linearized, and with standards, can be used to analyze unknown mixtures of coal liquids. The constraint on this analysis is that it be restricted to hexane soluble materials. Hexane insolubles precipitate in the system, contaminate columns and cause high pressure buildup.

HPLC Size Exclusion Chromatography

We have begun looking at HPLC size exclusion chromatography as a method of separating large molecules from smaller ones in coal liquefaction products. Since boiling point is related to molecular size for similar materials, we expect the smaller molecules to be low boiling. This technique is typically run with a strong solvent like THF, which dissolves the total coal liquefaction product.

We have obtained several coal liquefaction samples to test with size exclusion chromatography. A single sample of Wilsonville recycle bottoms from run 258, balance K, ran satisfactorily. This sample had been tested by ASTM D-1160 distillation and by TGA distillation at both HRI and Consol. As yet, we do not have enough information on the Wilsonville liquid to estimate its boiling point distribution

by size exclusion chromatography.

Simulated Distillation

Simulated distillation by gas chromatography is described by ASTM method D-2887 for petroleum distillates. The method works well when all of the sample elutes from the column. The chromatogram is then normalized, with the assumptions that all of the material injected is seen by the detector and that all of the compounds present have a similar response on a sample weight basis.

For a heavy product, normalization cannot be used since all of the sample injected does not elute from the column. We have found that the percentage of product detected can be determined with internal standards. Tests with petroleum vacuum gas oils showed that the uncertainty with an internal standard was less than 10% absolute. Applying this method with an internal standard to Wilsonville recycle bottoms produced results within several percent of the accepted value for the distillable fraction.

We have been providing simulated distillation service work for three other researchers at WVU. This has overloaded the instrument due to time required for the internal standard method. We plan to explore using external standards over the next reporting period, since this would reduce the number of runs by a factor of two, as well as simplifying sample preparation.

Two undergraduate students have started exploring simulated distillation by TGA using an older Netzsch thermal analyzer contributed by Exxon. We are setting up the instrument to do vacuum distillations. It has been calibrated at atmospheric pressure with NIST standards, but has not been run yet under vacuum conditions.

Plans

We are currently emphasizing boiling point analysis of liquefaction products. This will be done by HPLC size exclusion chromatography, GC simulated distillation and TGA simulated distillation. The size exclusion chromatography will involve collecting time fractions to correlate molecular size and boiling point with retention time. The GC simulated distillation will explore using external standards for

determining the amount of product that is detected when running high boiling samples. We hope to get the TGA equipment fully operational for vacuum distillations.

ELSD RESPONSE

Amount injected: 20 µg; Flow rate: 1.5 ml/min, pentane; N2 flow: 4 l/min

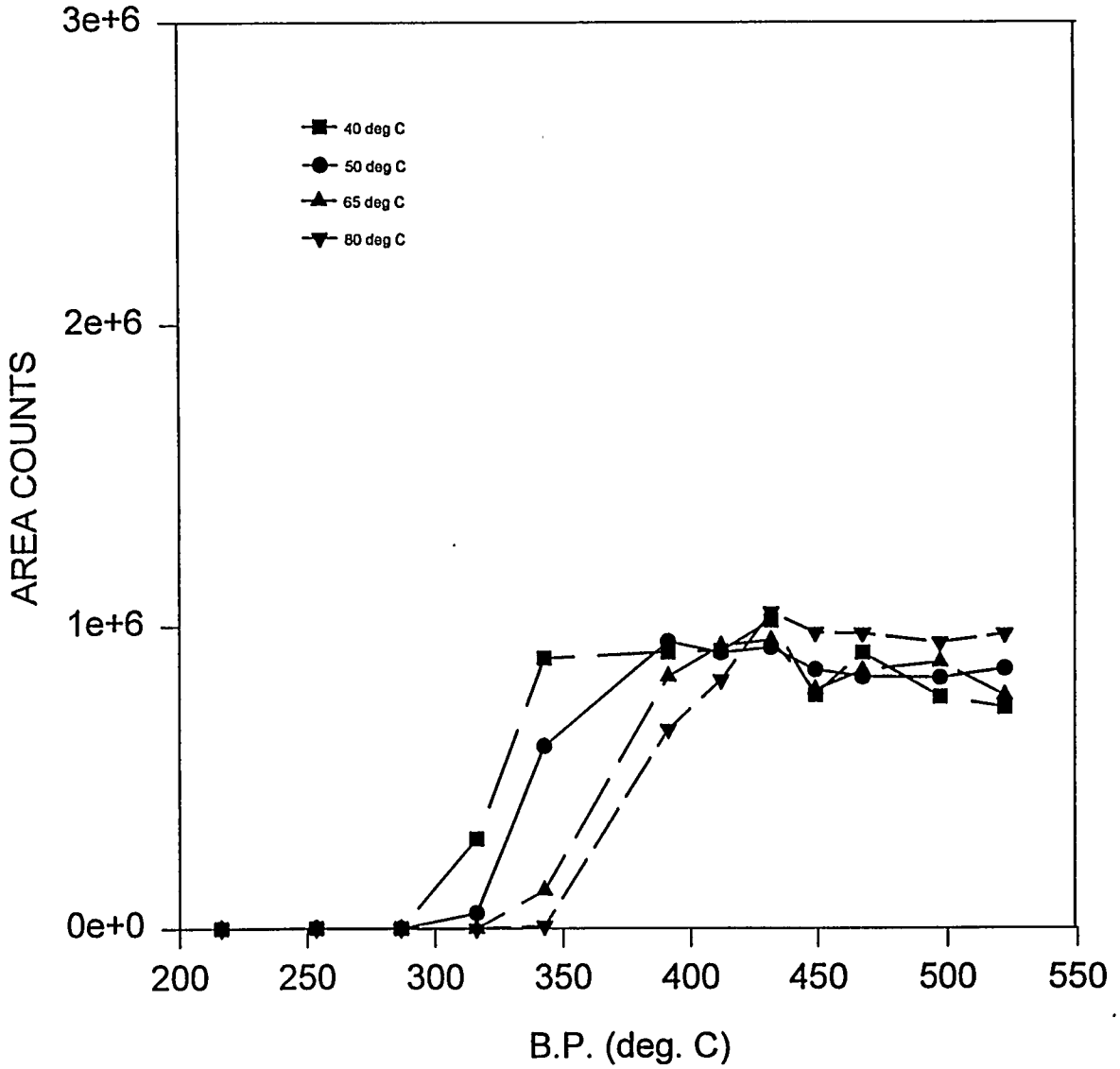

TASK III

Project III.4

COMPUTER MODELING OF LIQUEFACTION CATALYSTS AND REACTIONS

Harriet F. Ades and K.R. Subbaswamy
University of Kentucky

There were two main topics on which we worked during the first six months of this contract period (i) preliminary work on co-liquefaction: modeling the presence of LDP, and (ii) continuing work on DCL binary catalysts and iron sulfided catalysts.

I. Modeling Co-Liquefaction of Coal with Low Density Polyethylene (LDP): Preliminary Results

- Objective: Understand Synergism

Anderson and Tuntawiroon (1993) reported a synergism in the conversion yield of a 50/50 mixture of coal and polyethylene (PE). Of specific interest is whether the reported synergism results from more efficient hydrogen transfer to coal fragment dissociation products in the presence of PE as has been suggested by some investigators.

- Method

A new quantum mechanical force calculation method [Menon and Subbaswamy (1993)] (non-orthogonal tight-binding method: NTBMD) that has been successfully applied to silicon and carbon clusters, including fullerenes, has been used. It draws from extended Hückel and Slater-Koster methods. It can be used for finite temperature simulations as well. For simple organic compounds results from this method are comparable to those from MOPAC 5.2 quantum chemistry package.

- Modeling

We consider fragments of PE (LDP) characteristic of what is expected under experimental conditions. These are brought in contact with coal model compounds (initially toluene, later more complex ones) and H_2. Reaction pathways are studied.

- Preliminary Tests and Results

In Fig. 1 (a and b) we show the initial and final geometries when a neutral PE fragment is brought within reacting distance of a toluene molecule. As expected,

there is no tendency for any reaction to occur. In Fig. 2 (a and b) the initial and final geometries when a neutral PE radical fragment is brought within reacting distance of a toluene molecule are shown. While there is significant weakening of the proximate ring C-H bond, there is no scission. In Fig. 3 (a and b) the initial and final geometries for this same situation are shown, except that now a free H_2 molecule is also brought into the vicinity. As can be seen, the H_2 bond is broken with one hydrogen atom adding to the PE radical, one H atom adding to the β-position of the toluene molecule.

- Discussion

1. Comparison of bond strengths:

H-H	104	(Kcal/mole)
$H\text{-}CH_2CH_3$		98
$H\text{-}CH_2C6H_5$	85	
$CH_3\text{-}CH_3$	88	
$CH_3\text{-}CH_2CHCH_2$		72
$CH_3\text{-}C_6H_5$	93	

2. The C-C bonds near a branch are among the weakest bonds in the system; it is likely that these will be the first to break, creating PE radicals. According to our preliminary work, these, in the presence of H_2 appear to promote reactions such as β-scission of coal molecular fragments.

LDP radical fragments might promote hydrogenation of coal fragments, leading to easier bond scission. Since LDP radicals are more readily formed at lower temperatures, coal conversion can begin at lower temperatures.

In future work we will investigate more reaction pathways and try to construct kinetic models to gain better understanding of the influence of LDP. Also, the effect of catalysts will be studied.

II. Modeling DCL Catalysts

Effect of adding molybdenum to FeS based catalysts.

Motivation:Pradhan, et al. (1991)

Methods:Same as in Ades, et al., Energy Fuels, 1994, 8, 71.

We find that in the presence of the Mo impurity, the favored absorption site for the $Ph\text{-}CH_3$ is the so-called η^6-site. This corresponds to an arene-type complex. We

completed computations for the "fine-tuning" of geometries involving two surface-sites (A or B molybdenum position on the Fe 0001 surface as shown in Fig. 4). The results are given below:

Case	Ph--CH_3 BDE(eV)	Adsorption Energy (eV)
Free	4.25	
Mo(A)	2.85	5.62
Mo(B)	3.22	5.84

We conclude that Mo does not aid in depolymerization. The experimental results on increased yield is probably due to increased efficiency in hydrogenation.

We have continued work on different initial positions of toluene on the Fe 0001 surface of FeS. We find that there are two possible stable adsorption sites -- both with the center of the phenyl ring of toluene over an Fe atom (η^6-position). In one of these the Ph-CH_3 bond is over an Fe atom. The electron density from this bond is withdrawn by the Fe atom, weakening the bond more than in the other adsorption site.

In future work we will investigate more LDP reaction pathways and try to construct kinetic models to gain better understanding of the influence of LDP in co-liquefaction.

Fig. 1a (Initial)

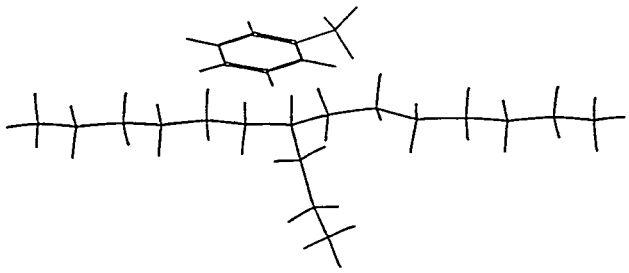

Fig. 1b (Final)

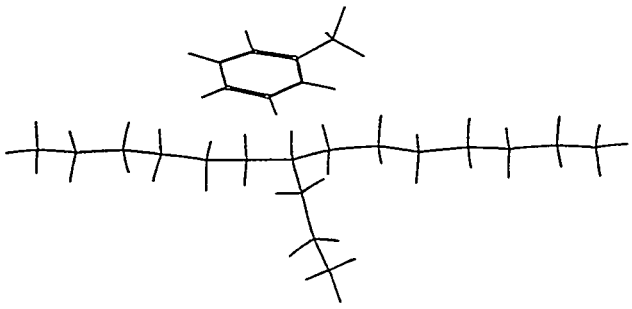

Fig. 2a (Initial)

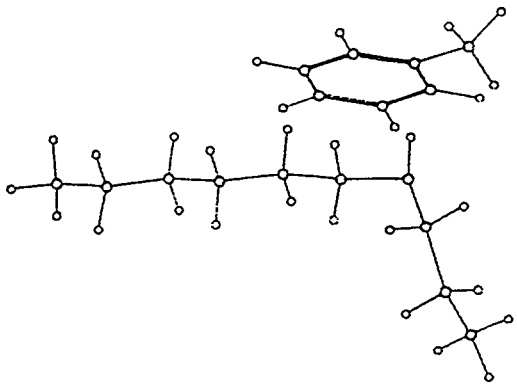

Fig. 2b (Final

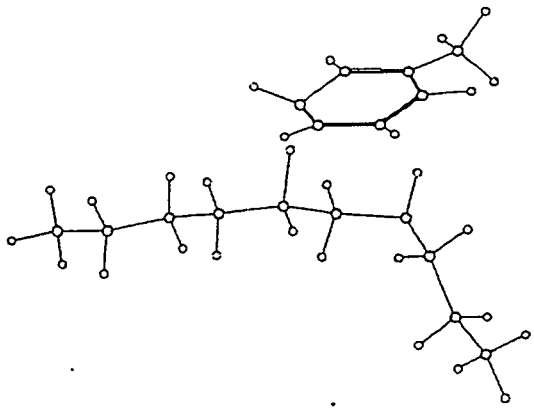

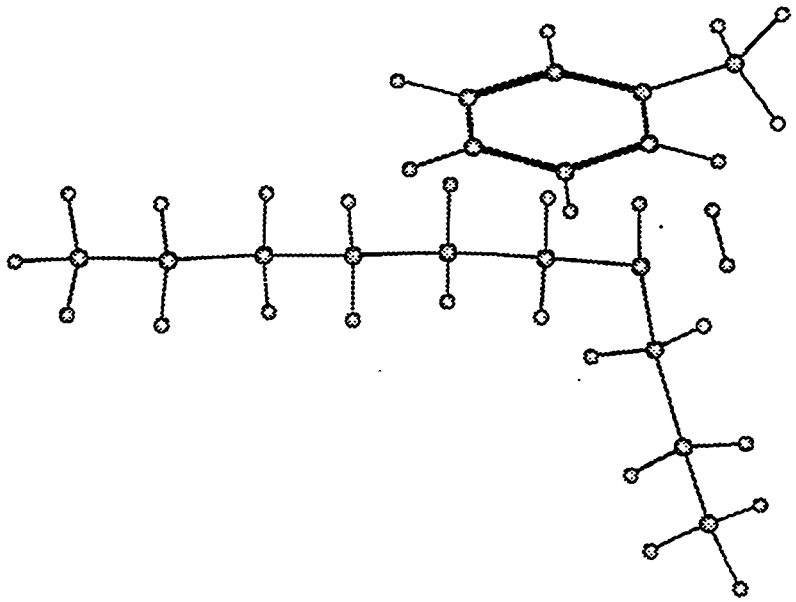

Fig. 3a
Initial

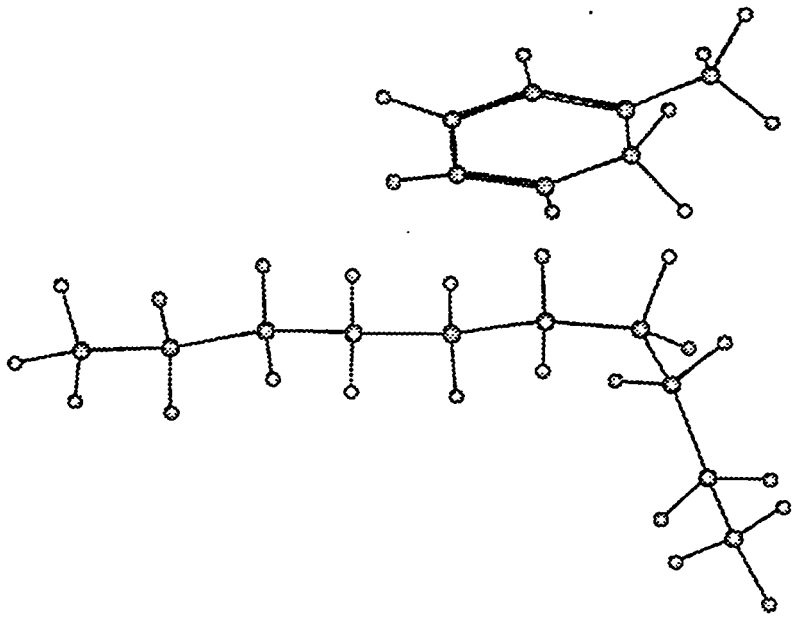

Fig. 3b
Final

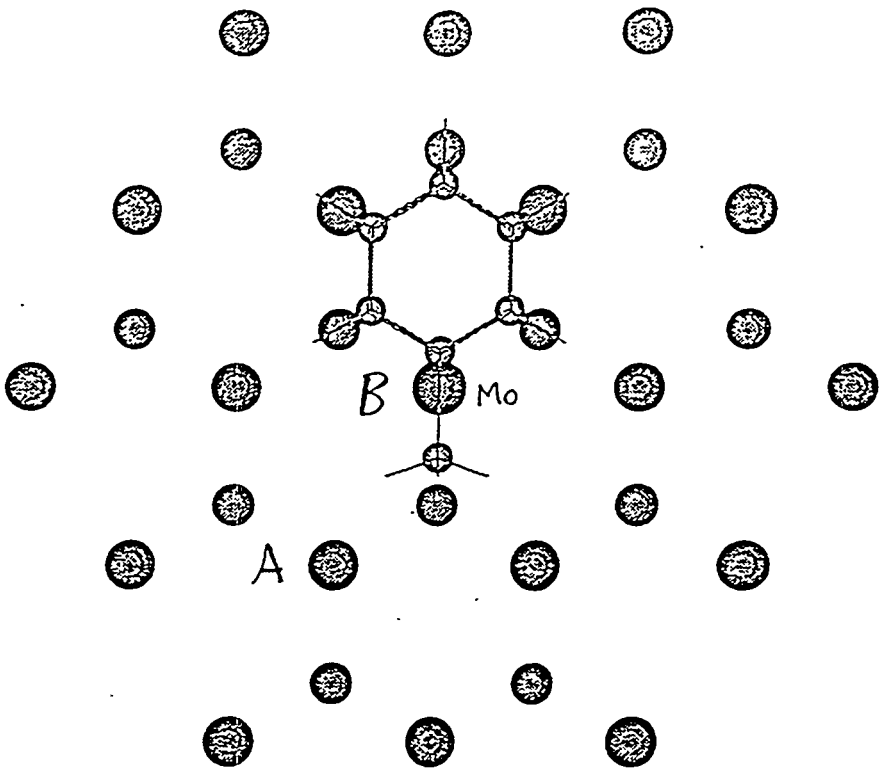

Figure 4

TASK III

Project III.5

BIOPROCESSING OF COAL

D. Bhattacharyya, M.I.H. Aleem, R.I. Kermode
M.V.S. Murty, D. Schieche
University of Kentucky

SUMMARY

In order to investigate the hydrogen limitation during the biohydrogenation of organics, high pressure (500 psig) hydrogen gas was applied in a multipurpose bioreactor. A preliminary study with *D. desulfuricans* under (normal and high pressure) hydrogen showed complete reduction of fumarate within 24 hours. The reaction rates of fumarate biohydrogenation were fully explained using Michaelis-Menten model and activated substrate model.

Time course experiment revealed that maximum liquefaction occurred at the end of 10th day of the treatment of coal IBC #105 in the presence of *Acidianus brierleyi*. A preliminary bioprocessing study was conducted on a mixture of polyethylene and IBC coal to increase *A. brierleyi* adsorption on PE and coal surfaces. The microbial adsorption may help in uniform distribution of reprecipitated iron catalyst (FeOOH) on the surface of PE and coal. This process in turn may enhance direct liquefaction and quality of oil. The results indeed showed an increase of 10 % liquefaction yield and about the double the amount of oil yield over the control sample. An extensive literature search was conducted on the thermal degradation of commercial polymers in order to effectively utilize them in coliquefaction with coal.

Reaction Rate Modeling of Fumarate Biohydrogenation Results

We have conducted several experiments on the biohydrogenation of coal and model compounds in the presence of microorganisms (1,2). *D. desulfuricans* was used in experiments to investigate the hydrogenation of soluble organics under low and high pressure hydrogen gas. Results of biohydrogenation of fumarate and effect of

bacterial cell concentration were given in last year's annual report (May 1994) (3). Data gathered from the fumarate reduction experiments were used to determine a reaction rate law for the biohydrogenation of fumarate to succinate under hydrogen gas using the anaerobic bacteria *D. desulfuricans*. Specifically, data from the experiment which investigated the effect of pressure on hydrogenation between 1 and 35 atm using acclimated bacteria were used.

The reaction rate models that were proposed were Michaelis-Menten and substrate activation. Model parameters were determined and all models were graphically fitted with each data set for comparison.

The rate law parameters were determined by the integral method using the Statistical Analysis Software (SAS) package. This package determined the model parameters along with an asymptotic standard error value for each parameter generated. Each rate law was integrated and the resulting nonlinear equation was entered into a procedure function with the data. The SAS program then used the procedure function to solve for the rate law parameters.

It was determined in that the chemical reaction for the biohydrogenation of fumarate to succinate was initially a zero-order reaction for the first six hours. A reaction rate model such as the Michaelis-Menten model was logical to try and fit to the data sets. It behaves as a zero-order reaction at high substrate concentration, then transfers to a first-order reaction rate type as the substrate concentration decreases.

$$-\frac{dC}{dt} = \frac{V_{max}\,C}{(K_m+C)} \qquad (1)$$

The model parameters were fit to the data sets using the SAS package as outlined above. These values are

$$Vmax = 0.98 \text{ mmol/(L-hr)}$$
$$Km = 1.26 \text{ mmol/L}$$

A graph of the model with the data is presented in Figure 1. The model fits the data

well in Figure 1, which was the 35 atm data set. The statistical method failed to determine parameters for the 1 atm data set. This fact suggests that the Michaelis-Menten reaction rate model might not be the best rate model to describe the biohydrogenation of fumarate.

The activated substrate model suggests that some substrate binds with the enzyme in the bacteria and activates it by forming an activated complex. This complex is the catalyst that carries out the biohydrogenation reaction.

$$-\frac{dC}{dt} = \frac{V_{max}\,C}{\left[K_1 + C + \frac{K_2}{C}\right]} \qquad (2)$$

The activated substrate model is similar to the Michaelis-Menten rate model in that it is initially zero-order at high substrate concentration, then changes reaction order as the substrate is depleted. But, instead of shifting to a first-order reaction, the activated substrate model follows second-order kinetics as the substrate concentration is decreased.

The model parameters for this reaction rate model as determined by SAS are given below.

	1 atm	35 atm
Vmax, mmol/(L-hr)	4.41	3.24
K1, mmol/L	6.55	8.83
K2 , (mmol/L)2	76.25	5.33

The graphical results for both the 1 and 35 atm reactions are given in Figure 2. The model fits both data sets well. Since the Michaelis-Menten model only fit one of the data sets, the activated substrate reaction rate model might be a better choice than the Michaelis-Menten reaction rate model for fumarate biohydrogenation with acclimated *D. desulfuricans*.

Dispersion of Reprecipitated Iron Catalysts on Coal and Polyethylene in the Presence of *Acidianus brierleyi*

This work deals with the formation of ultra-fine active iron particles and even

distribution of the fine FeOOH crystals on the surface of coal and waste polymers by using *Acidianus brierleyi*. Increase in microbial adsorption on polymer and coal surface for even dispersion of reprecipitated iron catalyst (FeOOH) on the surface of polymer and coal may enhance direct liquefaction and quality of oil.

We reported that *A. brierleyi* can change the iron forms of coals with enhanced liquefaction due to the FeOOH particles formation on the surface of coal (2-5). Treatment of high pyrite, high sulfur Illinois (IBC) coals and pyrite-free Blind Canyon (DECS) coal with added pyrite in the presence of *A. brierleyi*, showed catalyst formation and enhancement in liquefaction and oil yield (5). The direct liquefaction conversion and oil yield of the biotreated DECS #17 coal with added pyrite, went up by 14 and 5 % respectively over the control which did not contain A. brierleyi.(3,5) However, this process of biotreatment requires longer period (over 20 days) of incubation for the reprecipitation of liquid phase iron. A time course experiment where, the initial pH was maintained at 2.4 (constant) and at the end of 10th day the pH of the medium was shifted from 2.4 to 2.8 by the addition of 0.05 M NaOH. The liquefaction yield of the biotreated coal sample obtained at the end of 11th day, was increased by 12% over the control sample (Figure 3). The samples obtained after 11th day of treatment did not show any further increase in liquefaction.

We are trying to verify the formation of microcrystals of iron based catalysts on the coal and polymers surfaces by changing various physical and chemical parameters (pH, temperature, and different polymers) of the bio-reaction system. In a preliminary experiment, polyethylene (low density, 2.5 W%) and IBC coal #105 (2.5 W%) was treated with *A. brierleyi* at 68 C with a pH of 2.4. The pH of the medium was maintained at 2.4 for 9 days. At the end of 10th day, pH of the medium was raised to 2.8 for rapid precipitation of liquid phase iron. Coal + polymer mixture was collected at the end of 10th day by filtration and dried it overnight at 85 C. Our preliminary results showed that the liquefaction conversion and oil yield of the biotreated coal + polyethylene (1:1), were increased by 50 and 13 % respectively (Figure 4). Whereas control showed only 40 % liquefaction conversion and 6 % oil yield. We are in the process of repeating these experiments to establish the effect of polyethylene on liquefaction and oil yield.

Literature Review on Thermal and Liquefaction Kinetics of Commodity Polymers

Recycling of commodity polymers such as PVC, PET, and PS as high quality fuels (by co-liquefaction with coal) could be one of the best alternatives, since it improves the quality of the coal-based product and minimizes disposal in landfills. Although thermal degradation and pyrolysis of various polymers have been reported in literature, the fundamental information on direct liquefaction kinetics needed for process scale-up and optimization of oil properties is not available. The variables expected to be significant are: polymer type, solvent choice, degradation temperature range, catalyst (added or inherent in the polymer, such as metal stabilizers and fillers), and time of hydrogen addition. The thermal stability of PVC has been studied because it is particularly sensitive to temperature (6-11). These studies have focused on HCl evolution, with little information about the molecular weight distributions and conversions. The presence of PVC stabilizers will affect the thermal degradation properties. Several workers have reported that strong electrophilic chlorides such as ZnCl2, FeCl3, and AlCl3 (7) considerably accelerate the dehydrochlorination of PVC, except organotin chlorides of high Lewis acidity. However, in nitrogen atmosphere at 190o C, the samples with AlCl3 exhibited lower dechlorination rates than ordinary PVC. Depending on the source, there may be other additives with catalytic or inhibitory activity, such as calcium stearate, titanium dioxide, and butyl tin.

Pyrolysis and degradation of PS has been studied with the goal of converting the polymer to monomer as the method of recycling, rather than to produce a liquid fuel. Literature reports on the degradation of PS in several solvents (13,14) show that its conversion to low molecular weight products depended on the hydrogen-donating ability of the solvent used. Solvents with greater hydrogen-donated ability showed lower conversion of PS (14). Contamination of PS with other materials, such as lignin, affects extent of thermal degradation (15). To our knowledge, there are no reports of polymer (PVC, PS) degradation coupled with direct addition of hydrogen, as is anticipated in a liquefaction process. We will focus

on PS and PVC because of the available mechanism information about thermal degradation.

References

1. Murty, M.V.S., Aleem, M.I.H., Kermode, R.I., Bhattacharyya, D. (1994) J. Chem. Tech. Biotech. 60, 359-368.

2. Murty, M.V.S., Bhattacharyya, D., Aleem, M.I.H. (1994) In Biological Degradation and Bioremediation of Toxic Chemicals (Ed. G.R. Chaudhry), p. 470-492, Timber Press Inc. Portland, Oregon.

3. Bhattacharyya, D., Murty, Kermode, R.I., and Aleem, M.I.H., and D. Schieche (1994) "Bioprocessing of model organics by *Desulfovibrio sp.* and coal by *Acidianus brierleyi*" The VIIIth Annu. Tech. Meet., CFFLS, Snowbird, UT.

4. Kermode, R.I., Venkatachalam, M., Murty, M.V.S., Bhattacharyya, D., Aleem, M.I.H. (1994) "Microbially formed catalysts for enhancement of direct liquefaction yield". Chem. Eng. Commun. 128 (in press).

5. Murty, M.V.S., Huggins, F., Kermode, R.I., Bhattacharyya, D., Aleem, M.I.H. (1994) "Biogeneration of iron based catalysts by *Acidianus brierleyi* on high and low pyrite coals for direct liquefaction". Energy & Fuels (under revision).

6. Kim, C.H., Park, J.K., and Son, W.K. (1994) Polym. Deg. Stability, 44, 163-169.

7. Yassin, A.A., Sabaa, M.W. (1990) J. Macromol. Sci. Rev. Chem. C30, 491-5558.

8. Rogestedt, M. and Hjertberg, T. (1994) Polym. Deg. Stability, 45, 19-25.

9. Jimenez, A., Berenguer, V., Sanchez, A. (1993) J. Appl. Polym. Sci., 50, 1565-1573.

10. Benavides, R., Edge, M., and Allen, N.S. (1994) Polym. Deg. Stability, 44, 375-378.

11. Garrigues, C., Guyot, A., and Tran, V.H. (1994) Polym. Deg. Stability, 44, 63-70.

12. McNeill, I.C., Zulifquar, M., Kousas, T. (1994) Polym. Deg. Stability, 28, 131-151.

13. Sato, S., Murakata, S., Saito, Y., Watanabe, S. (1990) J. Appl. Polym. Sci. 40, 2065-75.

14. Murakata, T., Saito, Y., Yosikawa, T., Sato, S. (1993) Polymer, 34, 1436-39.

15. Mansour, O.Y. (1992) Polym.-Plast. Technol. Eng., 31, 747-758.

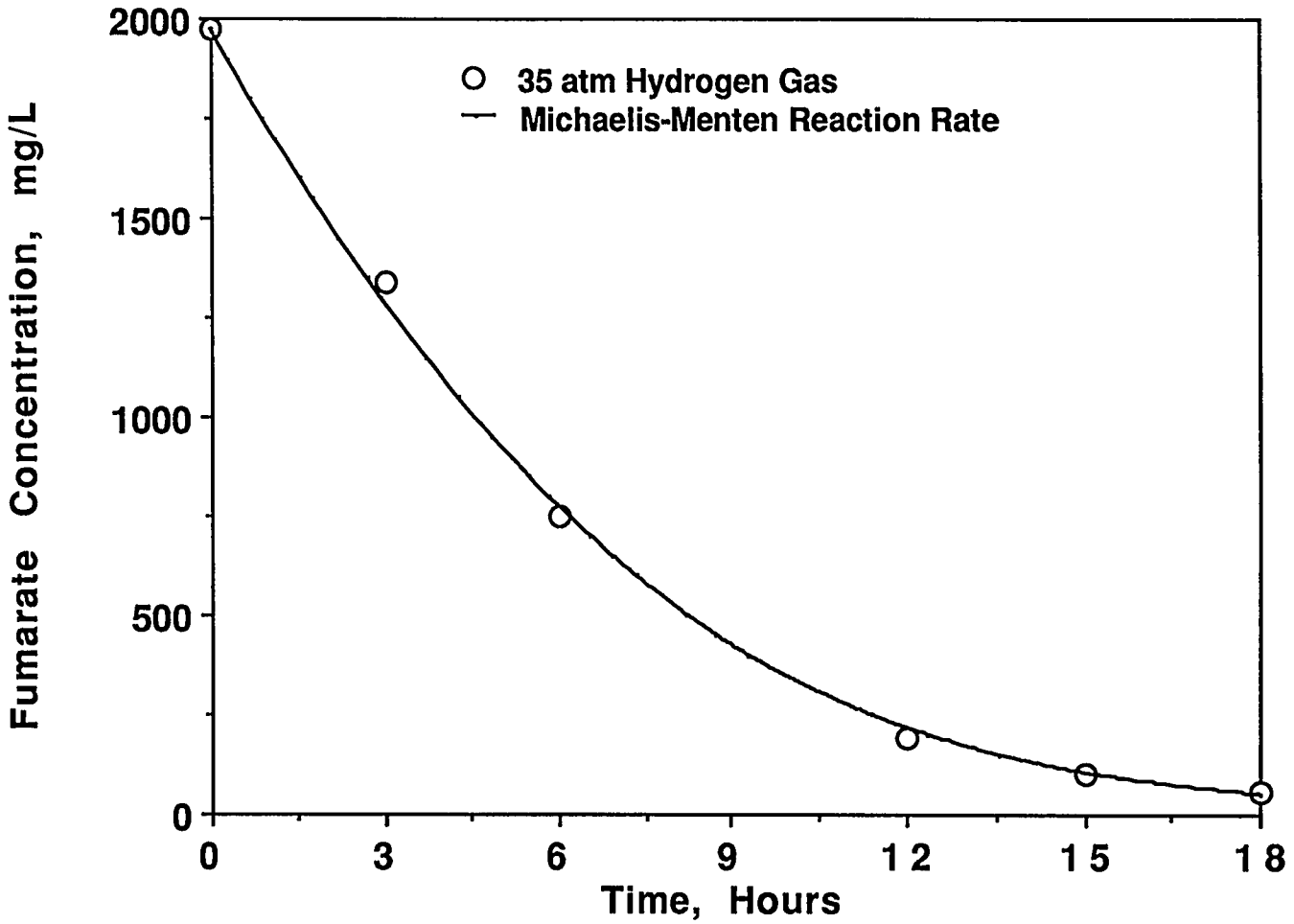

Figure 1. Michaelis-Menton Reaction Rate Fit of Fumarate Data for Fumarate Hydrogenated With D. desulfuricans at 35 atm, pH 7.4, 36°C, Using Hydrogen Gas

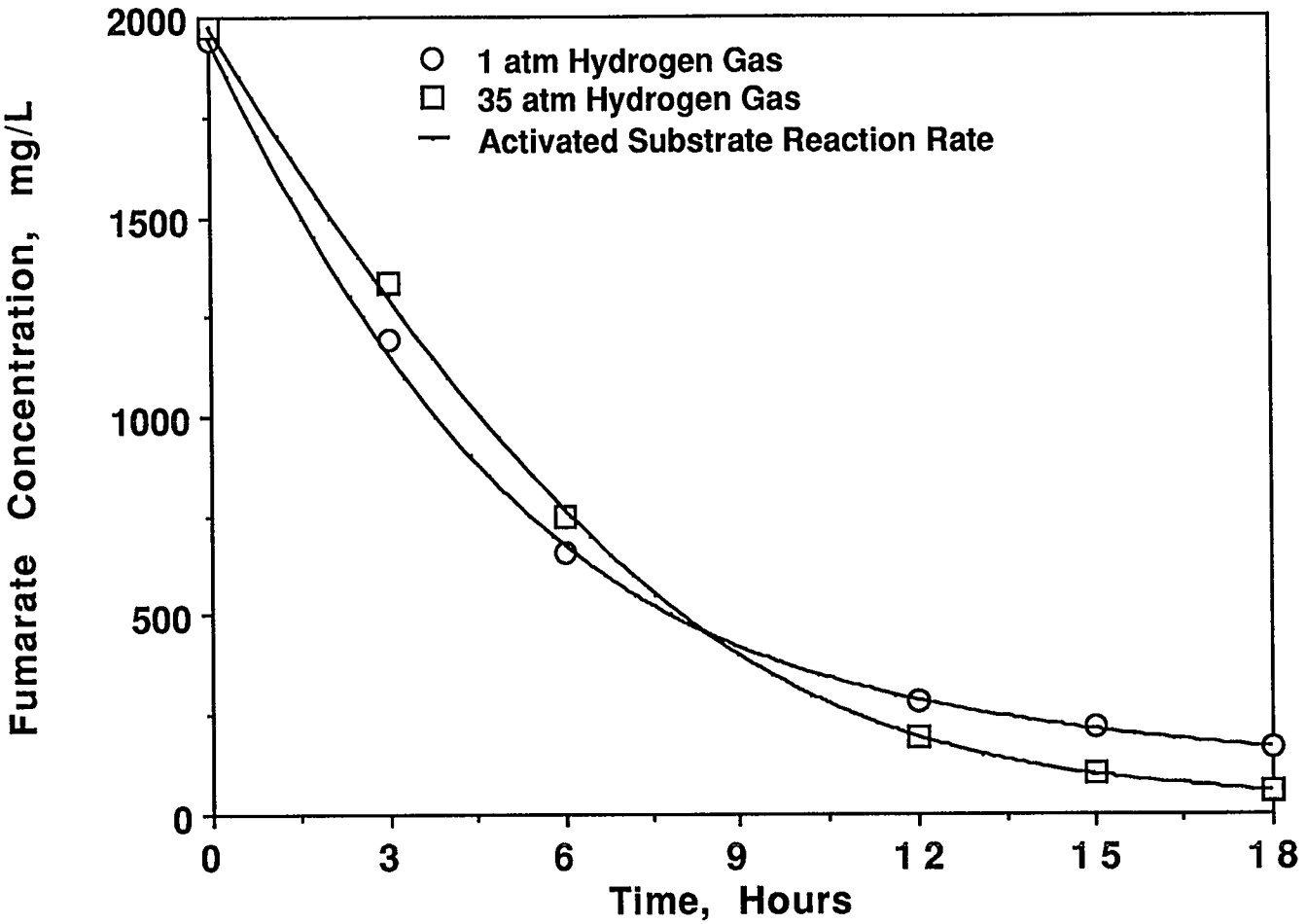

Figure 2. Activated Substrate Reaction Rate Fit of Fumarate Data for Fumarate Hydrogenated With D. desulfuricans at Both 1 and 35 atm, pH 7.4, 36°C, Using Hydrogen Gas

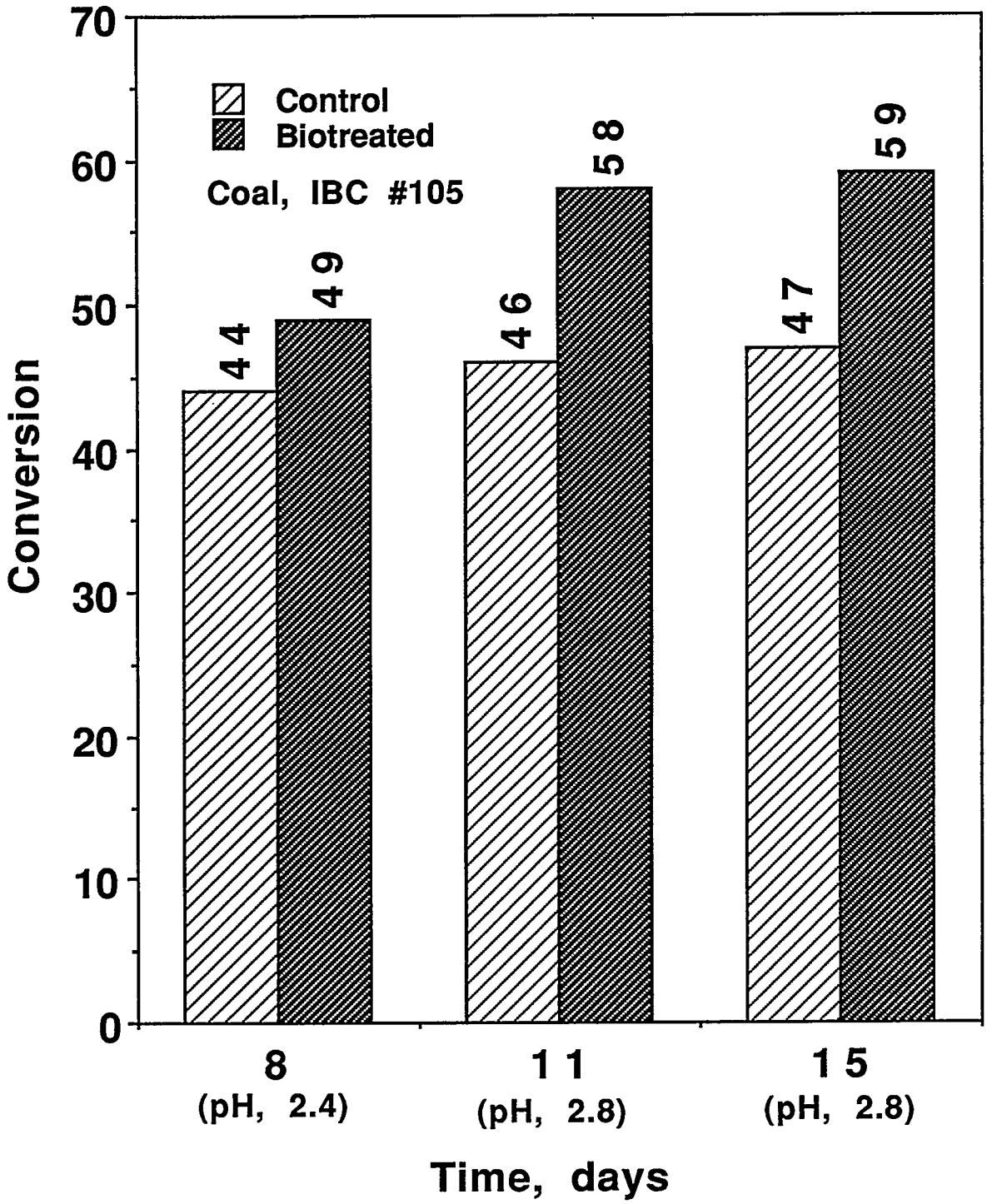

Figure 3. Time Course of Direct Conversion of Coal (5%) Treated with A. brierleyi at 68°C

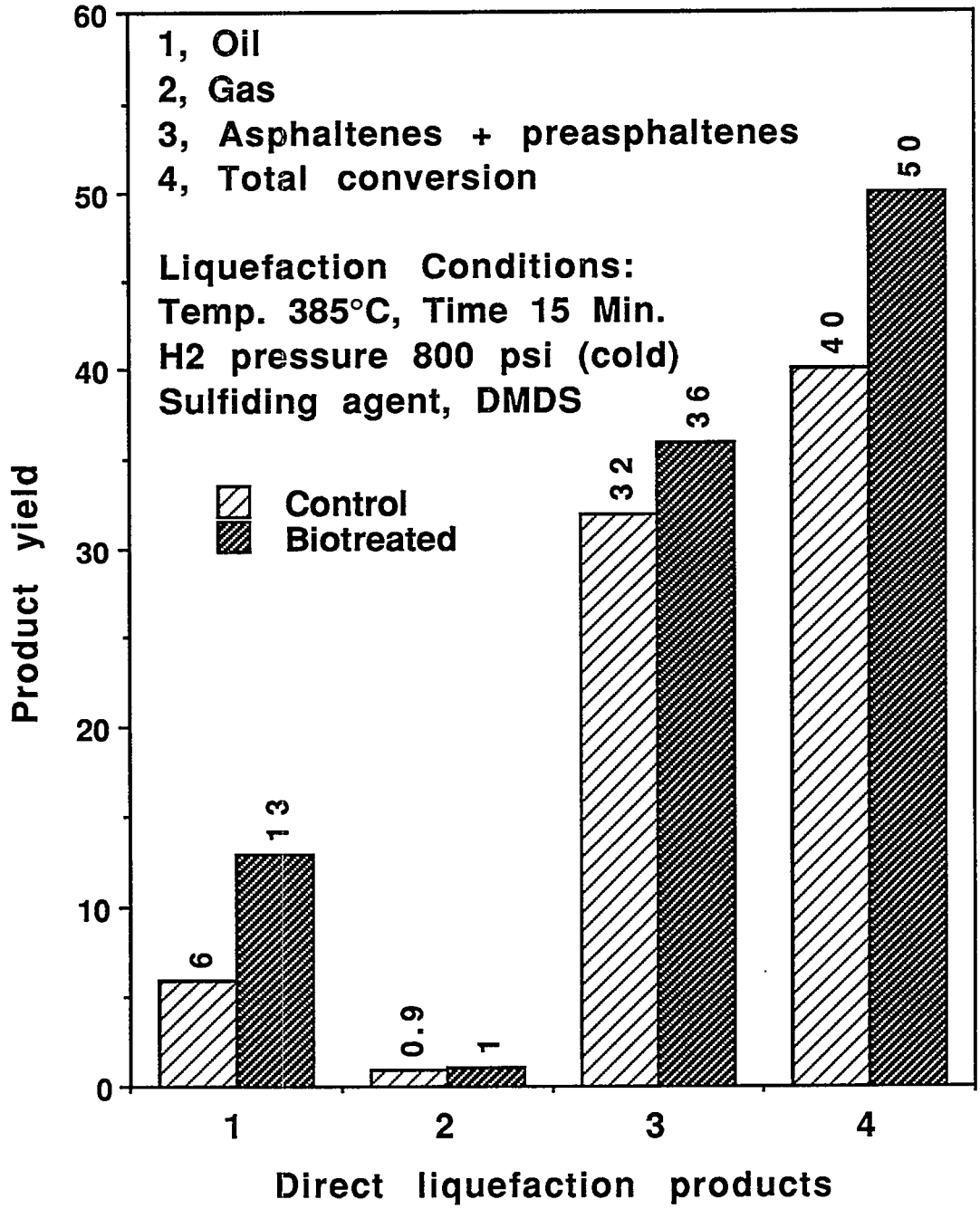

Figure 4. Direct Liquefaction Products of the Treated IBC #105 Coal in the Presence of Polyethylene Incubated with and without A.brierleyi at 68°C and pH 2.5

TASK IV

IN SITU ANALYTICAL TECHNIQUES FOR COAL LIQUEFACTION AND COAL LIQUEFACTION CATALYSTS

TASK IV

Project IV.1

HIGH PRESSURE/HIGH TEMPERATURE ESR SPECTROSCOPY OF FREE RADICALS IN COAL LIQUEFACTION AND COPROCESSING, AND CATALYST TESTING AND CHARACTERIZATION

M. S. Seehra and M. M. Ibrahim
Department of Physics
West Virginia University

OBJECTIVES

The primary objectives of this project are to investigate the coprocessing of coal with waste tires and plastics under both thermal and catalytic conditions and to characterize the catalysts used in coal liquefaction and coprocessing. High pressure/high temperature in-situ ESR (electron spin resonance) spectroscopy, x-ray diffraction (XRD) and thermogravimetric (TG) analysis are the primary techniques used in these investigations.

SUMMARY OF RESULTS

Results of our investigations during this period are best described by the four publications which were completed and submitted to various journals. A summary of these projects is given below.

a) Coprocessing of coal with waste tires and polymers: in-situ electron spin resonance investigations - accepted for publication for the ACS Symposium Series (Taylor & Francis, in press) --- In-situ ESR spectroscopy of free radicals is used to investigate the coprocessing of Blind Canyon coal with waste tire rubber (Goodyear Vector and Michelin tire rubber) and with polystyrene and polyethylene. The data of free radical density N versus temperature to 500°C, under vacuum and flowing H_2 gas conditions, show that the cracking temperature is lowered by about 100°C by the action of the tires and that the waste tire rubbers act as good hydrogen donors (Fig.

1). These findings suggest improved hydrogen transfer to coal with waste rubber. Similar experiments of coprocessing of coal with polystyrene and polyethylene show enhanced hydrocracking indicated by a large increase in N above 350°C (Fig. 2).

b) Free radical monitoring of the coprocessing of coal with chemical components of waste tires --- Abstract submitted for the April 1995 ACS meeting and a paper under preparation, with the following major points. In order to understand the mechanism for the improved liquefaction of coal with waste tires, we have investigated the effects of various chemical components of a tire (butadiene rubber, aromatic oil, carbon, ZnO, sulfur) on the free radical intensities of the Blind Canyon Coal using ESR spectroscopy from ambient to 525°C. Our results show that, individually and in selected combinations, the tire components promote enhanced cracking of the coal, especially above 320°C, as shown by the enhanced intensities of the free radical signal. However the hydrogenation type effect observed with the waste tires is not observed with the individual chemical components of the tire.

c) Thermal degradation of commingled plastics investigated by x-ray diffraction, ESR spectroscopy and thermogravimetry --- Abstract submitted for the April 1995 ACS meeting and a paper under preparation with the following major points. Ambient x-ray diffraction studies of the commingled plastics sample supplied by Larry Anderson of the University of Utah show the prominent (110) and (200) peaks of polyethylene (PE) and a weaker pattern due to TiO_2 (Fig. 3). The sample was then heated for one hour in air at selected temperatures shown in Fig. 3, cooling the sample to room temperature and followed by x-ray diffractometry. Above 360°C, irreversible degradation is observed, leading to complete disappearance of the PE peaks at 420°C but the TiO_2 peaks are still visible. The observation of free radical signal in ESR spectroscopy above 400°C signal the onset of thermal degradation. The free radical intensities are both time and temperature dependent (Fig. 4) and their magnitudes of about 10^{17} spin/gram are about 1/100 that of Blind Canyon coal at these temperatures. In TG, significant weight loss is observed above 400°C whose analysis at different heating rates provides a measure of the activation energy. These experiments show that major components of the commingled plastics are PE and TiO_2 and that PE begins to degrade irreversibly near 400°C.

d) Non-linear temperature variation of magnetic viscosity in nanoscale FeOOH particles --- Talk presented at the Consortium for Nanoscale Materials Meeting at the Oak Ridge National Laboratory in October 94 and a paper accepted for publication in the Physical Review. --- This work deals with the characterization of the electronic and magnetic properties of the 'Nanocat' FeOOH catalyst used for direct coal liquefaction. Our measurements show that in nanoscale FeOOH, magnetization is strongly time-dependent (magnetic viscosity) and its magnetic viscosity S has a non-linear temperature variation. At low temperatures (<7K), S is temperature independent because of quantum tunneling of the magnetization. For T>7 K, S begins to increase with temperature reaching a peak value at 47 K, followed by a monotonic decrease with temperature. We also show that in this sample of average particle diameter of about 30Å, 47 K is the average blocking temperature of the system above which temperature, the sample is superparamagnetic with the average magnetic moment ~ 7150 μ_B per particle. This large moment per particle may have a bearing on the catalytic properties of FeOOH. Several other magnetic parameters of this catalyst were also measured in this important work.

e) Miscellaneous: Other noteworthy activities under this project are as follows. H_2 pressures up to 1500 psi at 400°C have been obtained in in-situ ESR experiments using special sapphire tubes; Magnetic measurements on five other coated catalysts based on FeOOH and obtained from Dr. Huffman are nearing completion; M. Ibrahim attended the coal-plastic coprocessing meeting organized by V. Rao of PETC; Our TGA system broke down and it is now undergoing repair by Mettler Instruments; and a number of ESR experiments on the coal-commingled plastic coprocessing are underway. Results of these activities will be reported in future reports.

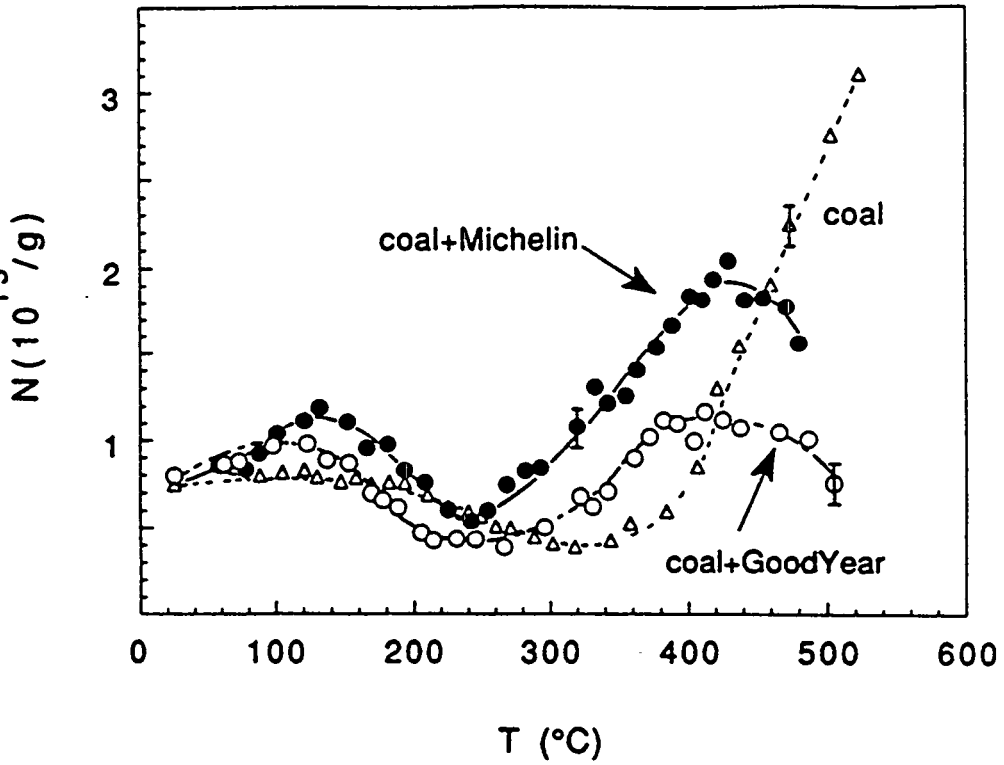

Fig. 1. Free radical density N versus temperature for Blind Canyon coal, and the coal (1:1) with mixed tire rubbers from Goodyear Vector and Michelin tires.

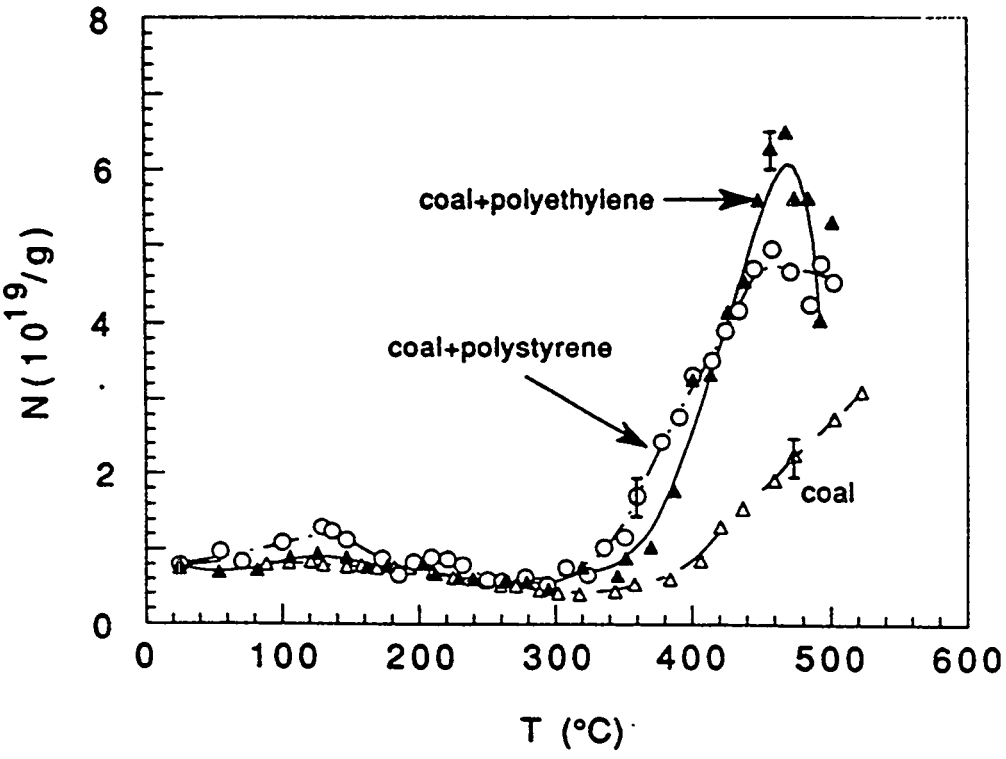

Fig. 2. Variation of free radical density N with temperature for Blind Canyon coal and the coal mixed with polyethylene and polystyrene under following H_2 gas.

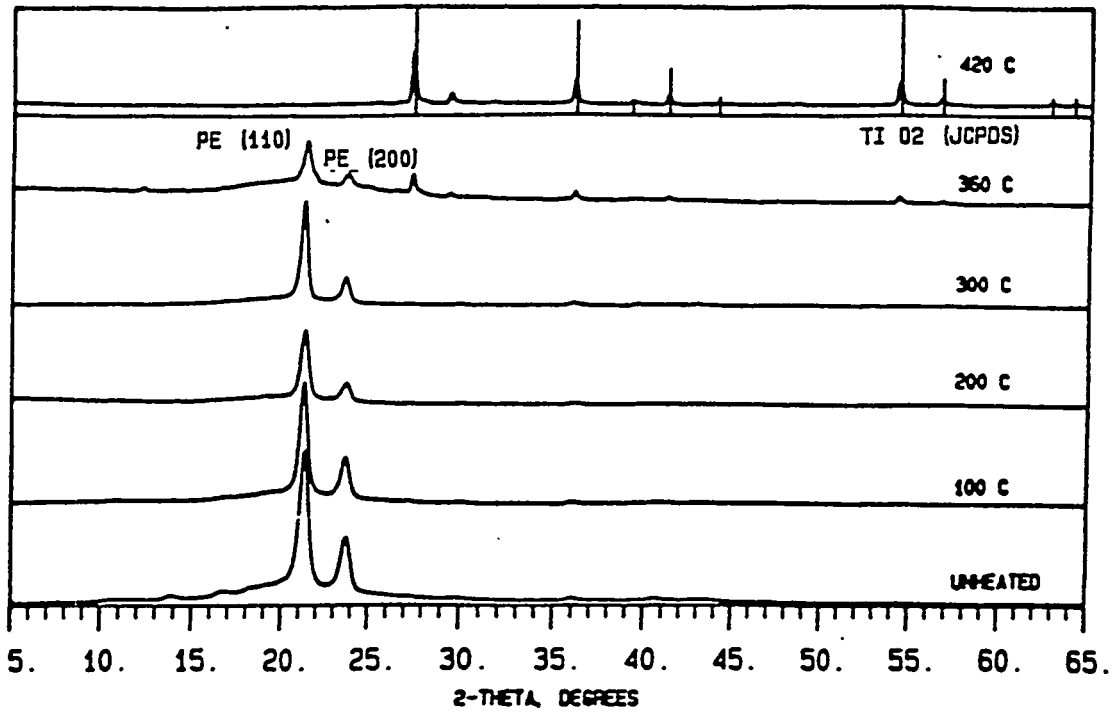

Fig. 3. Room temperature x-ray diffractograms of the commingled plastics heated for one-hour in air at various temperatures noted. PE stands for polyethylene and bar diffractogram is that expected for TiO_2.

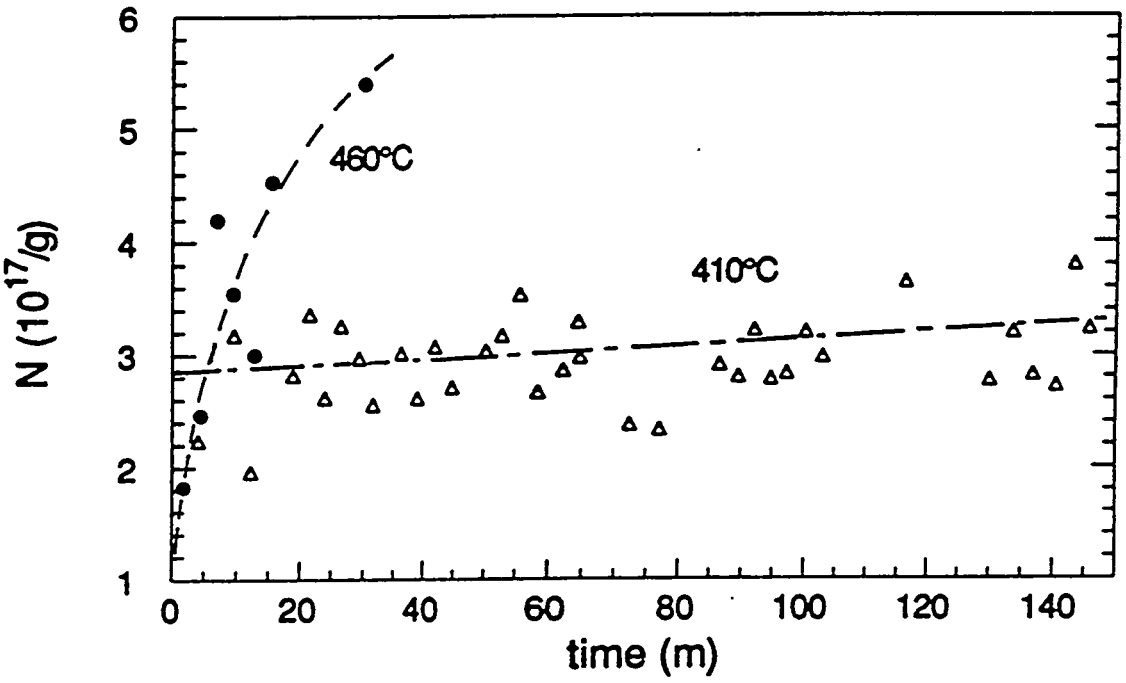

Fig. 4. Variation of the free radical density N with time at two temperatures for commingled plastics vacuum sealed in a pyrex tube.

TASK IV

Project IV.2

CATALYTIC REACTIONS IN WASTE PLASTICS AND COAL STUDIED BY HIGH PRESSURE TG/GC/MS

Henk L.C. Meuzelaar and Kui Liu
University of Utah

Recent work has focussed on studies of catalytic conversion of waste plastic and co-processing of coal with waste plastic using our high pressure TG/GC/MS instrument. This technique has proved to be very effective in bringing out the effects of different catalysts on decomposition reactions of commingled waste plastic and co-processing of coal with commingled waste plastic by comparing the relative reaction rates, residual char amounts and evolved product compositions.

1. Catalytic Effects on Decomposition Reactions of Commingled Waste Plastics

Commingled waste plastic (about 35 mg) was subjected to three different temperature programs using a constant heating rate of 20 C/min up to 410 C, 420 C or 430 C separately, isothermal hold for 30 mins and then heating up to 700 C at 20 C/min to observe how decomposition reactions occur at a hydrogen pressure of 900 psig.

Figure IV.2.1. illustrates how temperature affects the decomposition reactions as measured by the weight loss as a function of temperature history and reaction time. At the end of the 30 min isothermal period at 410 C, weight loss of the waste plastic is approx. 17%, whereas at 430 C, approx. 84% of the weight is lost. These results illustrate that thermal decomposition reactions of waste plastic (in hydrogen) are strongly dependent on relatively small changes in reaction temperature. An isothermal temperature of 420 C, producing approx. 54% weight loss within 30 min, was selected to investigate catalytic effects by comparing the relative decomposition reaction rates, residual char amounts and time-resolved product evolution profiles of thermal and catalytic runs, respectively.

Experiments on decomposition of the commingled waste plastic in two different reactor gas atmospheres (helium and hydrogen) and with several different catalysts were performed at 900 psig (except the helium run; 900 psig) using the temperature program mentioned above (isothermal at 420 C for 30 min). Catalysts studied include solid superacids such as Fe_2O_3/SO_4^{2-}, Al_2O_3/SO_4^{2-} (1% Pt promoted on Al_2O_3/SO_4^{2-}), and ZrO_2/SO_4^{2-} added at 10% to the feed, as well as conventional cracking catalyst; SiO_2/Al_2O_3 hydrocracking catalyst, $NiMo/Al_2O_3$ mixed with $SiO_2Al_2O_3$ in a 4:1 ratio (added at 50%) and HZSM-5 zeolite (added at 10%). The solid superacid catalysts were prepared by Dr. Shabtai's group. Different shapes of the TG profiles (weight loss vs. reaction time) in Figure IV 2.2 indicate catalytic effects on reaction rates and residue formation during waste plastic decomposition reactions.

At 420 C, all catalysts tested increase decomposition reaction rates to a varying degree, as indicated by the slopes of the curves in Figure IV.2.2. At these high catalyst addition levels, the SiO_2/Al_20_3 and HZSM-5 catalysts show the highest conversion rates. For the SiO_2/Al_2O_3 catalyst, measurable decomposition reactions occur at temperatures lower than 420 C. For the solid superacid catalysts studied, the approximate order of cracking activity is $ZrO_2/SO_4^{2-} > Al_2O_3/SO_4^{2-} > Pt/Al_20_3/SO_4^{2-} > Fe_2O_3/SO_4^{2-} >$ no catalyst. The weight loss after 30 min at 420°C is presented in Table IV 2.1 to illustrate how atmosphere and catalysts increase the yields of volatile products. In a hydrogen atmosphere the conversion yield is slightly increased compared to a helium atmosphere. Although $NiMo/Al_2O_3$, mixed with SiO_2/Al_2O_3 catalyst is not as effective as SiO_2/Al_20_3 in cracking ability, it gives less residue formation due to the hydrogenation activity of the sulfided metal component. For catalysts such as SiO_2/Al_20_3, $NiMo/Al_2O_3$ mixed with SiO_2/Al_20_3 and HZSM-5, the decomposition reactions are completed at 420°C within 30 minutes. Therefore, no further reactions occur upon the increase of temperature.

The catalysts tested clearly improve the conversion rate of the commingled waste plastic and lower the reaction temperature.

By examining the evolution profiles of volatile products by means of GC/MS changes in volatile product distributions as a function of reaction gas and catalysts can be measured. Several selected total ion chromatograms of one representative

sampling period at different conditions are presented in Figure IV 2.3. The results show that thermal cracking, either in helium or hydrogen (Figure IV.2.3a) produced more evenly distributed long straight chain aliphatics including alkenes and alkanes (alkenes and alkanes are not separated by the 2 meter short GC column). The stronger the cracking catalysts, the lighter the aliphatics (Figure IV.2.3b), and the more abundant the isomeric products (Figure IV.2.3c). Strong cracking catalysts such as SiO_2/Al_20_3 and HZSM-5 zeolite produce high yields of substituted aromatics due to cyclization reactions promoted by acid catalysts (shown in Figure IV.2.3d). The details will be demonstrated and discussed at the upcoming ACS Coal/Waste Materials Co-processing Symposium in Anaheim.

2. Catalytic Effects on Decomposition Reactions During Co-Processing of Coal with Commingled Waste Plastic

Co-processing runs of Blind Canyon DECS-6 coal with commingled waste plastic (in a ratio of 1:1) involved adding several selected catalysts. Samples were subjected to the same temperature history at a hydrogen pressure of 900 psig. Figure IV 2.4 illustrates the TG weight loss curves of the coal, the waste plastic as well as the coal plastic mixture under non-catalytic conditions. The dotted line is the predicted weight loss curve of the mixture which is the linear sum of the individual component curves. The mixture of coal with waste plastic shows a slightly lower reaction rate than the predicted value at 420 C (these findings were confirmed by Dr. Anderson's group using a sand bath tubing reactor). The product evolution profiles obtained by GC/MS will be examined and discussed in more detail in the next report. Catalysts which promote the decomposition reactions of the waste plastic are applied to the mixture of coal with plastic, including ZrO_2/SO_4^{2-}, SiO_2/Al_20_3, $NiMo/Al_2O_3$ mixed with SiO_2/Al_20_3 and HZSM-5 zeolite. The TG weight loss curves presented in Figure IV 2.5 indicate that catalytic co-processing of coal with plastic is more difficult than catalytic processing of the commingled waste plastic alone. The solid superacid catalyst ZrO_2/SO_4^{2-} and the cracking catalyst SiO_2/Al_20_3 (added at the 10% level) have little influence upon the decomposition reactions of the mixture. A possible explanation could be that the presence of nitrogen compounds poisons the active sites

of the acid catalysts resulting in no increase in total yield. By adding relatively large amounts (50%) of the SiO_2/Al_20_3 catalyst, the decomposition rate is increased, but to a lesser degree than for waste plastic alone. The HZSM-5 catalyst shows a very promising result for co-processing of coal and waste plastic by increasing both reaction rate and volatile product yield. This confirms earlier reports by Dr. Huffman's group. Apparently, the active sites of the HZSM-5 catalyst are much less poisoned by the coal compared to other catalysts. On the other hand, a mixture of $NiMo/Al_2O_3$ with SiO_2/Al_20_3 reveals better activity than the SiO_2/Al_20_3 catalysts, which is the opposite in case of plastic alone.

Further work needs to be done in examining how the product distribution changes for different catalysts during co-processing of coal with waste plastic and how the reactions are affected by lower temperatures at which no significant thermal reactions are expected to occur.

Table IV.2.1

Items	Weight Loss, %
He	55%
H2	59%
Fe_2O_3/SO_4^{2-}, 10%	75%
$Pt/Al_2O_3/SO_4^{2-}$, 10%	79%
Al_2O_3/SO_4^{2-}, 10%	83%
ZrO_2/SO_4^{2-}, 10%	86%
$NiMo/Al_2O_3$, mixed with SiO_2/Al_2O_3, 50%	97%
SiO_2 Al_2O_3, 50%	94%
HZSM-5, 10%	97%

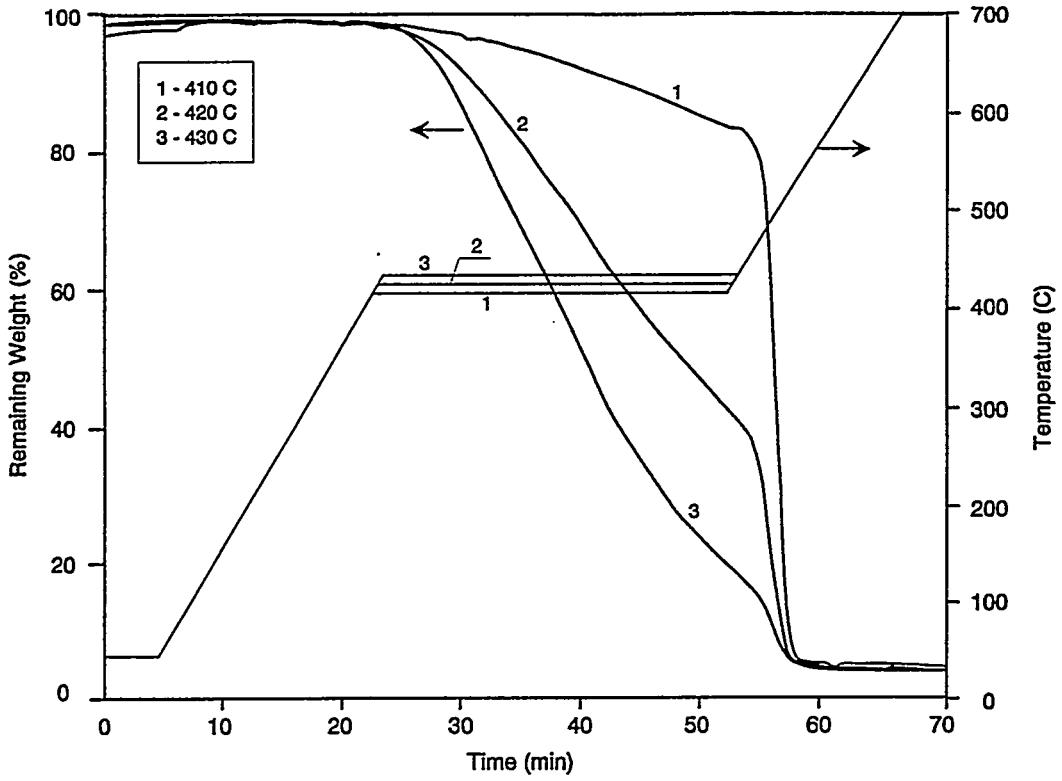

Figure IV.2.1. TG curves of the commingled waste plastic at 900 psig (H_2).

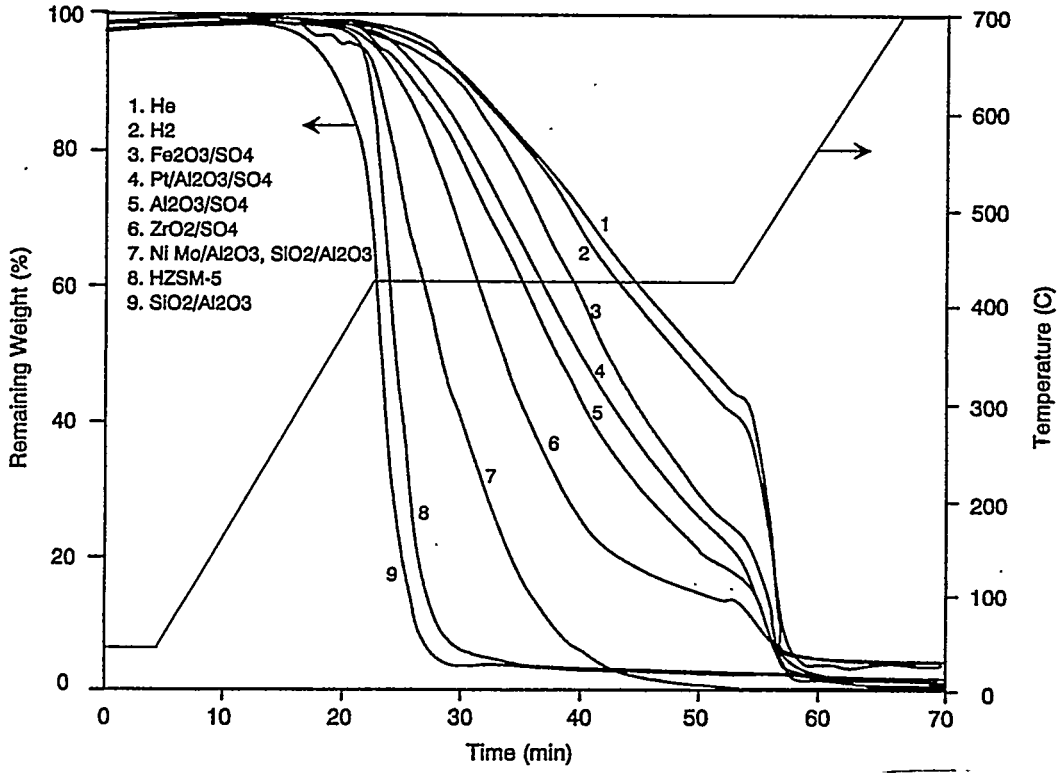

Figure IV.2.2. Effects of reactor gas atmospheres and catalysts on decomposition reactions of the commingled waste plastic at 900 psig.

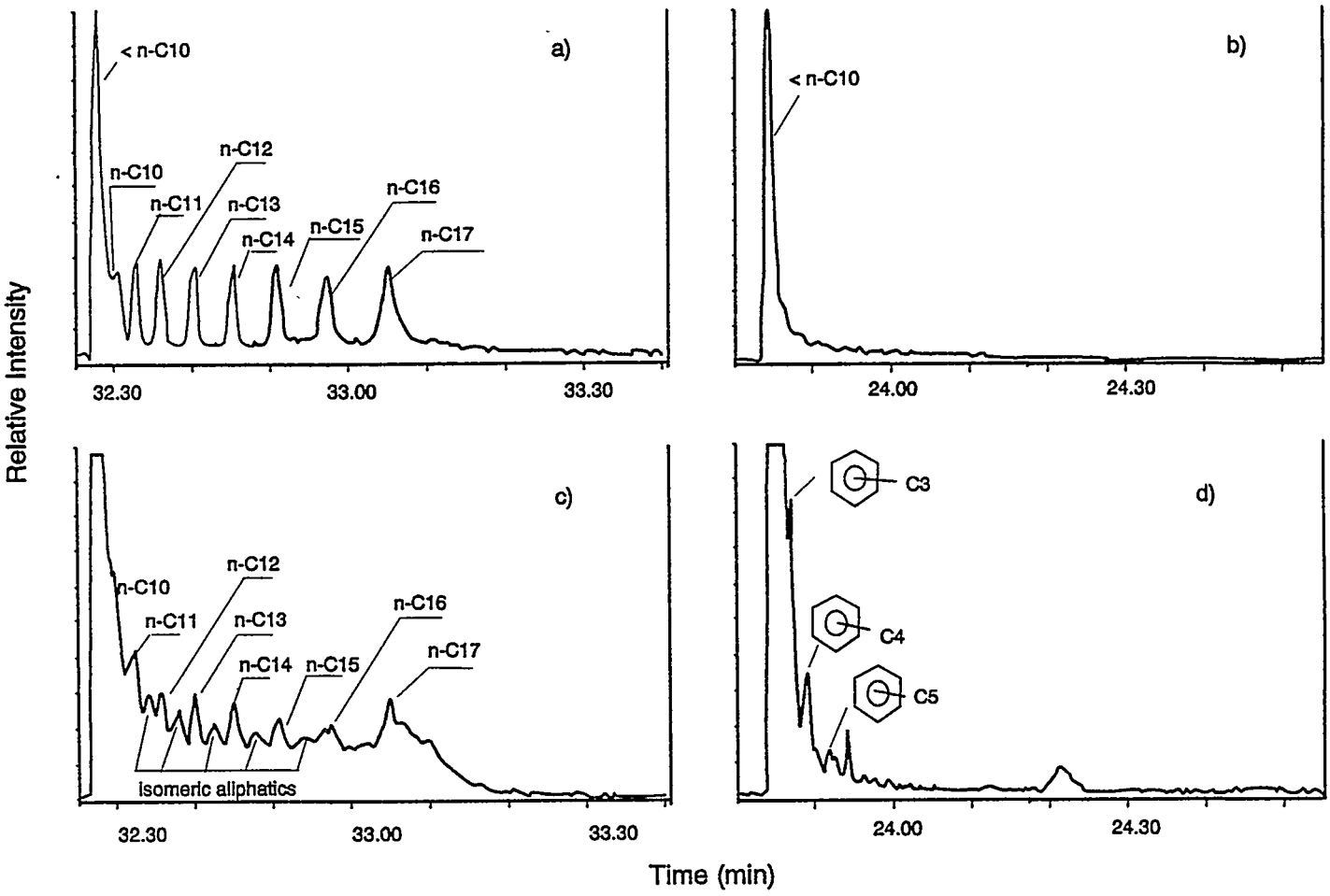

Figure IV.2.3. Total ion chromatograms of one sampling period of plastic decomposition products. a) in hydrogen; b) $SiO_2Al_2O_3$; c) ZrO_2/SO_4^{2-}; and d) HZSM-5.

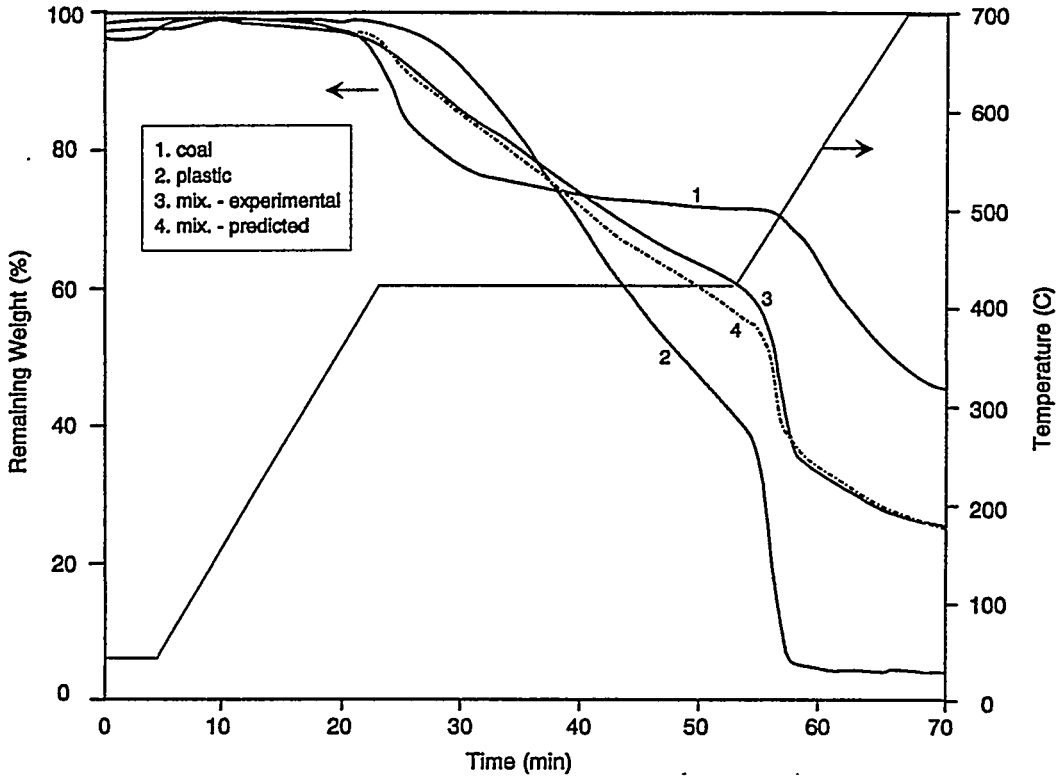

Figure IV.2.4. TG curves of co-processing of coal with plastic at 900 psig (H_2).

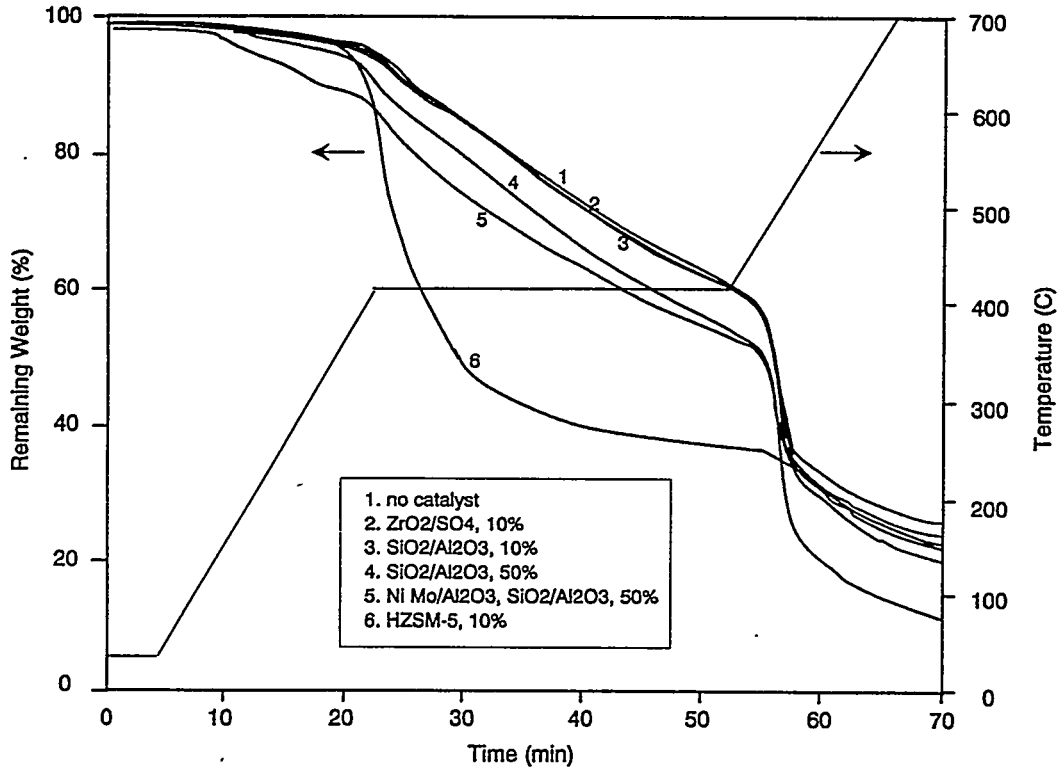

Figure IV.2.5. Effects of catalysts on co-processing of coal with plastic at 900 psig (H_2).

TASK IV

Project IV.3

IN-SITU XAFS AND MÖSSBAUER SPECTROSCOPIC STUDIES OF DCL CATALYSTS

N. Shah, J. Zhao, Z. Feng, F. Lu, K.R.P.M. Rao,
F.E. Huggins, G.P. Huffman
University of Kentucky

Introduction:

As noted in our last report, we have modified Neils and Burlitch design to build an *in-situ* cell for XAFS investigation of direct coal liquefaction (DCL) catalysts. This cell has been successfully used in investigating several catalysts at elevated temperature (up to 500 °C) and hydrogen pressure (100 psig cold) employed in the micro autoclave (tubing bomb) reactors. Recently, we tried to employ a novel XAFS technique to acquire data in a much shorter time. Dispersive XAFS technique can acquire entire XAFS spectra in about three orders of magnitude shorter time than the conventional XAFS technique.

Energy Dispersive XAFS:

Beamline X-6A at the National Synchrotron Light Source is designed for energy dispersive XAFS experiments. Figure 1 is a schematic diagram for the beamline setup. The beamline computer can control the 4-point crystal bender of Si [220] crystal to access incident energies between 6.5 and 21 KeV. The beam can be focussed to 100 μm spot size and by moving the detector radially inward/outward the energy range and the resolution can be adjusted. The angle of the flat mirror between the polychromator mirror and the sample is adjusted to allow only the first order radiation through. The higher order harmonics are blocked by a

vertical slit system between the sample and the harmonic rejection mirror.

Because there are no moving parts, no time is wasted in moving and waiting for stabilization.

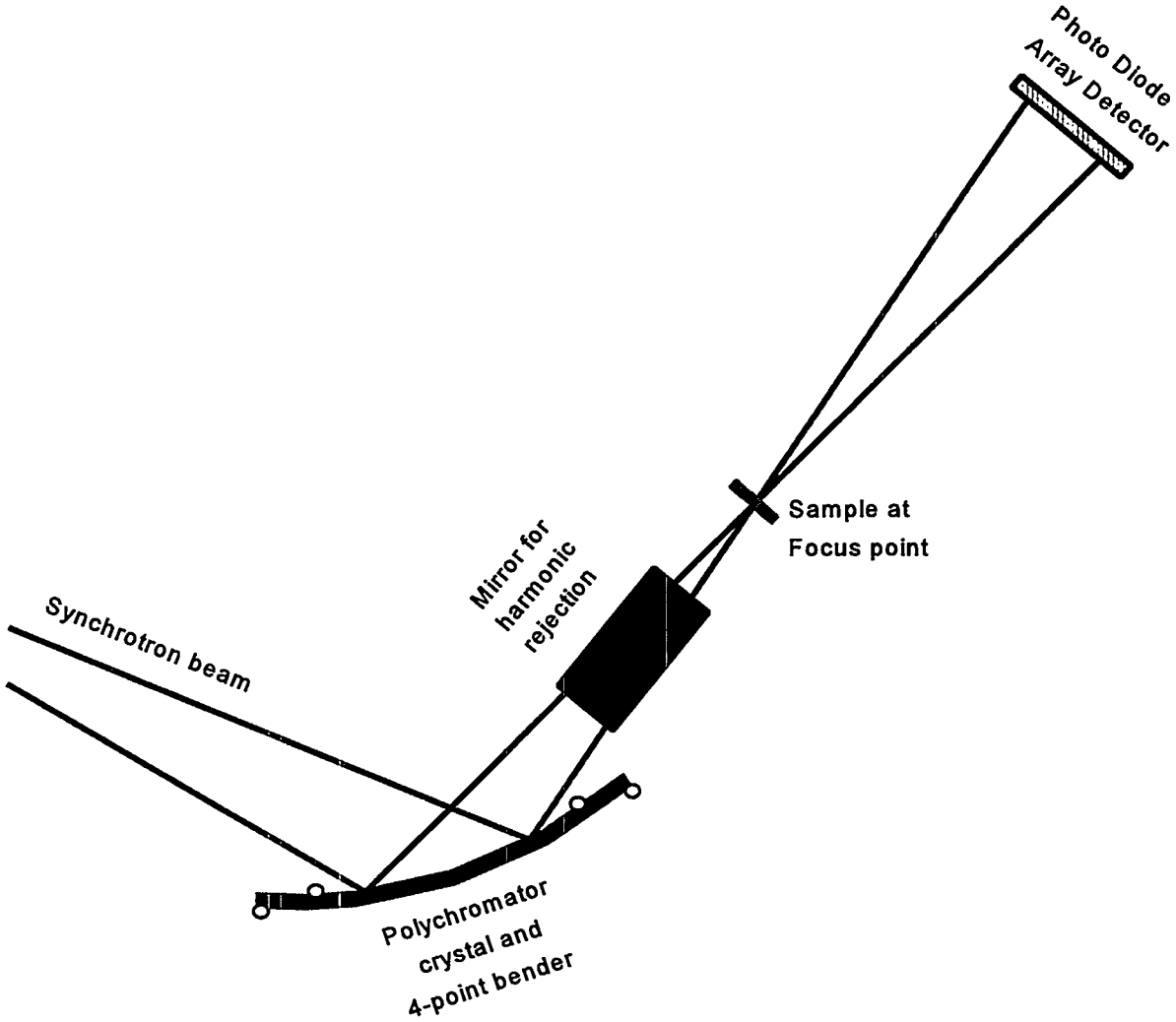

Figure 1. Schematic diagram showing the dispersive XAFS beamline components.

Results:

First the beamline components were aligned and calibrated using an iron foil calibration standard. Since there is only one crystal for energy dispersion, the intrinsic resolution of the beamline is worse than X-19A beamline with double crystal monochromator. Therefore, no attempt was made in measuring near edge XANES data. The detector was moved closer to

intercept approximately a 1000 eV range around 7500 Ev. This setting can measure data from about 100 Ev below the iron K-edge to a wave vector (k) of around 11 $(Å)^{-1}$. We could obtain excellent iron foil XAFS data within less than five seconds using these settings.

Blind Canyon (DECS-17) coal was mixed with 5% Fe loading citric acid treated ferrihydrite catalyst and sufficient elemental sulfur to convert all of the iron to $Fe_{1-x}S$ stoichiometry. A thin pellet of this sample was loaded within the *in-situ* XAFS cells and the cell was charged with 1000 psig (cold) hydrogen.

To align the cell, the harmonic rejection mirror was lowered from the beam path and a fluorescent screen showed x-rays transmitting through the cell. However, when an attempt was made to collect data, the detector did not register any x-ray signal. When only the cell was placed in the beam path, it was found that about 90% of the incident radiation was absorbed by the two graphite windows and only 10% of the incident radiation was transmitted through. Next, only the sample pellet was placed in the beam path and again only about 10% of the radiation was transmitting through. Thus, less than 1% of the incident flux can pass through both the cell and the sample. Hydrogen gas at high pressure can also absorb some radiation.

Since x-rays of 20 KeV energy are far more penetrating than that of 7KeV energy, we decided to try out an XAFS experiment at molybdenum K edge of a Fe-Mo dispersed catalyst. An EXAFS spectrum taken at room temperature showed much distortion of data. Moving the sample around moved the distorting features around in the spectra. Averaging the data taken at several spots also did not reduce this problem enough to achieve reasonable quality of information. The reason for these distortions is believed to be due to inhomogeneity of sample composition and density. All energy x-ray radiation passes through a 100 μm focussed spot. It is assumed that the composition and thickness of the sample are uniform within this spot. Since

the coal used is -100 mesh (<144 μm) particle size and the catalyst is only physically mixed, achieving isotropic uniformity is very difficult.

Conclusions:

Dispersive XAFS is a promising method for *in-situ* XAFS analysis of DCL catalysts. It can collect an entire XAFS spectrum in much shorter time and thereby provide valuable information on the kinetics of the catalyst transformations under reaction conditions. However, the following two major obstacles have to be overcome before it can be successfully used:

(1) The flux of the beamline, at iron K edge, is insufficient to penetrate the cell and the sample. A wiggler beamline or a next generation synchrotron source can provide enough flux to carry out the experiment.

(2) The sample has to be isotropically uniform both in density and composition over the focussed spot size. Physically mixed, dispersed catalysts cannot be mixed uniformly. Dispersed catalysts can be ground very finely and examined by themselves (without mixing with coal) under liquefaction conditions. An ion-exchanged catalyst may achieve more homogeneity.

TASK IV

Project IV.4

CATALYTIC DEHYDROGENATION OF PHENOLICS AND POLYCYCLIC OLEFINS IN THE PRESENCE OF HYDROAROMATIC COMPOUNDS

Irving Wender, John W. Tierney and Gerald D. Holder
University of Pittsburgh

Introduction

Hydrogen donor and hydrogen transfer reactions are of major important in direct coal liquefaction. Hydroaromatics, phenolics and polycyclic olefins are among the chief structures in coal or recycle solvents which can donate or transfer hydrogen. A measure of donatable hydrogen in coal liquefaction can be obtained by catalytic dehydrogenation of coal and model compounds[1-3]. Our work has shown that results obtained by catalytic dehydrogenation of three-ring polycyclic hydroaromatic and phenolic model compounds depend on factors such as configuration of the compounds, the catalyst and the degree of unsaturation[4,5].

The rate of evolution of hydrogen and the amount of hydrogen evolved from coal by catalytic dehydrogenation are indications of the reactivity of hydrogen donors. We hope to relate the rate or the amount of hydrogen removal either as H_2 gas or as hydrogen transferred to a hydrogen acceptor to their reactivities. This may furnish a qualitative method for rapid evaluation of the effectiveness of recycle solvents and coal liquefaction catalysts.

We have endeavored to ascertain the manner in which hydroaromatics, cyclic olefins and phenols influence each other in hydrogen transfer reactions. We have shown that the double bond in a polycyclic structure is responsible for the initiation of dehydrogenation. The hydrogen donor abilities of these compounds were compared under coal liquefaction conditions (400°C, 1000 psig of H_2). The product derived from the coal liquefaction was characterized by simulated distillation. It appears that structures resembling those in cholesterol may be good hydrogen donors in coal

liquefaction and may influence the hydrogen donor ability of hydroaromatics.

Results and Conclusions

Effect of Phenolic Groups on Catalytic Removal of Hydroaromatic Hydrogen

The model compound, 9-phenanthrol, released molecular hydrogen when catalytically dehydrogenated with Pd as the catalyst and phenanthridine as the vehicle. It was found by GC-MS that the evolution of H_2 was due to a reaction between phenanthrol molecules to form ethers. This must occur by reaction of the phenolic -OH groups with aromatic hydrogen in phenanthrol since no H_2 would be evolved if two hydroxyl groups in 9-phenanthrol condensed with the formation of water. The dehydrogenation of a mixture of 9,10-dihydroanthracene (9,10-DHA) and 9-phenanthrol gave off less molecular hydrogen than the sum expected from the dehydrogenation of the individual compounds. It seems likely that interaction between the hydroaromatic structures in 9,10-DHA and the phenolic group in 9-phenanthrol takes place during catalytic dehydrogenation. This type of interaction was studied by dehydrogenation of different ratios of 9-phenanthrol to 9,10-DHA. It was found that interaction between these two types of structures is significant and is maximum of 60-80% phenol. The dehydrogenation residue was analyzed by ^{1}H-NMR. A peak was observed at 5.4 ppm and indicates that reaction between the phenolic -OH and hydroaromatic structures does occur during catalytic dehydrogenation. This interaction between phenolic -OH groups and hydroaromatic structures has implications for the hydrogen donor ability of recycle solvents in direct coal liquefaction.

We carried out liquefaction of Illinois No. 6 coal with 9,10-dihydroanthracene (9,10-DHA) and a mixture of 9,10-DHA and 9-phenanthrol as solvents respectively. As shown in Table 1, the presence of 10 wt% phenolics in hydroaromatics slightly lowers the total conversion and oil yield. Simulated distillation showed that the interaction between phenolics during coal liquefaction reduced oil quality (C_5 soluble).

Catalytic Dehydrogenation of Polycyclic Olefins

An initial experiment was carried out on the catalytic dehydrogenation of

cholestane, a fully saturated compound. No hydrogen was removed from this compound. However, when cholesterol which has a single double bond in ring B, was dehydrogenated, about seven moles of hydrogen plus some methane per mole of cholesterol was obtained. We wondered whether this double bond in cholesterol or the hydroxyl group attached to the naphthenic structure (ring A) promotes the release of hydrogen. To study this, the hydroxyl group in cholesterol was blocked by silylation to form its trimethylsilyl ether. The silylated cholesterol was dehydrogenated and the hydrogen evolution rate was compared to the unsilylated cholesterol. There is less hydrogen evovlved from the silylated cholesterol and at the end of dehydrogenation, the silylated cholesterol had evolved one mole less of H_2/mole cholesterol than the unsilylated cholesterol. The silylation of the hydroxyl group does not affect the initial dehydrogenation rate, suggesting that the dehydrogenation of cholesterol starts from the ring containing the olefinic bond (ring B). It was ascertained by ^{1}H-NMR that the hydroxyl group was removed during catalytic dehydration. We believe that the cyclic hydrogen in ring A (1.0 mole H_2/ mole cholesterol) was removed after dehydration of the hydroxyl groups has occurred. The one mole difference in the amount of hydrogen evolution 2 indicates that the polycyclic hydrogen in ring A cannot be removed if the hydroxyl group has been blocked. It is likely that structures resembling cholesterol may be good hydrogen donors in coal liquefaction.

We liquefied Illinois No. 6 using cholesterol as a donor solvent (400°C, 1000 psig of He). Compared to the use of 9,10-DHA, cholesterol resulted in both higher conversion and oil yield. Even partially dehydrogenated cholesterol gave higher conversion and oil yield than 9,10-DHA. The oil quality was characterized by simulated distillation. Lighter oil was obtained from the reaction with cholesterol as solvent than with 9,10-DHA, indicating that cholesterol is a better hydrogen donor than 9,10-dihydroanthracene in conversion of coal.

Future Work

The interaction between phenolic and hydroaromatic compounds during catalytic dehydrogenation will be investigated further by dehydrogenation of a

mixture of phenolic and hydroaromatic compounds with a Pd catalyst in the presence of a hydrogen acceptor.

Polycyclic compounds such as cholesterol and ß-cholestanol (a compound resembling cholesterol but without a double bond) will be catalytically dehydrogenated alone and with hydroaromatics. The interaction between polycyclic olefins and hydroaromatics, if present, will be studied. Their performance in coal liquefaction will be compared in a microreactor.

We plan to use acenaphthylene (b.p. 280°C) as a hydrogen acceptor for dehydrogenation of hydroaromatics, phenolics and polycyclic olefins. It is believed that acenaphthylene is a better hydrogen acceptor than stilbene which we have been using. The effectiveness of these hydrogen acceptors in catalytic dehydrogenation will be compared.

Products derived from coprocessing of coal with various wastes and with heavy oils will be catalytically dehydrogenated using palladium catalyst. The donatable hydrogen content of the coprocessing products will be determined. The data obtained will be interpreted in light of the coprocessing process.

References

1. Reggel, L., I. Wender and R. Raymond, *Science*, Vol.137, 681-682 (1962).

2. Deshpande,A.P., *M.S. Thesis*, University of Pittsburgh (1991).

3. Fu, P.P., R.C. Harvey , *Chemical Reviews*, 78(4), 317-61 (1978).

4. Hu, J., J.H. Whitcomb, J.W. Tierney and I. Wender, preprint, Division of Fuel Chemistry of ACS, Washington, D.C., August 22, 1992, 37(3)1258-1265.

5. Hu, J., J.H. Whitcomb, J.W. Tierney and I. Wender, preprint, vol. 39, Division of Fuel Chemistry ACS, 208th ACS National Meeting, Washington, D.C., August 21-25, 1994.

Table 1. Effect of Donor Solvent on Liquefaction of Illinois No. 6 Coal (solvent/coal=2:1, 1000 psig He).

Donor Solvents	Conversion	Oil Yield
9,10-DHA	66.7	18.8
9,10-DHA + 10% 9-phenanthrol	63.2	17.0

Table 2. Comparison of Hydrogen Donor Ability of Cholesterol with 9,10-DHA in Liquefaction of Illinois No. 6 Coal (solvent/coal=2:1, 400°C, 100 psig He).

Donor Solvents	Total Conversion	Oil Yield
9,10-DHA	66.7	18.8
Cholesterol	78.2	22.1
Partially dehydrogenated cholesterol	75.4	20.3